



**HAL**  
open science

# Modulation of amphetamine-induced behaviors in mice by the atypical vesicular glutamate transporter type 3 (VGLUT3)

Nina Mansouri Guilani

► **To cite this version:**

Nina Mansouri Guilani. Modulation of amphetamine-induced behaviors in mice by the atypical vesicular glutamate transporter type 3 (VGLUT3). *Neurons and Cognition [q-bio.NC]*. Université Pierre et Marie Curie - Paris VI, 2017. English. NNT : 2017PA066538 . tel-01947557

**HAL Id: tel-01947557**

**<https://theses.hal.science/tel-01947557>**

Submitted on 7 Dec 2018

**HAL** is a multi-disciplinary open access archive for the deposit and dissemination of scientific research documents, whether they are published or not. The documents may come from teaching and research institutions in France or abroad, or from public or private research centers.

L'archive ouverte pluridisciplinaire **HAL**, est destinée au dépôt et à la diffusion de documents scientifiques de niveau recherche, publiés ou non, émanant des établissements d'enseignement et de recherche français ou étrangers, des laboratoires publics ou privés.

Université Pierre et Marie Curie  
École doctorale Cerveau, Cognition, Comportement  
*Neurosciences Paris Seine*  
*Systèmes Glutamatergiques Normaux et Pathologiques*

**Modulation of amphetamine-induced behaviors in mice by  
the atypical vesicular glutamate transporter type 3  
(VGLUT3)**

Par Nina MANSOURI-GUILANI

Thèse de doctorat de Neurosciences

Dirigée par le Dr. Salah EL MESTIKAWY

Présentée et soutenue publiquement le 5 décembre 2017

Devant un jury composé de :

Pr. Vania PRADO

Dr. Emmanuel VALJENT

Dr. Denis HERVÉ

Dr. Salah EL MESTIKAWY

Rapporteur

Rapporteur

Examineur

Directeur de thèse



## REMERCIEMENTS

Avant tout, je souhaiterais te remercier, Salah. D'abord, de m'avoir donné la chance de tracer mon chemin dans ton équipe. Tu as toujours fait preuve d'un enthousiasme débordant, quels que soient les résultats qui t'étaient présentés. Tu m'as constamment encouragée à discuter avec les autres chercheurs, et à collaborer avec eux. Grâce à toi, j'ai eu la chance de me former à de très nombreuses techniques, telles que la culture neuronale, l'électrophysiologie, la biologie moléculaire et l'anatomie. Bien que l'essentiel de ma thèse ait reposé sur du comportement, je suis fière d'avoir accumulé l'apprentissage de nombreuses autres connaissances. Malgré des désaccords récurrents, nous sommes toujours parvenus à trouver un terrain d'entente autour d'une bonne blague.

Je voudrais également remercier Stéphanie Daumas. Tu es celle qui m'a accueillie dans l'équipe, lorsque je n'étais qu'en L2. J'ai pu alors découvrir un groupe dynamique, une excellente ambiance et des thématiques très intéressantes. Ce stage, ainsi que l'idée de retravailler à tes côtés, m'ont poussée à reprendre contact avec toi pour rejoindre l'équipe. Je te remercie d'avoir appuyé mon retour en M2 auprès de Salah. Je te souhaite une belle continuation en tant que chef d'équipe, et je suis convaincue que des beaux jours s'offrent à vous.

Peppe, je te remercie pour l'aide conceptuelle que tu m'as apportée. Tu as su me stimuler aux moments où j'avais l'impression d'être dans l'impasse, et nos discussions m'ont été très précieuses. Dans ces moments-là, tu es parvenu à me remotiver. Ta / ton futur doctorant-e sera chanceux-se. Maintenant, on se concentre sur le futur papier.

Bien sûr, je veux chaleureusement remercier l'équipe « Systèmes glutamatergiques normaux et pathologiques », et plus généralement la grande famille du B4. Nous avons traversé beaucoup de choses ensemble. D'innombrables crises, certes, mais également beaucoup de moments de partage et de discussion, que ce soit au détour d'un couloir ou autour d'un plat picard dans la cuisine.

Odile, je tiens à te remercier particulièrement. Tu es vraiment l'ange-gardien de notre équipe, et le B4 a besoin de toi. Te voir chaque matin me redonnait du baume au cœur. Tu as toujours été disponible pour écouter, soutenir, enseigner, aider. J'ai de la chance de t'avoir connue. Tu es une personne merveilleuse, et je suis heureuse d'avoir rencontré l'homme qui partage ta vie. A ton image, c'est une personne dynamique et pleine d'humour.

Véronique B, nous aurons passé énormément de temps ensemble. Je te remercie d'avoir eu la patience de me transmettre ton savoir en culture cellulaire, en biologie moléculaire et en anatomie. Toi et moi avons beaucoup habité le B4 entre 7h30 et 9h du

matin ; c'était toujours réconfortant de te savoir présente, avec une oreille attentive et bienveillante. J'ai beaucoup aimé découvrir la facette musicale de ta personnalité, et j'espère avoir la chance d'entendre à nouveau tes performances.

Véronique F, je te remercie pour les discussions très intéressantes que nous avons eues pendant ces 4 années. J'admire ton ouverture d'esprit, et ta curiosité du monde et des gens ne connaît pas de limite.

Diana, Lauriane, je vous dois énormément. C'est vous qui m'avez appris la plupart des choses que je sais faire. Vous avez été de vrais modèles pour moi. Je suis heureuse que nous soyons devenues amies. Nos routes se sont séparées, mais vous revoir cet été pour célébrer ton union Lauriane restera un moment inoubliable. Je vous souhaite le meilleur pour la suite, quels que soient le pays ou la vocation qui paveront votre route.

Je remercie également les co-thésardes du bureau. Raphaële, j'admire ton ingéniosité, tu es une personne toujours droite dans ses bottes. Tout le monde t'apprécie, car tu es brillante, rigolote, et qu'on peut compter sur toi en toutes circonstances. Je suis sûre que cette dernière année de thèse sera une formalité pour toi. Sara, le détachement dont tu fais preuve m'a toujours impressionnée ; j'aurais aimé avoir ta faculté à laisser les contrariétés me passer au-dessus de la tête. Je te remercie de nous avoir ouvert la porte pour ces supers soirées sushis, et j'ai beaucoup aimé nos discussions et nos aventures chasse-aux-trésors. Je te souhaite beaucoup de réussite pour la suite, et plein de bonheur avec Zo. Nida, je te souhaite une bonne continuation, et ne doute pas que tu traceras ton sillon. Fiona, ou plutôt princesse Fiona, bravo pour tes talents de dessinatrice, c'est de famille ! Accroche-toi, envers et contre tous les problèmes techniques auxquels tu dois faire face au quotidien. Tu es pleine de ressource, et ta créativité et ton sérieux te conduiront très loin ! Toujours partante pour un repas Chez Ann ;) )

Je voudrais, Vincent, te saluer tout spécialement. Toi et moi nous entendons très bien. Je te remercie de n'avoir pas été brusqué par nos interactions, ou en tout cas d'avoir accepté ma personnalité. De nos premiers contacts, en cours de M2, jusqu'à ce jour, j'ai toujours eu ton soutien. Et je sais que nous continuerons à faire de nombreuses choses ensemble. Les discussions que nous aurons eues m'auront grandement élevée, que ce soit scientifiquement ou personnellement. Je te souhaite de merveilleuses choses pour la suite, j'ai hâte d'entendre tes histoires brésiliennes...et tes futures iraniennes !

Stéphanie De Gois. L'incontournable. Toujours prête à discuter. Merci pour ta droiture et ta rigueur. J'ai appris énormément à tes côtés, du fonctionnement du laboratoire, en passant par les potins, et en finissant par ta transmission de la BM et la culture cellulaire. Je me réjouis de savoir que tu es heureuse, et j'admire ton dynamisme. Tu sais toujours

ménager des temps pour faire du sport, et j'essaierai de m'inspirer de ça pour les années à venir !

Catalina, Sophie, nos chefs d'équipe. J'ai toujours apprécié nos discussions, et votre rigueur saura guider le B4 vers de beaux horizons.

J'en viens à une personne très spéciale, Sylvie. Ma chère Sylvie, merci de partager aussi volontiers tes expériences et ton savoir. Tu es un vrai souffle d'air dans le laboratoire, ton rire résonne dans nos couloirs et personne n'y reste insensible. J'espère que ce son tintera au B4 pendant longtemps encore, afin que les prochaines générations d'étudiants aient la chance d'appréhender *l'in situ* avec ton aisance. Tu es maintenant une initiée de la culture perse, j'espère que ta famille et toi franchirez le pas et vous laisserez tenter par un séjour en Iran. Merci pour ta gentillesse et ta générosité, nous avons encore beaucoup de choses à vivre ensemble.

Je voudrais également t'adresser des remerciements chaleureux Barbara. On se sera rapprochées en discutant de la Fête de l'Humanité, et tout au long de ces 4 années nous nous sommes trouvés de nombreux points communs. J'aime ta fantaisie. Je me rappellerai longtemps de cette Fête de l'Humanité que nous aurons passée ensemble. Je te remercie également pour toute l'aide administrative que tu m'as apportée, et je suis contente que tu sois devenue gestionnaire de notre équipe, ce qui nous aura permis de partager plus de moments ensemble. Je te souhaite de vite finir ta belle maison, et surtout d'en profiter à fond !!

Franck et Victor. Franck, papi Frankie .... Si je devais te décrire à quelqu'un, je dirai ; « Franck sait tout sur tout. Il a une théorie sur tous les sujets inimaginables. Attention, il est de mauvaise foi. » Ahlala quel roi de la mauvaise foi !! Franchement tu me tues !! Enfin bon, j'espère que nous aurons encore de nombreuses occasions de débattre, et de boire des coups. Ça va me manquer nos discussions. A défaut d'avoir facebook, j'ai un téléphone, et je ne suis pas loin du Long Hop haha. Merci pour ta gentillesse, ta disponibilité, et tes histoires. Je pense fort à toi pour ton EPHE, courage ! Victor, Victor... Malgré ton penchant pour les jeunes filles, je suis convaincue que tu arriveras d'ici tes 40 ans à rencontrer une personne de ta décennie haha. Ce qui était bien avec toi, c'est qu'on n'avait pas besoin de discuter, mais qu'on s'aimait bien. C'était un réconfort sans borne de te voir et de te savoir là les week-ends et les soirs au laboratoire. Merci d'avoir été disponible pour répondre aux questions, et pour tout le reste. T'es un type bien. Enfin bref, les garçons, je compte bien venir aux matchs de ligue des champions (il faut bien que quelqu'un soit contre le Bayern).

Enfin, je tiens à saluer les nombreuses personnes du laboratoire qui m'ont marquée. Steph Miot, Thomas, Elsa, Alejandro, Amaia, Hélène... Vous êtes de belles personnes et je vous souhaite beaucoup de bonheur dans vos nouvelles vies. Bon vent à vous !

Bien entendu, j'adresse mes sincères remerciements aux plateformes d'animalerie. Fabrice (B7), Goran, Odile, Julie, Marine, Fanny (B8), Doriane et Nathalie (NAC). Sans vous, nous ne pourrions rien faire. Je vous souhaite de bien vous porter, et surtout de garder le moral. Goran, toi et moi on a appris à bien se connaître, et je suis sûre que tu vas réussir à te plaire à Évreux. Bouger de Paris, c'est la voie de l'avenir. Tu as carrément raison !

Bien sûr, si je parle des animaux, comment ne pas parler de la plateforme du B7. Et de ses utilisateurs. A travers nos masques, et nos entrevues dans le couloir, nous aurons malgré tout réussi à nous connaître. Non, nous n'avons pas la même définition du mot silence. Non, nous n'avons pas toujours non plus la même définition du mot propreté. Nous ne partageons pas toujours les mêmes habitudes. Mais nous nous apprécions tous, et j'aurai rencontré des personnes au TOP dans ses couloirs. Je pense à Carole, Abdallah, Sébastien, Marine, Marc, Andry, Dorian, Soumee, Anne-Claire... Bonne chance pour vos manips à venir !!

Enfin, Isabelle Dusart, je t'adresse mes plus sincères remerciements. Tu as partagé ta passion de la médiation scientifique avec moi. Je t'en suis éternellement reconnaissante. Tu es une personne formidable, tu as marqué en profondeur la vie de nombreuses personnes. Ta générosité est sans borne, et je sais que j'aurai encore beaucoup d'occasions d'apprendre de toi.

Je clos ces remerciements adressés aux gens du laboratoire, et j'ouvre le chapitre concernant ma vie extérieure. La thèse l'aura gravement affectée, mais la vie post-thèse s'annonce riche en nouvelles aventures !

Bertrand, mon Doudou chéri. L'une des personnes les plus talentueuses que je connaisse. Et mon petit roro d'amour. Malcolm, le musico de ma vie. Garance, mon *alter ego*. Solène, la femme de ma vie culturelle. Héloïse, on s'est retrouvée, et comment ! Toujours sur la même longueur d'onde ! Benjamin, mon ami rosnéen. Adrien, barre de rire garantie. Merci pour tous ces moments passés ensemble, vous me donnez toujours le sourire !

Les copains de l'ENS, Pierre (PVG), le blondinet aux yeux bleus qui parlait persan. Que ton départ vers l'Ouest soit des plus doux, docteur ! Paupaul, mon co-respo volley ! On se sera bien marrés ensemble. Florian. Une simple rencontre en Australie, et nous voilà des années plus tard, toujours attachés comme quand on écrivait nos rapports à 00h30 avec des drosophiles dans la pièce d'à côté. Cheers mate ! Camille, je te remercie

pour ta douceur. J'espère que tu trouveras une vie qui saura t'épanouir. Je vous aime tous profondément.

Maria, my sweet Mia. Can you believe what our lives have turned into? Especially yours, of course... mamma Mia (haha). I love you, you are a real sunshine. Keep smiling, you're at the top of your game!! Can't wait to meet Charlotte Rose. You being here the D-day meant the world to me. Good luck for you thesis!!

J'en viens maintenant à Sébastien. L'homme qui partage ma vie. Tu as littéralement changé ma vie. Je te remercie pour ta patience. Pour ton soutien indéfectible. La vie avec toi est un bonheur au quotidien, et j'espère que tous les deux nous réussirons à nous tirer vers le haut et vivre de belles aventures ensemble. Je ne pense pas que j'aurais réussi à tenir ces 4 années sans toi à mes côtés. J'ai de la chance d'avoir un homme aussi bon dans ma vie. Je t'aime.

Enfin, je voudrais remercier ma famille. A mes parents que j'aime. Vous avez fait de moi ce que je suis, j'espère vous avoir rendus fiers. Je vous dois tout, je ne suis rien sans vous. Écrire ces mots m'émeut beaucoup, car je n'expose jamais mes sentiments. Je voudrais vous rendre au millième tout ce que vous faites pour moi, mais je suis tellement gâtée que je cela me paraît impossible. J'admire tout ce que vous êtes. De vrais humanistes. Des âmes pures. J'aimerais que le monde entier ait la chance de vous rencontrer, car tout ce que vous touchez s'améliore. Je n'ai qu'une envie, c'est que mes enfants aient la chance de passer le plus de temps possible à vos côtés. Quel honneur j'ai eu de côtoyer des gens aussi bons et aimants que vous, aussi cultivés, aussi curieux de la vie. Je vous souhaite de bien profiter de votre retraite prochaine.

J'adresse une pensée pleine d'émotions à ma grand-mère qui nous a quittés récemment. Cela m'a rappelé à quel point la famille est essentielle. Quelle que soit la distance qui nous sépare, nous restons et resterons soudés.

Je me dois de clore ces remerciements sur une note musicale. C'est le seul élément constant de ma vie. Je me cantonnerai à quelques sources d'inspiration.

**« Par un petit matin d'été / Quand le soleil vous chante au cœur  
Quelle est belle la liberté / la li-ber-té. »**

Georges Brassens

**« J'veux voir le cul de tes bouteilles / Et au diable leur pudeur  
Toutes il faut que j'les essaye / Que j'les dépucelle sur l'heure. »**

La Rue Ketanou

**« Breathe, keep breathing. I can't do this alone. »**

Radiohead

**« Dis-moi c'est quand / que ça commence si ce que l'on tient  
Est une absence ou un alibi / Et dis-moi aussi c'est quand que tu reviens »**

Louise Attaque

**« Je me souviendrai des beaux jours / Des roses et des lumières. »**

Deportivo

**« J'ai rien prévu pour demain / Mais c'est déjà bien d'y penser. »**

Tryo

**∞ Et à tout futur lecteur, merci de votre intérêt ∞**

## **ABSTRACT**

All drugs of abuse yield a greater release of dopamine in a cerebral structure called striatum. This structure is involved in motor control, but also in behaviors motivated by reward. Locally, striatal neurons are modulated by cholinergic interneurons (CINs). CINs have the particularity to express the vesicular glutamate transporter type 3 (VGLUT3) on top of the one for acetylcholine (VACHT). Therefore, these interneurons have the ability to release both glutamate and acetylcholine. In the striatum, VGLUT3 is also found in some serotonergic fibers. A genetic study revealed that the mutation rate of the gene encoding VGLUT3 is increased in human addicts. Moreover, mice lacking VGLUT3 (VGLUT3<sup>-/-</sup>) are pre-sensitized to cocaine, and present functional alterations in the striatum. Thus, VGLUT3 is involved in the response to drugs of abuse.

My work consisted in characterizing the effects of another psychostimulant, the amphetamine (AMPH), on VGLUT3<sup>-/-</sup> mice. This study revealed that VGLUT3<sup>-/-</sup> mice display locomotor sensitization to AMPH, to a higher extent than control mice. At high dose, psychostimulants produce abnormal movements called stereotypies. We observed that VGLUT3<sup>-/-</sup> mice are more resistant to AMPH-induced stereotypies. Further investigation showed that the glutamate released by CINs seems involved in these stereotypies, but not the serotonergic source.

Our result reveals an unsuspected role of the glutamate released by CINs in abnormal movements that are the hallmark of several pathologies.

### **Keywords:**

VGLUT3 ; striatum ; amphetamine; stereotypies; locomotor sensitization.



# RÉSUMÉ

Toutes les drogues entraînent une libération accrue de dopamine dans une structure cérébrale nommée striatum. Cette structure est impliquée à la fois dans le contrôle moteur et dans les comportements motivés par les récompenses. Localement, les neurones striataux sont modulés par des interneurons cholinergiques (CINs). Les CINs ont pour particularité d'exprimer le transporteur vésiculaire du glutamate de type 3 (VGLUT3) en plus de celui de l'acétylcholine (VACHT). Par conséquent, ces interneurons sont capables de libérer du glutamate et de l'acétylcholine. Dans le striatum, VGLUT3 est également retrouvé dans certaines fibres sérotoninergiques. Chez des patients toxicomanes, le taux de mutation du gène codant VGLUT3 est augmenté. De plus, les souris qui n'expriment pas VGLUT3 (VGLUT3<sup>-/-</sup>) sont pré-sensibilisées à la cocaïne, et présentent des changements fonctionnels dans le striatum. VGLUT3 est donc impliqué dans la réponse aux drogues d'abus.

Mes travaux de recherche ont consisté à caractériser l'effet d'un autre psychostimulant, l'amphétamine (AMPH), chez les souris VGLUT3<sup>-/-</sup>. Cela a permis de montrer que ces souris présentent une sensibilisation locomotrice à l'AMPH, plus forte que les contrôles. A forte dose, les psychostimulants entraînent l'apparition de mouvements anormaux appelés stéréotypies. Nous avons observé que les souris VGLUT3<sup>-/-</sup> sont plus résistantes aux stéréotypies induites par l'AMPH. Une étude plus approfondie a montré que le glutamate libéré par les CINs semble intervenir dans ces stéréotypies.

Ces résultats révèlent un rôle jusque-là insoupçonné du glutamate libéré par les CINs dans les mouvements anormaux, qui sont la signature de diverses pathologies.

## Mots-clés:

VGLUT3 ; striatum ; amphétamine ; stéréotypies ; sensibilisation locomotrice.



**TABLE OF ILLUSTRATIONS** **I**

**LIST OF TABLES** **V**

**ABBREVIATION LIST** **VII**

**INTRODUCTION** **1**

**PART I.**

**GLUTAMATE: A FUNDAMENTAL NEUROTRANSMITTER** **1**

- 1. Generalities about neurotransmission** ..... **2**
- 2. History of glutamate identification as a neurotransmitter**..... **3**
- 3. Glutamate receptors and related signaling** ..... **4**
  - 3.1 Ionotropic glutamate receptors 5
  - 3.2 Metabotropic glutamate receptors 8
- 4. Glutamate transporters**..... **10**
  - 4.1 Plasma membrane glutamate transporters 12
  - 4.2 Vesicular neurotransmitter transporters 15

**PART II.**

**VESICULAR GLUTAMATE TRANSPORTER TYPE 3 (VGLUT3)** **23**

- 1. Vesicular glutamate transporters**..... **23**
  - 1.1 A history of VGLUTs 23
  - 1.2 VGLUTs cellular and subcellular distributions 25
  - 1.3 VGLUTs structure 26
  - 1.4 Mechanism of glutamate uptake by VGLUTs 28
  - 1.5 VGLUTs during development 31
  - 1.6 VGLUTs pharmacology 32
- 2. Vesicular glutamate transporter type 3 (VGLUT3)** ..... **35**
  - 2.1 Anatomical distribution 35
    - 2.1.1 Regional distribution 35
    - 2.1.2 Ultrastructural distribution 38
    - 2.1.3 Neuronal subtypes distribution 39
  - 2.2 Functional roles: overview 41
    - 2.2.1 Dual release of transmitters 41
    - 2.2.2 Vesicular synergy 44
    - 2.2.3 Related phenotypes 46

## **PART III.**

### **THE STRIATUM**

**51**

<b>1. Anatomy of the striatum .....</b>	<b>51</b>
1.1 Matrix <i>versus</i> striosomes	51
1.2 Functional compartmentalization	52
1.3 Striatal cytoarchitecture	53
1.3.1 Medium spiny neurons	53
1.3.2 Striatal interneurons	55
<b>2. Striatal connectivity .....</b>	<b>58</b>
2.1 Striatal afferents	58
2.1.1 Glutamatergic innervation	58
2.1.2 Midbrain DA neuromodulation	59
2.1.3 Serotonergic innervation	61
2.1.4 Cholinergic innervation	62
2.1 Striatal activity modulation	63
2.1.1 DAergic modulation	63
2.1.2 Cholinergic modulation	65
2.1.3 Acetylcholine / dopamine activity during behavior	66
2.2 Striatal efferent to basal ganglia	68
2.2.1 Basal ganglia	68
2.2.2 The striatonigral (direct) pathway	69
2.2.3 The striatopallidal (indirect) pathway	69
2.2.4 The striosomal pathway	70
2.2.1 Current view on striatal function	71

## **PART IV.**

### **STRIATAL DYSREGULATIONS AND ASSOCIATED PATHOLOGIES**

**73**

<b>1. The reward system .....</b>	<b>73</b>
1.1 Reward circuitry	73
1.2 Mode of action of drugs	74
1.3 Drug addiction	75
1.4 Molecular basis of drug addiction	78
1.5 Role of VGLUT3 in addiction	82
1.6 Amphetamine	85
<b>2. Dorsal striatum defects .....</b>	<b>87</b>
2.1 Parkinson's disease	87
2.2 Obsessive-compulsive disorders	93

<b>3. Stereotypies.....</b>	<b>93</b>
3.1 Definition and general considerations	93
3.2 Animal models to elicit stereotypies	94
3.2.1 L-DOPA-induced dyskinesia	94
3.2.1 Drug-induced stereotypies	94
3.3 Functional and biochemical correlates of stereotypies	96
3.4 Methods to assess drug-induced stereotypies	98
3.5 Role of VGLUT3 in LID	100

## **MATERIALS AND METHODS 107**

<b>1. Animal models .....</b>	<b>107</b>
1.1 VGLUT3 <sup>-/-</sup>	107
1.2 VGLUT3 <sup>LoxP/LoxP</sup>	108
1.3 VGLUT3 conditional knock-out: genetic approach	109
1.3.1 SERT-Cre conditional knock-out	110
1.3.2 ChAT-IRES-Cre conditional knock-out	111
1.4 VGLUT3 conditional knock-out: viral approach	112
1.4.1 Surgical procedure	112
1.4.2 Cre-expressing virus	113
<b>2. Behavioral experiments .....</b>	<b>113</b>
2.1 Spontaneous locomotor activity	114
2.2 Anxiety tests	115
2.2.1 Open field	115
2.2.2 O maze	115
2.3 Behavioral sensitizations	115
2.3.1 Behavioral sensitization to amphetamine	116
2.3.2 Locomotor sensitization to cocaine	116
2.4 Stereotypy scoring	117
2.4.1 Categorial scoring	117
2.4.2 Rating-scale-based scoring of general stereotypies	119
2.4.3 Rating-scale-based scoring of orofacial stereotypies	119
<b>3. Drug treatments .....</b>	<b>120</b>
<b>4. Anatomical studies by immunohistochemistry .....</b>	<b>120</b>
4.1 Immunofluorescence	120
4.1.1 Conditional knock-outs validation: VGLUT3, VACHT and 5-HT	120
4.1.2 ΔFosB immunofluorescence	121
4.2 Immunoautoradiography	122
<b>5. Statistics .....</b>	<b>122</b>
<b>6. Experiments color code .....</b>	<b>123</b>

**PART I.****VGLUT3 FULL KNOCK-OUT AND AMPHETAMINE 125**

<b>1. Basal characterization.....</b>	<b>126</b>
1.1 Number of VGLUT3 <sup>-/-</sup> used	126
1.2 VGLUT3 <sup>-/-</sup> mice weight	126
1.3 Spontaneous locomotion	127
<b>2. VGLUT3<sup>-/-</sup> and amphetamine 1 mg/kg.....</b>	<b>127</b>
2.1 Acute injection of amphetamine 1 mg/kg	127
2.1 Repeated injections of amphetamine 1 mg/kg	128
<b>3. VGLUT3<sup>-/-</sup> and amphetamine 3 mg/kg.....</b>	<b>130</b>
3.1 Acute injection of amphetamine 3 mg/kg	130
3.1 Repeated injections of amphetamine 3 mg/kg	130
<b>4. VGLUT3<sup>-/-</sup> and amphetamine 5 mg/kg.....</b>	<b>132</b>
4.1 Effect on locomotion	132
4.1.1 Acute injection of amphetamine 5 mg/kg	132
4.1.2 Repeated injections of amphetamine 5 mg/kg	133
4.2 Effect on stereotypies	134
4.2.1 General stereotypies	134
4.2.2 Orofacial stereotypies	136
<b>5. Discussion.....</b>	<b>138</b>

**PART II.****CONTRIBUTION OF VGLUT3-POSITIVE SYSTEMS IN THE RESPONSE TO AMPHETAMINE 147**

<b>1. The VGLUT3-positive serotonergic drive of the striatum.....</b>	<b>148</b>
1.1 Anatomical characterization of cKO-VGLUT3 <sub>5-HT</sub>	148
1.2 Behavioral characterization of cKO-VGLUT3 <sub>5-HT</sub>	149
1.2.1 Weight	149
1.2.2 Basal locomotion	149
1.2.3 Anxiety tests	150
1.2.4 Spontaneous locomotion before sensitization	152
1.3 cKO-VGLUT3 <sub>5-HT</sub> and amphetamine 5 mg/kg	152
1.3.1 Effect on locomotion	152
1.3.2 Effect on stereotypies	154
<b>2. The VGLUT3-positive cholinergic drive of the striatum .....</b>	<b>157</b>
2.1 Anatomical characterization of cKO-VGLUT3 <sub>ACh</sub>	158
2.2 Behavioral characterization of cKO-VGLUT3 <sub>ACh</sub>	158
2.2.1 Weight	158
2.2.2 Basal locomotion	159
2.2.3 Anxiety tests	160

2.2.4 Spontaneous locomotion before sensitization	162
2.3 cKO-VGLUT3 <sub>ACh</sub> and amphetamine 5 mg/kg	162
2.3.1 Effect on locomotion	162
2.3.2 Effect on stereotypies	165
2.4 cKO-VGLUT3 <sub>ACh</sub> and cocaine 10 mg/kg	168
<b>3. Discussion.....</b>	<b>169</b>
<b>PART III.</b>	
<b>STUDY OF THE ROLE OF VGLUT3 IN THE NUCLEUS ACCUMBENS IN THE</b>	
<b>RESPONSE TO COCAINE</b>	<b>177</b>
<b>1. Development of viral injections.....</b>	<b>178</b>
1.1 Choice of virus	178
1.2 Experimental groups	179
<b>2. Anatomical validation .....</b>	<b>180</b>
<b>3. Behavioral characterization .....</b>	<b>181</b>
3.1 Mice weight	181
3.2 Basal locomotion	182
3.3 Anxiety levels	183
<b>4. Locomotor sensitization to cocaine .....</b>	<b>185</b>
<b>5. Discussion.....</b>	<b>187</b>
<b>GENERAL CONCLUSION</b>	<b>189</b>
<hr/>	
<b>APPENDICES</b>	<b>II</b>
<hr/>	
<b>1. Temporal course of AMPH injections .....</b>	<b>ii</b>
1.1 VGLUT3 <sup>-/-</sup> and AMPH 1 mg/kg	ii
1.2 VGLUT3 <sup>-/-</sup> and AMPH 3 mg/kg	iii
1.3 VGLUT3 <sup>-/-</sup> and AMPH 5 mg/kg	iv
1.4 cKO-VGLUT3 <sub>5-HT</sub> and AMPH 5 mg/kg	v
1.5 cKO-VGLUT3 <sub>ACh</sub> and AMPH 5 mg/kg	vi
<b>2. Publications .....</b>	<b>vii</b>
<b>REFERENCES</b>	<b>VIII</b>
<hr/>	



# **Table of illustrations**

## **INTRODUCTION**

<i>Figure A.1: L-glutamic acid and L-glutamate structures.....</i>	<i>1</i>
<i>Figure A.2: Electron micrograph of an excitatory synapse in the mouse neocortex .....</i>	<i>3</i>
<i>Figure A.3: Term “glutamate” occurrence in the literature since 1912 .....</i>	<i>4</i>
<i>Figure A.4: Schematic view of a glutamatergic synapse .....</i>	<i>5</i>
<i>Figure A.5: Glutamate excitatory post - synaptic current has two components.....</i>	<i>6</i>
<i>Figure A.6: LTD / LTP in hippocampus, electrophysiological and structural features .....</i>	<i>7</i>
<i>Figure A.7: Duration range of iGluRs and mGluRs responses.....</i>	<i>8</i>
<i>Figure A.8: mGluRs coupling and intracellular cascades.....</i>	<i>9</i>
<i>Figure A.9: Glutamate concentration in the brain.....</i>	<i>11</i>
<i>Figure A.10: Modeling of glutamate diffusion in a three - dimensional structure.....</i>	<i>12</i>
<i>Figure A.11: EAATs electrochemical and molecular properties.....</i>	<i>13</i>
<i>Figure A.12: Subcellular distribution of EAATs in the hippocampus.....</i>	<i>14</i>
<i>Figure A.13: Synaptic vesicle properties.....</i>	<i>16</i>
<i>Figure A.14: SVs lateral mobility along axon.....</i>	<i>17</i>
<i>Figure A.15: Serotonin and catecholamines biosynthesis pathways.....</i>	<i>19</i>
<i>Figure A.16: VNTs electrochemical dependence.....</i>	<i>20</i>
<i>Figure A.17: Glutamate gradients at excitatory presynaptic terminals .....</i>	<i>23</i>
<i>Figure A.18: VGLUT3 expression promotes glutamate release by GABAergic neurons .....</i>	<i>25</i>
<i>Figure A.19: Alignment of Homo sapiens VGLUTs amino acid sequences .....</i>	<i>27</i>
<i>Figure A.20: VGLUT topology model .....</i>	<i>28</i>
<i>Figure A.21: SV endocytosis at the plasma membrane .....</i>	<i>30</i>
<i>Figure A.22: VGLUT1 - 3 protein expression during post - natal development.....</i>	<i>32</i>
<i>Figure A.23: VGLUT family inhibitors.....</i>	<i>34</i>
<i>Figure A.24: Regional distribution of VGLUT3 transcript and VGLUT1, - 2 and - 3 proteins .....</i>	<i>37</i>
<i>Figure A.25: VGLUT3 at asymmetrical or symmetrical synapses.....</i>	<i>38</i>
<i>Figure A.26: Co - release and co - transmission in neurons.....</i>	<i>41</i>
<i>Figure A.27: VGLUT3 and VIAAT are expressed on the same SVs.....</i>	<i>43</i>
<i>Figure A.28: Vesicular synergy between VGLUT3 and VAcHT.....</i>	<i>44</i>
<i>Figure A.29: Hyperlocomotion induced by acetylcholine or glutamate detuning (60min).....</i>	<i>48</i>
<i>Figure A.30: Functional subdivisions of the striatum in humans and rodents .....</i>	<i>52</i>
<i>Figure A.31: Cytology of striatal interneurons.....</i>	<i>55</i>
<i>Figure A.32: VGLUT1 and VGLUT2 distribution in the striatum .....</i>	<i>59</i>
<i>Figure A.33: Organization of dopaminergic projections to different striatal subregions .....</i>	<i>60</i>
<i>Figure A.34: Dopaminergic and cholinergic modulation of striatal neurons.....</i>	<i>62</i>
<i>Figure A.35: D<sub>1</sub>R and D<sub>2</sub>R signaling cascades.....</i>	<i>64</i>
<i>Figure A.36: Opposite responses of DA neuron and CINs during operant conditioning .....</i>	<i>67</i>
<i>Figure A.37: Basal ganglia circuit.....</i>	<i>68</i>
<i>Figure A.38: The striosomal pathway.....</i>	<i>70</i>
<i>Figure A.39: The reward circuitry (sagittal view of mouse brain).....</i>	<i>73</i>
<i>Figure A.40: Major targets of addictive drugs.....</i>	<i>75</i>
<i>Figure A.41: ERK activation in D<sub>1</sub> - and D<sub>2</sub> - MSNs following acute cocaine .....</i>	<i>79</i>
<i>Figure A.42: IEG activation cascade time -course .....</i>	<i>80</i>
<i>Figure A.43: Locomotor sensitization to cocaine in VGLUT3<sup>-/-</sup> mice.....</i>	<i>83</i>
<i>Figure A.44: D<sub>1</sub> -MSNs characteristics in VGLUT3<sup>-/-</sup> mice.....</i>	<i>83</i>
<i>Figure A.45: Dual regulation of DA efflux by ACh and Glu from CINs in the Acb.....</i>	<i>84</i>

Figure A.46: Prevalence of amphetamine - type stimulants (excluding ecstasy) in 2010.....	85
Figure A.47: Amphetamine modes of action .....	86
Figure A.48: Anatomical and cellular defects in human PD .....	87
Figure A.49: Enkephalin and opioid receptors expression in toxin - induced parkinsonism .....	88
Figure A.50: Presynaptic model of 5 - HT - mediated LID .....	92
Figure A.51: Amphetamine biphasic effect on locomotion and stereotypies.....	95
Figure A.52: Model of CalDAG - GEFs striatal signaling to ERK in LID.....	97
Figure A.53: LID in VGLUT3 <sup>-/-</sup> and Drd2-Cre::VACHT <sup>LoxP/LoxP</sup> .....	101
Figure A.54: VGLUT3 mutations in humans with severe drug abuse .....	103

## MATERIALS AND METHODS

Figure B.1: VGLUT3 <sup>-/-</sup> construct.....	108
Figure B.2: VGLUT3 <sup>LoxP/LoxP</sup> construct.....	109
Figure B.3: VGLUT3 conditional knock - out breeding strategy.....	110
Figure B.4: Set - ups used for behavior.....	114
Figure B.5: Protocol for behavioral sensitization to amphetamine.....	116
Figure B.6: Protocol for behavioral sensitization to cocaine.....	117

## RESULTS

Figure C.1: VGLUT3 <sup>-/-</sup> mouse weight .....	126
Figure C.2: VGLUT3 <sup>-/-</sup> mice spontaneous activity.....	127
Figure C.3: VGLUT3 <sup>-/-</sup> locomotor sensitization to AMPH 1 mg/kg.....	129
Figure C.4: VGLUT3 <sup>-/-</sup> locomotor sensitization to AMPH 3 mg/kg.....	131
Figure C.5: VGLUT3 <sup>-/-</sup> locomotor sensitization to AMPH 5 mg/kg.....	133
Figure C.6: VGLUT3 <sup>-/-</sup> general stereotypies with AMPH 5 mg/kg.....	136
Figure C.7: VGLUT3 <sup>-/-</sup> orofacial stereotypies with AMPH 5 mg/kg.....	138
Figure C.8: Model of cocaine and amphetamine action in VGLUT3 <sup>-/-</sup> mice .....	140
Figure C.9: Striatal evoked dopamine levels in VGLUT3 <sup>-/-</sup> mice.....	144
Figure C.10: Immunoautoradiography for VGLUT3 in cKO-VGLUT3 <sup>5-HT</sup> mice .....	148
Figure C.11: cKO-VGLUT3 <sup>5-HT</sup> mice weight .....	149
Figure C.12: cKO-VGLUT3 <sup>5-HT</sup> circadian locomotor activity .....	150
Figure C.13: cKO-VGLUT3 <sup>5-HT</sup> anxiety levels in the open field test.....	151
Figure C.14: cKO-VGLUT3 <sup>5-HT</sup> anxiety levels in the 0 maze test .....	151
Figure C.15: cKO-VGLUT3 <sup>5-HT</sup> spontaneous activity .....	152
Figure C.16: cKO-VGLUT3 <sup>5-HT</sup> locomotor sensitization to AMPH 5 mg/kg.....	153
Figure C.17: cKO-VGLUT3 <sup>5-HT</sup> general stereotypies with AMPH 5 mg/kg .....	155
Figure C.18: cKO-VGLUT3 <sup>5-HT</sup> orofacial stereotypies with AMPH 5 mg/kg.....	157
Figure C.19: Immunoautoradiography for VGLUT3 in cKO-VGLUT3 <sup>ACH</sup> mice (n = 5-5).....	158
Figure C.20: cKO-VGLUT3 <sup>ACH</sup> mice weight.....	159
Figure C.21: cKO-VGLUT3 <sup>ACH</sup> circadian locomotor activity.....	160
Figure C.22: cKO-VGLUT3 <sup>ACH</sup> anxiety levels in the open field test.....	161
Figure C.23: cKO-VGLUT3 <sup>ACH</sup> anxiety levels in the 0 maze test.....	161
Figure C.24: cKO-VGLUT3 <sup>ACH</sup> spontaneous activity .....	162
Figure C.25: cKO-VGLUT3 <sup>ACH</sup> locomotor sensitization to AMPH 5 mg/kg.....	164
Figure C.26: cKO-VGLUT3 <sup>ACH</sup> general stereotypies with AMPH 5 mg/kg.....	166
Figure C.27: cKO-VGLUT3 <sup>ACH</sup> orofacial stereotypies with AMPH 5 mg/kg.....	167
Figure C.28: cKO-VGLUT3 <sup>ACH</sup> locomotor response to acute AMPH 5 mg/kg or COC 10 mg/kg .....	168
Figure C.29: VGLUT3 striatal expression in cholinergic interneurons and 5 - HT fibers.....	169
Figure C.30: Striatal evoked dopamine levels in mice lacking VGLUT3 or VACHT in CINs .....	172
Figure C.31: Immunoautoradiography for VGLUT3 in cKO-VGLUT3 <sup>GABA</sup> mice.....	174
Figure C.32: Determination of the virus and time post - injection for a VGLUT3 accumbal depletion.....	178

<i>Figure C.33: Immunofluorescence against VGLUT3 in the Acb after AAV injection.....</i>	<i>179</i>
<i>Figure C.34: Anatomical verification of VGLUT3 level in VGLUT3<sup>LoxP/LoxP</sup> AAV - injected mice .....</i>	<i>180</i>
<i>Figure C.35: Quantification of VGLUT3 in the VGLUT3<sup>LoxP/LoxP</sup> mice injected with AAVs .....</i>	<i>181</i>
<i>Figure C.36: VGLUT3<sup>LoxP/LoxP</sup> AAV - injected mice weight.....</i>	<i>182</i>
<i>Figure C.37: VGLUT3<sup>LoxP/LoxP</sup> AAV - injected circadian locomotor activity.....</i>	<i>183</i>
<i>Figure C.38: VGLUT3<sup>LoxP/LoxP</sup> AAV - injected anxiety levels in the open field test.....</i>	<i>184</i>
<i>Figure C.39: VGLUT3<sup>LoxP/LoxP</sup> AAV - injected anxiety levels in the O maze test.....</i>	<i>184</i>
<i>Figure C.40: VGLUT3<sup>LoxP/LoxP</sup> AAV - injected locomotor sensitization to cocaine.....</i>	<i>185</i>
<i>Figure C.41: Correlation between VGLUT3 accumbal level and cocaine - induced locomotion .....</i>	<i>186</i>

## **APPENDICES**

---

<i>Figure E.1: VGLUT3<sup>-/-</sup> horizontal locomotion in response to AMPH 1 mg/kg .....</i>	<i>ii</i>
<i>Figure E.2: VGLUT3<sup>-/-</sup> horizontal locomotion in response to AMPH 3 mg/kg .....</i>	<i>iii</i>
<i>Figure E.3: VGLUT3<sup>-/-</sup> horizontal locomotion in response to AMPH 5 mg/kg .....</i>	<i>iv</i>
<i>Figure E.4: cKO-VGLUT3<sup>5-HT</sup> horizontal locomotion in response to AMPH 5 mg/kg.....</i>	<i>v</i>
<i>Figure E.5: cKO-VGLUT3<sup>ACH</sup> horizontal locomotion in response to AMPH 5 mg/kg.....</i>	<i>vi</i>



# **List of tables**

## **INTRODUCTION**

---

<i>Table A.1: Excitatory amino acid transporters characteristics.....</i>	<i>13</i>
<i>Table A.2: Vesicular neurotransmitter transporters characteristics.....</i>	<i>18</i>
<i>Table A.3: VGLUT1 and VGLUT2 characteristics.....</i>	<i>26</i>
<i>Table A.4: VGLUT3 structural expression in mammalian brain.....</i>	<i>36</i>
<i>Table A.5: Insight of abusive drugs and their targets .....</i>	<i>74</i>
<i>Table A.6: Creese &amp; Iversen stereotypy rating scale.....</i>	<i>99</i>

## **MATERIALS AND METHODS**

---

<i>Table B.1: Primers for VGLUT3<sup>-/-</sup> PCR .....</i>	<i>107</i>
<i>Table B.2: Primers for VGLUT3<sup>LoxP/LoxP</sup> PCR.....</i>	<i>109</i>
<i>Table B.3: Primers for SERT - Cre PCR.....</i>	<i>111</i>
<i>Table B.4: Primers for universal Cre PCR.....</i>	<i>112</i>
<i>Table B.5: Primers for ChAT - Cre PCR.....</i>	<i>112</i>
<i>Table B.6: List of viruses used .....</i>	<i>113</i>
<i>Table B.7: Categorical scoring of stereotypies .....</i>	<i>118</i>
<i>Table B.8: Rating scale for general stereotypies .....</i>	<i>119</i>
<i>Table B.9: Rating scale for orofacial stereotypies.....</i>	<i>120</i>

## **RESULTS**

---

<i>Table C.1: CIN - related phenotypes.....</i>	<i>173</i>
<i>Table C.2: Percentage of VGLUT3 decrease after unilateral viral injection .....</i>	<i>178</i>



## Abbreviation list

<b>5- HT:</b> 5- hydroxytryptamine (serotonin)	<b>CaIDAG- GEF:</b> calcium- diacylglycerol- guanine- nucleotide exchange factor
<b>6- OHDA:</b> 6- hydroxydopamine	<b>CaMK:</b> calmodulin- kinase
<b>AAV:</b> adeno-associated virus	<b>cAMP:</b> cyclic adenosine monophosphate
<b>AC:</b> adenylyl cyclase	<b>CB1R:</b> cannabinoid receptor type 1
<b>ACPD:</b> 1- amino- 1,3- dicarboxycyclopentane	<b>cc:</b> corpus callosum
<b>Acb:</b> nucleus accumbens	<b>CCK:</b> cholecystokinin
<b>AcbC:</b> nucleus accumbens, core	<b>CDK:</b> cyclin- dependent kinase
<b>AcbSh:</b> nucleus accumbens, shell	<b>ChAT:</b> choline acetyltransferase
<b>ACh:</b> acetylcholine	<b>CIN:</b> cholinergic interneuron (see TAN)
<b>AChE:</b> acetylcholine esterase	<b>CIN-KO:</b> mice with CIN ablation
<b>AD:</b> adrenalin	<b>CMV:</b> cytomegalovirus
<b>ADP:</b> adenosine diphosphate	<b>CNS:</b> central nervous system
<b>AIM:</b> abnormal involuntary movement	<b>COC:</b> cocaine
<b>AMG:</b> amygdala	<b>CPP:</b> conditioned place preference
<b>AMPA:</b> $\alpha$ -amino-3-hydroxy-5-methyl-4-isoxazole propionic acid	<b>CPu:</b> caudate- putamen nuclei
<b>AMPAR:</b> $\alpha$ -amino-3-hydroxy-5-methyl-4-isoxazole propionic acid receptor	<b>CR:</b> calretinin
<b>AMPH:</b> D-amphetamine	<b>CTD:</b> C- terminal domain
<b>AP:</b> action potential	<b>Cx:</b> cerebral cortex
<b>AP1:</b> activator protein 1	$\Delta\mu_{H^+}$ : electrochemical gradient
<b>ARC:</b> activity- regulated cytoskeleton- associated protein	<b><math>\Delta\psi</math>:</b> electrical gradient
<b>Arg:</b> arginine	<b>DA:</b> dopamine
<b>ASD:</b> autism spectrum disorder	<b>DAG:</b> diacylglycerol
<b>Asp:</b> aspartate	<b>DARPP- 32:</b> DA- and cAMP-regulated phosphoprotein 32 kDa
<b>ATP:</b> adenosine triphosphate	<b>DAT:</b> dopamine transporter
<b>AUC:</b> area under curve	<b>DCQ:</b> dicarboxylic quinoline
<b>BAC:</b> bacterial artificial chromosome	<b>DG:</b> dentate gyrus
<b>BF:</b> basal forebrain	<b>DIS:</b> drug- induced stereotypies
<b>BG:</b> basal ganglia	<b>DLS:</b> dorsolateral striatum
<b>BLA:</b> basolateral amygdala	<b>DMS:</b> dorsomedial striatum
<b>BNPI:</b> brain-specific $Na^+$ -dependent inorganic phosphate transporter	<b>DNA:</b> deoxyribonucleic acid
<b>BST:</b> bed nucleus of the <i>stria terminalis</i>	<b>DNPI:</b> differentiation- associated $Na^+$ -dependent inorganic phosphate transporter
<b>BY:</b> Brilliant Yellow dye	<b>DOR:</b> $\delta$ opioid receptor
<b>BYA:</b> Brilliant Yellow analog	<b>DRN:</b> dorsal raphe nucleus
<b>CA1- 3:</b> field CA1- 3 of the hippocampus	<b>dStr:</b> dorsal striatum

**Dyn:** dynorphin

**E:** glutamate

**EAAC:** excitatory amino acid carrier

**EAAT:** excitatory amino acid transporter

**EB:** Evans Blue dye

**Enk:** enkephalin

**EPSC:** excitatory post- synaptic current

**ERK:** extracellular signal- related kinase

**FS:** fast- spiking

**GABA:**  $\gamma$ - aminobutyric acid

**GAD:** glutamate decarboxylase

**GAPDH:** glyceraldehyde- 3- phosphate dehydrogenase

**GDB:** goal- directed behavior

**GDP:** guanosine diphosphate

**GLAST:** glutamate aspartate transporter

**GlpT:** glycerol- 3- phosphate transporter

**GLT:** glutamate transporter

**Glu:** glutamate

**GPCR:** G- protein- coupled receptor

**GPe:** globus pallidus *externum*

**GPI:** globus pallidus *internum*

**GTP:** guanosine triphosphate

**Hb:** habenula

**Hc:** hippocampus

**His:** histidine

**hSyn:** human synapsin

**Hyp:** hypothalamus

**IAR:** immunoautoradiography

**IC<sub>50</sub>:** half maximal inhibitory concentration

**IEG:** immediate early gene

**IHC:** inner hair cell

**IF:** immunofluorescence

**iGluR:** ionotropic glutamate receptor

**IN:** interneuron

**i.p.:** intraperitoneal injection

**IP3:** inositol triphosphate

**IPSC:** inhibitory post- synaptic current

**ir:** immunoreactivity

**ISH:** *in situ* hybridization

**KA:** kainate

**KAR:** kainate receptor

**kb:** kilobase

**K<sub>i</sub>:** dissociation constant of inhibitor

**K<sub>m</sub>:** Michaelis constant

**KO:** homozygous knock- out

**KOR:**  $\kappa$  opioid receptor

**L- DOPA:** L-3,4-dihydroxyphenylalanine

**LHb:** lateral habenula

**LID:** L- DOPA- induced dyskinesia

**LTD:** long- term depression

**LTP:** long- term potentiation

**LTS:** low threshold spiking

**MA:** monoamine

**mAChR:** muscarinic acetylcholine receptor

**MAO:** monoamine oxidase

**MDMA:** 3,4- methylenedioxymethamphetamine

**METH:** methamphetamine

**mGluR:** metabotropic glutamate receptor

**MNK1:** mitogen-activated protein kinase interacting kinase-1

**MOR:**  $\mu$  opioid receptor

**MPP<sup>+</sup>:** 1- methyl- 4- phenylpyridinium

**MPTP:** 1- methyl- 4- phenyl- 1,2,3,6- tetrahydropyridine

**MRN:** median raphe nucleus

**mRNA:** messenger ribonucleic acid

**MSK:** mitogen and stress- activated protein kinase- 1

**MSN:** medium spiny neuron

**NA:** noradrenalin

**nAChR:** nicotinic ACh receptor

**NK-1:** neurokinin 1

**NMDA:** N- methyl- D- aspartate

**NMDAR:** N- methyl- D- aspartate receptor

**NO:** nitric oxide

**NOS:** nitric oxide synthase

**NPY:** neuropeptide Y

**nT:** neurotransmitter

**NTD:** N- terminal domain  
**OCD:** obsessive-compulsive disorder  
**OF:** open field  
**OFC:** orbitofrontal cortex  
**ON:** overnight  
**OT:** olfactory tubercle  
**PBS:** phosphate buffer saline  
**PFA:** paraformaldehyde  
**PFC:** prefrontal cortex  
**PKA:** protein kinase A  
**PKC:** protein kinase C  
**PLC:** phospholipase C  
**PP:** protein phosphatase  
**PPN:** pedunculopontine nucleus  
**PSD:** post- synaptic density  
**PSU:** polysubstance use  
**PV:** parvalbumin  
**Pyr:** pyramidal cell layer  
**RB:** Rose Bengal dye  
**RBA:** Rose Bengal analog  
**ROS:** reactive oxygen species  
**RT:** room temperature  
**rpS6:** ribosomal protein S6  
**RRP:** ready releasable pool  
**SERT:** serotonin transporter  
**SLC:** solute carrier  
**SN:** substantia nigra  
**SNc:** substantia nigra *pars compacta*  
**SNr:** substantia nigra *pars reticulata*  
**SP:** substance P  
**SS:** somatostatin  
**SSRI:** selective serotonin reuptake inhibitor  
**STN:** subthalamic nucleus  
**Str:** striatum  
**SV:** synaptic vesicle  
**TAN:** tonically activated neuron (see CIN)  
**TB:** Trypan Blue dye  
**TH:** tyrosine hydroxylase  
**Thal:** thalamus  
**Thr:** threonine  
**V- ATPase:** vacuolar ATPase  
**VACHT:** vesicular acetylcholine transporter  
**VEAT:** vesicular excitatory amino acid transporter  
**VGAT:** vesicular GABA transporter  
**VGLUT:** vesicular glutamate transporter  
**VIAAT:** vesicular inhibitory amino acid transporter  
**V<sub>max</sub>:** maximum rate of reaction  
**VMAT:** vesicular monoamine transporter  
**VNT:** vesicular neurotransmitter transporter  
**VNUT:** vesicular nucleotide transporter  
**vStr:** ventral striatum  
**VTA:** ventral tegmental area  
**WB:** western blot  
**WPRE:** Woodchuck hepatitis virus posttranscriptional regulatory element  
**WT:** wild- type



# INTRODUCTION

## PART I.

## GLUTAMATE: A FUNDAMENTAL NEUROTRANSMITTER

Glutamic acid (Glu, or E) is one of the twenty-one proteogenic  $\alpha$ - amino acid found in eukaryotes. Like all amino acids, it is a fundamental structural unit to build proteins. In humans, it can be classified as a non- essential amino acid, because it can be produced from the transformation of  $\alpha$ - ketoglutarate, a citric acid cycle intermediate.

Ritthausen initially discovered this amino acid by first digesting gluten with sulfuric acid (Ritthausen 1866), and subsequently named it glutamic acid; he later confirmed this result by digesting other vegetable proteins (Ritthausen 1869). But the first description of its constitution, structural and chemical properties came years later, in 1890, with Wolff's work (Wolff 1890): its formula was demonstrated to be **C<sub>5</sub>H<sub>9</sub>NO<sub>4</sub>** (Figure A.1a). This amino acid carries a carboxyl group on its side chain (Figure A.1b).

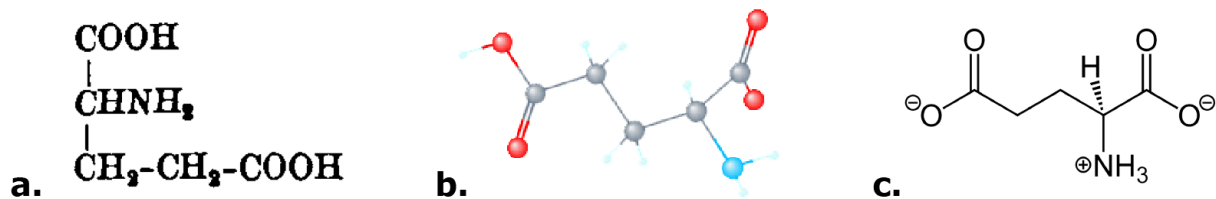


**Figure A.1: L-glutamic acid and L-glutamate structures**

**a.** L-glutamic acid structural formula (from Wolff 1890). **b.** L-glutamic acid molecular representation. **c.** L-glutamate structural formula.

At physiological pH, the side chain is deprotonated, which provides the amino acid the property of being negatively charged ( $pK_a=4.45$  for the  $\gamma$ - carboxyl group; Nagai *et al.* (2008)). This anionic form of glutamic acid is called glutamate (Figure A.1c). Thanks to its negative charge, glutamate is quite hydrophilic based on the hydropathy index (Kyte and Doolittle 1982). Like the other amino acids, the clear majority of glutamate in the body is the levogyre enantiomer, or L- glutamate. Therefore, unless specifically denoted by the appropriate prefix, all amino acids and other optically active substances mentioned are understood to be naturally occurring isomers, and the term glutamate will be referring to L- glutamate thereafter.

Glutamate is an essential amino acid for its metabolic role. In addition, it is also the most abundant excitatory neurotransmitter in the vertebrate nervous system (Erecinska and Silver 1990). Moreover, it is the precursor of  $\gamma$ -aminobutyric acid (GABA).

## **1. Generalities about neurotransmission**

The human brain contains about 86 billion neurons and virtually the same number of glial cells (Azevedo *et al.* 2009, Herculano-Houzel 2009). Against Golgi's reticular theory, which stated that brain is a continuum, Ramon y Cajal introduced at the end of the nineteenth century the notion that brain cells are unique elements that are arranged into networks to communicate together.

In the vertebrate central nervous system (CNS), neurons communicate with one another by a combination of electrical and chemical signals – the latter are called neurotransmitters. Neurons can be classified according to the neurotransmitter(s) they release. Nerve endings contain specialized organelles called synaptic vesicles (SVs) that are loaded with neurotransmitters. When the presynaptic terminal is depolarized, SVs fuse with the plasma membrane and release their content in the synaptic cleft. Neurotransmitters then bond to their specific receptors. The nature and localization of these receptors determine the recruitment of second messengers and is followed by intracellular signaling cascades. To end the signal, neurotransmitters are either reuptaken, degraded, or diffuse out of the synaptic cleft.

### **To be considered as a neurotransmitter, a chemical substance must**

- 1** Be present in the presynaptic terminal
- 2** Be released in a calcium- dependent manner
- 3** Act on specific targets
- 4** Be mimicked / inhibited by application of specific ago- / antagonists

Excitatory synapses are morphologically different from inhibitory synapses. In their presynaptic element, SVs are small and rounded. The post-synaptic element contains a zone that appears dense to electrons (Figure A.2). This area rich in proteins is called post- synaptic density (PSD). PSD is particularly prominent at excitatory synapses and for that reason asymmetrical synapse is a hallmark of excitatory neurons (Figure A.2).

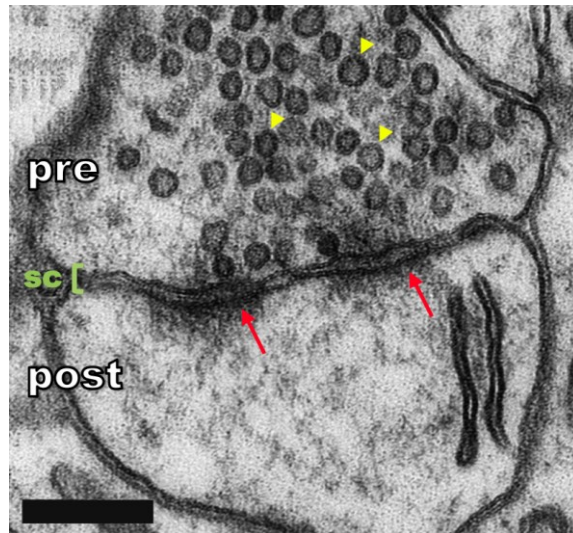


**Figure A.2: Electron micrograph of an excitatory synapse in the mouse neocortex**

The presynaptic element (pre) contains synaptic vesicles (yellow arrowheads) filled with glutamate. Glutamate is released into the synaptic cleft (sc). The postsynaptic element on this illustration (post) contains two PSDs (red arrows). Scale bar = 200  $\mu\text{m}$ .

Adapted from Korogod *et al.* (2015)

## **2. History of glutamate identification as a neurotransmitter**

It is well established since the fifties that glutamate is highly abundant and plays an important role in the CNS (Krebs 1935, Krebs *et al.* 1949, Schwerin *et al.* 1950). The first evidence that glutamate was involved in neurotransmission came in the early 1950s. First, glutamate was shown to be involved in the occurrence of seizures in patients suffering from *petit mal* epilepsy (Goodman *et al.* 1946, Wager 1946, Pond and Pond 1951). Later on, Hayashi revealed the ability of glutamate to trigger convulsions in humans, monkeys and dogs (Hayashi 1952, 1954). Interestingly this study also reported a toxic effect of high dose of glutamate. About the same time, glutamate was identified as the precursor for GABA (Roberts and Frankel 1950). Hayashi demonstrated that GABA antagonizes glutamate-induced seizures in dogs (Hayashi 1959). In 1954, Cole & Oikemus showed that intraperitoneal injection (i.p.) of glutamate in anaesthetized mouse has a stimulant effect (Cole and Oikemus 1954). In the late fifties, it was found that glutamate has the ability to depolarize and excite individual neurons in the spinal cord (Curtis *et al.* 1959, 1960). This established that glutamate is a potent major excitatory neurotransmitter in the CNS. Glutamate was then found to be enriched in synaptosomes and transported into synaptic vesicles (Kuhar and Snyder 1970, Disbrow *et al.* 1982).

At that time, data had accumulated showing that glutamate met the criteria required for a molecule to be considered as a neurotransmitter, as written by Fonnum (1984):

*"Glutamate satisfies today to a large extent the four main criteria for classification as a neurotransmitter: (1) it is pre-synaptically localized in specific neurons; (2) it is specifically released by physiological stimuli in concentrations high enough to elicit postsynaptic response; (3) it demonstrates identity of action with the naturally occurring transmitter, including response to antagonists; and (4) mechanisms exist that will terminate transmitter action rapidly."*

After suspicions about a potential role as neurotransmitter in the fifties, followed by twenty years of doubts, it was settled in the eighties that glutamate is definitely the main excitatory neurotransmitter in the CNS. Since, glutamate has remained one of the most studied transmitters in neuroscience (Figure A.3).

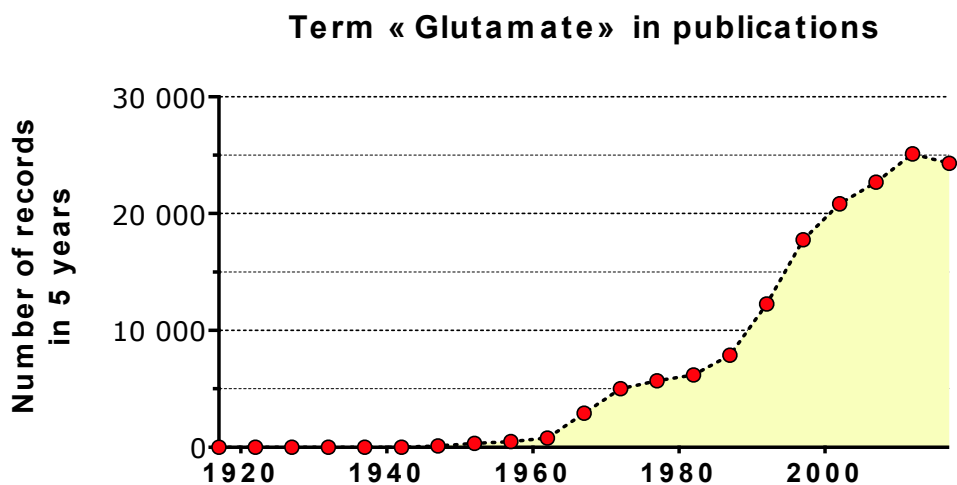


**Figure A.3: Term "glutamate" occurrence in the literature since 1912**

### **3. Glutamate receptors and related signaling**

In the brain, more than 70% of synapses are glutamatergic (as depicted in Figure A.4; Purves *et al.* (2012)). Once in the synaptic cleft, glutamate exerts its action by stimulating glutamate receptors. There are two kinds of glutamate receptors: ionotropic glutamate receptors (iGluRs) and metabotropic glutamate receptors (mGluRs).

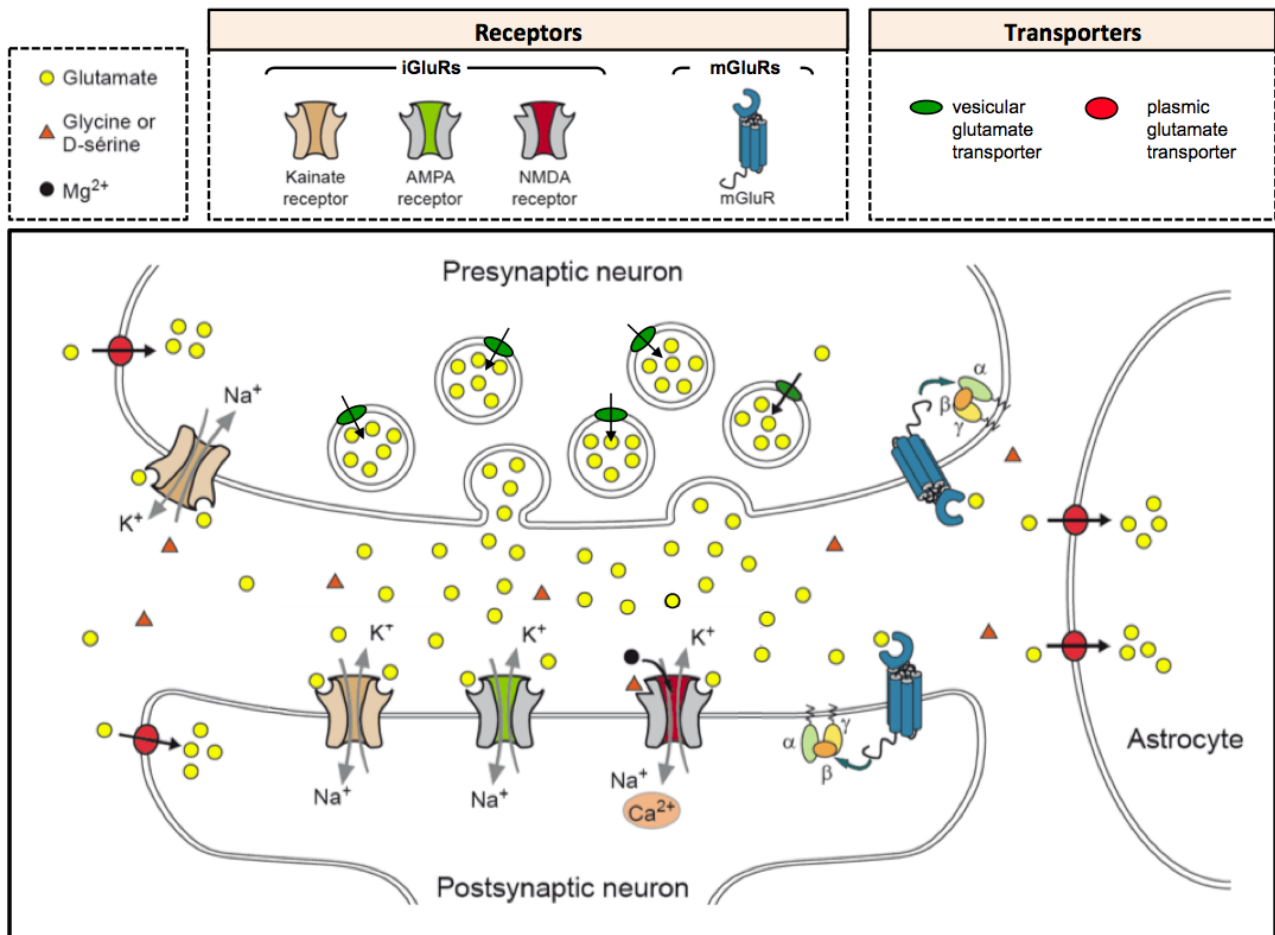


**Figure A.4: Schematic view of a glutamatergic synapse**

Glutamate is accumulated in SVs and released in the synaptic cleft. Glutamate then binds to post- and pre-synaptic receptors. Binding to iGluRs (NMDAR, AMPAR, KAR) induces ions movements. In contrast, mGluR activation triggers intracellular cascades mediated by G- proteins. To terminate the signal, glutamate is removed from the cleft by plasmalemmal transporters located on glia and neurons.

### 3.1 Ionotropic glutamate receptors

Ionotropic glutamate receptors are glutamate-gated ion channels permeable to cations (Na<sup>+</sup>, K<sup>+</sup>). Once activated, they mediate a fast transmission of signal, by inward or outward ion movements. In the mammalian brain, iGluRs are the most prevalent type of glutamate receptors, roughly expressed by 70% of the synapses (Purves *et al.* 2012).

Three main classes of iGluRs have been discovered, and named after their specific agonists: N- methyl- D- aspartate (**NMDA**),  $\alpha$ - amino- 3- hydroxy-5- methylisoxazole-4- propionic acid (**AMPA**) and kainate (**KA**). Recently, a fourth category of iGluR has been discovered, called  $\delta$  receptors. This subtype is quite atypical because it is not activated by glutamate (orphan receptor; Hepp *et al.* (2015)). Interestingly, more potent agonists for each receptor subtypes have been discovered, but NMDAR, AMPAR and KAR nomenclature has been retained (Lodge 2009).

All iGluRs are composed of 4 subunits, whose combination confers particular properties (affinity for ligands, ionic conductance, trafficking, intracellular interactions, desensitization). Their dysfunctions have been related to pathological states such as stroke, epilepsy, neuropathic pain or schizophrenia (Niciu *et al.* 2012).

Most excitatory central synapses coexpress AMPA and NMDA receptors. AMPA receptors mediate a fast excitation (Figure A.5a), whereas NMDA receptors generate a much slower and longer-lasting current besides fluxing  $\text{Ca}^{2+}$  (Figure A.5b). Thus, in response to specific patterns of presynaptic activity, the ratio between these two types of receptors at a synapse will influence the time course and summation of synaptic currents, and also the amount of  $\text{Ca}^{2+}$  entry (Watt *et al.* 2000). The magnitude of  $\text{Ca}^{2+}$  entry in the postsynaptic element largely determines whether long-term potentiation (LTP) or depression (LTD) of AMPARs occurs (Paoletti *et al.* 2013, Zhu *et al.* 2013).

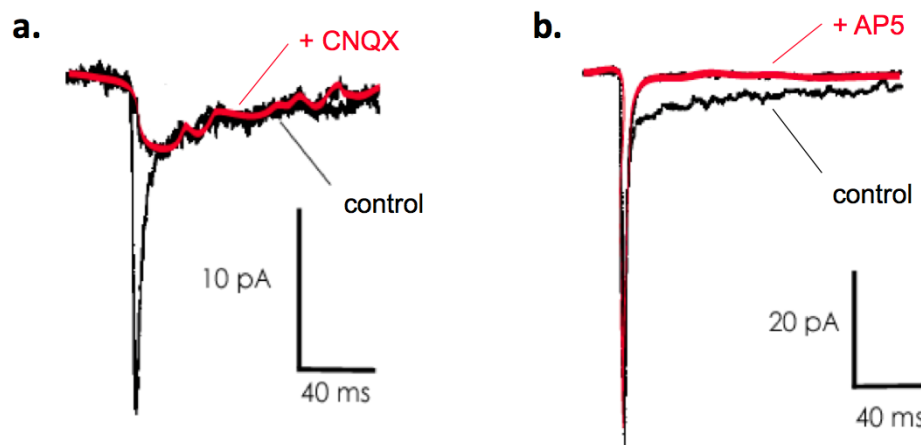


**Figure A.5: Glutamate excitatory post- synaptic current has two components**

**a.** Presynaptic stimulation leads to a strong and fast inward current that slowly decreases and is long-lasting in the postsynaptic neuron voltage-clamped at  $-70$  mV. When CNQX is added (selective AMPAR competitive antagonist), the fast-component is blocked. **b.** The addition of AP5 (selective NMDAR competitive antagonist), blocks the slow component of the EPSC.

Adapted from Watt *et al.* (2000)

NMDARs exhibit a voltage-dependent block by extracellular magnesium ( $\text{Mg}^{2+}$ ). This  $\text{Mg}^{2+}$ -block can be relieved by a prior cell depolarization, often mediated by AMPAR current (Nowak *et al.* 1984). Unlike NMDARs, AMPARs are impermeable to  $\text{Ca}^{2+}$  due to a constitutive glutamine/arginine editing of their GluA2 subunit (Gan *et al.* 2015). Thus, the presence of calcium-permeable GluA2-lacking receptors at the synaptic membrane will confer dramatic excitability properties to the postsynaptic element.

- iGluRs and synaptic plasticity

Synaptic plasticity is a mechanism that gives rise to a long-lasting and activity-dependent modification of synaptic strength ( $\uparrow$  in LTP,  $\downarrow$  in LTD). It is believed that LTP and LTD underlie many forms of learning and memory (Lamprecht and LeDoux 2004, Takeuchi *et al.* 2014). Dysregulation of synaptic plasticity probably contributes to a wide range of brain disorders (Irving and Harvey 2014, Nistico *et al.* 2014, Zhuo 2014).

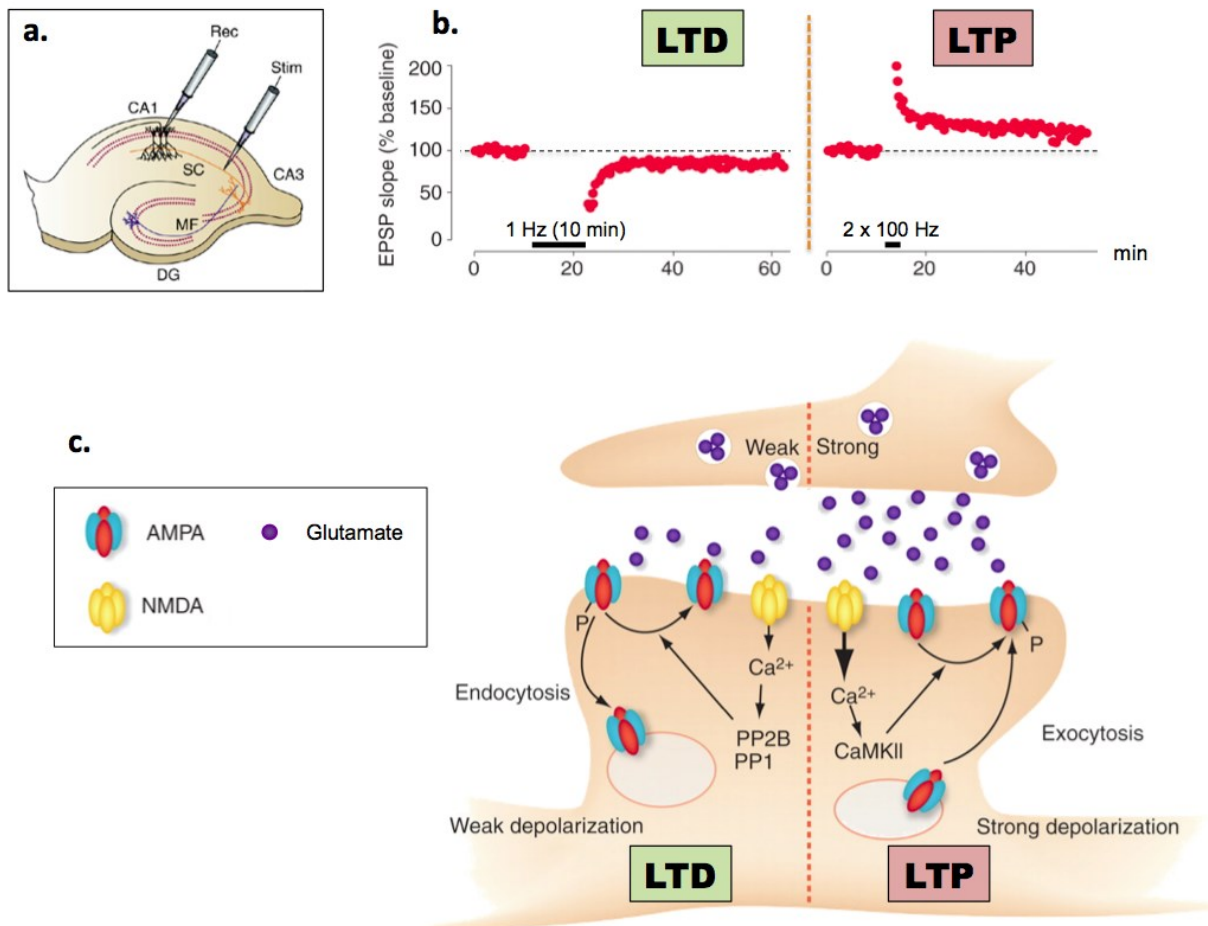


**Figure A.6: LTD / LTP in hippocampus, electrophysiological and structural features**

**a.** Schematic representation of a hippocampal slice of rodent brain, demonstrating the CA1, CA3 and dentate gyrus (DG), with typical electrodes placement for studying synaptic plasticity at CA3 neurons projection onto CA1. SC=Schaffer collateral; MF=mossy fiber; Stim=stimulating electrode; Rec=recording electrode. (From Citri and Malenka 2008) **b.** CA3- CA1 synapses monitored by extracellular field recordings in a hippocampal slice preparation. **Left panel:** Low-frequency stimulations elicit LTD. **Right panel:** High-frequency tetanic stimulations elicit LTP. (Adapted from Luscher and Malenka 2012) **c.** Postsynaptic expression mechanisms of LTP and LTD. **Left side:** A weak activity of the presynaptic neuron leads to a modest depolarization and calcium influx through NMDA receptors. This preferentially activates phosphatases that dephosphorylate AMPA receptors, thus promoting receptor endocytosis. **Right side:** A strong activity paired with a strong depolarization triggers LTP in part via CaMKII, receptor phosphorylation, and exocytosis. (Adapted from Luscher *et al.* 2012)

Both LTP and LTD are initiated the same way (Figure A.6). A presynaptic depolarization releases an amount of glutamate sufficient enough to activate NMDARs,

leading to a postsynaptic  $\text{Ca}^{2+}$  influx. A strong but brief increase of intracellular  $\text{Ca}^{2+}$  promotes LTP. In contrast, a low but sustained amount of  $\text{Ca}^{2+}$  induces LTD. In a general way, AMPARs are responsible for LTP/LTD induction (by postsynaptic depolarization) whereas NMDARs allow their expression (via  $\text{Ca}^{2+}$  entry). The elevation of calcium level drives the recruitment of several signaling pathways involving kinases or phosphatases contributing to LTP and LTD respectively. This includes: i) regulation of AMPAR trafficking to and from the post-synaptic membrane, ii) short-term post-translational modifications (phospho- or dephosphorylation) of pre-existing AMPARs, or iii) modification of subunit composition over a longer term (Lamprecht *et al.* 2004, Bassani *et al.* 2013, Park *et al.* 2014). Another feature of LTP is the modification of dendritic spines (Lamprecht *et al.* 2004). For instance, there can be spine head enlargement, or spine perforation leading to generation of new PSDs. Conversely, in LTD protocols, spine number is decreased (Luscher *et al.* 2012).

### 3.2 Metabotropic glutamate receptors

Metabotropic glutamate receptors are coupled to trimeric G-proteins (G-protein-coupled receptor, GPCR) and second messenger systems. They are seven-transmembrane-domain proteins, with a large extracellular N-terminal domain (NTD) that binds their ligand, and an intracellular C-terminal domain (CTD) that is linked to different G-proteins.

The mGluRs recruit and activate G-proteins and downstream signaling cascades, resulting in short-term effects (post-translational modifications of pre-existing proteins), and long-term effects (recruitment of transcription factors and gene activation); overall, their kinetics of activation is slower than iGluRs (Figure A.7). mGluRs are involved in synaptic plasticity through long-term modifications of receptors and synapses, neurotransmitter release and neuronal excitability tuning (Swanson *et al.* 2005).

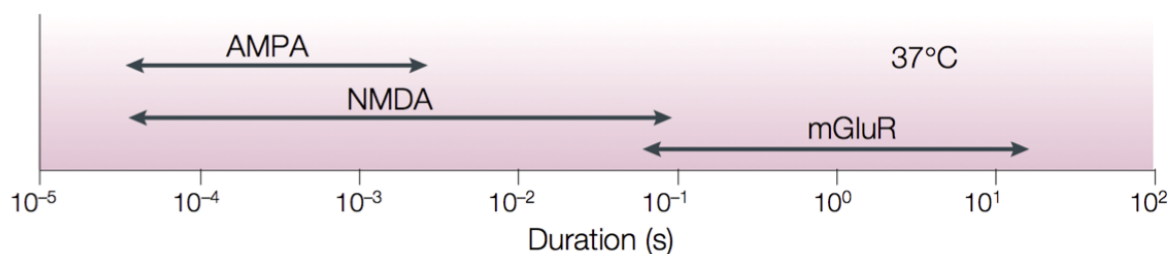


**Figure A.7: Duration range of iGluRs and mGluRs responses**

NMDARs and AMPARs exhibit a fast response to glutamate whereas mGluR kinetics is slower (time scale of hundreds of milliseconds to seconds) due to intracellular signaling cascades recruitment.

The mGluRs were identified in the mid-eighties, when it was demonstrated that L-glutamate could stimulate phosphatidylinositol hydrolysis and intracellular  $\text{Ca}^{2+}$

mobilization, effect not reversed by the then-known iGluRs antagonists. Since then, eight mGluRs have been discovered (mGluR1- 8), and are divided in three groups, based on their structure, pharmacology and signal transduction.

These receptors are located on both glutamatergic and non- glutamatergic neurons. They can be pre- or post- synaptic and also perisynaptic. Postsynaptic mGluRs modulate ion channel activity and therefore neuronal excitability. On the other hand, presynaptic mGluRs inhibit neurotransmitter release (Pineiro and Mulle 2008). Studies indicate that mGluRs have an important role in anxiety- related disorders, and group I antagonists / group II agonists are proposed as potential anxiolytics (Swanson *et al.* 2005). From a functional point of view, these receptors can be stabilized by an inter-subunit disulfide bridge (Rondard *et al.* 2011).

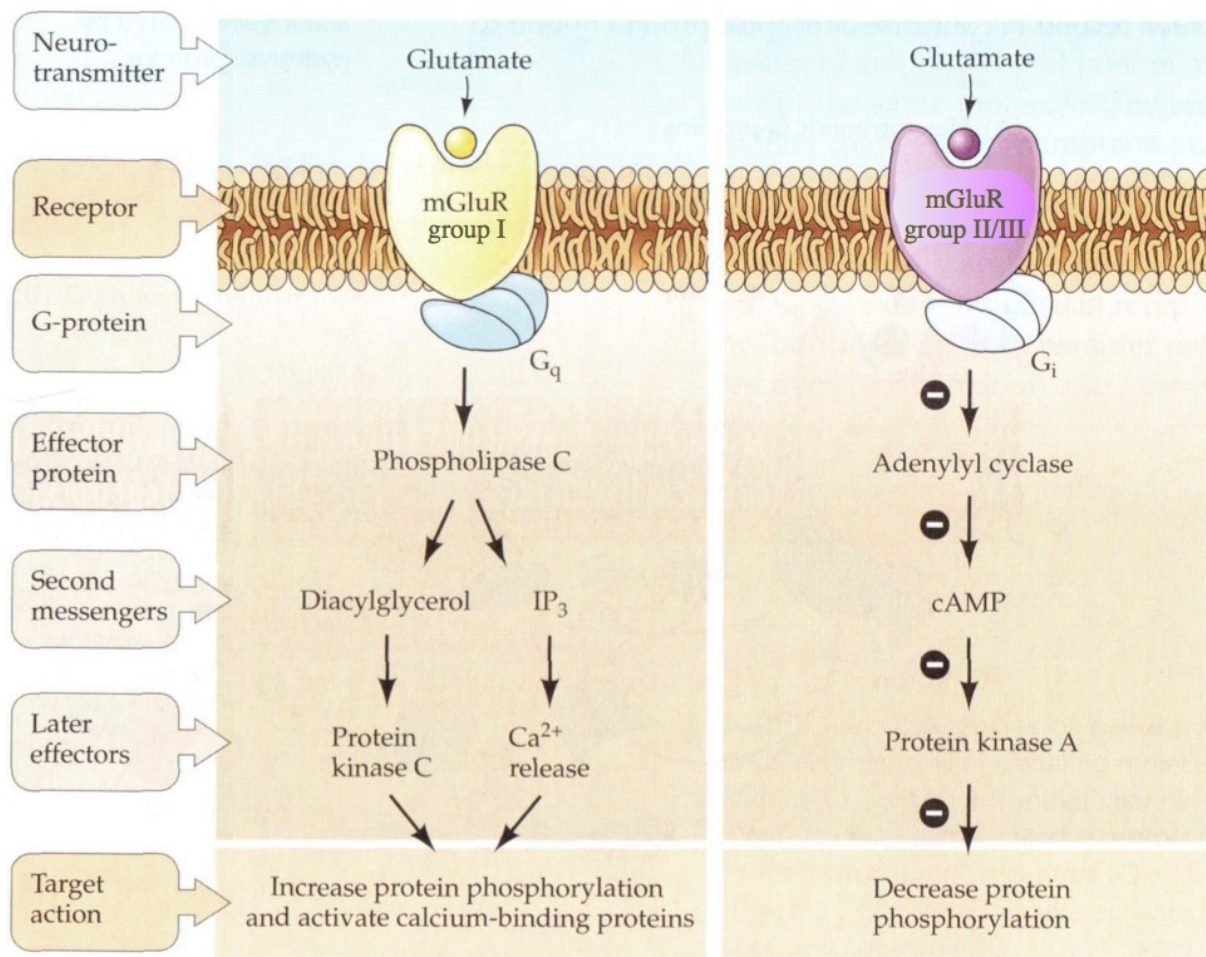


**Figure A.8: mGluRs coupling and intracellular cascades**

**Left panel:** Group I mGluRs are coupled to G<sub>q</sub>. Activation of G<sub>q</sub> leads to an overall increase of the intracellular calcium level and related signaling, including phosphorylation cascades via protein kinase C (PKC) or calmodulin- kinase (CaMK). **Right panel:** Group II/III mGluRs are coupled to G<sub>i/o</sub>. Activation of G<sub>i/o</sub> inhibits adenylyl cyclase, therefore decreasing the turnover of cAMP.

(Adapted from Neuroscience, fifth edition, 2012)

- Group I mGluRs

Group I mGluRs (mGluR1 and mGluR5) are coupled to the G- protein  $G_{\alpha_q}$ , which activates phospholipase C (PLC) and thereby also produces inositol triphosphate ( $IP_3$ ) and diacylglycerol (DAG).  $IP_3$  promotes the release of sequestered  $Ca^{2+}$  from intracellular stores. Therefore, group I is involved in the increase of  $Ca^{2+}$  signaling and in turn to protein kinase C (PKC) and calmodulin- kinase activation (Figure A.8, left panel). Group I mGluRs are predominantly localized on postsynaptic neurons, lateral to the PSD; but they can also be found presynaptically (Swanson *et al.* 2005). They are involved in synaptic plasticity associated with learning processes, and in synaptic pathways linked to the transmission of pain (Watkins 2000).

- Group II mGluRs

Group II mGluRs is constituted of mGluR2 and mGluR3. These receptors are negatively coupled to adenylyl cyclase (AC) via G- protein  $G_{\alpha_{i/o}}$ . AC inhibition causes a drop in cAMP levels, and subsequently a decrease in active protein kinase A (PKA) resulting in an overall diminution of phosphorylation cascades (Figure A.8, right panel). Group II presynaptic mGluRs are localized away from release sites in the preterminal portion of axons (Pinheiro *et al.* 2008).

- Group III mGluRs

Group III mGluRs consist of mGluR4, - 6, - 7 and - 8. As for group II, they are negatively coupled to AC (Figure A.8, right panel). Group III presynaptic mGluRs are mostly localized at the active zone of presynaptic terminals (Pinheiro *et al.* 2008). At many synapses, these inhibitory receptors segregate with facilitatory presynaptic iGluRs and act as a homeostatic switch that keeps synaptic transmission in a physiological range.

#### **4. Glutamate transporters**

Glutamate synaptic release is followed by an increase of extracellular glutamate concentration up to 1mM, during 1ms. After its release, glutamate is cleared from the synaptic cleft by transporters (Clark and Barbour 1997). When glutamate is not removed from the extra-neuronal space, there is an overstimulation of receptors (NMDARs in particular). This results in an excessive calcium influx inside the cytoplasm that will activate enzymes that in turn will injure the overexcited neuron. This phenomenon is called excitotoxicity, and can naturally occur when the neuron is oxygen- starved (case of hypoxia).

Thus, it is crucial that extracellular glutamate levels remain low at basal state, around 1 $\mu$ M (Figure A.9; Nicholls and Attwell (1990)).

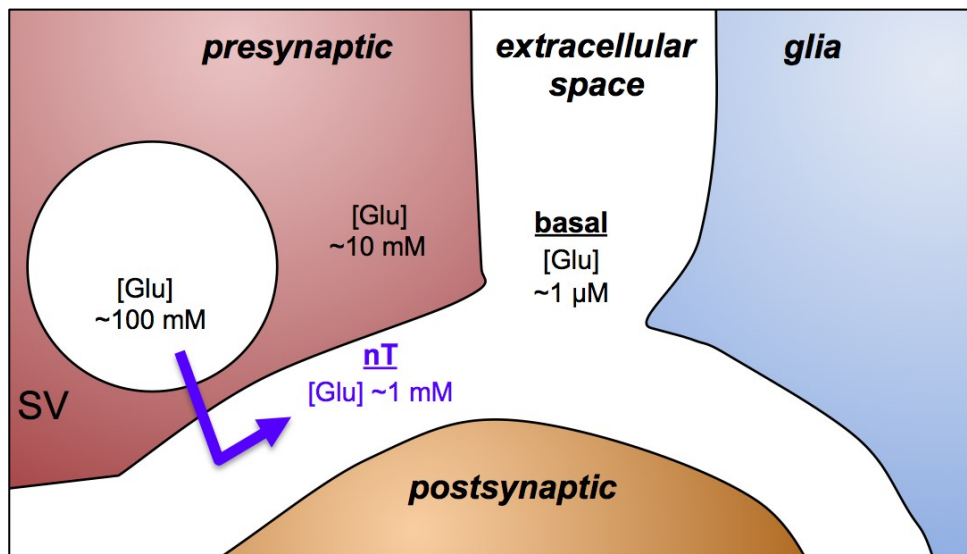


**Figure A.9: Glutamate concentration in the brain**

In the cell, cytoplasmic level of glutamate is around 10mM, while intravesicular level is ten times higher. At basal state, extracellular glutamate level is kept low, at around 1μM. Glutamate release during neurotransmission leads to a transient increase up to 1mM. Glu: glutamate; nT: neurotransmitter; SV: synaptic vesicle.

In the CNS, extracellular glutamate is eliminated by either passive diffusion or active reuptake. To date, there is no knowledge of extracellular enzymatic degradation for glutamate.

#### Passive diffusion:

This phenomenon, also called spillover, occurs *in vivo* (Figure A.10). Released glutamate diffuses out of the synapse and for example binds to presynaptic GluRs on adjacent GABAergic or glutamatergic terminals (Pinheiro *et al.* 2008). It has been modeled that glutamate release at one synapse has around 5% chance to elicit a response at the nearest neighboring synapse (Barbour 2001). However, this process is slow, and thus incompatible with rapid glutamatergic signaling.

#### Active reuptake:

Reuptake of glutamate into neurons and glial cells represents the prime mechanism by which the amino acid is removed from the synaptic cleft (Nicholls *et al.* 1990).

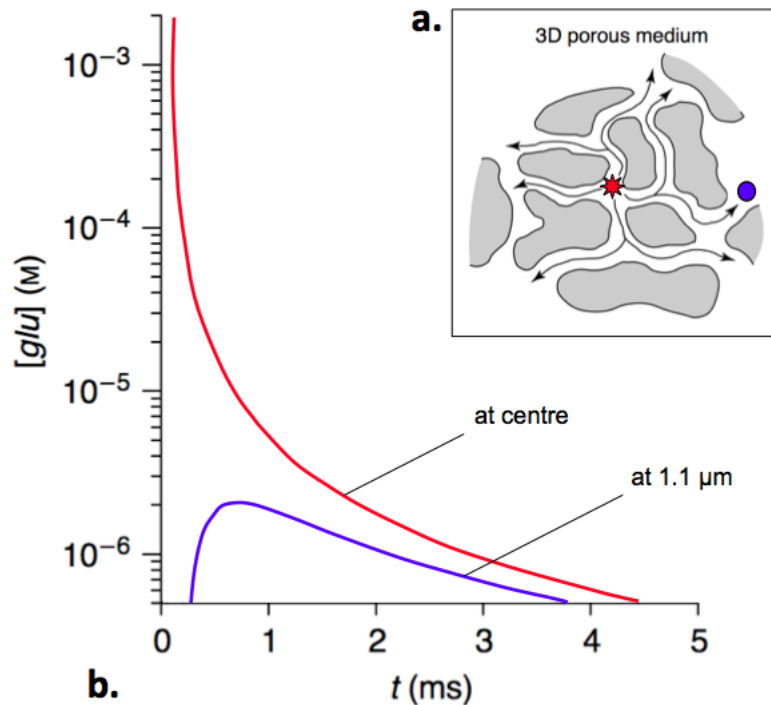


**Figure A.10: Modeling of glutamate diffusion in a three- dimensional structure**

**a.** Diagram of a porous medium containing obstacles to diffusion. The *red star* indicates the point of release and the *blue circle* the point of detection of neurotransmitter. **b.** Modeling for neurotransmitter diffusion in a porous medium by simple diffusion (without binding or uptake), for example in cortex of hippocampus. Curves represent concentration time- course at the point of release (*in red*) or at a distance of 1.1 μm (*in blue*), which corresponds to a neighboring synapse.

Adapted from Barbour and Hausser (1997)

#### 4.1 Plasma membrane glutamate transporters

- High- affinity  $\text{Na}^+/\text{K}^+$  glutamate transporters

Glutamate plasmalemmal transporters are high-affinity  $\text{Na}^+/\text{K}^+$  transporters belonging to solute carrier (SLC) family that were relatively conserved during evolution (Slotboom *et al.* 1999). Five glutamate plasmalemmal transporters have been identified in humans: EAAT1- 5 (excitatory amino acid transporter). They are selective for L- glutamate and D/L- aspartate. EAATs have a high micromolar affinity for their substrates. In the literature, these proteins can be found with other names according to the species studied (Table A.1; Niciu *et al.* (2012)).

EAATs are highly conserved ( $\approx$  50- 60% homology), especially within their CTD, and EAAT analogs from other species are very similar to their corresponding human form, with more than 90% homology (Figure A.11a; Danbolt (2001)). The five isoforms principally differ by their expression pattern. They are expressed by neurons and astrocytes (Table A.1). The most abundant glutamate transporters are EAAT2 (in glial cells) and EAAT3 (in neurons). Glutamate transporters concentrate intracellular glutamate up to 10'000- fold relatively to the extracellular space (Nicholls *et al.* 1990).

**Table A.1: Excitatory amino acid transporters characteristics**

Name	Gene	Expression	Localization	Cell type
<b>EAAT1</b> (GLAST1)	SLC1A3	<b>Astrocytes</b>	Neocortex Cerebellum	Retinal Muller cells Cerebellar Bergmann glia
<b>EAAT2</b> (GLT- 1)	SLC1A2		Forebrain	Ubiquitous
<b>EAAT3</b> (EAAC1)	SLC1A1	<b>Neurons</b>	CNS Peripheral tissues	Soma Dendrites GABAergic or Glu neurons
<b>EAAT4</b>	SLC1A6		Cerebellum	Purkinje cells
<b>EAAT5</b>	SLC1A7		Retina	Photoreceptors Bipolar cells

GLAST: glutamate/aspartate transporter (in rat); GLT: glutamate transporter (in rat); EAAC: excitatory amino acid carrier (in rabbit/rat).

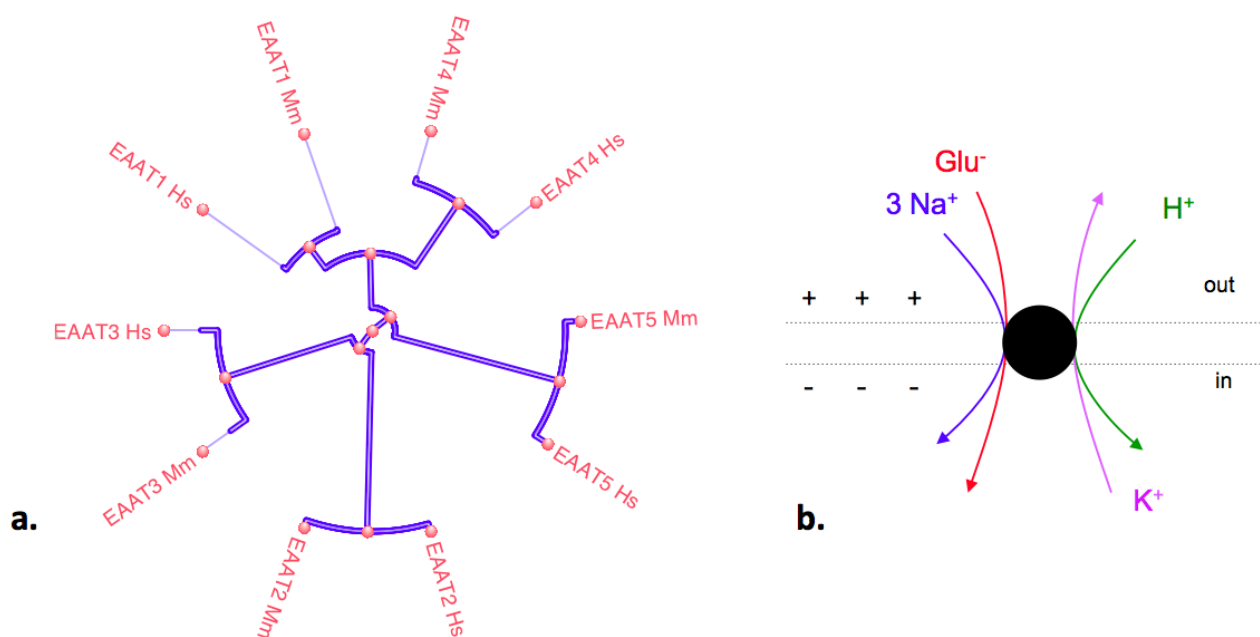


**Figure A.11: EAATs electrochemical and molecular properties**

**a.** Phylogenetic tree of EAATs based on protein alignment. Mm: *Mus musculus*; Hs: *Homo sapiens* (Source: sequences from NCBI, Newick file generated online on [www.phylogeny.fr](http://www.phylogeny.fr), tree generated with NCBI tree viewer tool). **b.** EAATs mediate the entry of three  $\text{Na}^+$  and one  $\text{H}^+$  in, and one  $\text{K}^+$  out of the cell to power glutamate uptake.

The mechanistic of glutamate transport is not trivial (Attwell 2000). Glutamate bears a net negative charge and is imported inside the cell, which is also negative compared to the extracellular environment. This transport against the electrochemical gradient requires energy. This energy derives from the cotransport of ions moving down their

electrochemical gradients. For each imported glutamate molecule, three Na<sup>+</sup> and one proton move in, while one K<sup>+</sup> is extruded (Figure A.11b). Therefore, this transport is electrogenic and uses Na<sup>+</sup> gradient as the driving force, with a net entry of two positive charges for each imported glutamate (Vandenberg *et al.* 2013). It has been estimated that the energy consumed by glutamate transporters in the cerebral cortex represents about 2% of total energy consumption of the tissue (Danbolt 2001).

EAATs have a very specific subcellular distribution, as depicted in Figure A.12 (Danbolt 2001).

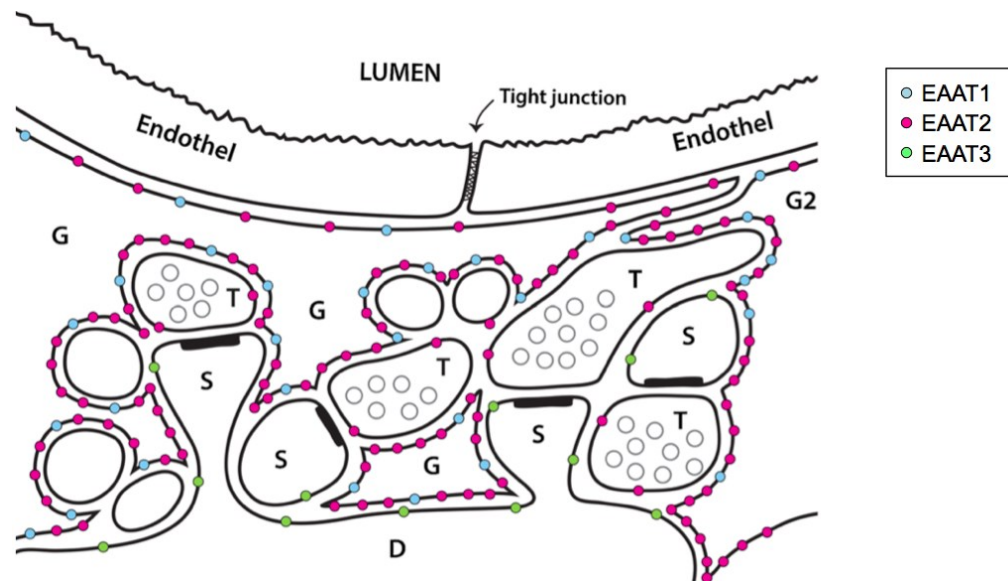


**Figure A.12: Subcellular distribution of EAATs in the hippocampus**

Glutamatergic nerve terminals (T) are shown forming synapses onto dendritic spines (S). Astrocyte branches are indicated (G). Astrocytes have very high densities of both EAAT1 (*blue dots*) and EAAT2 (*red dots*), with the highest densities found in membranes facing the neuropil, and low densities on membranes facing endothelium. EAAT1/2 are astrocytic, but EAAT2 can also be found in about 10% of hippocampal nerve terminals. EAAT3 (*green dots*) is selective for neurons, but is expressed at levels two orders of magnitude lower than EAAT2 and is targeted to dendrites and cell bodies.

From Zhou and Danbolt (2014)

- Astrocytic recapture of glutamate

Most of glutamate recapture is mediated by astrocytes. Indeed, astrocytes are glial cells that have many fine membrane processes, and are found in very close association with synapses. They are essential actors of synaptic activity, in that they can shape the spatio-temporal glutamate concentration profile by glutamate uptake, but also by releasing it as a “gliotransmitter”. As such, astrocytes are the third member of the tripartite synapse alongside with the presynaptic terminal and the postsynaptic process (Perea *et al.* 2009).

## 4.2 Vesicular neurotransmitter transporters

- General considerations

Glutamate identity switches from metabolic amino acid to neurotransmitter when neurons have the ability to accumulate it presynaptically. The neurotransmitter is stored in spherical SVs (40 nm diameter) by specific vesicular transporters. The neurotransmitter content of a single vesicle is the elementary unit, or quantum, of synaptic transmission (Katz 1979). Quantal size modification can be the consequence of postsynaptic adjustments, *i.e.* number of receptors at the membrane, or receptor sensitivity (single-channel conductance). It has been proposed that presynaptic changes such as alterations in vesicle filling or vesicle swelling can impact on the quantum size (Edwards 2007). However this hypothesis is still debated.

- Synaptic vesicle cycle

During the neurotransmission cycle, an incoming action potential (AP) activates voltage-gated calcium channels that mediate an important calcium influx from extracellular stores into the nerve ending. The transient rise in  $Ca^{2+}$  triggers the fusion of SVs with the plasma membrane and release of their chemical content into the synaptic cleft (Katz 1979, Attwell 2000, Sudhof 2004). In most terminals, only 10- 20% action potentials trigger release (Sudhof 2004). For non- neuropeptide transmitters such as glutamate, the streamline consists in repeated cycles of exo/endocytosis and transmitter refilling of the pre- existing pool of SVs present at nerve terminals (Gasnier 2000).

SVs form clusters at a specialized area of the membrane called the active zone and apposed to the postsynaptic structures (Figure A.2). Although morphologically indistinct, SVs are classically organized into three pools: the ready releasable pool (RRP), the recycling pool and the reserve pool (Figure A.13a,b). RRP defines the pool of vesicles that are first to undergo fusion during synaptic activity and are docked at the active zone. Their number is estimated around 5- 15 in hippocampal neurons, and they are thought to represent ~1- 2% of total SVs. The recycling pool is a pool of SVs than can be mobilized under appropriate stimulation and represents about 15% of total SVs. SVs from the reserve pool are not recruited by the AP. They represent the vast majority of SVs in the terminal (~85%). However, they occasionally spontaneously fuse with the plasma membrane (Figure A.13c; Fowler and Staras (2015)). SVs can be refilled with transmitters in the early steps of the recycling pathway. Therefore, a given nerve terminal has the ability to sustain nT release at high frequency with a limited number of vesicles (according to Gasnier, a few hundred per terminal (Gasnier 2000)).

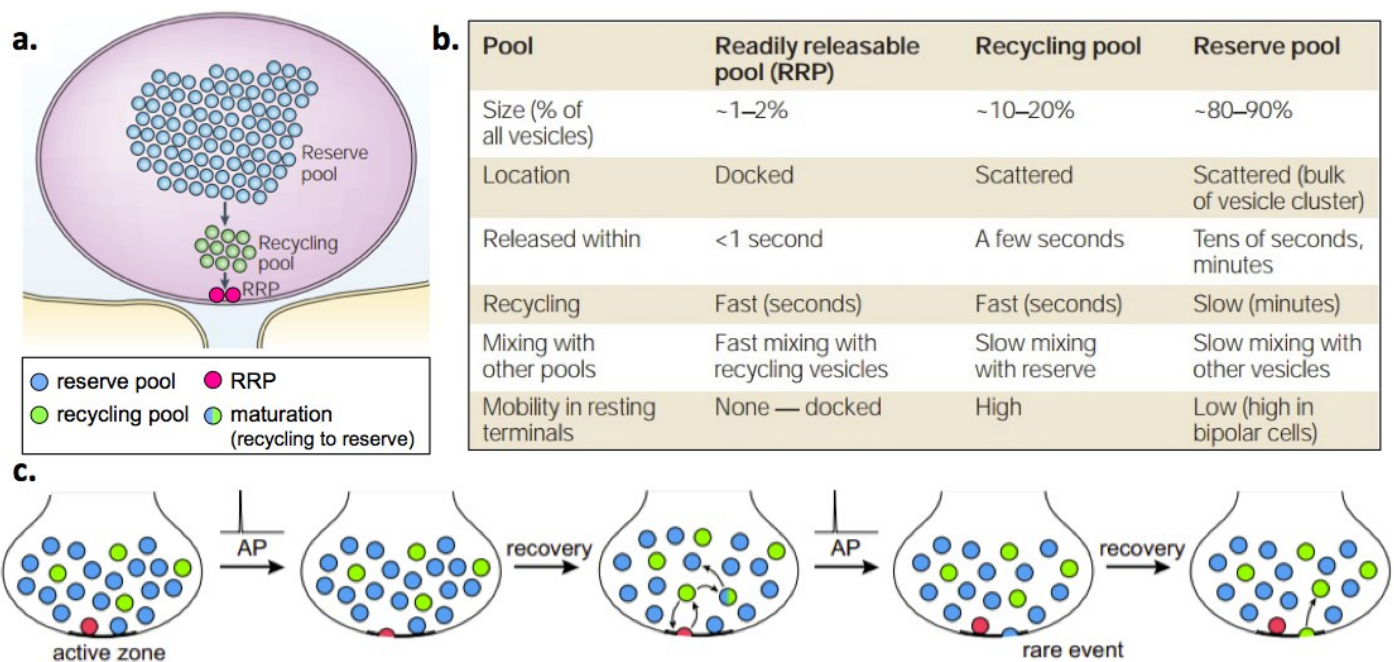


**Figure A.13: Synaptic vesicle properties**

**a.** Schematic view of SV proportions in the presynaptic terminal. There are three pools of SVs: the reserve pool (~80–90% of total pool, *blue dots*), the recycling pool (~10–20%, *green dots*) and the ready releasable pool (RRP; ~1–2%, *red dots*) that is docked and primed for release. **b.** Characteristics of the vesicle pools. **c.** Model for vesicle release under physiological stimulation. Upon arrival of an action potential (AP), some of the RRP vesicles docked at the active zone are released. However, the mild stimulation paradigm employed allows for a recovery phase, during which these vesicles are retrieved as recycling pool vesicles. They can then either transform into reserve pool vesicles (*green-blue gradient dots*) or maintain their recycling pool status. Repeated action potentials cause further release of vesicles docked at the active zone. Occasionally, a reserve pool vesicle docked at the active zone will also undergo fusion with the plasma membrane. Upon endocytosis, it will replenish the recycling pool. *Arrows* indicate vesicle trafficking.

From Rizzoli and Betz (2005), Denker and Rizzoli (2010)

Recently, this vision of SVs organization has been challenged by the idea of a labile pool of SVs that could move along the axon between different presynaptic terminals (Staras and Branco 2010, Herzog *et al.* 2011). This lateral mobility offers a new view of presynaptic organization, in which synapses can be functionally coupled via shared SVs population because the labile SVs can be mobilized at their new and spatially remote locus (Figure A.14).

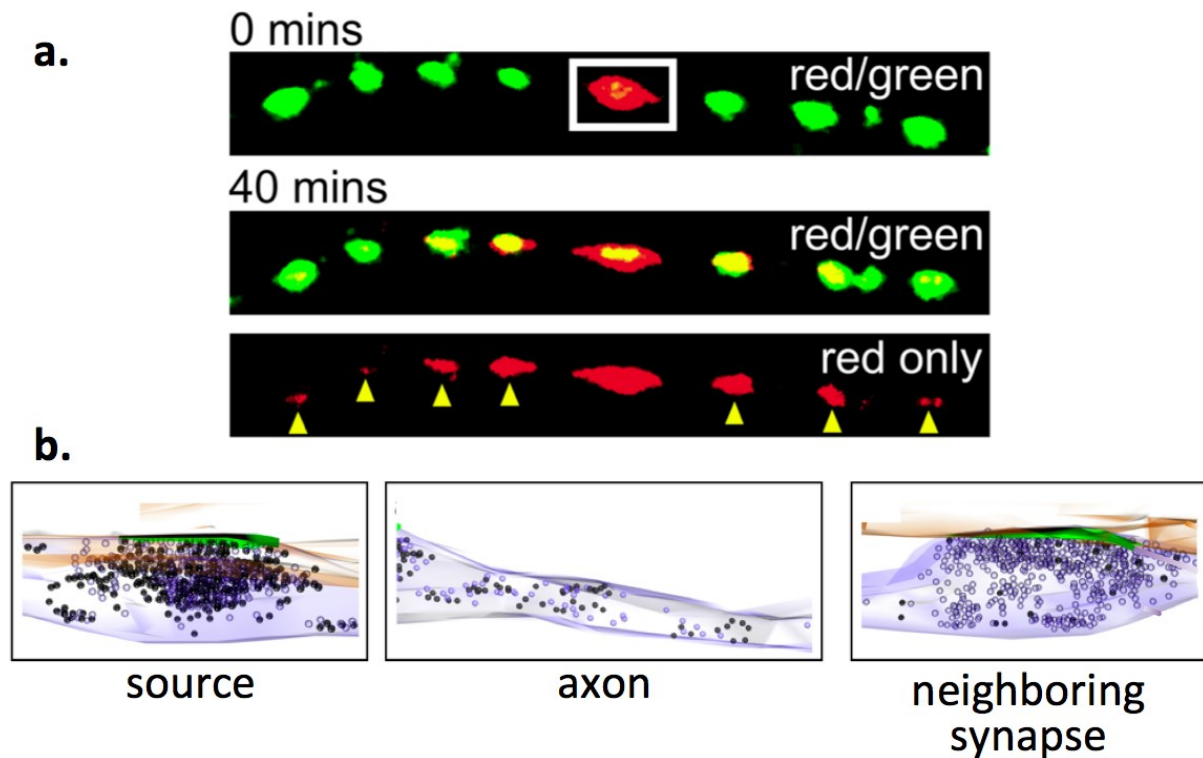


**Figure A.14: SVs lateral mobility along axon**

**a.** SV sharing across multiple synapses monitored using a photoswitchable vesicle marker, synaptophysinI-Dendra2 (SypI-Dendra2). **Top panel:** Red/green overlay showing a synapse along an axon being selectively photoswitched (*white rectangle*) from a green-emitting to a red-emitting form. **Middle panel:** The anterograde and retrograde spreads of red vesicles to neighboring green synapses are monitored over time for up to 40 min. **Bottom panel:** Same image showing red fluorescence only, detailing the contribution of vesicles made from a target synapse to neighbors (*yellow arrowheads*). **b.** Ultrastructural readout of functional vesicle sharing from a target to a neighboring synapse after 5 min of diffusion. *Orange element:* dendrite; *green element:* active zone; *black dots:* photoconverted SVs; *blue dots:* native SVs.

Adapted from Staras *et al.* (2010)

- Vesicular neurotransmitter transporters

Neurotransmitter uptake into SVs is mediated by specific vesicular transporters that belong to SLC family. So far, nine vesicular neurotransmitter transporters (VNTs) have been identified. They belong to three families: SLC17, SLC18 and SLC32 (Table A.2). Their classification is based on their substrate specificity and sequence homology. SLC17, -18 and -32 achieve vesicular uptake of anionic, cationic or electroneutral neurotransmitters (nTs) respectively (Chaudhry *et al.* 2008).

Members of the SLC17 family transport anionic molecules. This family includes three vesicular glutamate transporters (VGLUT1-3), the H<sup>+</sup>/sialic acid cotransporter (also named vesicular excitatory amino acid transporter, or VEAT), and four sodium-dependent phosphate transporters that are not present in the CNS (vesicular nucleotide transporters, or VNUT).

**Table A.2: Vesicular neurotransmitter transporters characteristics**

Transporter	Gene	Substrate	Localization	Driving force & Transport mode
<b>Sialin or VEAT</b>	SLC17A5	Sialic acid Asp	Lysosomes Pinealocytes Hippocampal neurons	$\Delta\psi$ Uniport
<b>VGLUT2</b>	SLC17A6	Glu	Glu neurons	
<b>VGLUT1</b>	SLC17A7		Astrocytes?	
<b>VGLUT3</b>	SLC17A8		Glu neurons + Ach, 5- HT, GABA neurons Astrocytes?	
<b>VNUT</b>	SLC17A9	ATP, ADP		
<b>VMAT1</b>	SLC18A1	5- HT, catecholamines, $\pm$ histamine	Endocrine cells	$\Delta\psi$ , $\Delta\text{pH}$ , $\text{H}^+$ Antiport
<b>VMAT2</b>	SLC18A2		Monoamine neurons	
<b>VACHT</b>	SLC18A3	ACh	ACh neurons	$\Delta\psi$ , $\Delta\text{pH}$ , $\text{H}^+$ Antiport
<b>VIAAT</b>	SLC32A1	GABA Gly	GABA and Gly neurons	$\Delta\psi$ , $\text{Cl}^-$ Cotransport

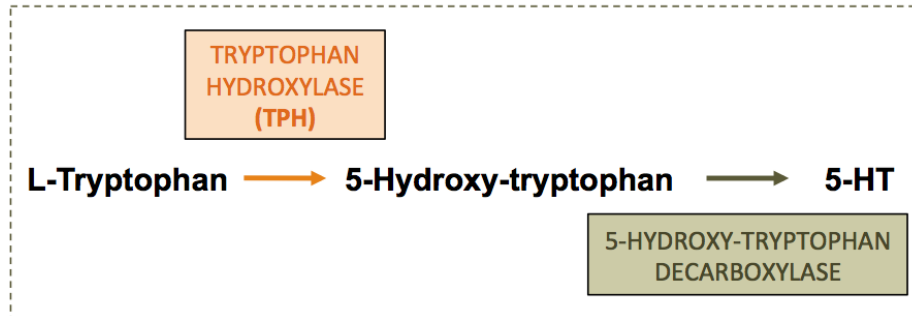
VEAT: vesicular excitatory amino acid transporter; VGLUT: vesicular glutamate transporter; VNUT: vesicular nucleotide transporter; VMAT: vesicular monoamine transporter; VACHT: vesicular acetylcholine transporter; VIAAT: vesicular inhibitory amino acid transporter.

Adapted from Omote *et al.* (2011)

Members of the SLC18 family perform vesicular uptake of cationic neurotransmitters, *i.e.*, acetylcholine (ACh) serotonin (5- HT), histamine, and catecholamines (Figure A.15) - dopamine (DA), adrenalin (AD), noradrenalin (NA). This family is composed of the vesicular acetylcholine transporter (VACHT) and of two vesicular monoamine transporters (VMAT1- 2). VMAT2 is the isoform that is used by monoaminergic neurons in the CNS.

The only member of SLC32 family is the vesicular inhibitory amino acid transporter (VIAAT, or VGAT, for vesicular GABA transporter) that is selective for two electroneutral amino acids, *i.e.*, GABA and glycine (Dumoulin *et al.* 1999).

## SEROTONIN



## CATHECHOLAMINES

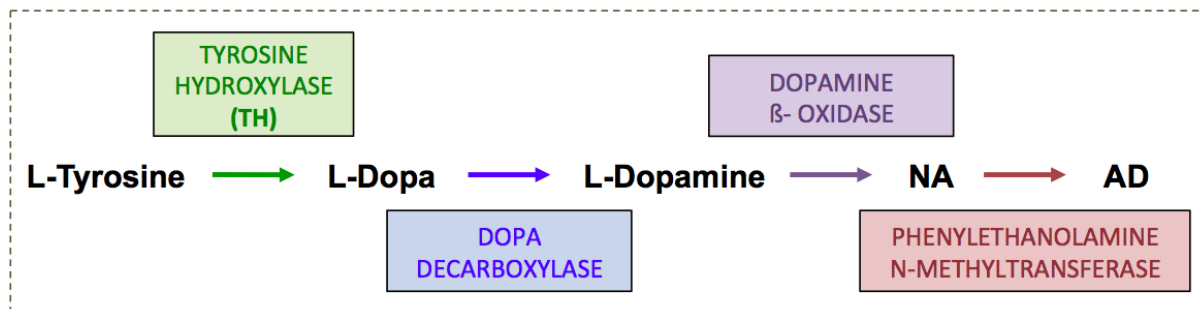


**Figure A.15: Serotonin and catecholamines biosynthesis pathways**

- Mechanistic of vesicular transport

All VNTs achieve an uptake against the nT electrochemical gradient. Therefore, this transport requires an energetic fuel. In the early nineties, it was established that nT transport is a secondary active transport, driven by an electrochemical proton gradient (Maycox *et al.* 1990). The ATPase responsible for generating the energy gradient was identified in 1987 (Nelson 1987). All synaptic vesicles carry a copy of the vacuolar H<sup>+</sup>-ATPase (Takamori *et al.* 2006). This primary transporter belongs to the vacuolar class of proton pumps. V-ATPases use the energy released by ATP hydrolysis to direct a flow of H<sup>+</sup> into SVs. The influx of H<sup>+</sup> generates an overall **electrochemical proton gradient ( $\Delta\mu_{H^+}$ )** through the SV membrane, which can be decomposed into:

- a **chemical component ( $\Delta pH$ )** because the intra-vesicular compartment is acidified;
- an **electrical component ( $\Delta\psi$ )** because the accumulation of positive charges inside the SV generates a membrane potential. (Ozkan and Ueda 1998)

VNTs then use this proton gradient to exchange luminal protons for cytoplasmic transmitters. However, all VNTs do not display the same dependence on the two components of the electrochemical proton gradient (Figure A.16). Indeed, the transport of monoamines and acetylcholine primarily depends on the chemical component ( $\Delta pH$ ), whereas the transport of glutamate depends predominantly on the electrical component ( $\Delta\psi$ ). Accumulation of the inhibitory transmitters GABA and glycine relies on both  $\Delta pH$

and  $\Delta\psi$ . Regarding transport stoichiometry, the species that move across SV membrane depend on the imported neurotransmitter (mainly its charge).

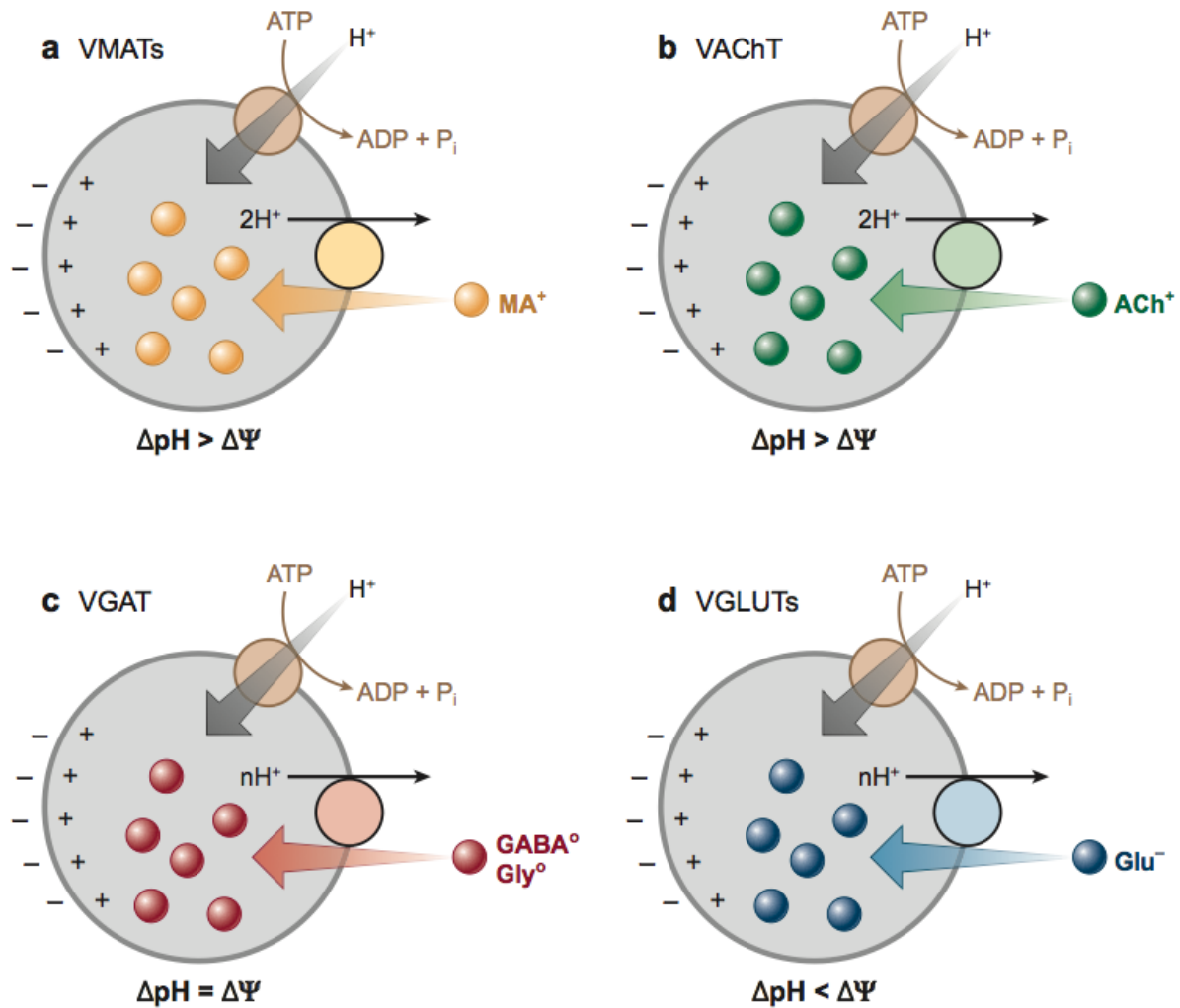


**Figure A.16: VNTs electrochemical dependence**

A V-ATPase generates an electrochemical gradient ( $\Delta\mu_{H^+}$ ) across the vesicle membrane. VNTs use this gradient to drive the transport of transmitters into SVs by coupling the transmitter translocation to H<sup>+</sup> running down  $\Delta\mu_{H^+}$ . The different vesicular transporters rely to different extents on the two components ( $\Delta pH$  and  $\Delta\psi$ ) of this gradient. **a.** VMATs and **b.** VACHT transport their positively charged substrates coupled to the exchange of two H<sup>+</sup>, and hence rely primarily on  $\Delta pH$ . **c.** GABA and glycine are transported as neutral zwitterions by VIAAT (VGAT), which depends equally on the chemical and the electrical component of  $\Delta\mu_{H^+}$ . **d.** VGLUTs transport the negatively charged glutamate and thus rely more on  $\Delta\psi$  than  $\Delta pH$ .

From Chaudhry *et al.* (2008)

Vesicular glutamate transporters (VGLUTs), in particular the third isoform called VGLUT3, will be discussed in the following section, as it is the main focus of the present work.

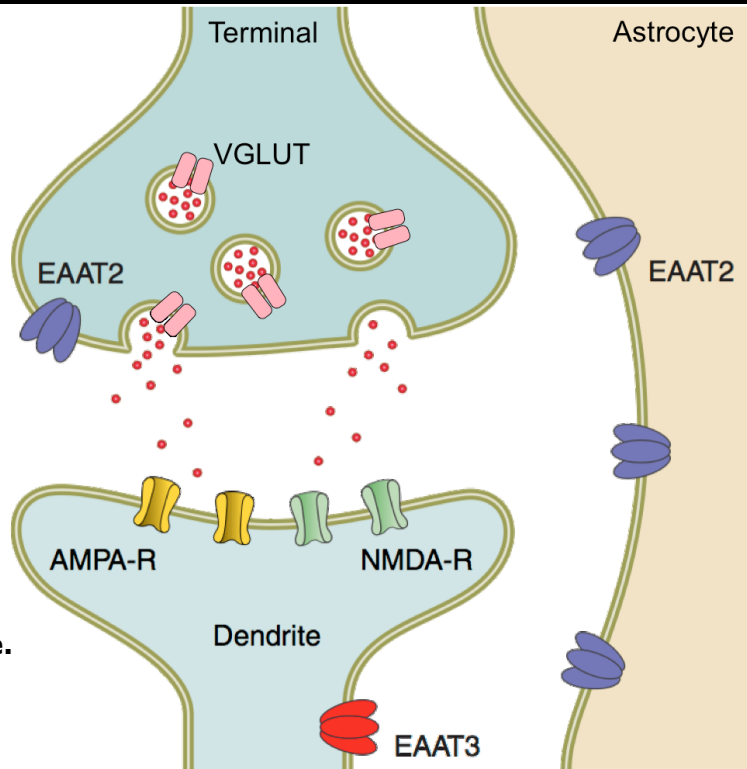
**Glutamate is the major excitatory neurotransmitter in the CNS.**

**It is accumulated into synaptic vesicles by VGLUTs.**

**Once released, it acts on its pre- and postsynaptic receptors (AMPA-R, NMDAR and mGluR).**

**Then, it is captured by EAAT to start a new cycle.**

Adapted from Vandenberg and Ryan (2013)





## PART II.

# VESICULAR GLUTAMATE TRANSPORTER TYPE 3 (VGLUT3)

## 1. Vesicular glutamate transporters

Glutamate is accumulated into SVs. The intravesicular concentration of glutamate varies between 100 and 400 mM, which is 10 to 100 times higher than the cytosolic concentration (Figure A.17); therefore there is a massive glutamate gradient ( $>10^6$ ) between intravesicular and extracellular glutamate (Disbrow *et al.* 1982, Burger *et al.* 1989, Erecinska *et al.* 1990, Danbolt 2001, Otis 2001).

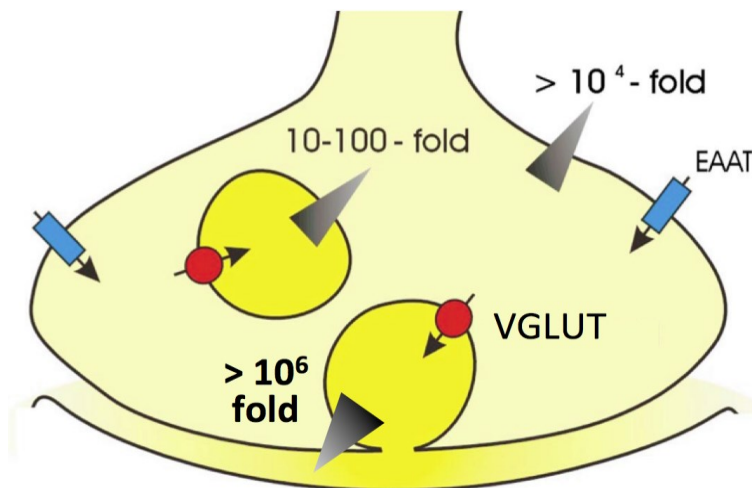


**Figure A.17: Glutamate gradients at excitatory presynaptic terminals**

Plasmalemmal EAATs (*in blue*) accumulate glutamate in the cell with a  $10^4$  gradient. Vesicular VGLUTs (*in red*) accumulate glutamate in the SV, up to 100-fold. The resulting gradient between intravesicular and extracellular glutamate is about  $10^6$ . Gradients are depicted by *shaded black triangles*.

Adapted from Otis (2001)

VGLUTs are present throughout the vertebrate class, with minor changes regarding their transport function (Tabb and Ueda 1991). Recent studies indicate that 80% of all synaptic vesicles contain VGLUT1 and - 2 (Takamori *et al.* 2006). Three VGLUTs have been discovered in vertebrates: VGLUT1, VGLUT2 and VGLUT3, encoded by SLC17A7, - A6 and - A8 respectively (Table A.2).

### 1.1 A history of VGLUTs

Vesicular glutamate transport features were identified prior to their isoforms discovery. Thanks to pure synaptic vesicles (synapsin I- positive), it was demonstrated

that glutamate is stored into SVs (Burger *et al.* 1989). Glutamate synaptic accumulation is adenosine triphosphate (ATP)-dependent and Na<sup>+</sup>-independent. Unlike EAATs that carry either L- Glu or L- Asp with a high affinity ( $K_m \sim \mu\text{M}$  range), VGLUTs are only selective for L- Glu (and D- Glu to some extent) with a low affinity (in the mM range). The transport demonstrates biphasic dependence to chloride. The optimal Cl<sup>-</sup> concentration is between 4 and 10 mM (Maycox *et al.* 1990, Nicholls *et al.* 1990, Bellocchio 2000). The transport requires a proton electrochemical gradient, and mainly relies on its chemical component (Herzog *et al.* 2001).

The first member discovered was named BNPI, for brain- specific sodium- dependent inorganic phosphate transporter. In 1994, this protein was initially characterized as a phosphate transporter at the plasma membrane, where it imports inorganic phosphate inside the cytoplasm in an Na<sup>+</sup>-dependent manner (Ni *et al.* 1994). It was only in 2000 that a predominant vesicular transport function for glutamate was inferred (Bellocchio 2000, Takamori *et al.* 2000). BNPI was renamed VGLUT1. It was found that the expression of VGLUT1 is sufficient to induce a glutamatergic phenotype in inhibitory GABAergic neurons (Takamori *et al.* 2000). However, VGLUT1 would was not present in all glutamatergic synapses in the brain (Bellocchio *et al.* 1998, Otis 2001). Therefore it was surmised there might be additional members of VGLUTs family.

Shortly after, different teams identified a second member of the VGLUT family. First called DNPI, for differentiation-associated sodium- dependent inorganic phosphate transporter, this transporter was renamed VGLUT2. It shared many structural and functional properties with VGLUT1 (Aihara *et al.* 2000, Fremeau *et al.* 2001, Fujiyama *et al.* 2001, Hayashi *et al.* 2001, Herzog *et al.* 2001).

A year later an additional member of VGLUT family was discovered and named VGLUT3 (Fremeau *et al.* 2002, Gras *et al.* 2002, Schafer *et al.* 2002, Takamori *et al.* 2002).

All three VGLUTs confer an excitatory phenotype to GABAergic neurons when exogenously expressed. This has been long known for VGLUT1 and - 2 (Takamori *et al.* 2000, 2001), and was also demonstrated recently for VGLUT3 (Figure A.18; Zimmermann *et al.* (2015)).

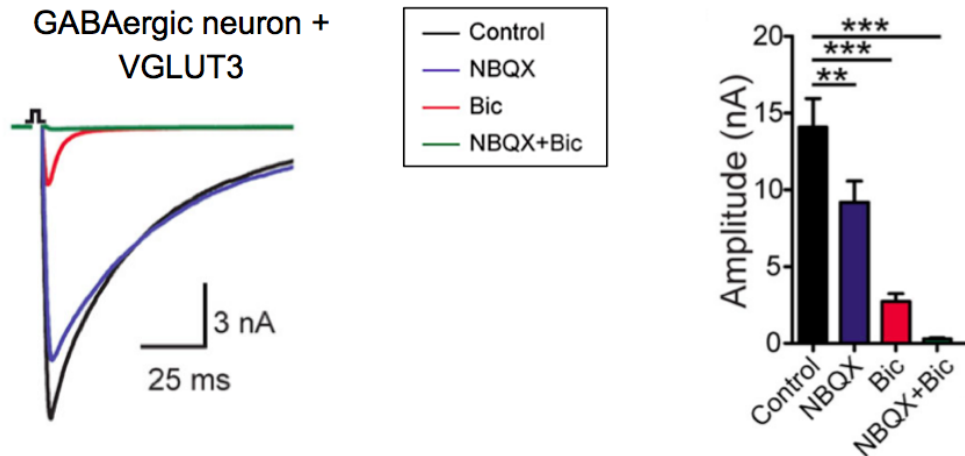


**Figure A.18: VGLUT3 expression promotes glutamate release by GABAergic neurons**

Striatal GABAergic neurons expressing VGLUT3 release GABA. GABA effect is blocked by adding the GABA<sub>A</sub>R antagonist bicuculline (*in red*) in the extracellular medium. The remaining current is attributed to glutamate and is blocked by the application of AMPAR antagonist CNQX (*in blue*).

Adapted from Zimmermann *et al.* (2015)

## 1.2 VGLUTs cellular and subcellular distributions

- VGLUT1 and VGLUT2 distributions

The mRNA coding for VGLUT1 and VGLUT2 and the two proteins have complementary patterns of expression (Aihara *et al.* 2000, Fujiyama *et al.* 2001, Herzog *et al.* 2001, Boulland *et al.* 2004). VGLUT1 and VGLUT2 define two distinct classes of excitatory synapses in the CNS and can be used as *bona fide* markers for glutamatergic neurons (Fremeau *et al.* 2001, Kaneko and Fujiyama 2002). In a nutshell, VGLUT1 is expressed in cortical regions (*i.e.* cerebral and cerebellar cortices, hippocampus), whereas VGLUT2 is found in subcortical areas of the brain (*i.e.* diencephalon & brainstem). This pattern is highly conserved between rodents and human (Vigneault *et al.* 2015). For a more detailed expression pattern see Table A.3.

A slight note of caution needs to be put forward: in the brain, there is a coexpression of VGLUT1 and -2 to some extent. Mixed VGLUT1/VGLUT2 mRNA-expressing neurons were identified in the lateral olfactory tract and some thalamic nuclei, but proteins do not colocalize (Herzog *et al.* 2001). VGLUT1 and -2 can also be transiently co-expressed during development, as explained later (1.5: VGLUTs during development).

**Table A.3: VGLUT1 and VGLUT2 characteristics**

<b>Protein</b>	<b>VGLUT1</b>	<b>VGLUT2</b>
<b>Gene</b>	SLC17A7	SLC17A6
<b>Human locus</b>	19q13	11p14.3
<b>Distribution</b>	<p><b>Esophagus</b> (motor nerve terminal)</p> <p><b>Muscle</b> (afferent endings)</p> <p><b>Bone</b> (osteoclasts)</p> <p><b>Pineal gland</b></p> <p><b>Pancreas</b> (α cells)</p> <p><b>Brain</b></p> <p>Cx (II / III - VI)</p> <p>Hc (pyramidal layer)</p> <p>DG (granular layer)</p> <p>Olfactory bulb</p> <p>Striatum (exclusive)</p>	<p><b>Lungs</b> (sensory nerve terminal)</p> <p><b>Intestine</b> (L cells)</p> <p><b>Pineal gland</b></p> <p><b>Pancreas</b> (α cells)</p> <p><b>Stomach</b></p> <p><b>Brain</b></p> <p>Cx (IV)</p> <p>Thalamus</p> <p>Habenula (medial / lateral)</p> <p>Hypothalamus</p> <p>Cerebellum</p> <p>Striatum (exclusive)</p>
<b>Subcellular localization</b>	Axon terminal	
<b>K<sub>m</sub> for L- Glu</b>	~ 4 mM	~ 2 mM
<b>V<sub>max</sub></b>	~ 500 pmol.min <sup>-1</sup> .mg <sup>-1</sup> prot	
<b>IC<sub>50</sub> for Evans Blue dye</b>	~ 300 nM	

- [VGLUT3 distribution](#)

VGLUT3 expression is quite unusual compared to the large and complementary patterns of VGLUT1 and -2 expression. VGLUT3 distribution will be further discussed in the next section (PART II.2.1: Anatomical distribution).

### 1.3 VGLUTs structure

The three isoforms, which are largely conserved in mammals, share a high homology of sequence (Fremeau *et al.* 2002, Gras *et al.* 2002, Takamori *et al.* 2002). For example, human VGLUT3 shares more than 72% with VGLUT1 and VGLUT2 (Figure A.19). Most of the differences between the three proteins are observed in their N- and C- termini (Gras *et al.* 2002, Schafer *et al.* 2002, Almqvist *et al.* 2007). Therefore, their biochemical functional properties do not differ much. The most divergent region is the CTD, with only

2% homology between the three isoforms (Almqvist *et al.* 2007). Their molecular weight is around 55- 60 kDa (Gras *et al.* 2005).

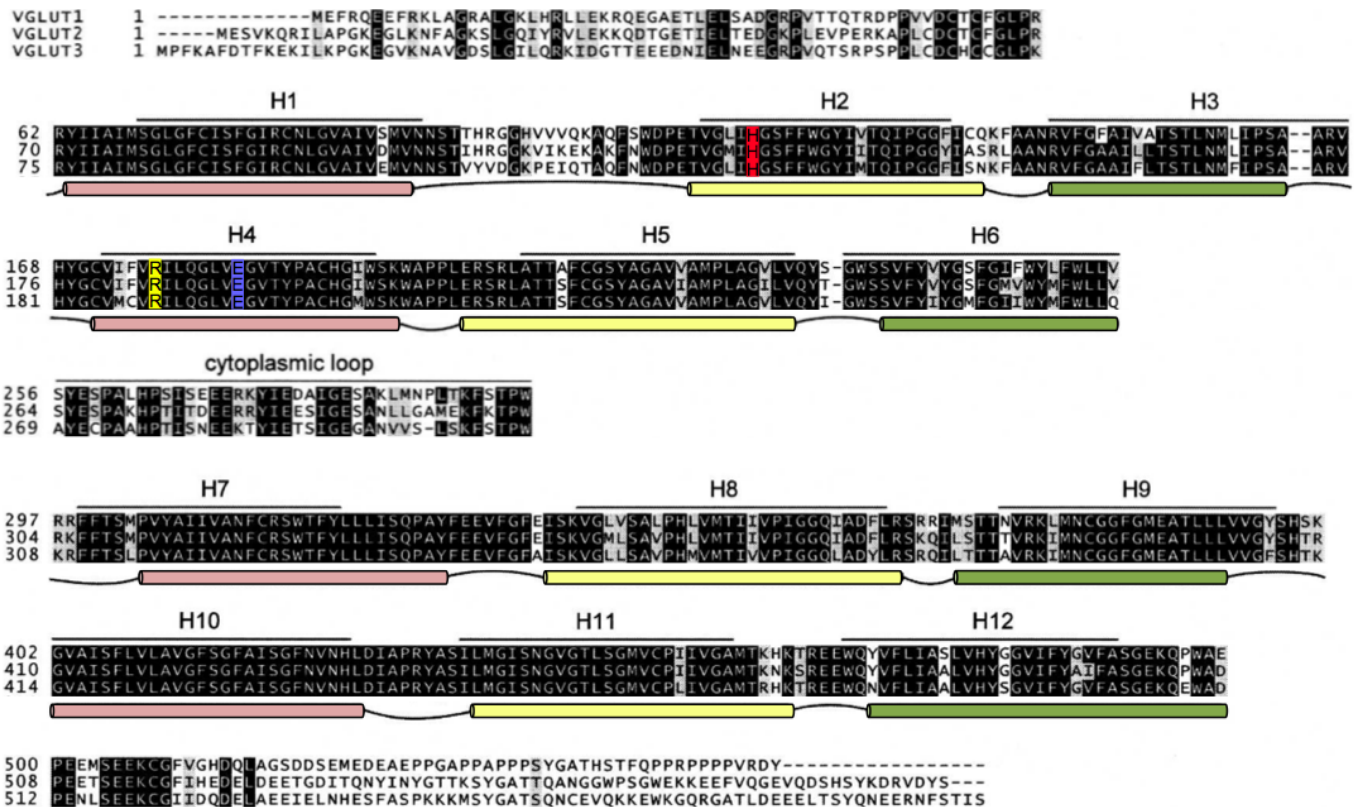


**Figure A.19: Alignment of *Homo sapiens* VGLUTs amino acid sequences**

VGLUT1, - 2 and - 3 are highly homologous in their central portion, with the majority of divergences being concentrated in NTD and CTD. His<sup>128</sup> (in red), Arg<sup>184</sup> (in yellow) and Glu<sup>191</sup> (in blue), charged amino acids in the TMDs, are responsible for L- Glu transport activity for VGLUT2. Conserved amino acids are highlighted in black. Solid lines mark the 12 predicted helical regions (H1- H12) and the predicted cytoplasmic loop. Colored tubes correspond to regions with transmembrane helices for the bacterial homolog GlpT, connected by cytoplasmic (convex) and luminal (concave) loops.

Adapted from Almqvist *et al.* (2007)

VGLUTs topology has been inferred in two studies (VGLUT2 in Jung *et al.* 2005, VGLUT1 in Almqvist *et al.* 2007). A putative model was proposed for the three VGLUTS. This model is based on the structure of glycerol- 3- phosphate transporter (GlpT), a distant bacterial homolog (Almqvist *et al.* 2007). According to this 3D model, VGLUTs have twelve  $\alpha$ - helices TMD organized in two clusters that are separated by a long central loop (Figure A.20). The N- and CTD are cytoplasmic, as for the big central loop (Almqvist *et al.* 2007). The pore is constituted with 45 residues (44 of them are fully conserved among VGLUTs, in black in Figure A.20a).

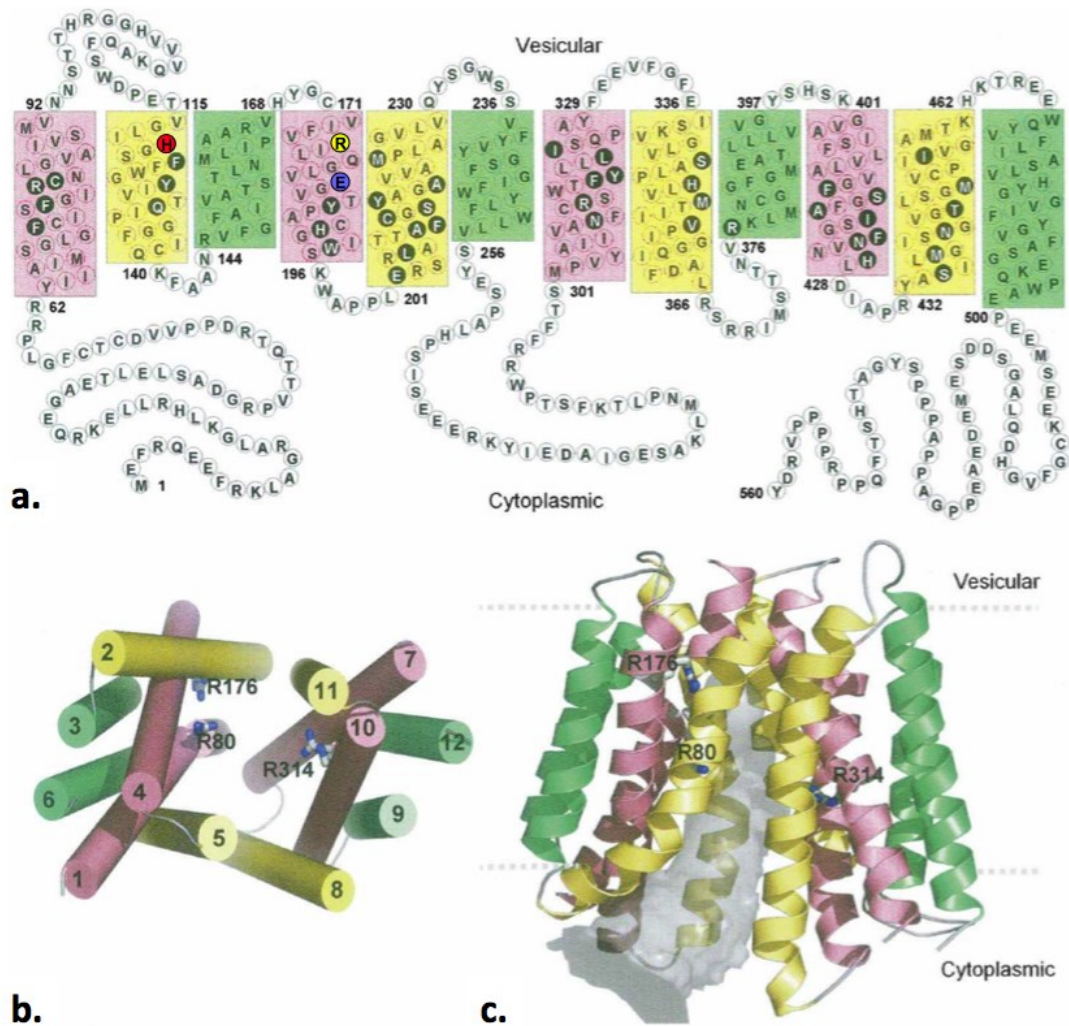


**Figure A.20: VGLUT topology model**

**a.** Proposed topology for VGLUT1. Residues that face the center of the pore are represented *in black circles*, and the ones involved in glutamate transport *in color* (His<sup>128</sup> *in red*, Arg<sup>184</sup> *in yellow* and Glu<sup>191</sup> *in blue*). **b.** VGLUT1 viewed from the cytoplasmic side. **c.** 3D representation of VGLUT model. The 12 transmembrane helices form a pore (*gray volume*) that is open to the cytoplasmic side. The highly variable first and last 60 residues of the N- and C-terminal are not shown.

Adapted from Almqvist *et al.* (2007)

#### 1.4 Mechanism of glutamate uptake by VGLUTs

VGLUT1 and -2 functional properties for glutamate transport are very similar and match those previously described for glutamate transport in brain SVs (see 1.1: A history of VGLUTs). This transport is Mg<sup>2+</sup> and Cl<sup>-</sup> - dependent, requires a proton electrochemical gradient and relies on its  $\Delta\psi$  component. It is highly selective for L- glutamate, and it is inhibited by dyes such as Evans Blue. Characteristics of VGLUT3- driven glutamate transport are closely related to those of VGLUT1 and VGLUT2, despite minor differences (Gras *et al.* 2002, Takamori *et al.* 2002).

In theory, VGLUTs possess two independent transport machineries: the Na<sup>+</sup>- dependent Pi transport, which was the first historical function attributed to VGLUTs,

and the  $\Delta\psi$ -dependent L- glutamate uptake. However, the  $\text{Na}^+$ -dependent  $\text{P}_i$  transport is poorly established. Here, we will only discuss this second mechanism (Juge *et al.* 2006).

- Release probability

It was suggested that the differential distribution of VGLUT1 and VGLUT2 could be linked to a difference in the probability of transmitter release (Fremeau *et al.* 2001). Indeed, VGLUT2- expressing terminals have a high release probability and could provide a high- fidelity transfer of information (Weston *et al.* 2011). These synapses are common in sensory and autonomic nervous systems (*e.g.* cerebellum, brainstem, thalamocortical projections, blood- pressure controlling presympathetic neurons, inspiratory augmenting neurons, chemosensory neurons innervating the main respiratory center, nociception- mediating spinal cord dorsal root ganglia neurons; Ueda (2016)). In contrast, VGLUT1 is associated with synapses that have low release probability (*e.g.* hippocampus) and appears important for synaptic plasticity (Varoqui *et al.* 2002, Fremeau *et al.* 2004).

- Substrate recognition

VGLUTs selectively transport L- glutamate and D- glutamate to some extent, but not aspartate, GABA or glutamine. They fail to recognize glutamate analogs that lack free  $\alpha$ - amine,  $\alpha$ - and  $\gamma$ - carboxyl and three- carbon skeleton between the two carboxylate groups (Ueda 2016). By directed mutagenesis, three residues conserved among VGLUTs were proven to be responsible for L- glutamate transport activity (*i.e.* Arg<sup>184</sup>, His<sup>128</sup> and Glu<sup>191</sup>; Figure A.19; Juge *et al.* (2006)).

The affinity of VGLUTs for their substrate is in the millimolar range ( $10^3$ - fold of that of plasma transporter). This is consistent with the high cytoplasmic level of glutamate (Figure A.9).

- ATP- dependence

As previously discussed, VGLUT- mediated glutamate uptake is ATP- dependent. The ATP used as the energy source for proton influx in SV does not originate from mitochondria. It is rather produced locally during glycolysis, which is why synaptic vesicles are endowed with the glycolytic ATP- generating enzyme complex GAPDH/3- PGK (glyceraldehyde-3- phosphate dehydrogenase / 3- phosphoglycerate kinase). This seems to be also valid for other VNTs (Ikemoto *et al.* 2003, Ueda 2016).

- Chloride- dependence

The function of chloride in VGLUT-positive SVs is still a matter of debate.  $\text{Cl}^-$  leads to an increased  $\Delta\text{pH}$ , presumably by dissipating  $\Delta\psi$  (Omote *et al.* 2011). VGLUTs have a biphasic dependence on chloride for the uptake. The transport is inhibited at low

(< 4 mM) and high (> 10 mM)  $\text{Cl}^-$  concentrations. In physiological conditions, extracellular and intraneuronal chloride concentrations are about 150 mM and 20 mM respectively (Ueda 2016).

After fusion with the plasma membrane, SVs undergo endocytosis. During endocytosis, the outer layer of the plasma membrane becomes the inner layer of SV, and *vice versa*, with the extracellular fluid being trapped in the SV. Therefore, the inside of SV is rich in chloride and sodium ions (Figure A.21).

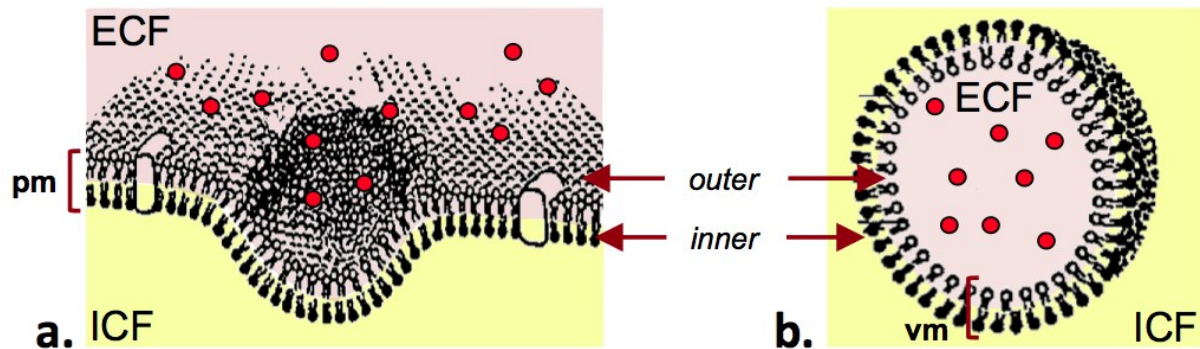


**Figure A.21: SV endocytosis at the plasma membrane**

**a.** Plasma membrane (pm) is a lipid bilayer that delimits the inside of the cell, which is made of intracellular fluid (ICF), from the outside medium constituted by the extracellular fluid (ECF). ECF is rich in chloride (red dots). **b.** After endocytosis, the outer layer of pm becomes the inner layer of SV membrane (vm) and *vice versa*. Thus, after endocytosis, the inside of SV is enriched in  $\text{Cl}^-$ .

Adapted from Trkanjec and Demarin (2001)

- A highly modulated system

Several different hypothetical mechanisms have been proposed for glutamate uptake. Globally they share a common idea, but they distinguish themselves through the molecular players that intervene in ion movements (Edwards 2007, Hnasko and Edwards 2012, Ueda 2016). Recent studies support the idea that extravesicular  $\text{K}^+$  also plays a role and suggest that VGLUT-mediated uptake is highly flexible in regards with the changing ionic environment during transport (Preobraschenski *et al.* 2014, Ueda 2016).

- Number of copy and transport

It has been proposed that each SV in glutamatergic neurons carries either 4 or 9 copies of VGLUT1 (depending on the study), or 14 copies of VGLUT2, and that there is little intervesicle variation in the number of VGLUTs (Takamori *et al.* 2006, Mutch *et al.* 2011). It is assumed that VGLUT3 is present within the same range in SVs.

Several studies indicate that the copy number of VGLUT1 and VGLUT2 per vesicle can affect quantal size (Daniels *et al.* 2004, Wojcik *et al.* 2004, Wilson *et al.* 2005, Wu *et al.* 2007, Ueda 2016). Yet, it was also shown that a single VGLUT on SV is sufficient to ensure glutamate uptake (Daniels *et al.* 2006).

A recent study conducted in our team revealed that the copy number of VGLUT3 on SVs could be non-uniform (Ramet *et al.* 2017). A transgenic mouse carrying a mutated version of VGLUT3 (p.A211V) has a substantial decrease of the transporter level (up to 70%). Even by decreasing this level to 85%, mice do not display behavioral alterations, and VGLUT3 uptake function appears unaltered. Since there is a decrease of mEPSC in mutant mice, this suggests that VGLUT3 number could vary among SVs. This also points towards non-uptake-related roles of VGLUT3. Or else to differential roles of VGLUT3 according to the neural types that express it.

## 1.5 VGLUTs during development

Glutamatergic pathways undergo major adjustments during development. A highly differentiated spatial and age-dependent expression of the three VGLUTs is observed (Figure A.22). VGLUT1 concentration is very low at birth. Its expression increases steadily throughout postnatal development. It reaches a peak after postnatal day 14 (P14). Interestingly, VGLUT1 progressively replaces VGLUT2 in several regions such as the cortex or the hippocampus.

VGLUT2 represents the major VGLUT isoform during embryonic and early postnatal phases. Its expression occurs early in the embryonic life and reaches its maximum level at P7. VGLUT2 is first distributed homogeneously all over the cerebral cortex, but in the adult brain the labeling becomes more concentrated in cortical layers IV and VI. This has been named the "VGLUT2 - VGLUT1 switch" (Wojcik *et al.* 2004).

VGLUT3 expression increases progressively during postnatal development. It is increasingly present in the rostral brain (striatum & hippocampus) throughout post-natal development. VGLUT3 is strongly and transiently expressed in the caudal brain (cerebellum & superior olive complex) during early post-natal life (Schafer *et al.* 2002, Boulland *et al.* 2004, Gras *et al.* 2005). Then it disappears from these areas after P20 (Gras *et al.* 2005).

VGLUTs are essential regulators of vital functions in mammals. Deletion of VGLUT1 or VGLUT2 is lethal. VGLUT2-lacking mice die immediately after birth as a result of respiratory failure (Wallen-Mackenzie *et al.* 2010). VGLUT1-lacking mice die toward the end of the postnatal third week, precisely when the "VGLUT2 - VGLUT1 switch" occurs most likely due to diminished functioning of their cortex (Wojcik *et al.* 2004).

VGLUT3 shows a transient expression in several cell types. It is found in progenitor-like cells in the paraventricular zone at early developmental stages (Boulland *et al.* 2004). Moreover, cell cultures enriched with progenitor cells seem to have a high level of coexpression between VGLUT3 and Nestin (marker for progenitor cell). VGLUT3 is

also transiently expressed in Purkinje cells in the cerebellum (Boulland *et al.* 2004, Gras *et al.* 2005).

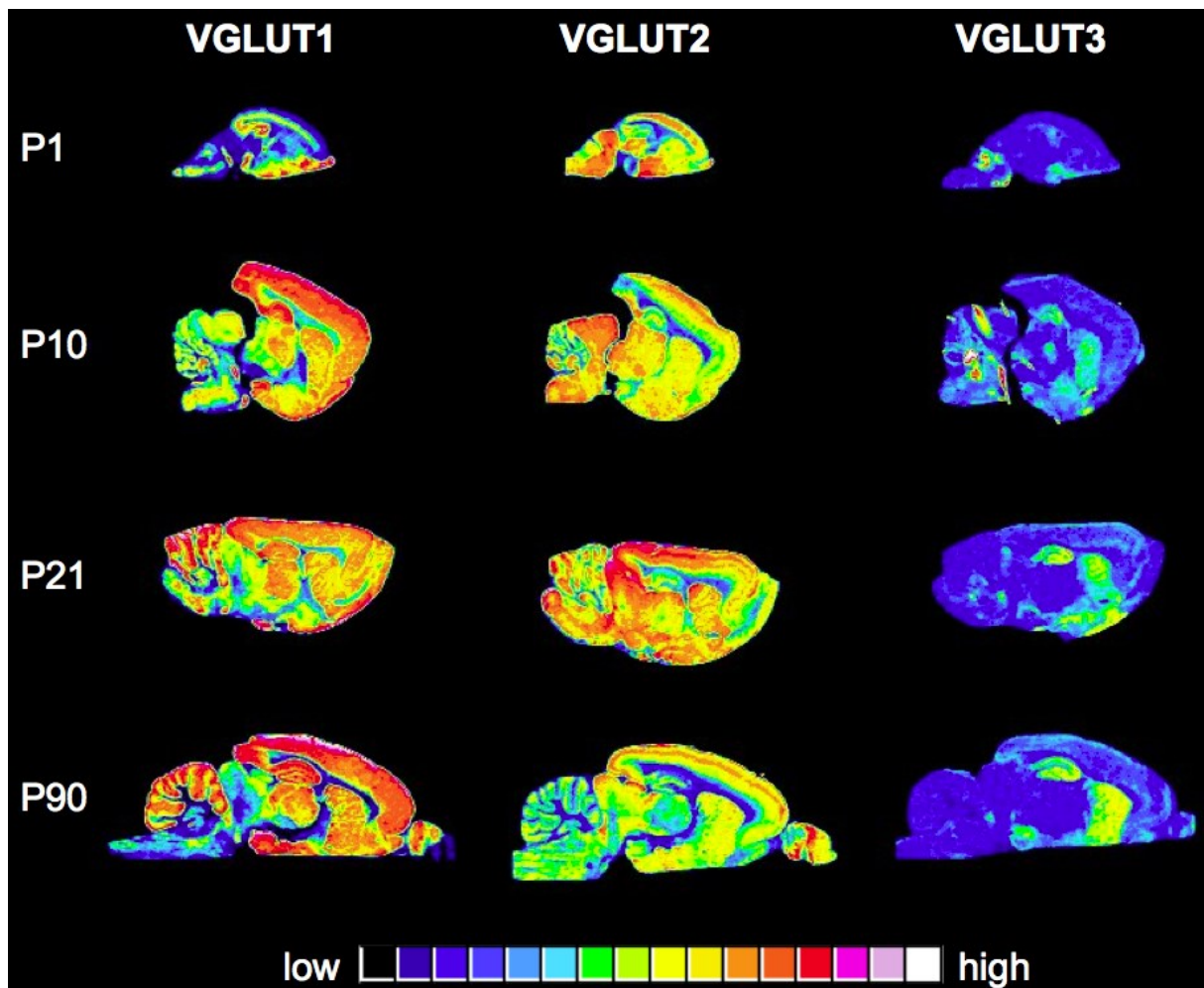


**Figure A.22: VGLUT1- 3 protein expression during post- natal development**

VGLUT1, - 2 and - 3 immunoautoradiography at different developmental stages in the rat brain (*sagittal view*) represented in pseudocolor. **Left column:** VGLUT1 expression at birth is low. Its expression then increases throughout development and appears especially in cortical regions. **Middle column:** VGLUT2 shows strong staining in the first few postnatal days, with the highest intensity in the brainstem regions and in the cerebellum. The cerebellum and midbrain levels then fade with development. In the adult, VGLUT2 shows an expression pattern complementary to that of VGLUT1; only low levels of VGLUT2 are seen in the neocortical regions. **Right column:** VGLUT3 expression increases until the third week postnatal. Its cerebellar expression is transient.

Adapted from Gras *et al.* (2005)

## 1.6 VGLUTs pharmacology

Through time, many selective compounds have been found to bind glutamate- related proteins (transporters, receptors, enzymes). This stems from the fact that glutamate is very flexible, and can adopt several relatively stable conformations (Danbolt 2001). Unlike the plasma membrane transporters and receptors, the three VGLUTs share a very high level of homology. For that reason, so far there are no specific pharmacological

agents that specifically target one subtype of VGLUT. Glutamatergic systems dysfunctions are involved in a variety of pathological states (Meldrum 2000, Swanson *et al.* 2005, Niciu *et al.* 2012, Schwartz *et al.* 2012) Therefore, VGLUTs represent therapeutic targets of choice. Discovery of subtype- specific VGLUT modulator should be a major field of research.

Three kinds of VGLUTs inhibitor have been identified: dyes ( $K_i$  10 nM - 10  $\mu$ M), substituted quinolines (DCQ;  $K_i$  40 nM - 300  $\mu$ M), and glutamate analogs ( $IC_{50}$  > 230  $\mu$ M; Figure A.23).

The best VGLUT uptake inhibitors are large aromatic hydrophobic dyes (Chaudhry *et al.* 2008). They contain two large azo groups. To name a few, Trypan blue (TB; Figure A.23a), Evans blue, Chicago sky blue dyes were first discovered. Another series of aromatic dyes include Rose Bengal (RB; Figure A.23b), only non- competitive inhibitor that exhibits a high affinity ( $K_i$  = 19nM), although it also inhibits VMAT2 (Pietrancosta *et al.* 2010). Recently, a new class of VGLUT inhibitors consisting of Brilliant Yellow dyes (BY; Figure A.23e) was discovered ( $K_i$  = 12 nM; Tamura *et al.* (2014)). Because of their structure (diazo groups and highly charged sulfonic acid groups), all these dyes are membrane- impermeable and potentially cytotoxic. Therefore, new inhibitory agents development are needed.

Due to its high potency to inhibit VGLUTs and to cross membranes, RB was used as a support to synthesize new analogs. However, they failed to be more potent than the original molecule (Pietrancosta *et al.* 2010).

Another research direction adopted for the design of more potent VGLUT inhibitors was the synthesis of small molecules that combine benefits of TB and DCQs (Figure A.23f). On top of being able to inhibit VGLUT uptake activity within a micromolar range, these compounds offered the advantage of being easily synthesized in two steps (Favre-Besse *et al.* 2014).

A new study published this year consisted in producing Brilliant Yellow dye analogs (BYA; Figure A.23g). Despite their reduced potency, these membrane- permeable new compounds proved to be highly specific for VGLUT uptake inhibition both *in vitro* in heterologous system, and *ex vivo* on hippocampal slices. An interesting feature of Brilliant Yellow dye analogs is that they are fluorescent (Kehrl *et al.* 2017).

A new study report the generation of nanobodies directed against the membrane portion of VGLUT1 (Schenck *et al.* 2017). Nanobodies have the ability to block their target in a given conformation, thus preventing proteic activity. Even if not specific for one of VGLUTs isoforms, nanobodies could efficiently block glutamate uptake. Schenk *et al.* expressed nanobodies under control of cell- type specific promoters in order to

block VGLUT activity. This approach could be of particular interest in the case of VGLUT3, which is mainly expressed by non- glutamatergic neurons. In addition nanobodies can be coupled to fluorescent proteins to become immunocytochemical tools (Schenck *et al.* 2017).

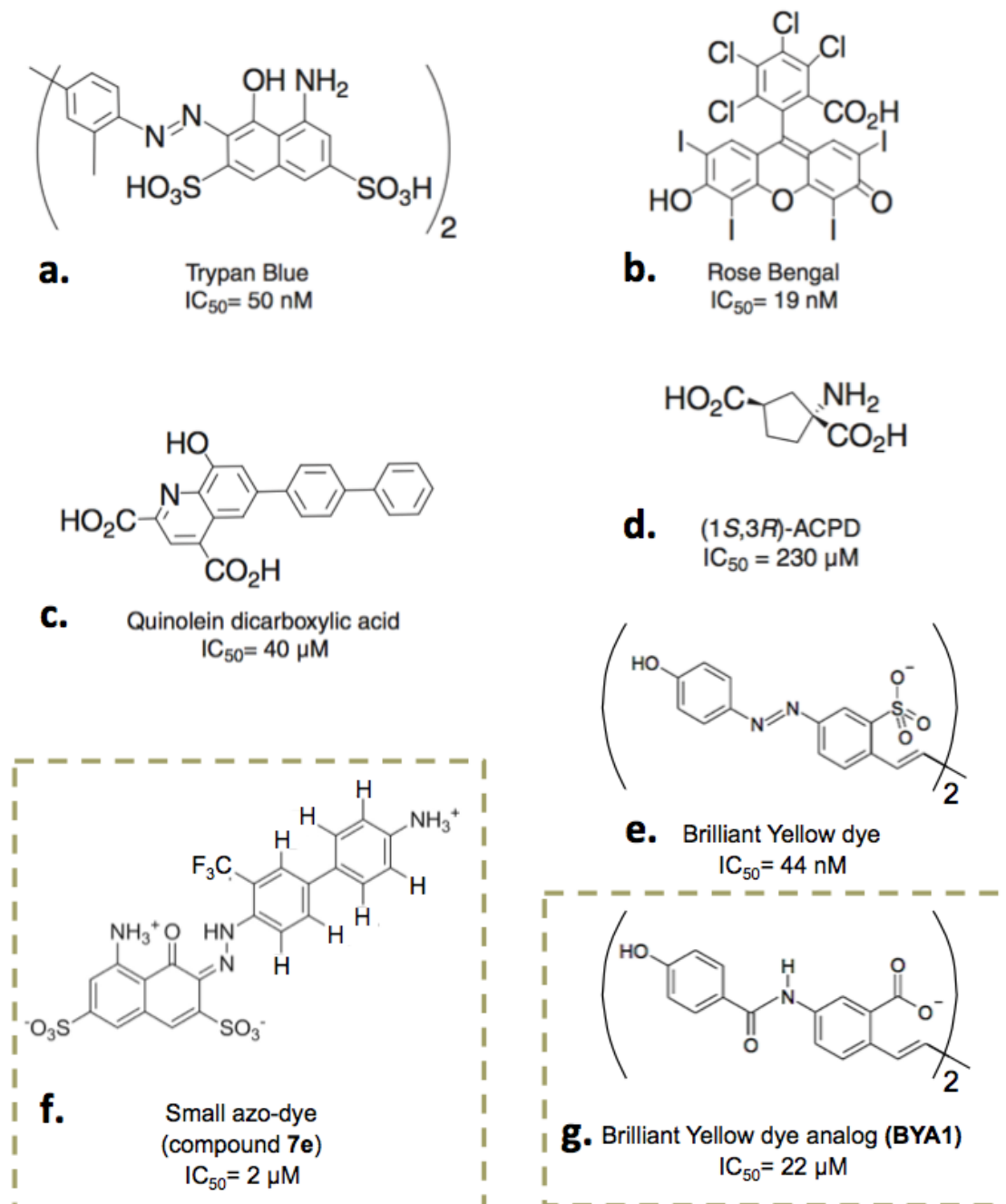


**Figure A.23: VGLUT family inhibitors**

**a, b** and **e.** Trypan Blue (TB), Rose Bengal and Brilliant Yellow (BY) are part of the dyes that inhibit VGLUTs. **c.** Quinolein dicarboxylic acid belongs to the substituted quinoline class (DCQ). **d.** Trans-1- amino- cyclopentane-1,3- dicarboxylate ((1*S*,3*R*)- ACPD) is a glutamate analog. **f.** Example of a new compound designed based on TB and DCQ properties. Here is represented the compound **7e** described in Favre-Besse *et al.* (2014). **g.** Another example of a new compound, derived from BY (BYA1, described in Kehrl *et al.* (2017)).

Adapted from Pietrancosta *et al.* (2010), Favre-Besse *et al.* (2014), Kehrl *et al.* (2017)

## **2. Vesicular glutamate transporter type 3 (VGLUT3)**

Human VGLUT3 (*SLC17A8*) is encoded by an 80 kb gene located on chromosome 12, and is constituted by 12 exons.

### **2.1 Anatomical distribution**

#### **2.1.1 Regional distribution**

In contrast with VGLUT1 and VGLUT2, VGLUT3 has a restricted pattern of expression that overlaps with the formers in some brain areas, but never in the same terminals (Schafer *et al.* 2002). This pattern of expression is shared between rodents and human (Vigneault *et al.* 2015). VGLUT3 is present in several structures in the CNS as well as in peripheral organs such as liver and kidney (Fremeau *et al.* 2002).

- Distribution in the brain

The anatomical distributions of VGLUT3 transcript and protein are summarized in the Table A.4 (Herzog *et al.* 2004).

Most VGLUT3- positive structures display both the expression of mRNA and protein, suggesting a preferential role in local projection neurons (Figure A.24). They include the cerebral cortex (Cx; Figure A.24a- e), the striatum (Str; Figure A.24a- b), the bed nucleus *stria terminalis* (BST; Figure A.24b), the hippocampus (Hc; Figure A.24c- d), the dorsal and median raphe nuclei (DRN and MRN respectively; Figure A.24e) and the interpeduncular nucleus (IP; Figure A.24e).

However, some structures only have the transcript (projecting structures). This is the case for the lateral habenula (Hb), which display high levels of transcript but no protein (Figure A.24c).

On the other hand, some structures only express VGLUT3 protein, and correspond to structures innervated by long- projecting VGLUT3-positive neurons. For example, the mesencephalon, thalamus (Thal) and hypothalamus (Hyp) are moderately stained (Figure A.24c- d). The substantia nigra *pars compacta* (SNc) and ventral tegmental area (VTA) are heavily stained, and VGLUT3 seems to account for the majority of VGLUT- positive terminals in these structures (Figure A.24d). The amygdala (AMG) - and more precisely its basolateral nucleus (BLA) - displays high levels of VGLUT3 protein (Figure A.24c).

**Table A.4: VGLUT3 structural expression in mammalian brain**

VGLUT3	Transcript	Protein
<b>Gene</b>	SLC17A8	
<b>Human locus</b>	12q23.2	
<b>Distribution</b>	<p><b>Eyes</b><sup>a</sup>  <b>Inner ear</b>  <b>Kidney</b><sup>a</sup>  <b>Liver</b><sup>a, b</sup>  <b>Spinal cord</b><sup>d, e</sup>  <b>Brain</b></p> <p>Cerebral cortex<sup>a, b, c</sup>            Striatum (CPu &amp; Acb)<sup>a, c</sup>            Bed nucleus<sup>c</sup>            Hippocampus (DG<sup>a, b, c</sup> &amp; CA1- 3<sup>a, b, c</sup> &amp; stratum radiatum<sup>b, c</sup>)<sup>a, b, c, d</sup>            Amygdala<sup>b, d</sup>            Habenula<sup>a</sup>            Thalamus (median nuclei)<sup>c, d</sup>            Hypothalamus<sup>b, c</sup>            Nucleus tractus solitarii<sup>c</sup>            SNc<sup>b</sup>            Ventral pallidum<sup>c</sup>            Raphe (DRN&amp; MRN)<sup>a, b, c</sup>            Cerebellum (granule layer)<sup>b, d</sup></p>	<p><b>Retina</b><sup>b</sup>  <b>Inner ear</b>  <b>Kidney</b><sup>a</sup>  <b>Pancreas</b> (<math>\beta</math> cells)<sup>f</sup>  <b>Skeletal muscle</b><sup>b</sup>  <b>Spinal cord</b><sup>e</sup>  <b>Brain</b>  <b>Only in grey matter</b><sup>a</sup></p> <p>Olfactory tubercles<sup>a</sup>            Cerebral cortex (II / VI)<sup>a, b</sup> (IV / V)<sup>c</sup>            Striatum (CPu &amp; AcbSh&gt;AcbC<sup>a</sup>)<sup>a, b, c</sup>            Bed nucleus<sup>c</sup>            Stria terminalis<sup>c</sup>            Hippocampus (Pyr &amp; Gran layers)<sup>a, c</sup>            Hippocampus (stratum radiatum)<sup>b, c</sup>            Amygdala<sup>a, b, c</sup>            Thalamus<sup>c</sup>            Hypothalamus<sup>c</sup>            SNc<sup>a</sup>            Ventral pallidum<sup>c</sup>            Globus pallidus (GPi &gt; GPe)<sup>c</sup>            Raphe (DRN&amp; MRN)<sup>a, b</sup>            Periaqueductal grey<sup>c</sup></p>
<b>Subcellular localization</b>	Neurons: Axon terminals; dendrites; perikarya Astrocytes? Progenitor cell?	
<b>K<sub>m</sub> for L- Glu</b>	~ 1 mM	
<b>V<sub>max</sub></b>	~ 20 pmol.min <sup>-1</sup> .mg <sup>-1</sup> prot	
<b>IC<sub>50</sub> for Evans Blue dye</b>	~ mM	

**a**, Gras *et al.* (2002), Herzog *et al.* (2004); **b**, Fremeau *et al.* (2002), (Boulland *et al.* 2004); **c**, Schafer *et al.* (2002); **d**, Takamori *et al.* (2002); **e**, Oliveira *et al.* (2003); **f**, Gammelsaeter *et al.* (2011).

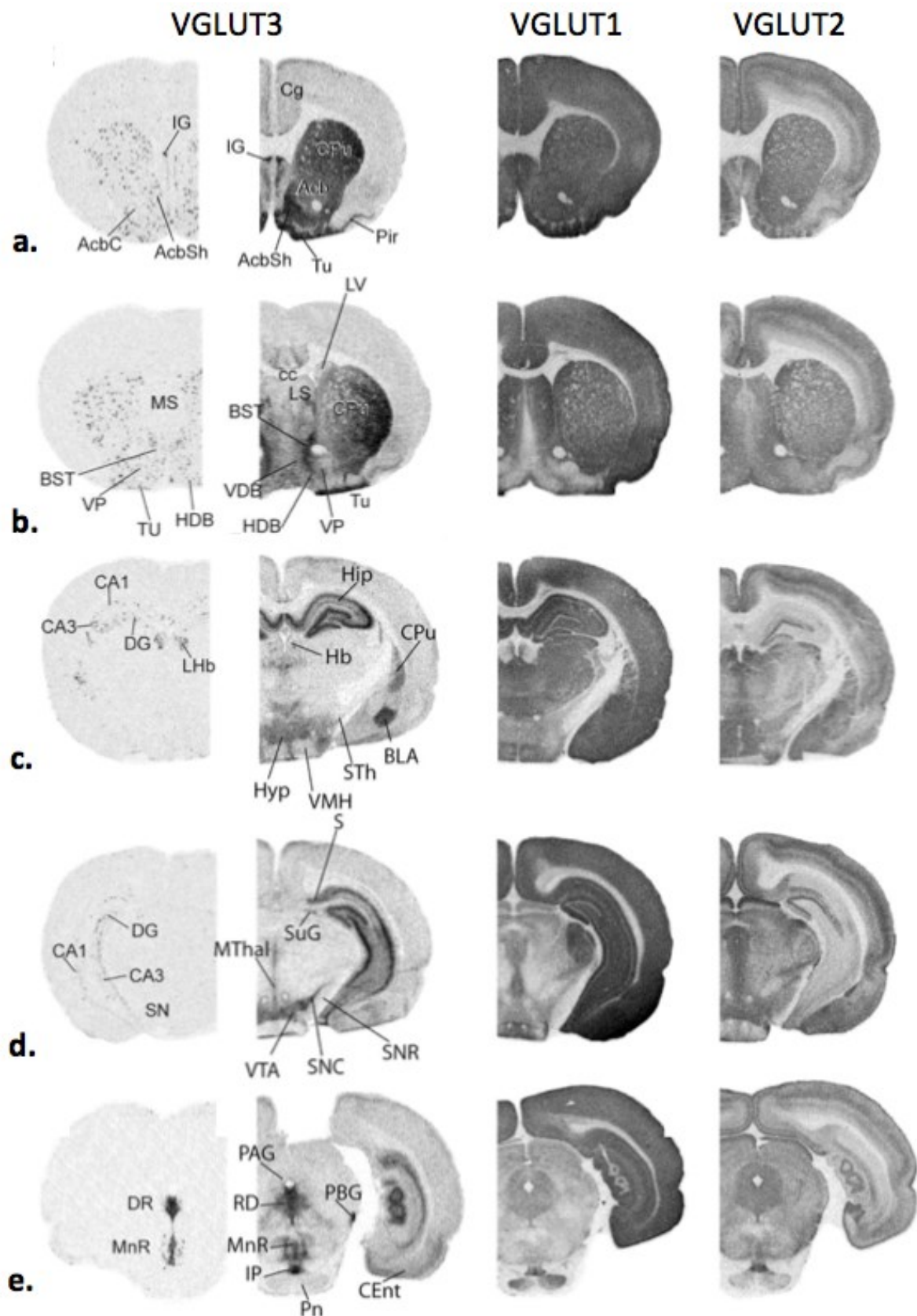


**Figure A.24: Regional distribution of VGLUT3 transcript and VGLUT1, - 2 and - 3 proteins**  
 VGLUT3 transcript (**left**) was visualized by radioactive *in situ* hybridization, while the protein (**right**) was labeled by immunohistochemistry, as for VGLUT1 (**third panel**) and VGLUT2 (**forth panel**)

Adapted from Herzog *et al.* (2004)

- [Distribution in other structures](#)

#### Corti organ:

VGLUT3 is expressed in the inner ear sensory cells, also referred to as inner hair cells (IHC). These cells represent the first synapse in the auditory pathway, and convert auditory stimuli into electric signal to the auditory nerve (Ruel *et al.* 2008, Seal *et al.* 2008).

#### Spinal cord:

VGLUT3 expression in the spinal cord is controversial. One study stated that VGLUT3 protein is found in the ventral horn of the cervical and thoracic spinal cord, with a supraspinal origin, probably from raphe nuclei (Oliveira *et al.* 2003). Another study showed that VGLUT3 is present in the dorsal horn of the spinal cord and identified some functional correlate associated with this location (Seal *et al.* 2009).

#### Dental pulp:

Along with VGLUT1 and - 2, VGLUT3 is expressed in dental pulp sensory afferents that regulate local microcirculation blood flow (Zerari-Mailly *et al.* 2012).

#### Bladder:

VGLUT3 is expressed by a subpopulation of neurons in the bladder dorsal root ganglion (Brumovsky *et al.* 2013).

### 2.1.2 Ultrastructural distribution

VGLUT1 and VGLUT2 that are located almost exclusively in nerve terminals. In contrast, VGLUT3 is found in the perikarya and proximal dendrites of some neurons in addition to their terminals. They include cholinergic interneurons of the striatum and GABAergic interneurons in hippocampus and cortex (Fremeau *et al.* 2002, Gras *et al.* 2002, Schafer *et al.* 2002, Herzog *et al.* 2004).

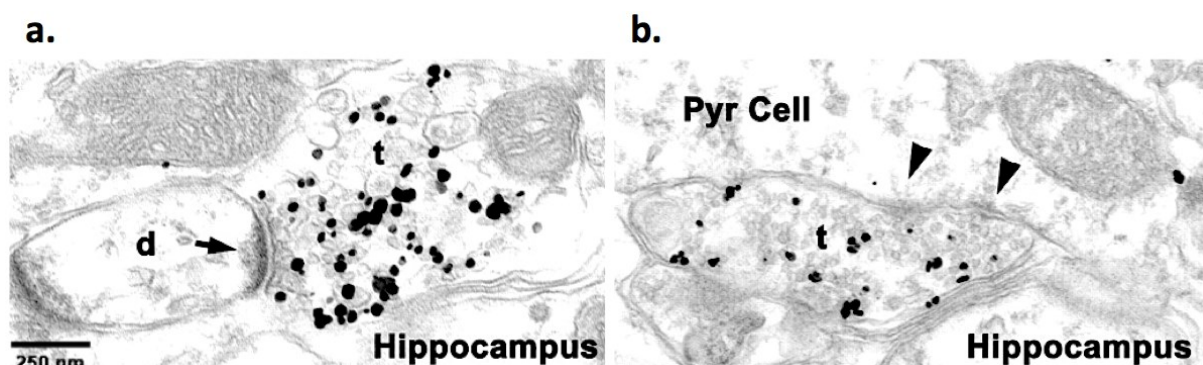


**Figure A.25: VGLUT3 at asymmetrical or symmetrical synapses**

Electron microscopy visualization of immunoparticles against VGLUT3 at an asymmetrical (**a**, arrow) or symmetrical (**b**, arrowhead) synapse in the hippocampus. t: terminal; d: dendrite; Pyr cell: pyramidal cell. Scale bar = 250 nm.

From Gras *et al.* (2002)

Electron microscopy detections revealed that VGLUT3 is also found in terminals forming either asymmetrical or symmetrical synapses (Figure A.25). This suggests that VGLUT3 is expressed by excitatory or inhibitory/modulatory neurons respectively (Freneau *et al.* 2002, Gras *et al.* 2002).

### 2.1.3 Neuronal subtypes distribution

VGLUT3 was identified in non- glutamatergic neurons, *i.e.*, these neurons were initially identified as using another neurotransmitter than glutamate. VGLUT3 is expressed by subsets of serotonergic neurons, GABAergic neurons and cholinergic neurons.

- [VGLUT3 in serotonergic neurons](#)

#### Raphe

VGLUT3 is expressed in all raphe nuclei, with a more prominent distribution in the dorsal and medial raphe (Hioki *et al.* 2010). Costaining with serotonergic markers (5- HT or SERT, for plasmalemmal serotonin transporter) showed that in these nuclei there are three populations of neurons: **i)** purely glutamatergic neurons (VGLUT3- positive), **ii)** purely serotonergic neurons (SERT- positive), and **iii)** mixed Glu / 5- HT neurons (Schafer *et al.* 2002). Recent studies provided anatomical support for VGLUT3 sorting in the axonal arborization of a single DR neuron (Gagnon and Parent 2014, Voisin *et al.* 2016). Along a single axon, some varicosities have VGLUT3, when others are devoid of it. This highlights the complexity of the 5- HT network. It suggests that VGLUT3 sorting in different branches of serotonergic neurons is regulated and confers differential functional properties to terminals (Amilhon *et al.* 2010). Serotonergic neurons have a very profuse ascending axonal arborization. However, only half of their branches make synaptic contacts. The other half mediates a diffuse transmission through asynaptic *en passant* contacts. It is possible that VGLUT3 would be preferentially targeted to varicosities making synaptic contacts, also because these varicosities appear larger in electron microscopy than the VGLUT3- devoid ones (Gagnon *et al.* 2014).

A large number of 5- HT neurons in the DRN and MRN express VGLUT3 mRNA (Gras *et al.* 2002, Shutoh *et al.* 2008, Crawford *et al.* 2011). However, in the DRN and MRN, VGLUT3 is mainly expressed in fibers and terminals lacking 5- HT (Amilhon *et al.* 2010). In the projecting areas of serotonergic neurons (*i.e.* forebrain and brainstem), VGLUT3 is expressed in ~ 50% of 5- HT fibers in the cortex, and between 30 to 80% in the hippocampus. Surprisingly, there is almost no dual expression of SERT and VGLUT3 in the brain (Gras *et al.* 2008, Amilhon *et al.* 2010). This observation suggests enhanced levels of 5- HT transmission by VGLUT3/5-HT fibers due to the lack of serotonin reuptake.

There is a double origin for VGLUT3- positive 5- HT neurons in the raphe, regarding the expression of the transcription factor Pet- 1 (~55% are Pet- 1- positive in MNR; Kiyasova *et al.* (2011), Sos *et al.* (2017)).

### **Purely glutamatergic neurons in the raphe**

In the raphe, some neurons express VGLUT3 without SERT or VMAT2. It has been estimated that the proportion of VGLUT3- positive neurons that are not serotonergic is around 20% (Hioki *et al.* 2010). These neurons are mainly located in the dorsal part of the DRN and project to many areas, including the VTA and SNc. These neurons have not been characterized yet.

- [VGLUT3 in GABAergic neurons](#)

### **Hippocampus**

In the hippocampus, VGLUT3 is expressed by GABAergic cholecystokinin (CCK)- positive basket cells in the *Pyramidale* layer (Somogyi *et al.* 2004, Fasano *et al.* 2017). Their terminals contact somata and proximal dendrites in CA1- 3. VGLUT3 is also expressed by GABAergic interneurons (INs) in the granule layer of DG.

### **Cerebral cortex & neocortex**

VGLUT3 is expressed by sparse populations of GABAergic interneurons in layers II and VI of the cerebral cortex. The strongest labeling is found in the outer layer II. These interneurons are mainly CCK- and cannabinoid receptor type 1 (CB1R)- positive (Harkany *et al.* 2004, Somogyi *et al.* 2004). In the neocortex, VGLUT3 is expressed by CCK- and preprotachykinin B- positive GABAergic interneurons (Hioki *et al.* 2004).

In summary, VGLUT3 is preferentially expressed by subpopulations of GABAergic CCK- positive interneurons in the cerebral cortex and hippocampus.

- [VGLUT3 in cholinergic neurons](#)

### **Striatum**

VGLUT3 is expressed by all cholinergic interneurons (CINs) of the striatum (Gras *et al.* 2002, Herzog *et al.* 2004, Nickerson Poulin *et al.* 2006, Gras *et al.* 2008, Commons and Serock 2009). Both the dorsal part and the ventral part (or nucleus accumbens, Acb) are labeled. In the Acb, the outer part (shell, AcbSh) is more intensely stained compared to the inner part (core, AcbC; Herzog *et al.* (2004)). All VGLUT3- positive terminals express ChAT (choline acetyltransferase, ACh biosynthetic enzyme); inversely, 80% of ChAT- ir (immunoreactive) terminals express VGLUT3 (Stensrud *et al.* 2013).

### **Basal forebrain**

The basal forebrain (BF) is a brain region that has a strong cholinergic component. It contains an important mixed population of VGLUT3 / ChAT- positive neurons (30% of

magnocellular cholinergic neurons in the ventral pallidum, and up to 10% in the caudal BF) that projects to the BLA (Nickerson Poulin *et al.* 2006).

## 2.2 Functional roles: overview

### 2.2.1 Dual release of transmitters

The presence of VGLUT3 in subgroups of GABAergic, serotonergic or cholinergic terminals raised the possibility that two neurotransmitters could be released within the same neuron.

For years, Dale's principle ruled for neurotransmission: **a given neuron releases a single neurotransmitter**. However, increasing number of reports referring to colocalization of neuropeptide and nT, or of several nTs or VNTs within a single neuron, crippled this theory and were soon followed by electrophysiological and functional studies.

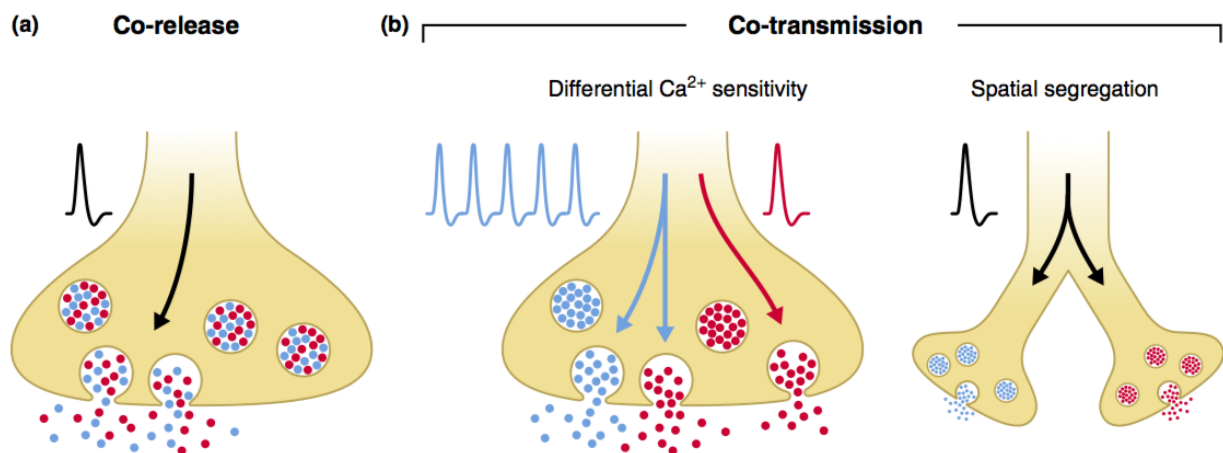


**Figure A.26: Co- release and co- transmission in neurons**

**a.** With co-release, both nTs (*red and blue dots*) are packaged into the same set of SVs, which will be released in the synaptic cleft upon an AP. **b.** In co-transmission, the nTs are sequestered into distinct populations of SVs, which leads to a differential release. It might rise from differential  $\text{Ca}^{2+}$  sensitivity (*left panel*), implying the requirement of specific stimulation pattern for SV recruitment. Or it can rely on spatial segregation of SV populations to different boutons (*right panel*), in which case, a single incoming information is transmitted to different postsynaptic targets.

From Vaaga *et al.* (2014)

The release of multiple neurotransmitters from a single neuron does not necessarily imply that they have to be packaged in the same SVs (Figure A.26; (Vaaga *et al.* 2014)). If they are, then the two transmitters are released together, which means there is a **co-release** (Figure A.26a). If they are in non-overlapping SVs, then it is a **co-transmission** (Figure A.26b). This co-transmission can be either co-temporal (the two transmitters are located in different terminals and thus released simultaneously, but with distinct downstream target; Figure A.26b right panel) or sequential (*i.e.* nTs are packaged in different SVs within the same terminal and their release can be uncoupled in

a frequency- or intensity-dependent way; Figure A.26b left panel). Many brain structures possess neurons carrying both a neurotransmitter and a neuropeptide, e.g. [5-HT / substance P]-expressing neurons in the medulla oblongata, or [DA / CCK]-expressing neurons in the VTA (Hokfelt *et al.* 1984, Johnson 1994). With the existence of several messengers, neurons can transmit differentiated messages at synapses.

In the case of VGLUT3-positive neurons, the multiple messengers are glutamate and either a neuromodulator (5-HT, ACh) or the inhibitory neurotransmitter GABA. However, it should be noted that for 5-HT and GABA, there seems to be axon terminal heterogeneity, i.e. that some terminals will express either one of the corresponding transporters, or the two together.

- [Serotonin- glutamate dual release](#)

The first clue for a dual transmitter release in 5-HT neurons was that extracellular stimulation of raphe nuclei leads to non-serotonergic excitatory post-synaptic currents (EPSCs) in the striatum, followed by longer latency serotonergic potentials (Park *et al.* 1982). Later, another study stated that cultured serotonergic neurons have the ability to elicit fast AMPAR-mediated post-synaptic currents (Johnson 1994). Then, it was demonstrated that activation of raphe nuclei leads to i) fast AMPAR- and ionotropic 5-HT<sub>3</sub>R-mediated EPSCs in hippocampal GABAergic interneurons and ii) a slow-rising putatively metabotropic 5-HT<sub>1A</sub>R-mediated inhibitory post-synaptic currents (IPSCs) in CA1 hippocampal neurons, or indirect inhibition via GABAergic interneurons (Varga *et al.* 2009). Recently, *in vivo* studies using optogenetic activation of serotonergic neurons from the DRN showed that AMPAR-mediated EPSCs are elicited in the VTA and AcbSh, comforting the idea that there is indeed a serotonin-glutamate dual release (Liu *et al.* 2014).

- [GABA- glutamate dual release](#)

Several cases involve GABA / Glu co-release. The first description of a VGLUT3-dependent GABA / Glu dual release was reported in the developing auditory system at inhibitory synapse that are also VGLUT3-positive (Gillespie *et al.* 2005). This transient expression (~ until P7) during the auditory map peak sharpening has been hypothesized to help eliminate or strengthen connections between medial nucleus of the trapezoid body and the lateral superior olive.

There is some ultrastructural evidence for VGLUT3 and VIAAT colocalization on the same SVs membranes in the cortex and hippocampus, but not in the striatum (Stensrud *et al.* 2013). This is a clue for an *in vivo* storage of GABA and Glu within the same SVs, and for a subsequent co-release (Figure A.27). More recently, our team revealed that CCK-positive basket cells in the hippocampus signal with GABA and use glutamate as a

secondary transmitter to retro-inhibit GABA signaling onto pyramidal cells (Fasano *et al.* 2017). In this situation, VGLUT3-dependent glutamate is acting upon mGluR.

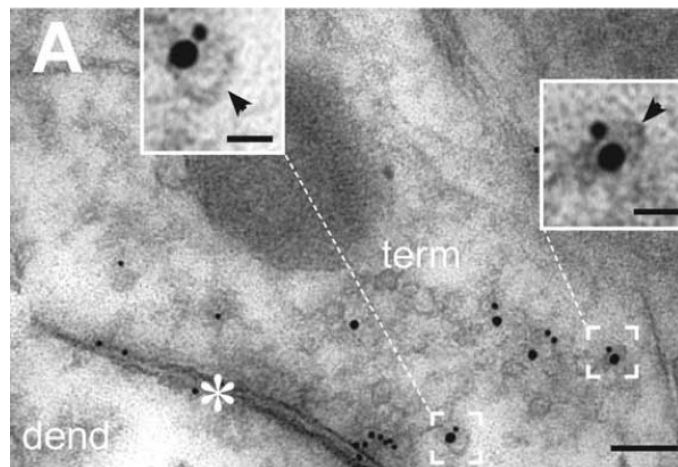


**Figure A.27: VGLUT3 and VIAAT are expressed on the same SVs**

Electron micrograph of a CA3 pyramidal cell layer terminal (term) forming a symmetric synapse (asterisk) on a stem dendrite (dend). VIAAT (large gold particles) and VGLUT3 (small gold particles) are colocalized on the same SV membranes (inset, arrowheads). Scale bars = 100 nm and 25 nm (inset).

From Stensrud *et al.* (2013)

- Acetylcholine- glutamate dual release

VGLUT3 is expressed by all CINs of the striatum. Using SV immunopurification, Gras *et al.* confirmed that VGLUT3 and VACHT were co-expressed in SV subsets from the striatum (Gras *et al.* 2008). This result was confirmed by electron microscopy with post-embedding gold particles (Stensrud *et al.* 2013).

Two local intrastriatal sources were identified as being able to elicit EPSCs: i) nicotinic ACh receptors (nAChRs) and ii) AMPARs / NMDARs (Cherubini *et al.* 1988). Later, it was demonstrated that these currents are imputable to local cholinergic interneurons, as striatal cholinergic autaptic cultures release both glutamate and acetylcholine, which respectively elicit AMPAR- and nAChR- mediated currents (Allen *et al.* 2006, Huh *et al.* 2008). More recently, it was observed that mice depleted for VACHT specifically in the CINs do not reproduce the phenotype observed by CINs toxin-mediated ablation, suggesting that these neurons use another transmitter than ACh (Guzman *et al.* 2011). Moreover, optogenetic activation of CINs triggers glutamatergic EPSCs in principal striatal neurons (Higley *et al.* 2011).

Therefore, CINs release both glutamate and acetylcholine.

### 2.2.2 Vesicular synergy

We saw that VGLUT3 expression by non- glutamatergic neurons enables them to co- release glutamate. Additionally, VGLUT3 presence in terminals increases the filling of SVs with the primary transmitter, leading to a potentiated release of the latter. This mechanism is called **vesicular synergy**.

- VGLUT3 / VAcHT synergy

Mice constitutively lacking VGLUT3 (VGLUT3<sup>-/-</sup>) show a two- fold decrease of ACh uptake, along with a two- fold reduction of evoked striatal ACh release (Gras *et al.* 2008). Both the presence of VGLUT3 and glutamate are necessary to maintain WT- level uptake activity. The positive effect of glutamate on [<sup>3</sup>H]ACh uptake is lost with the application of VGLUT inhibitor Evans Blue. Overall, this study reported for the first time that VGLUT3- dependent glutamate stimulates ACh vesicular loading (Figure A.28; Gras *et al.* (2008)).

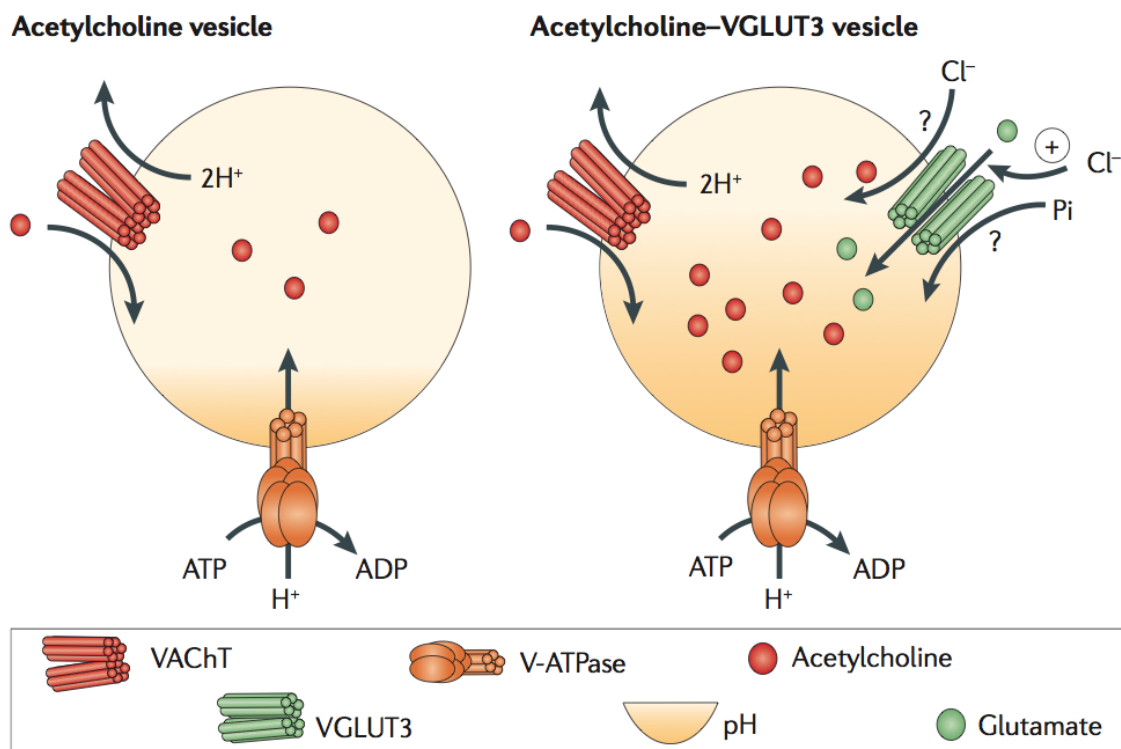


**Figure A.28: Vesicular synergy between VGLUT3 and VAcHT**

The kinetic properties of VAcHT (*in red*) are such that to accumulate one molecule of acetylcholine (*red circles*), two protons are extruded from the vesicle (**left panel**). Thus, VAcHT rapidly dissipates  $\Delta$ pH. Glutamate (*green circles*) and chloride acidify SVs through distinct and additive mechanisms. It can thus be proposed that the presence of VGLUT (*in green*) on SVs results in more acidified vesicles, which enables VAcHT to accumulate higher amounts of acetylcholine (**right panel**). The VGLUT-dependent increased vesicular accumulation of serotonin, acetylcholine, dopamine or GABA is known as vesicular synergy.

From El Mestikawy *et al.* (2011)

They postulated that the entry of glutamate would counterbalance VAcHT stoichiometry: for each positively-charged ACh influx, two protons are exported, resulting in a faster dissipation of  $\Delta\text{pH}$  gradient over  $\Delta\psi$ . Glutamate, which is negatively charged, would stimulate the accumulation of protons inside cholinergic SVs.

This interplay between the two transporters was validated with an electrophysiology study. The activation of CINA lacking VGLUT3 results in a strong attenuation of cholinergic signaling in the dorsal striatum (Nelson *et al.* 2014).

- [VGLUT3 / VMAT2 synergy](#)

Amilhon *et al.* highlighted the fact that VGLUT3 also enhances VMAT2-mediated [<sup>3</sup>H]5-HT vesicular loading by about 30% in the cortex and hippocampus (Amilhon *et al.* 2010). This increased accumulation is reduced in presence of VGLUT inhibitors and absent in VGLUT3<sup>-/-</sup> mice. Such a synergy was rationale since VMAT2 and VAcHT share bioenergetic transport properties (Figure A.16). It should be noted that the stimulation of 5-HT loading by VGLUT3 is probably higher than 30%, since uptake experiments assess VMAT2 global activity. Yet, VMAT2 is also expressed in histaminergic, dopaminergic and noradrenergic terminals.

Thus, VGLUT3<sup>-/-</sup> mice have a decreased accumulation and hence efflux of 5-HT in the cortex and hippocampus, and VGLUT3 seems to positively regulate 5-HT transmission in limbic areas.

- [VGLUT3 / VIAAT synergy](#)

To this date, there is no strong evidence for VIAAT / VGLUT3 vesicular synergy.

One study showed that VIAAT-immunoprecipitated SVs accumulate glutamate in addition to GABA. Trypan Blue inhibits GABA uptake from 15%, suggesting that VGLUT promotes GABA loading into SVs (Zander *et al.* 2010). In addition, Fasano *et al.* observed that the amplitude of GABA mini is decreased in the hippocampus of VGLUT3<sup>-/-</sup> (Fasano *et al.* 2017). This observation suggests that VGLUT3-dependent glutamate accelerates GABA loading into SVs.

However, two studies did not replicate these findings. In one study VGLUT3 was exogenously expressed in striatal GABAergic neurons. It was then found that glutamate and GABA are released from the same vesicles but do not synergize (Zimmermann *et al.* 2015). Another study stated that the expression of VGLUT3 during development in GABAergic neurons of the auditory brainstem leads to a synaptic accumulation of glutamate but does not synergize GABA release (Case *et al.* 2014).

The synergistic role of VGLUT3 onto VIAAT activity is not easy to detect. Unlike VAcHT and VMAT2, VIAAT activity is driven by both components of the electrochemical

proton gradient. Therefore, the accumulation of glutamate in GABA- containing SVs, as previously described, will increase  $\Delta\psi$  and  $\Delta\text{pH}$ . In theory, glutamate could have a slight effect on VIAAT activity.

### 2.2.3 Related phenotypes

- [Anxiety-related behaviors](#)

Augmentation of the serotonergic tone is a therapeutic thread to prevent mood and anxiety disorders (Renoir *et al.* 2012). VGLUT3<sup>-/-</sup> mice have a lower 5-HT efflux (Amilhon *et al.* 2010). Behavioral tests ran on mutant mice revealed that null mice have a marked neophobia (marble burying test, novelty- suppressed feeding) and an increased anxiety (elevated plus maze, open field) related to their decreased 5-HT levels. The onset of hyper-anxiety in mutants is very early, as demonstrated by the increased distress call in P8 pups. VGLUT3<sup>-/-</sup> mice are not prone to aggressive behaviors or social avoidance compared to WT littermates (Amilhon *et al.* 2010).

- [Deafness](#)

VGLUT3 is expressed by inner hair cells of the cochlea (Ruel *et al.* 2008, Seal *et al.* 2008). Mice constitutively lacking VGLUT3 are completely deaf, but maintain normal motor and vestibular function (Ruel *et al.* 2008, Seal *et al.* 2008). Their deafness stems from the impossibility for IHCs to release glutamate to convert auditory stimuli into electric signal. Thus, VGLUT3 is involved in maintaining a functional transmission at the first auditory relay. In these mice, the rest of the auditory system is still functioning. Hence, hearing can be restored (up to seven weeks) by VGLUT3 virally-mediated gene delivery in IHCs (Akil *et al.* 2012).

- [Electrographic seizures](#)

The electroencephalogram recordings of VGLUT3<sup>-/-</sup> mice depict some unusual cortical activity that spontaneously and intermittently synchronizes (Seal *et al.* 2008). This demonstrates a neocortical hyperexcitability, characteristic usually associated with convulsive seizures in epilepsy. However, these electrographic seizures are not accompanied by any convulsion (Seal *et al.* 2008).

- [Mechanical hypersensitivity](#)

VGLUT3 is expressed by the low-threshold C-fibre mechanoreceptors of the skin. These cells are activated by light touch and brush, and form unmyelinated fibers that terminate in laminae II and I in the spinal cord dorsal horn. Upon activation, they release glutamate in the dorsal horn (Drew and MacDermott 2009).

VGLUT3<sup>-/-</sup> mice show normal response to low-intensity mechanical stimuli. Yet, VGLUT3 plays a role in mechanical hypersensitivity after inflammation (Seal *et al.* 2009).

Another study demonstrated that under specific etiologic conditions, VGLUT3-positive fibers contribute to the development of mechano-cold hypersensitivity (Draxler *et al.* 2014).

- [Insulin secretion](#)

VGLUT3 is expressed in the pancreatic islets of Langerhans, which mainly contain insulin-secreting  $\beta$ -cells and glucagon-secreting  $\alpha$ -cells. Insulin and glucagon are two hormones that differentially regulate circulating plasma glucose level: insulin promotes glycogenesis and lipogenesis (hypoglycemia) while glucagon favors glycogenolysis and gluconeogenesis (hyperglycemia). These two hormones are stored in secretory vesicles within pancreatic cells cytoplasm.

VGLUT3 is expressed by  $\beta$ -cells, in the insulin-containing secretory granules, along with EAAT2, which is usually associated with the plasmalemma. However, the concentration of glutamate in the secretory granules is maintained low: while VGLUT3 imports the amino acid, EAAT2 extrudes it. The packaged amount of glutamate influences the electrochemical gradient across the secretory granule membrane, and hence regulates insulin secretion (Gammelsaeter *et al.* 2011).

- [Thermoregulation](#)

VGLUT3 is expressed in non-serotonergic neurons of the medullary raphe region. By innervating thermoregulatory effector organs, these neurons mediate thermoregulatory functions, including fever. Glutamate injection in the thoracic spinal cord is followed by thermogenesis in the brown adipose tissue, which suggests a descending control of thermoregulatory functions by non-serotonergic glutamatergic pathways (Nakamura *et al.* 2004). This is coherent with the putative expression of VGLUT3 at the thoracic level of the spinal cord ventral horn (Oliveira *et al.* 2003).

- [Hyperactivity](#)

VGLUT3<sup>-/-</sup> mice have a slight basal hyperlocomotion, similar to that obtained by striatal cholinergic interneuron ablation (CIN-KO; Figure A.29), but preserved motor skills (Kitabatake *et al.* 2003, Gras *et al.* 2008). This hyperlocomotor activity can be rescued with donepezil administration, a centrally AChE (catabolic enzyme of ACh) inhibitor, which suggests the involvement of acetylcholine in the observed phenotype. A more recent study proposed that this hyperlocomotion is circadian-dependent (Divito *et al.* 2015). They found that VGLUT3<sup>-/-</sup> mice are more hyperlocomotive at night, in relation with an increased DA release during the dark cycle (Divito *et al.* 2015).

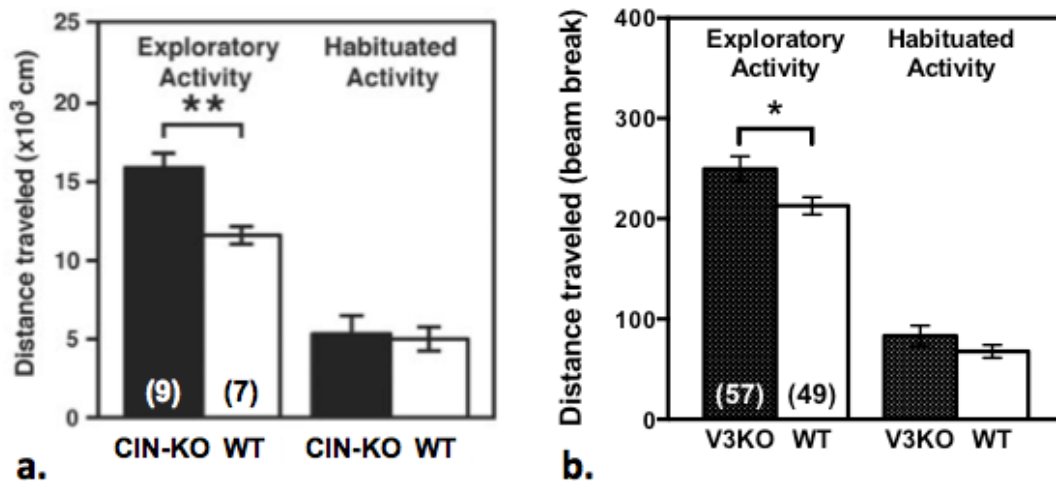


**Figure A.29: Hyperlocomotion induced by acetylcholine or glutamate detuning (60min)**

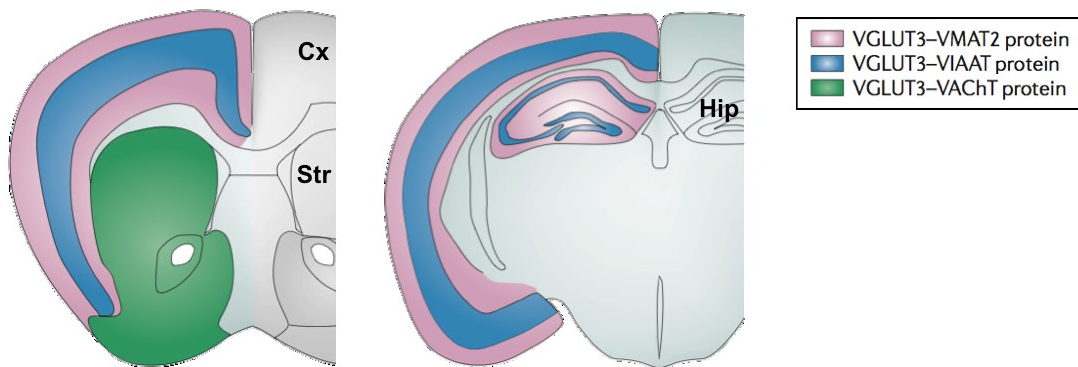
**a.** Selective ablation of cholinergic interneurons (CINs) results in an increased exploratory behavior (CIN- KO, *black bar*) compared to control animals (WT, *white bar*). (Adapted from Kitabatake *et al.* 2003) **b.** As for striatal cholinergic knockouts, VGLUT3<sup>-/-</sup> mice (V3KO, *black bar*) have an increased basal locomotion compared to WT littermates (WT, *white bar*). (NMG, unpublished data).

However, two studies demonstrate that transgenic mice specifically lacking VACHT or VGLUT3 in CINs (VACHT<sup>LoxP/LoxP</sup> x D<sub>2</sub>R-Cre, named Drd2-Cre::VACHT<sup>LoxP/LoxP</sup> or VGLUT3<sup>LoxP/LoxP</sup> x ChAT-IRES-Cre, named ChAT-IRES-Cre::VGLUT3<sup>LoxP/LoxP</sup> respectively) show normal locomotion and motor skills. This suggests that the hyperlocomotive phenotype could have another origin than CINs (Guzman *et al.* 2011, Divito *et al.* 2015).

- Drug-related behaviors

CINs are important regulators of striatal activity. VGLUT3<sup>-/-</sup> mice are hypersensitive to the hyperlocomotor effect of cocaine, with a 2.5-fold hyperlocomotion compared to wild-type (WT) siblings (Gras *et al.* 2008). A more recent study, also conducted by our team, focused on a full characterization of cocaine effects on VGLUT3<sup>-/-</sup> mice (Sakae *et al.* 2015). This work will be further discussed in the final part of the introduction.

**VGLUT3 is expressed in non-glutamatergic neurons, along with other vesicular transporters. These cophenotypes suggest an interplay between glutamate transmission and other neurotransmission systems through co-release (5-HT, ACh and GABA) and have implications for behavioral, neurological and mental disorders.**



Adapted from El Mestikawy *et al.* (2011)



## PART III.

# THE STRIATUM



### 1. Anatomy of the striatum

Striatum is a brain region of the basal ganglia that receives massive excitatory inputs from the cortex and the thalamus. These inputs convey sensorimotor, limbic and cognitive information. Striatum mainly projects to the substantia nigra and the globus pallidus to encode motor control. It is also involved in motivational and reward processes, as well as learning of skills and habits.

#### 1.1 Matrix versus striosomes

Striatum is a macroscopically heterogenous structure in terms of cell distribution. Some regions are densely packed (clusters of 1'500 to 15'000 cells; Goldman-Rakic (1982)) and called **striosomes** (or patches). These regions are surrounded by loosely- packed cells that form the so-called **matrix**. The striosomal volume represents 15 to 20 percent of striatal total volume (Gerfen 1992).

The striosomal organization into two compartments is associated with a differential expression of a large number of transmitter- related markers. For instance, striosomes are defined as [ $\mu$ - opioid receptor (MOR) / substance P (SP)]- rich and AChE- poor regions whereas the matrix is rather an [enkephalin (Enk) / AChE]- rich compartment (Graybiel and Ragsdale 1978, Bolam *et al.* 1988, McGeorge and Faull 1989, Crittenden and Graybiel 2011).

Moreover, striatal organization into patch and matrix compartments is also related to input- output connections, including the laminar organization of the cortex. Striatal patches preferentially receive afferents from deep cortical layers whereas superficial cortical layers send projections to the matrix (Gerfen 1992). Limbic cortical areas (orbitofrontal, anterior cingulate, and insular cortices) preferentially innervate striosomes, whereas projections from the somatosensory, motor, and associative cortices terminate mainly in the matrix. Since the amygdala, hippocampus, and nucleus accumbens are interconnected with the orbitofrontal, anterior cingulate, and insular cortices, this supports the idea that striosomes are part of a limbic circuit embedded in the sensorimotor and associative striatum (Figure A.38a; Crittenden *et al.* (2011)).

In summary, the traditional view of striatal connectivity stated that striosomal compartment participates to limbic forebrain circuits, while extra- striosomal

compartment is involved in sensorimotor / associative forebrain circuits (Brimblecombe and Cragg 2017).

Contrary to the previous studies, results show that patch / exo-patch and matrix neurons receive both limbic and sensorimotor information (Smith *et al.* 2016). This new vision raises many functional questions about striatal activity.

## 1.2 Functional compartmentalization

Striatum can be divided in functionally different sub-areas, based on the nature of their inputs: the ventral striatum, and the caudate and putamen nuclei (Figure A.30). In humans the internal capsule separates the caudate and the putamen, while they are merged together in rodents. More recently, it was proposed that striatum should be divided in three communities based on the cortico-striatal projectome: the rostral, the intermediate and the caudal striata (Hintiryan *et al.* 2016).

Globally, striatum receives glutamatergic inputs (cortex, thalamus, amygdala and hippocampus), as well as midbrain DA and GABA projections, but also cholinergic innervation from the brainstem...

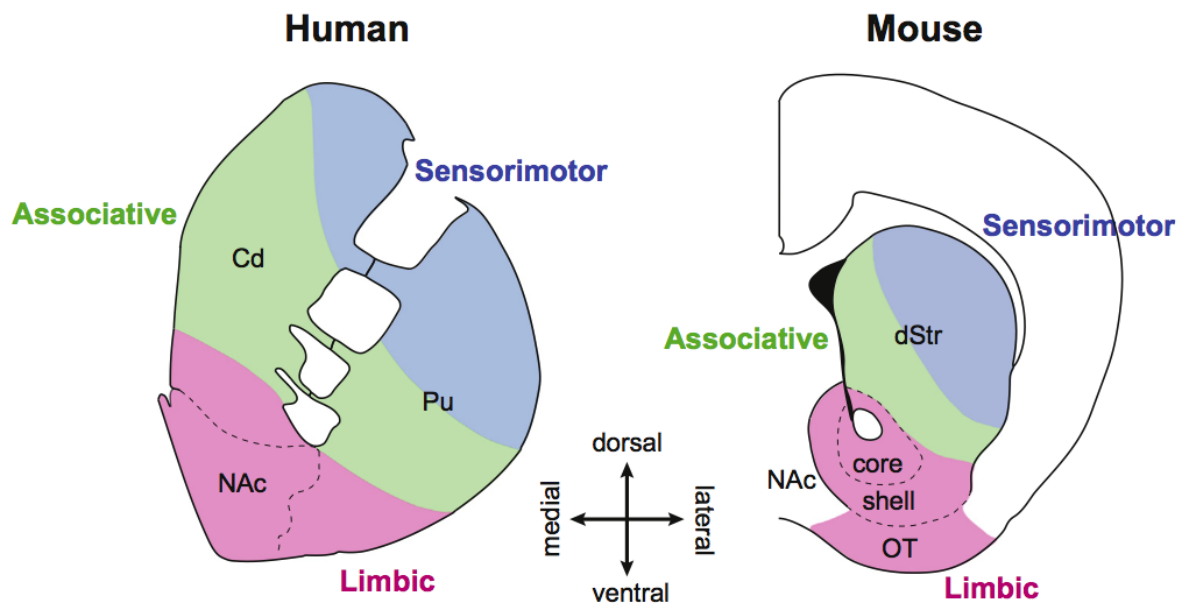


**Figure A.30: Functional subdivisions of the striatum in humans and rodents**

Functionally, the striatum (Str) can be divided into limbic (*magenta*), associative (*green*), and sensorimotor (*blue*) regions, in both human (**left**) and rodent (**right**), determined by cortical inputs mediating each function. The nucleus accumbens, which makes up the ventral Str, is indicated by the *dashed lines*. In mouse, a *second dashed line* indicates the border between the NAc core and shell. Cd, caudate; dStr, dorsal striatum; OT, olfactory tubercle; Pu, putamen.

From Chuhma *et al.* (2017)

- Nucleus accumbens

Along with the olfactory tubercles, the **nucleus accumbens (Acb)** constitutes the ventral striatum (vStr). Acb is part of the limbic striatum (Figure A.30). It is a central structure that participates in higher order brain functions, such as reward-related behaviors, motivation, learning and memory (Di Chiara 2002). It has been considered as an interface between the limbic and motor systems (Zahm and Brog 1992). It integrates signals arising from limbic areas (amygdala, hippocampus and hypothalamus) and cortical areas (prefrontal cortex). It also modulates reward-related motor output of various goal-directed behaviors, through dopaminergic afferents arising from the VTA. The nucleus accumbens consists in two distinct subregions. The accumbens shell (AcbSh) is part of a limbic circuit, with primarily projections to limbic structures. The accumbens core (AcbC) projects to motor-related regions of basal ganglia (Heimer *et al.* 1991).

- Dorsal striatum

The dorsal striatum (dStr) participates to habit formation, motor functions, cognitive flexibility and cue-induced behaviors (Everitt and Robbins 2013, Prado *et al.* 2017). It can be divided in two parts: the dorsolateral striatum and the dorsomedial striatum. The **dorsomedial striatum (DMS)** is the associative part of the striatum. It receives inputs from the prefrontal cortex and limbic regions (Gerfen 1992). It is involved in behavioral flexibility, reward-associated motor learning and reaction time.

The **dorsolateral striatum (DLS)** constitutes the striatal sensorimotor territory. It receives strong afferents from the motor and premotor cortices, and is particularly important for habit formation (Gerfen 1992). In human, the dStr is formed of two distinct nuclei: the caudate nucleus corresponds to the DMS, while the putamen nucleus corresponds to the DLS. Together, they form the caudate-putamen (CPU).

### **1.3 Striatal cytoarchitecture**

The vast majority of striatal neurons are GABAergic spiny projection neurons (~ 95%) called medium spiny neurons. They are the only neurons projecting out of the striatum. The remaining 5 % are mainly local interneurons, either cholinergic or GABAergic.

#### **1.3.1 Medium spiny neurons**

Against the popular belief, medium spiny neurons (MSNs) differ in their anatomical and physiological properties, which mirror differences in their network connections and biochemistry (Gertler *et al.* 2008). They can also be distinguished by the expression of specific DA receptor subtypes: **i)** the D<sub>1</sub>R-expressing MSNs, which project to the substantia nigra (SN) and **ii)** the D<sub>2</sub>R-expressing MSNs, which project to the globus

pallidus (GP). Each of these two types expresses a specific set of signaling molecules, as detailed below.

The majority of MSNs are located in the matrix regardless of their downstream connectivity (Crittenden *et al.* 2011). In terms of proportion, there is as much D<sub>1</sub>R- and D<sub>2</sub>R- in the striatum, and these two populations are intermingled (Gangarossa *et al.* 2013, Ren *et al.* 2017).

MSNs share baseline electrophysiological properties. Their resting potentials are very negative (-90 mV) and they have a low input resistance. This makes them silent at basal state. They are densely studded with dendritic spines, where they are connected by a large number of glutamatergic and dopaminergic afferents (Smith and Bolam 1990, Jiang and North 1991). Locally, MSNs send axon collaterals that supply the striatum with a large and dense arborization (Kreitzer 2009). This network allows synaptic interconnectivity with other MSNs and striatal interneurons.

Their activity is related to the execution of a task or movement, and they usually fire before or right after the onset of the movement (Kimura 1986).

### **D<sub>1</sub>R-expressing MSNs**

D<sub>1</sub>R-expressing MSNs (D1-MSNs) project monosynaptically to the globus pallidus *internalis* (GPi, medial part) and the substantia nigra *pars reticulata* (SNr). Yet, most D1-MSNs also send collaterals to the GPe, thus forming a functional bridge between the direct and indirect pathways (Cazorla *et al.* 2015).

D1-MSNs express two neuropeptides that are very important for local modulation of other neurons: substance P and dynorphin (Dyn). The endogenous opioid Dyn acts on  $\kappa$ -opioid receptors that are homogeneously distributed within the striatum. They also express high levels of the muscarinic receptor M<sub>4</sub>R, which exerts an opposing effect compared to D<sub>1</sub>R (Ena *et al.* 2011). They also carry the GPCR adenosine receptor 1 (A<sub>1</sub>R), which is coupled to G $\alpha_{i/o}$  and leads to AC inhibition upon adenosine binding (Beaulieu *et al.* 2015).

### **D<sub>2</sub>R-expressing MSNs**

D<sub>2</sub>R-expressing MSNs (D2-MSNs) project to the globus pallidus *externalis* (GPe, lateral part). They form a multisynaptic pathway to the output nuclei of basal ganglia. They are enriched with the neuropeptide enkephalin. This endogenous opioid acts on  $\delta$ - and  $\mu$ -opioid receptors (DOR and MOR) that are highly enriched in the striatum, especially in the striosomes (Figure A.49; Koizumi *et al.* (2013)). Opioid receptors are GPCRs negatively coupled to AC. Conversely to D1-MSNs, D2-MSNs carry the GPCR adenosine receptor 2A (A<sub>2A</sub>R), which is coupled to G $\alpha_s$  and leads to cAMP stimulation upon adenosine binding and thus antagonizes D<sub>2</sub>R (Ena *et al.* 2011).

### D<sub>1</sub>R/D<sub>2</sub>R-expressing MSNs

The majority of D<sub>1</sub>- or D<sub>2</sub>- expressing neurons are segregated in two populations. Yet, it was observed that in the dStr, approximately 5% of MSNs co-express D<sub>1</sub>- and D<sub>2</sub>R, whereas this number reaches 15 - 30% in Acb subregions (Matamales *et al.* 2009). D<sub>1</sub>R and D<sub>2</sub>R can form heteromers in a region-dependent proportion (Bertran-Gonzalez *et al.* 2008, Perreault *et al.* 2010). They seem to constitute a third pathway that mostly targets the substantia nigra *pars compacta* and that is differentially affected by dopaminergic deafferentation (Gagnon *et al.* 2017). A recent study using a double BAC (bacterial artificial chromosome) transgenic mouse (D1-tdTomato and D2-eGFP) found less than 1% co-localization of the two receptors in the CPu, suggesting the previous values may be overestimated (Ren *et al.* 2017).

From a molecular point of view, these cells express peptidic markers of both D<sub>1</sub>- and D<sub>2</sub>- MSNs, *i.e.* dynorphin and enkephalin respectively (Perreault *et al.* 2010). It has been proposed that D<sub>1</sub>/D<sub>2</sub>R heteromers are coupled to another G- protein, G<sub>αq/11</sub> that activates PLC (Perreault *et al.* 2011). Yet, this specific coupling to G<sub>αq</sub> has been recently challenged (Frederick *et al.* 2015).

### 1.3.2 Striatal interneurons

Apart from the principal GABAergic spiny population of the striatum, a small number of aspiny interneurons play a critical role in local modulation of signal integration and striatal output (Figure A.31). These interneurons consist in large cholinergic interneurons and medium- sized GABAergic interneurons (Kreitzer 2009).

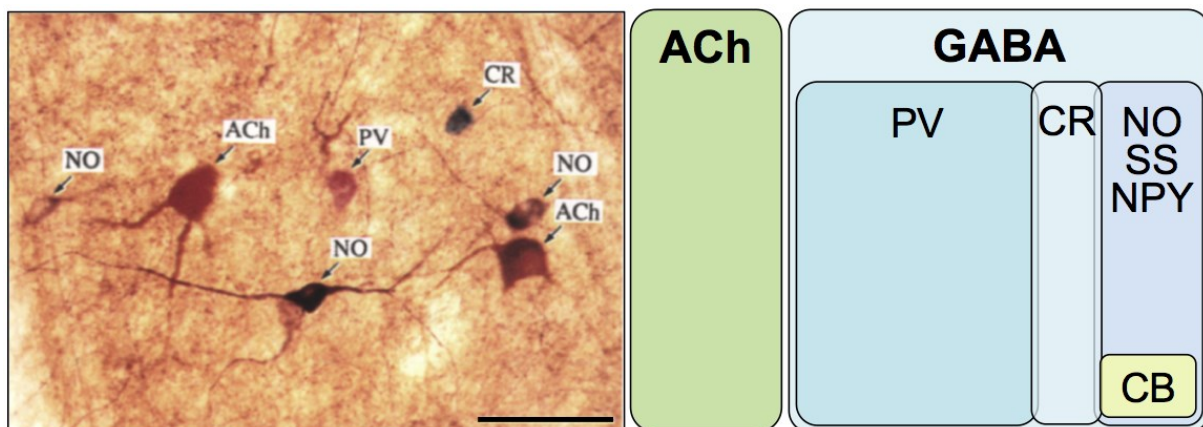


**Figure A.31: Cytology of striatal interneurons**

**Left side:** Immunohistochemistry of cholinergic INs (ACh, *in brown*) and GABAergic nitric oxide- (NO, *in purple*), parvalbumin- (PV, *in red*) and calretinin- expressing (CR, *in green*) GABAergic INs. Scale bar = 50  $\mu$ m. **Right side:** Shared chemical compositions of striatal INs. The size of the boxes is proportional to the relative number of cells that are immunoreactive for a substance. CB, calbindin D<sub>28k</sub>; SS, somatostatin; NPY, neuropeptide Y.

Adapted from Kawaguchi *et al.* (1995)

- Cholinergic interneurons

Cholinergic interneurons, also known as tonically active neurons (TANs), are large aspiny neurons that account for about 1-3% of striatal neurons (Zhou *et al.* 2002). Despite their small number, they have particularly widespread dendritic and axonal arborizations that densely innervate the entire striatum. They are considered as major regulators of striatal activity (Kreitzer 2009). It has been estimated that each CIN possess around 500'000 varicosities (Lim *et al.* 2014).

CINs receive direct afferents from the thalamus and cortex, as well as dopaminergic inputs (Wilson *et al.* 1990, Kawaguchi *et al.* 1995). Their somata are mainly localized in the matrix, close to matrix-striosome boundaries. Their axonal arborization is found in both compartments, while the dendrites are restricted to the matrix (Crittenden *et al.* 2014, Crittenden *et al.* 2017). In terms of general distribution, the rostral striatum contains a higher density of CINs than the caudal one, and the distribution in the dStr is much larger than in the vStr (Matamales *et al.* 2016). Moreover, CINs are more numerous in the AcbSh than the AcbC, in line with VGLUT3 distribution (Herzog *et al.* 2004, Matamales *et al.* 2016).

### **Electrophysiological and chemical properties**

CINs are tonically active. They present small spontaneous depolarizing potentials that summate to trigger APs, because their resting potential (-60 mV) is only 5 mV below the AP threshold (Wilson *et al.* 1990). Therefore, there is a constant exocytic efflux of ACh in the striatum, as Ca<sup>2+</sup> removal from the medium leads to a rapid decline of extracellular ACh levels (Mandel *et al.* 1994, Bickerdike and Abercrombie 1997). This sustained efflux ensures relatively high extracellular levels of ACh, especially in the striosomes where AChE activity is lower.

Three reliable markers are used to identify CINs: ChAT, VACHT and the choline plasmalemmal transporter CHT (Prado *et al.* 2017). The gene encoding VACHT is entirely embedded in the first intron of ChAT encoding gene. Despite their common locus, their corresponding mRNAs are expressed with different ratios throughout the brain (Eiden 1998, Weihe *et al.* 1998). There is also one reliable surrogate marker of CINs activity, which has been shown to follow their spiking pattern under basal and stimulated conditions: the phospho-ribosomal protein S6 (p-rpS6; Bertran-Gonzalez *et al.* (2012)).

CINs express different plasmalemmal receptors. For example, 80% of CINs express the dopamine receptor D<sub>2</sub>R and D<sub>5</sub>R, and DA inhibits ACh release in the dorsal striatum (Bernard *et al.* 1991, DeBoer *et al.* 1996, Chuhma *et al.* 2014). On the other hand, DA neurons photostimulation induces action potentials in CINs of the AcbSh (Chuhma *et al.* 2014). They also carry type 2 muscarinic receptors (M<sub>2</sub>R) as autoreceptors, which are negatively coupled to AC (Bernard *et al.* 1992). Thus, ACh negatively regulates its own

release (Alexander 2004). Interestingly, all CINs express VGLUT3, which synergizes acetylcholine tone (Gras *et al.* 2008), and about 85% of VGLUT3-positive varicosities are cholinergic (Sakae *et al.* 2015). CINs also express NK-1 (neurokinin 1), the SP receptor. Therefore, these cells are subjected to a phasic regulation by D1-MSNs that release SP (Gerfen 1992, Commons *et al.* 2009). It is important to note that the receptors described here only represent a few receptors on CINs surface. The regulation exerted by neuropeptides and other neurotransmitters is very complex. CINs have been described as expressing thirty different types of receptors (for an exhaustive listing, refer to Lim *et al.* (2014)).

### Functional properties

Striatal cholinergic interneurons are involved in many processes, such as associative learning, reward processing and motor control (Prado *et al.* 2017). Their impairment leads to cognitive flexibility deficits in reversal learning tasks, or to hypersensitivity to drugs (Kitabatake *et al.* 2003, Prado *et al.* 2017). CINs ablation also yields important motor and procedural learning defects (Kaneko *et al.* 2000, Kitabatake *et al.* 2003). In addition, it was demonstrated that in the nucleus accumbens, CINs play a critical role in drug response. Mice lacking CINs are more sensitive to drugs, while accumbal ACh enhancement prevents their addictive effects (Hikida *et al.* 2001, Hikida *et al.* 2003). They play a critical role in network regulation during presentation of learned or salient sensory cues, and demonstrate a particular “fire-pause-rebound” pattern of activity (see au-dessous 2.1.3: Acetylcholine / dopamine activity during behavior).

- GABAergic interneurons

There are several non-overlapping classes of striatal GABAergic interneurons. They are sorted according to their morphological and electrophysiological properties, but mainly on their neuropeptide content: the parvalbumin (PV)-expressing, the calretinin (CR)-expressing and the [somatostatin (SS)-, neuropeptide Y (NPY)- and nitric oxide synthase (NOS)]-expressing interneurons (Kawaguchi *et al.* 1995). The GABA synthesizing enzyme, glutamate decarboxylase (GAD67), densely stains all these interneurons, unlike MSNs that express the GAD65 isoform.

### Parvalbumin-expressing INs

The parvalbumin-expressing interneurons (PV-INs) are the most common GABAergic interneurons in the striatum. They are expressed in both striosomal and matrixial compartments. However, they are enriched in the DLS, suggesting a role in sensorimotor integration. They are thought to represent about ~2% of total striatal neuronal population. They have large dendritic and axonal arborizations without apparent regard for the boundaries between compartments (Kreitzer 2009). They receive a large number of afferents from the cortex and thalamus, and make somatodendritic asymmetric

synapses on MSNs. They also have Gap junctions, which means they form electrical synapses and thus form a continuous network (Kawaguchi *et al.* 1995). These neurons have a very dynamic electrophysiological activity, and are also called fast-spiking (FS) interneurons. They can fire at high frequency with short-duration APs (Kreitzer 2009).

### **Somatostatin/neuropeptide Y/NO synthase-expressing INs**

Somatostatin /neuropeptide Y /NO synthase-expressing interneurons are found in both compartments. They preferentially innervate the matrix, and their axons often cross the compartmental boundaries (Kreitzer 2009). Their aspiny dendritic and axonal fields are larger than that of other interneurons (Centonze *et al.* 1999). Since they express NOS, they can release NO. They receive cortical, dopaminergic and cholinergic innervation, and make somatodendritic synapses onto MSNs (Kawaguchi *et al.* 1995). In addition to fast spikes, they can generate large and persistent plateau depolarizations, and thus are classified as low-threshold spiking (LTS)-interneurons (Kreitzer 2009).

These neurons release different transmitters depending on their pattern of firing: GABA, NO, NPY, SS. For example, it was demonstrated that upon high-frequency stimulation, they release NO, which blocks NMDARs on MSNs upon intracellular signaling (Centonze *et al.* 1999). Like CINs, they carry the SP receptor NK-1, and the muscarinic receptor M<sub>2</sub>R (Bernard *et al.* 1998).

### **Calretinin-expressing INs**

Calretinin-expressing (CR)-interneurons are LTS-interneurons. They are not well characterized. They do not receive thalamic projections (Kreitzer 2009).

## **2. Striatal connectivity**

### **2.1 Striatal afferents**

#### **2.1.1 Glutamatergic innervation**

Cortical and thalamic neurons make excitatory synaptic connections onto MSNs in similar proportions.

- Cortical innervation

All major cerebral cortex regions send excitatory glutamatergic projections to the striatum with an ipsilateral predominance, and each striatal locus receives projections from several cortical regions (McGeorge *et al.* 1989). Individual axons from the cerebral cortex innervate MSNs within a single compartment. These MSNs process the information and communicate with neighboring areas via GABAergic interneurons and CINs, whose dendrites can cross patch/matrix delineation. Additionally, these corticostriatal projections make monosynaptic contacts onto CINs and LTS-interneurons (Kreitzer

2009). The corticostriatal projections are VGLUT1-ir, as this transporter is responsible for glutamatergic uptake in SVs (Figure A.30; Wouterlood *et al.* (2012)). Two recent studies, based on tracing experiments, reveal that cortico-striatal and thalamo-striatal projections are more complex than previously described. Together, they define more striatal subterritories than associative, sensorimotor and limbic areas (Hintiryan *et al.* 2016, Hunnicutt *et al.* 2016).

- Subcortical innervation

The thalamus sends VGLUT2-ir excitatory terminals to the striatum. These projections reach both MSNs and CINs and make asymmetric synapses onto dendritic shafts (mainly in the matrix) and dendritic spines (Smith *et al.* 1990). The synapses made on dendritic shafts are thought to be projections from the thalamic parafascicular nucleus on the CINs. There is a dorsolateral-ventromedial gradient of VGLUT2 in the striatum, with a predominant innervation of the medial AcbSh (Figure A.32; Wouterlood *et al.* (2012)).

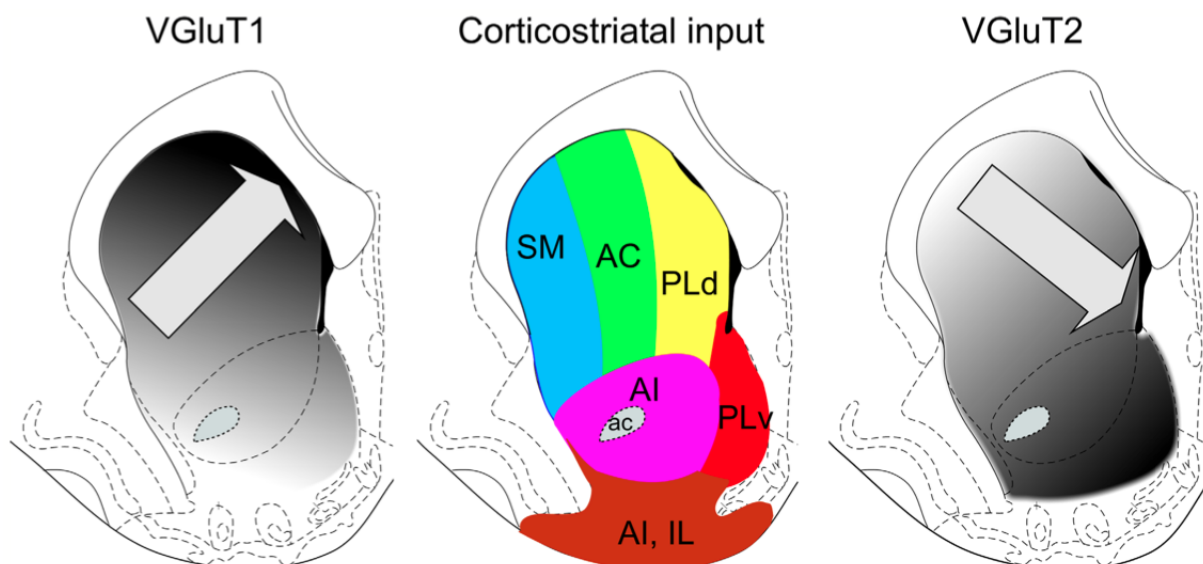


**Figure A.32: VGLUT1 and VGLUT2 distribution in the striatum**

VGLUT1 (**left section**) and -2 (**right section**) predominantly represent cortical and thalamic inputs respectively. The striatal subregions in the **central section** delineate inputs from midline and intralaminar thalamic nuclei and prefrontal cortical regions. SM: somatomotor cortex; AC: anterior cingulate cortex; PLd: dorsal prelimbic cortex; PLv: ventral prelimbic cortex; AI: anterior insular cortex; IL: infralimbic cortex.

From Wouterlood *et al.* (2012)

### 2.1.2 Midbrain DA neuromodulation

Two midbrain structures send dopaminergic projections to the striatum: i) the mesolimbic pathway originating from the VTA and ii) the nigrostriatal pathway originating from the SNc (Figure A.33). These projections are topographically organized along a dorsoventral, mediolateral, and rostrocaudal axes (Gerfen and Surmeier 2011). The dStr

receives more DAergic inputs than the vStr. However, DA equivalently modulates cortical and thalamic inputs (Chuhma *et al.* 2017).

Dopaminergic neurons have two modes of firing. At basal state, they exhibit a tonic firing ( $\sim 4$  Hz in rodents) that sustains striatum with low levels of DA. Superimposed on this activity are phasic bursts of APs ( $\sim 15$  Hz), which yield an extracellular DA concentration of 500 nM (Kreitzer 2009, Sulzer 2011). These bursts can be elicited by unexpected reward and reward-related cues. This will be further discussed in the following section. Extracellular levels of DA are finely regulated thanks to the presence of DA transporter (DAT) on their terminals and also of D<sub>2</sub>R autoreceptors that inhibit DA release.

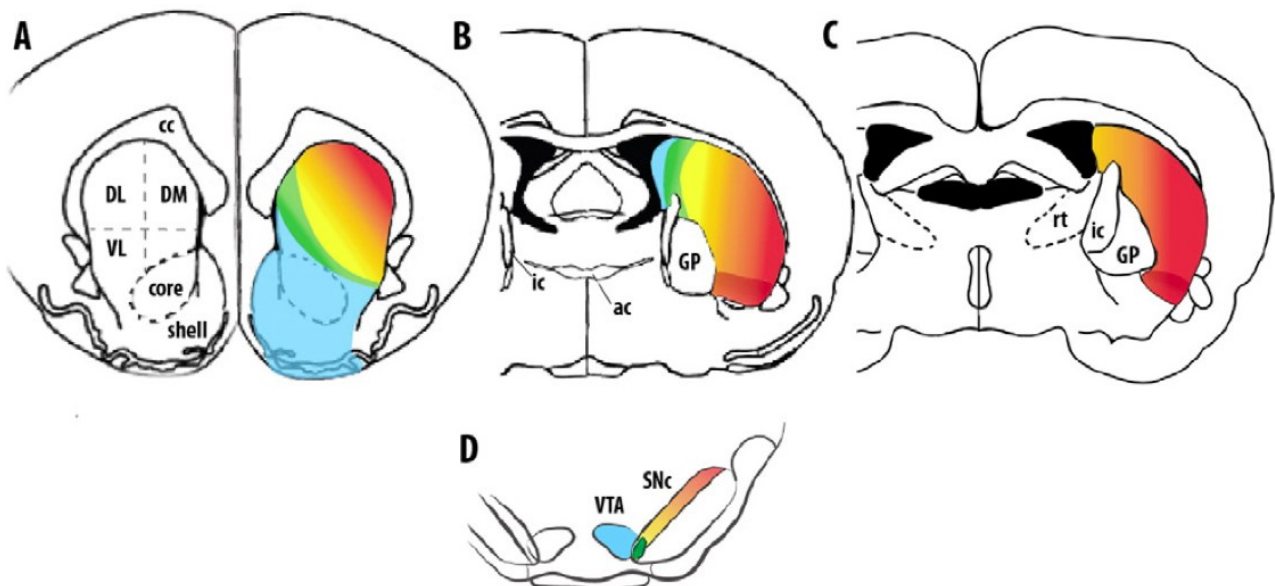


**Figure A.33: Organization of dopaminergic projections to different striatal subregions**

Midbrain DA neurons (**D**) project topographically (*indicated by color spectrum*) to the striatum along the mediolateral axis (**A**, **B**, **C** illustrate three rostrocaudal levels). More medially located DA neurons in the ventral tegmental area (VTA) project to the ventral Str, (nucleus accumbens shell and core). More laterally located DA neurons in the substantia nigra *pars compacta* (SNc) project to more lateral dorsal Str regions (DL). DM: dorsomedial Str; VL: ventrolateral Str.

From Cenci *et al.* (2015)

- [Mesolimbic pathway](#)

The mesolimbic dopaminergic system is involved in reward-guided behaviors. It is important for the acquisition of behaviors that are reinforced by salient drives of the environment or by addictive drugs. Drugs act specifically on this pathway, either locally in the VTA, or in the target region Acb, to elevate accumbal DA level (Luscher and Ungless 2006).

- [Nigrostriatal pathway](#)

The nigrostriatal pathway originates from the SNc and projects to the dorsal striatum. It is involved in locomotor tasks and its defects are responsible for the locomotor phenotypes occurring in Parkinson's disease (PD) or Huntington's disease (HD). The ventral part of the SNc mainly innervates the striosomal compartment, while the dorsal part seems to aim the matrix.

### 2.1.3 Serotonergic innervation

Serotonin (5-HT) is a neuromediator involved in mood regulation, pain and vigilance states. The dorsal raphe sends projections to the striatum, more particularly to the Acb (Geyer *et al.* 1976, Vertes 1991). Projections arising from the DRN connect many structures thanks to their numerous collaterals. Most of these fibers form *en passant* synapses and have more than two thousands varicosities (Gagnon *et al.* 2014). These varicosities are either 5-HT-positive / VGLUT3-positive (large varicosities) or 5-HT-positive / VGLUT3-negative (small varicosities). In the striatum, around 15% of VGLUT3-positive terminals are serotonergic (Sakae *et al.* 2015). Serotonergic fibers in the striatum are often collaterals of axons innervating the substantia nigra *pars compacta*. These fibers are believed to exert a double control over the striatum, both on the striatonigral and the nigrostriatal projections (Vertes 1991, Gagnon *et al.* 2014).

Many studies have supported the idea that DRN is involved in the reward circuitry because of its extensive connections to reward-related structures. It had been proposed that DRN neurons would encode punishment by antagonizing DA action (Daw *et al.* 2002, Cools *et al.* 2011). However, other studies have shown that activation of serotonergic DRN neurons positively signals reward via 5-HT / glutamate action (Liu *et al.* 2014). A more recent study redirected the discussion by proposing that serotonergic neurons from the DRN would signal both types of information, but on different timescales (Cohen *et al.* 2015).

Serotonergic striatal projections exert dual effects on CINs (Virk *et al.* 2016). In the dorsal striatum, 5-HT stimulates CINs by acting on 5-HT<sub>2</sub>Rs (G<sub>αq</sub>-coupled), 5-HT<sub>6</sub>Rs and 5-HT<sub>7</sub>Rs (G<sub>αs</sub>-coupled), whereas it hyperpolarizes them in the Acb via 5-HT<sub>1A</sub>R and 5-HT<sub>1B</sub>R (Blomeley and Bracci 2005, Lim *et al.* 2014, Virk *et al.* 2016). The 5-HT system also regulates all major dopaminergic pathways through several 5-HT receptors subtypes. The following 5-HT receptors subtypes facilitate DA release: 5-HT<sub>1A</sub>R, 5-HT<sub>1B</sub>R, 5-HT<sub>2A</sub>R, 5-HT<sub>3</sub>R and 5-HT<sub>4</sub>R. In contrast, 5-HT<sub>2c</sub>R, which is characterized by high levels of constitutive activity, inhibits both tonic and phasic DA release (Alex and Pehek 2007).

### 2.1.4 Cholinergic innervation

Classically, CINs have been considered as the sole source of acetylcholine in the striatum. However, different studies proved that projections arising from the mesopontine tegmentum of the brainstem provide a monosynaptic cholinergic innervation to the striatum (Woolf and Butcher 1986, Dautan *et al.* 2014). This cholinergic projection is topographically organized. The pedunculopontine nucleus (PPN) preferentially innervates the DLS, while the medial and ventral striata are targeted by the laterodorsal tegmental nucleus (LDT Dautan *et al.* 2014). It has been proposed that this cholinergic pathway plays an essential role in striatal modulation. Indeed, cholinergic projections arising from PPN and LDT specifically innervate the matrix, and also send collaterals to both thalamus and VTA (Dautan *et al.* 2014). However, it seems likely that this striatal innervation is minimal, because mice depleted from VACHT specifically in the CINs have less than 1% residual VACHT labelling in the striatum (Guzman *et al.* 2011). Another study also supported this idea by crossing VGLUT3-Cre mice with a reporter line (Isl-tdTomato); no Tomato staining was visible in the hindbrain cholinergic nuclei (Divito *et al.* 2015).

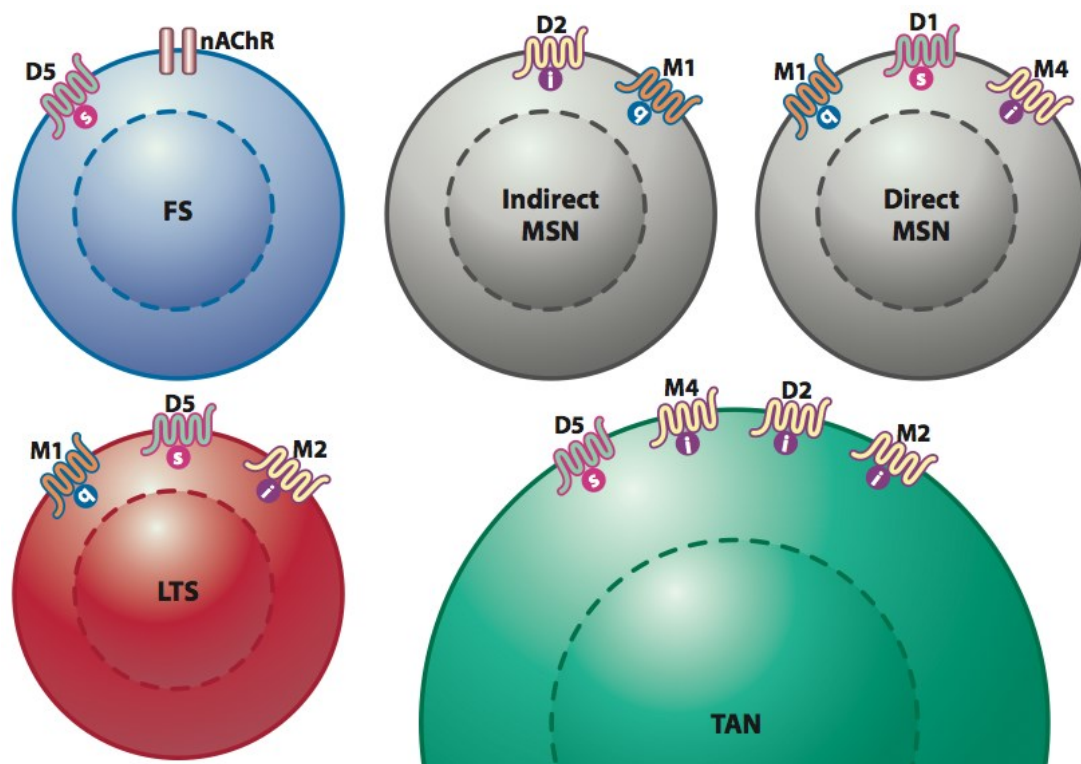


**Figure A.34: Dopaminergic and cholinergic modulation of striatal neurons**

Striatal neurons express different types of dopamine and acetylcholine receptors. Striatopallidal (indirect) and striatonigral (direct) MSNs are shown *in gray*. FS and LTS GABAergic interneurons are depicted *in blue and red*, respectively, and cholinergic interneuron is shown *in green*. GPCRs are displayed with their associated G-protein:  $G\alpha_s$  (magenta),  $G\alpha_i$  (purple), or  $G\alpha_q$  (blue). FS interneurons also express the ionotropic nicotinic ACh receptor.

From Kreitzer (2009)

## 2.1 Striatal activity modulation

In the striatum, both CINs and DA fibers form dense intermingled arborizations. ACh and dopamine convergently but antagonistically regulate the activity of principal MSNs (Kaneko *et al.* 2000). These two neurotransmitters are tonically released in the striatum and act by a widespread volumic transmission (Kreitzer 2009). Striatum neurons display different sets of DA and ACh receptors (Figure A.34). Likewise, both transmitters act on glutamatergic or dopaminergic terminals in the striatum, thus exerting a presynaptic control (Calabresi *et al.* 2000).

### 2.1.1 DAergic modulation

Each DAergic neuron sends axonal varicosities to a compact zone of the striatum, representing up to 5% of the total striatal volume. Altogether, DAergic boutons represent nearly 10% of all striatal synapses (Kreitzer 2009). The non-synaptic release of DA yields a volumic transmission that targets extrasynaptic receptors. The nature and location of these receptors determines the output. DA can modulate cell excitability when acting on postsynaptic targets, or exocytic release when binding to presynaptic targets on the excitatory inputs. All striatal cells express DA receptors.

- Dopamine receptors

Five subtypes of DA receptors mediate the physiological functions of DA, namely D<sub>1</sub>-D<sub>5</sub>R, encoded in human by *DRD1-5* genes respectively. They can be classified into two categories regarding their coupling to G- proteins. Canonically, DA receptors are coupled to adenylate cyclase, but recent evidence stressed out the fact that cAMP-independent mechanisms are involved in their functions (for review, see Beaulieu *et al.* 2015).

#### D<sub>1</sub>- class receptors

This class, which comprises D<sub>1</sub>R and D<sub>5</sub>R, is positively coupled to G<sub>α<sub>s,olf</sub></sub> and to cAMP pathway (Figure A.35, left panel). The production of cAMP results in PKA activation. One of PKA substrates is DARPP- 32 (dopamine and cAMP- regulated phosphoprotein), which acts as a negative regulator of protein phosphatase 1 (PP-1) when phosphorylated on Thr34, therefore promoting iGluRs phosphorylation to increase glutamatergic signaling. On the other hand, DARPP- 32 phosphorylation on Thr75 by the cyclin- dependent kinase 5 (CDK5) results in a negative retrocontrol of PKA (Greengard 2001, Gerfen *et al.* 2011, Beaulieu *et al.* 2015). More recently, some evidence showed that these receptors are also coupled to G<sub>q</sub> and to PLC transduction cascade (Beaulieu *et al.* 2015).

Striatal INs all express D<sub>5</sub>R (Figure A.35; Kreitzer (2009)). D<sub>1</sub>-class receptors have a low affinity for DA and thus need a prior elevation of extracellular DA to be recruited. Therefore, D<sub>1</sub>-like receptors are preferentially activated during phasic activity of DAergic neurons (Kreitzer 2009).

## D<sub>2</sub>- class receptors

This class is composed of D<sub>2</sub>R, D<sub>3</sub>R and D<sub>4</sub>R. They are coupled to G<sub>αi,o</sub> and inhibit cAMP production (Figure A.35, right panel). These receptors have a high affinity for DA, and are activated at basal state thanks to the tonic activity of DAergic neurons (Kreitzer 2009). In the striatum D<sub>2</sub>- MSNs and CINs express D<sub>2</sub>R (only 20% of CINs express D<sub>2</sub>R in the AcbSh).

Recent reports also impute non- canonical roles to D<sub>2</sub>R (for review, see Beaulieu *et al.* 2015). For example, G<sub>βγ</sub> subunits are linked to PLC activation and promote calcium release from intracellular stores to activate downstream calcium- dependent kinases such as PKC and CaMKII (Beaulieu *et al.* 2015).

As for D<sub>1</sub>R, Activation of D<sub>2</sub>R recruits several cascades converging on NMDAR and AMPAR subunits phosphorylation.

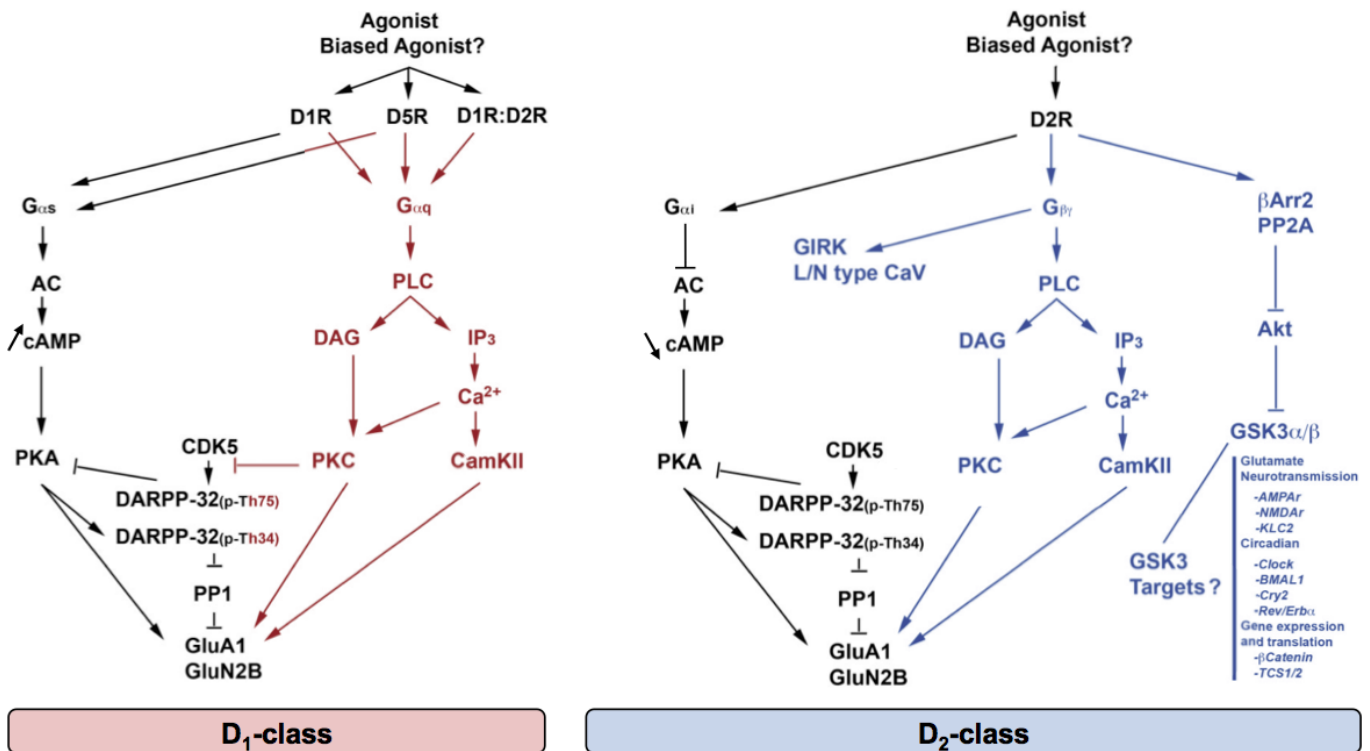


**Figure A.35: D<sub>1</sub>R and D<sub>2</sub>R signaling cascades**

Canonical coupling of DA receptor class I (**left side**) and class II (**right side**) to G<sub>α</sub> and cAMP transduction cascade (*in black*). D<sub>1</sub>- class receptors and D<sub>2</sub>R are also involved in cAMP- independent cascades (*in red or blue respectively*).

Adapted from Beaulieu *et al.* (2015)

- [DA is released along with other nTs](#)

However, the picture is not that simple. Indeed, within the past few years, DAergic neurons were demonstrated to release multiple nTs (Vaaga *et al.* 2014, Chuhma *et al.* 2017). For example, glutamate is released by some VTA- originating DA neurons after its vesicular accumulation by VGLUT2 (Hnasko *et al.* 2012). Co-transmitted glutamate elicits EPSC in both MSNs and CINs in the vStr, and particularly in the medial AcbSh. Surprisingly, it was reported that GABA is packaged in a VIAAT-independent / VMAT2-dependent way by DA-containing SVs (Tritsch *et al.* 2012). Co-released GABA will elicit IPSCs mostly in MSNs in the AcbC and the dStr (Chuhma *et al.* 2017). Overall, it appears that DA phasic firing in the vStr activates CINs thanks to glutamatergic signaling, whereas in the dStr, MSNs and CINs express a pause of firing mediated by D<sub>2</sub>R and GABA signaling {Chuhma, 2014 #43; Nelson, 2014 #1140; Chuhma, 2017 #979}.

### 2.1.2 Cholinergic modulation

In the striatum, all neural types express either nicotinic AChR receptors and / or muscarinic AChR receptors (mAChR). Therefore, CINs exert a strong modulation over the entire striatum, including themselves (Gonzales and Smith 2015). By their pivotal location at matrix/striosome boundary, they also mediate the transfer of information between the two compartments. Unlike DA that is loaded back into DAergic nerve terminals by DAT, ACh is rapidly locally degraded by AChE, which serves to limit its diffusion (Kreitzer 2009).

- [Acetylcholine receptors](#)

#### Nicotinic acetylcholine receptors

Nicotinic acetylcholine receptors are pentameric ligand-gated cationic channels. Upon binding of ACh molecules, they mediate influx of cations and produce an EPSC. Their subunit composition is region-specific and defines the channel properties. The neuronal types only comprise  $\alpha$  ( $\alpha_{1-10}$ ) and  $\beta$  ( $\beta_{1-4}$ ) subunits. They can either form homopentamers (*e.g.*  $\alpha_7$  in the striatum) or  $3\alpha:2\beta$  heteromers (*e.g.*  $\alpha_4\beta_2$ ,  $\alpha_6\alpha_4\beta_2\beta_3$  and  $\alpha_6\beta_2\beta_3$  in the striatum; Quirk *et al.* (2007)). All cell types in the striatum express the nAChR  $\beta_2$  subunit (Bernard *et al.* 1995).

#### Muscarinic acetylcholine receptors

Five muscarinic acetylcholine receptors have been identified in mammals (M<sub>1-5</sub>R). M<sub>1</sub>, M<sub>3</sub> and M<sub>5</sub>R are G<sub>q</sub>-coupled GPCRs, while M<sub>2</sub> and M<sub>4</sub>R are G<sub>i</sub>-coupled (Kemel *et al.* 1989). M<sub>1</sub>R, M<sub>2</sub>R and M<sub>4</sub>R are expressed in the striatum with a neuronal-specific distribution (Bernard *et al.* 1992). Almost all striatal neurons carry M<sub>1</sub>R. D1-MSNs and CINs express M<sub>4</sub>R, with a predominant cytoplasmic localization in CINs, and

plasmalemmal in D1- MSNs especially in the striosomes (Bernard *et al.* 1991). M<sub>2</sub>R is used by CINs as an autoreceptor, and is also present in FTS-interneurons (Bernard *et al.* 1998). In addition, M<sub>5</sub>R is present on DAergic varicosities.

- Cholinergic modulation

Cholinergic interneurons form a dense striatal network and are tonically active. Several studies indicate a high overlap between this network and the dopaminergic terminals (Zhou *et al.* 2002). The released ACh interacts with nAChRs on striatal neurons and on nerve endings from glutamatergic and dopaminergic afferents (Calabresi *et al.* 2000).

It was demonstrated that acetylcholine has the ability to stimulate DA release in the striatum (Kemel *et al.* 1989). Indeed, DAergic projections from nigrostriatal and mesolimbic pathways both carry presynaptic mAChRs. The regulatory mechanisms involved are different in the matrix and striosome compartments. In the matrix, the facilitating effect seems to rely on both nAChRs and mAChRs (Kemel *et al.* 1989). As for the glutamatergic projections, they express both presynaptic nAChRs and mAChRs (M<sub>2</sub>R and M<sub>4</sub>R); thus, ACh can either enhance or decrease glutamate release.

### 2.1.3 Acetylcholine / dopamine activity during behavior

The antagonist balance between ACh and DA in the striatum has been long known. DA negatively regulates ACh release via presynaptic D<sub>2</sub>R while ACh enhances DA release via presynaptic nAChR (DeBoer *et al.* 1996, Threlfell *et al.* 2012).

Dopaminergic neurons from the VTA and cholinergic interneurons of the striatum both present firing patterns related to motor and reinforcement learning (Figure A.36). Their reward-related activities, even though temporally coincident, greatly differ in terms of polarity and dependence on reward probability (Morris *et al.* 2004, Cragg 2006). *In vivo*, CIN activity recording was initially performed during an operant conditioning task where a tune would announce to monkeys the delivery of a reward (juice; Kimura *et al.* (1984), Kimura (1986)). Monkeys had to move an arm to reach the reward. After conditioning, CINs would discharge briefly and synchronously following the presentation of the conditioned sensory stimulus, but pause their tonic activity during the execution of the movement.

Morris *et al.* nicely illustrated this DA / ACh activity interplay during an operant conditioning task (Figure A.36), where the animal learns to associate a cue (here, a visual cue) with a probabilistic reward schedule (juice; Morris *et al.* (2004)).

**Dopaminergic neurons from the VTA** burst right after the cue presentation and the reward delivery. During cue presentation, their firing is proportional to the probability of

reward (*i.e.* maximum response when probability of reward  $P=1$ ). On the other hand, during the reward delivery, the firing is proportional to the uncertainty of the reward (*i.e.* maximum response when probability of reward  $P=0.5$ ). When the reward is omitted, there is a transient decrease in their firing precisely when the neuronal response would have signaled the presence of a reward (Schultz *et al.* 1997).

On another note, **cholinergic interneurons'** firing does not depend on the probability of reward or uncertainty. As for DA neurons, they are responsive to cue presentation, but respond antagonistically with a decreased firing. During the reward presentation, they have a typical firing-pause-rebound response, directly opposite to that of DA neurons. During reward omission, they have a slight decrease of firing (Morris *et al.* 2004). These neurons are also responsive to aversive stimuli, but not to neutral ones; so their pause in activity would encode the salience value (Cragg 2006).

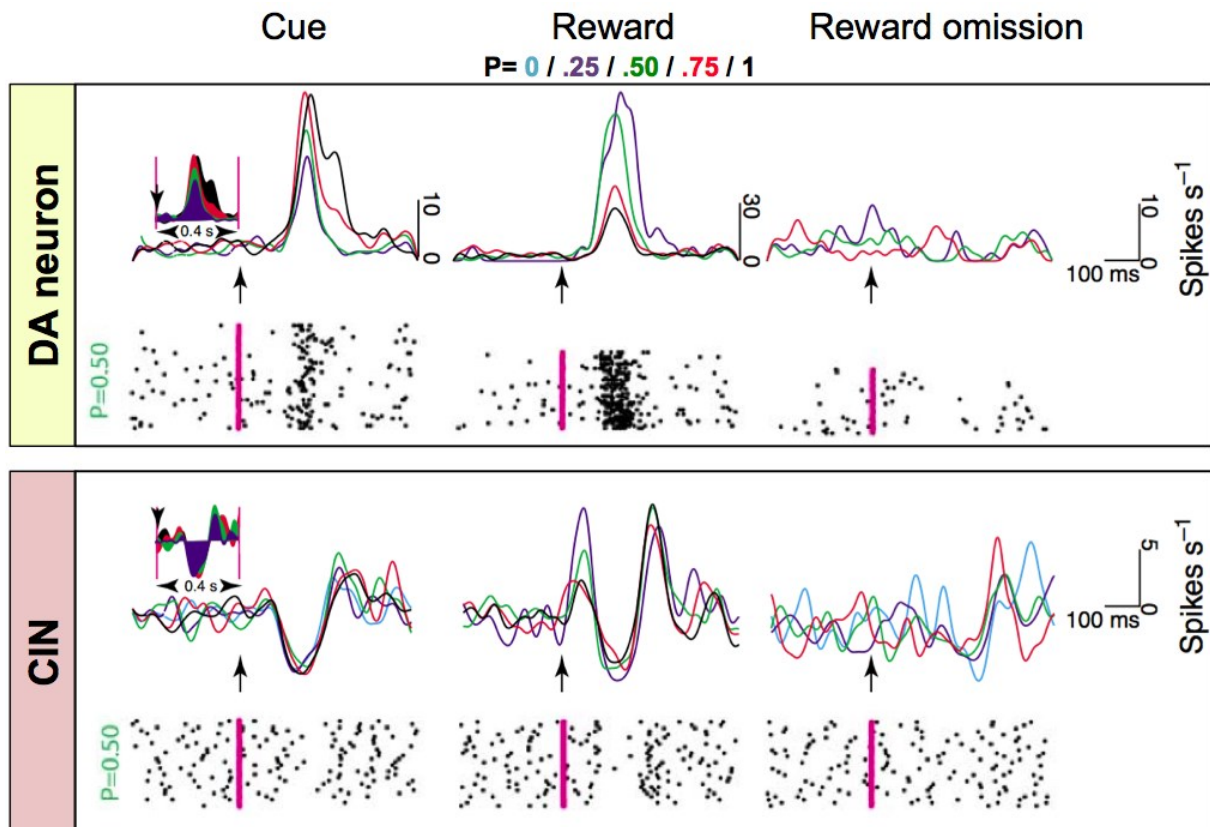


**Figure A.36: Opposite responses of DA neuron and CINs during operant conditioning**

**Top panel:** DA neurons have an increased firing during cue presentation (**left**) and reward delivery (**middle**), and a transient depression when the reward is omitted (**right**).

**Bottom panel:** CINs respond to both cue presentation and reward by pausing their firing.

**Top:** Alignment of mean firing rates; the *colors* represent responses for different probability of reward ( $P$ ).

**Bottom:** Raster plot of the response for  $P=0.5$ .

Adapted from Morris *et al.* (2004)

In summary, CINs signal for the prediction of a reward but their activity does not depend on the reward probability. In contrast DA neurons encode the predictive value of

various events in relation to reward. Thus, CINs serve as a temporal frame for the DA signal to be processed in the striatum (Cragg 2006).

## 2.2 Striatal efferent to basal ganglia

The output neurons of the striatum are the long- projecting GABAergic MSNs that provide GABAergic innervation to the basal ganglia. They are mainly segregated in three populations, the D1- and D2- MSNs, and the mixed D1/D2- MSN population.

### 2.2.1 Basal ganglia

Basal ganglia (BG) are a group of subcortical structures involved in the control of voluntary movement and in our ability to learn patterns of behavior to maximize reward. Striatum is the major input of the BG.

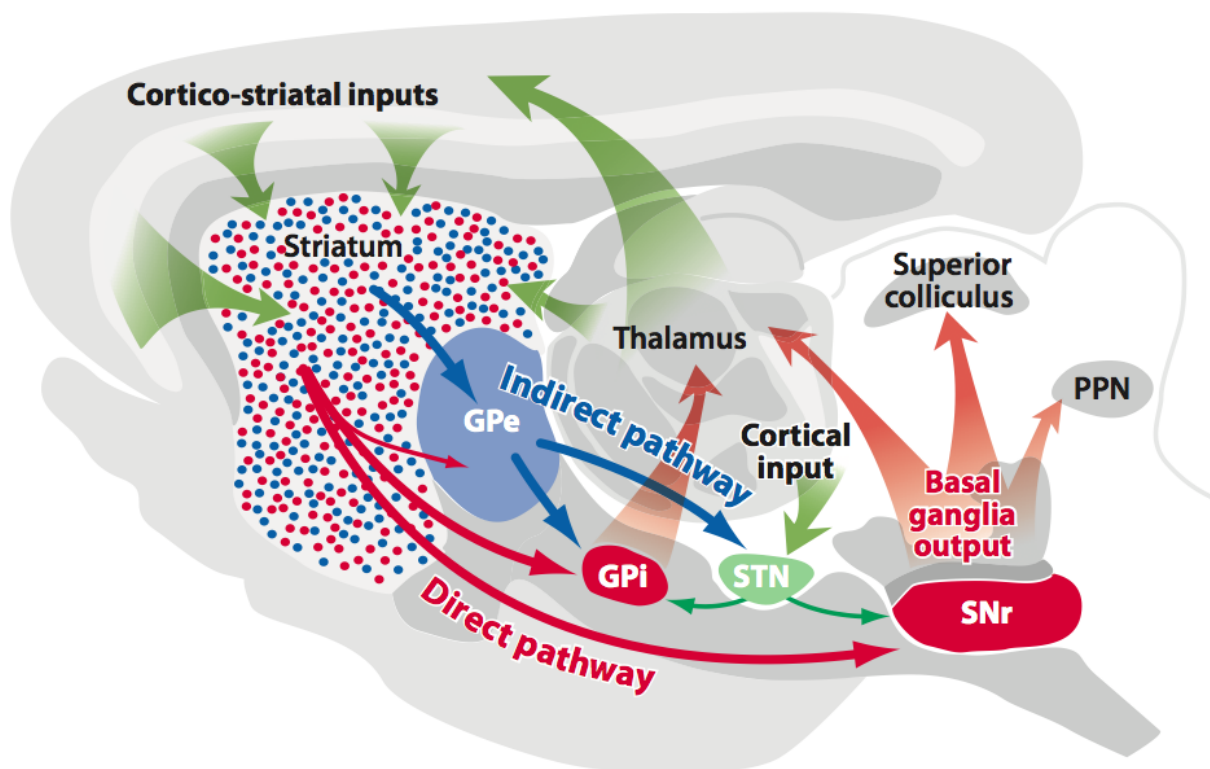


**Figure A.37: Basal ganglia circuit**

Striatum receives excitatory corticostriatal and thalamic inputs. Outputs of the basal ganglia arise from the internal segment of the globus pallidus (GPi) and substantia nigra *pars reticulata* (SNr), which are directed to the thalamus, superior colliculus, and pedunculo-pontine nucleus (PPN). The direct pathway originates from D<sub>1</sub>R-expressing MSNs (*red dots*) that project to the GPi and SNr output nuclei. The indirect pathway originates from D<sub>2</sub>R-expressing MSNs (*blue dots*) that project only to the external segment of the globus pallidus (GPe), which together with the subthalamic nucleus (STN) contain transsynaptic circuits connecting to the basal output nuclei. The direct and indirect pathways provide opponent regulation of the basal ganglia output interface. GABAergic and glutamatergic projections are represented with *blue/red arrows* and *green arrows* respectively.

From Gerfen *et al.* (2011)

The two main efferent pathways emerging from the striatum are the **striatonigral (direct)** and **striatopallidal (indirect) pathways** (Figure A.37). Their function is to transform the excitatory inputs from the cortex into balanced antagonistic inputs to the major output neurons of the basal ganglia. A third pathway, which appears to be **striosome-specific**, involves striosomal MSNs targeting SNc in a monosynaptic way.

### **2.2.2 The striatonigral (direct) pathway**

The D1-MSNs directly project to BG output nuclei, globus pallidus *internum* and substantia nigra *pars reticulata*, via the direct pathway. GPi is involved in axial and limb and SNr in eye and head movements. These two nuclei exert an inhibitory GABAergic drive on the thalamus. Activation of this pathway leads to a disinhibition of the thalamus (Gerfen *et al.* 2011). GPi projects to the centromedial thalamus, that in turn sends glutamatergic projections to the sensorimotor putamen, on D1-MSNs. On the other hand, SNr targets the parafascicular thalamus, which projects to the limbic part of the dStr and to the vStr (Gerfen 1992).

Activation of D1-expressing MSNs decreases basal ganglia output by directly suppressing activity at the level of GPi / SNr. D1-MSNs receive strong cortical inputs from layers III and superficial V that form the intratelenchephalic tract. Given the reentrant nature of BG-thalamocortical connections, cortically initiated activation of the direct pathway therefore results in a positive feedback at cortical levels, due to thalamic disinhibition. For this reason, the direct pathway is also called the pro- movement or “go” pathway (Gerfen *et al.* 2011).

### **2.2.3 The striatopallidal (indirect) pathway**

The D2-MSNs are part of the “two-armed” indirect pathway. First, the striatopallidal projections inhibit the globus pallidus *externum*. In the first arm, GPe GABAergic neurons project to the subthalamic nucleus (STN), whose excitatory glutamatergic neurons send feedforward connections to the GPi / SNr, as well as feedback connections to the GPe. The second arm of the indirect pathway is formed by direct GPe projections to the GPi / SNr. A consequence of this arrangement is that activation of D2-MSNs tends to increase neuronal activity at the level of GPi / SNr in both arms; in one case by disinhibiting the STN along with its excitatory projections to the GPi / SNr, and in the other by directly disinhibiting the GPi / SNr (Gerfen *et al.* 2011).

There is an additional loop in the indirect pathway, where STN sends reciprocal projections to the GPe. This loop has a pacemaker activity, through the presence of low-threshold T-type Ca<sup>2+</sup>-channels in both STN and GPe that create oscillatory interactions between GPe and STN. This synchronized activity is normally restrained by

powerful local GABAergic feedback that desynchronizes the output of neighboring neurons in the GPe (Gerfen *et al.* 2011).

Conversely to the direct pathway, cortically-initiated activation of the indirect pathway has the opposite effect on movement. This is due to the presence of an intermediate GABAergic stage of processing within the GPe. Cortical projections to matricial D2- MSNs preferentially arise from the motor cortex and deep layer V, which constitutes the pyramidal tract. In this tract, the main projections target the spinal cord and command movements, but send a collateral to striatum (Lei *et al.* 2004). The activation of these projections, as it is a copy of the motor command, is believed to act as a suppressor of unwanted movements.

### 2.2.4 The striosomal pathway

Striosomal and matricial MSNs indifferently project to BG direct and indirect pathways. However, there is an alternative input to the BG, where some striosomal MSNs from the dStr directly project to the SNc with collaterals to the GPi / GPe (Figure A.38). This pathway is named the **striosomal pathway**.

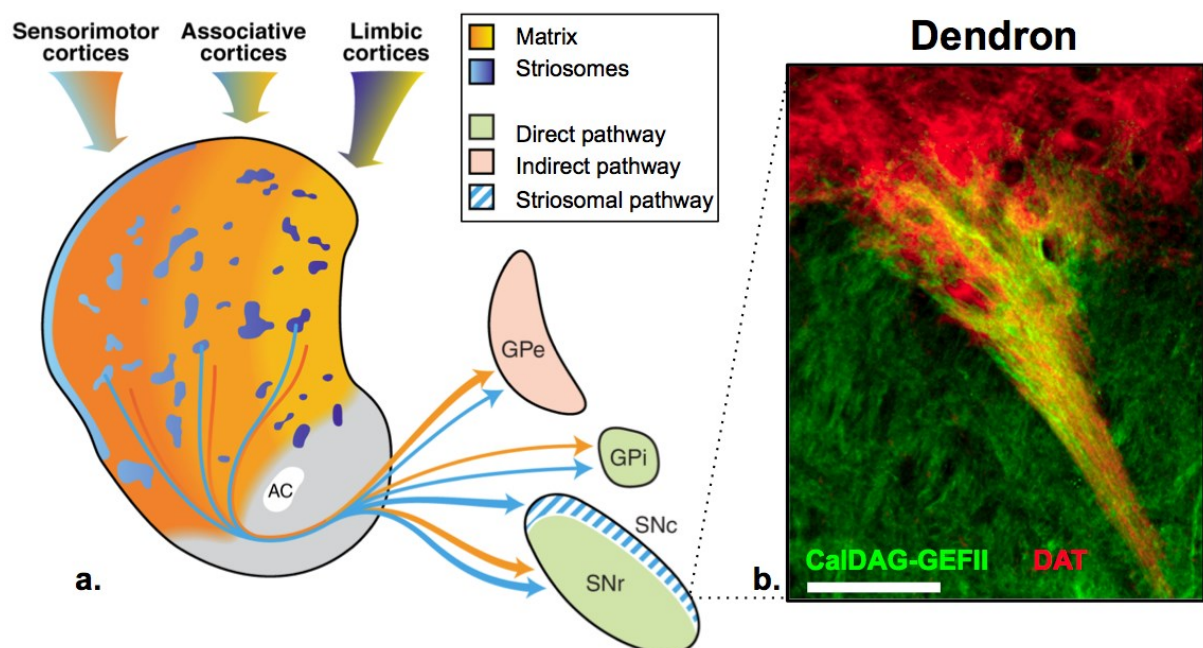


**Figure A.38: The striosomal pathway**

**a.** Striosomes (in blue) send direct GABAergic projections to the substantia nigra *pars compacta* (SNc, hatched blue and white area) and constitute the striosomal pathway. From Crittenden *et al.* (2011) **b.** Their GABAergic axonal projections (CalDAG-GEFII-ir, in green) are tightly entwined with ventral dendrite clusters arising from dopaminergic neurons of the SNc (DAT-ir, in red) that form dendrons. Scale bar = 50  $\mu$ m. From Crittenden *et al.* (2016)

Striosomal MSNs preferentially receive inputs from limbic cortical areas such as the orbitofrontal cortex (OFC). These MSNs then project to bouquet of dendrites arising from clusters of dopaminergic neurons in the SNc, called dendrons. Striosomal projections and

dendrons are tightly intertwined (Crittenden *et al.* 2016). Not only do dendrons receive GABAergic afferents from striosomes, but also cholinergic and glutamatergic projections from other brain areas. Together, these different sources can strongly influence DAergic SNc neurons activity. These dopaminergic fibers project back to the dorsal striatum, thus forming a striato-nigro-striatal circuit, but they also project ventrally to the SNr and thus can influence BG output. Along with the CINs, this pathway is of central importance in the balance of signaling between direct and indirect pathways. By modulating SNc activity, the striosomal pathway directly controls DA levels in the dorsal striatum (Crittenden *et al.* 2011, Brimblecombe *et al.* 2017).

### 2.2.1 Current view on striatal function

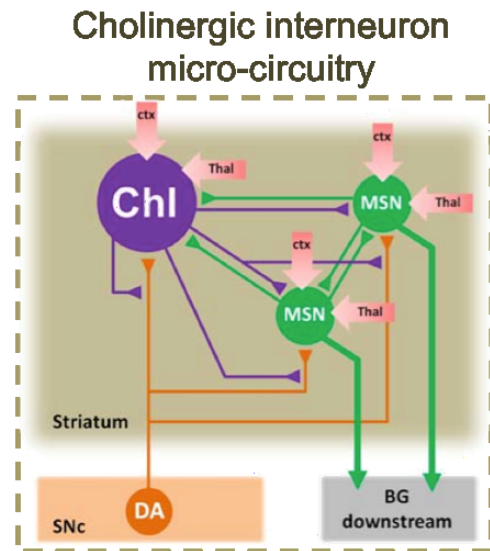
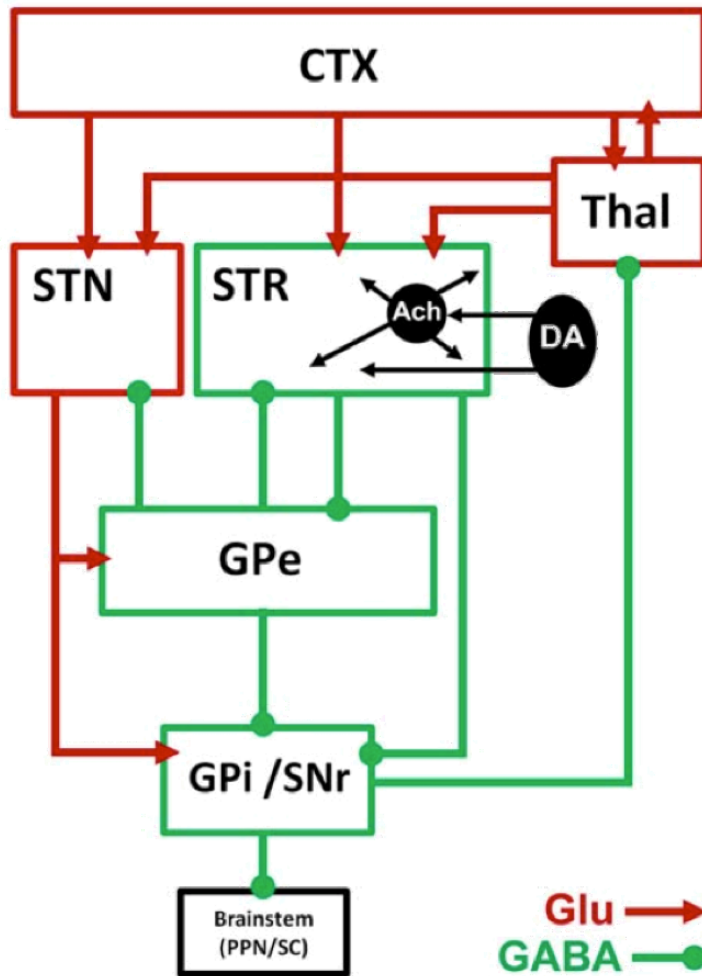
The classical model of striatal function proposed that the activity of direct and indirect pathways is coordinated to select specific motor programs and to inhibit the competing ones. This model predicted that during ongoing behavior, there would be an increased activity in neuronal ensembles constituted of neurons from both pathways rather than one or the other. The execution of a movement sequence would then generate a complex pattern of activity in specific neuronal ensembles.

Based on this model, the current view is that the striatum performs a computation of emotional / motivational, cognitive and sensorimotor information provided by the cerebral cortex to facilitate the selection of the appropriate action out of a collection of possibilities. Distinct cortico-BG loops are thought to perform different aspects of this sorting. They are also believed to play different roles in the acquisition and stabilization of context-dependent action selection. DMS-associative cortex connection seems to play an important role in the early phases of skill acquisition, whereas the DLS-sensorimotor cortex loop would be involved in later phases, once the skill has been established and the action program becomes more automated and inflexible (Gerfen *et al.* 2011). This last statement is consistent with the current view on the repeated exposure to drugs (Everitt *et al.* 2013).

The program selection is modulated by DA, which yields synaptic LTP on D1-MSNs and LDP on D2-MSNs in a given neuronal ensemble upon corticostriatal activation. Therefore, in this neuronal ensemble, reward will promote the ability:

- to turn on direct-pathway-associated MSNs linked to action initiation;
- to repress the indirect-pathway MSNs responsible for action suppression.

On the contrary, transient depression of DA release associated with aversive events will promote action suppression (Gerfen *et al.* 2011).



Deffains and Bergman (2015)

The striatum is the main input of basal ganglia, a set of subcortical structures important for the control of voluntary movement and our ability to learn patterns of behavior that maximize reward.

The striatum is principally composed of GABAergic neurons, MSNs, which mainly receive information from the cortex and thalamus. This integration is modulated by dopaminergic innervation from midbrain structures (VTA and SNc) and serotonergic afferents from the dorsal raphe nucleus. Locally, several tiny populations of interneurons massively regulate the striatal network, in particular the cholinergic interneurons. These neurons express VACHT and VGLUT3 and release both acetylcholine and glutamate. Dopamine and acetylcholine exert a reciprocal control on their respective release.

MSNs project to basal ganglia via the striatonigral pathway that promotes movement by disinhibiting the thalamo-cortical connections, or via the striatopallidal pathway that represses movement. The balance between these two pathways, together with cortical control, determines the motor outcome of an action.

## PART IV.

# STRIATAL DYSREGULATIONS AND ASSOCIATED PATHOLOGIES

Pathological changes of striatal activity are associated with a wide range of neurological and psychiatric disorders. Alterations in dopamine signaling induce differential activation of D<sub>1</sub>R- and D<sub>2</sub>R-expressing MSNs. For example, a hyper-responsive DAergic signaling is associated with drug addiction or L-DOPA-induced dyskinesia (LID). On the other hand, hypo-active DAergic signaling is the hallmark of Parkinson's disease.

### 1. The reward system

#### 1.1 Reward circuitry

The reward circuitry is a set of structures comprising: the ventral tegmental area, the striatum, several limbic structures (such as hippocampus, basolateral amygdala, lateral habenula (LHb)) and the prefrontal cortex (PFC; Figure A.39). It is activated by stimuli or pursuits that promote evolutionary fitness of the organism, such as social stimulation, nutrient-rich food or sex.

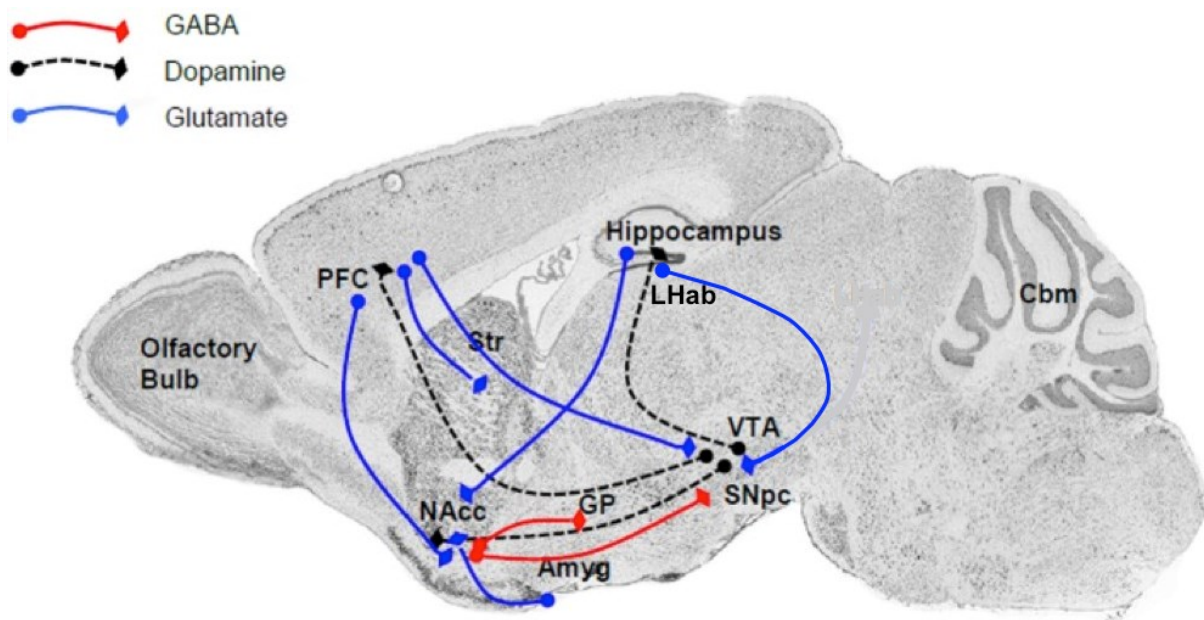


**Figure A.39: The reward circuitry** (sagittal view of mouse brain)

Adapted from Franklin *et al.* (2014)

The striatum is a key neural substrate for many drugs of abuse. It plays a role in reward-related learning as well as addictive behaviors. As mentioned above, the DLS and DMS receive excitatory inputs from the sensorimotor and limbic cortices respectively, with the intermediate region being connected to the associative cortex (Figure A.38; Crittenden *et al.* (2011)). The nucleus accumbens receives projections from the Hc, BLA and medial PFC. Cortico-accumbal projections can be further differentiated, as the prelimbic cortex and the infralimbic cortex preferentially project to the Acb core (AcbC) and shell (AcbSh) respectively. All together, these projections determine the addictive state of an individual (Russo and Nestler 2013).

## 1.2 Mode of action of drugs

Drugs of abuse have the property to activate the reward circuitry in a stronger and more persistent way than natural rewards.

Drugs of abuse are a chemically heterogeneous group with very distinct molecular targets and different site of actions in the reward circuit. But they all share the same overall effect: they increase DA efflux in the striatum, especially in the nucleus accumbens (Figure A.40; Nestler (2005), Luscher *et al.* (2006)). On the contrary, drugs with aversive properties (*e.g.* agonist of  $\kappa$ -opioid receptor, or bremazocine) decrease DA release, while non-abusive drugs (*e.g.* atropine) do not modify DA levels in the striatum (Di Chiara and Imperato 1988).

Based on their synaptic targets, drugs can be sorted in three classes: drugs that activate GPCRs (I), drugs that modulate ionotropic receptors (II), and drugs that inhibit/reverse transporters of biogenic amines (III), as described in Table A.5.

**Table A.5: Insight of abusive drugs and their targets**

Class	Drug	Target	Effect	Endogenous ligand / substrate
<b>I</b>	Morphine	Opioid receptors ( $G_{i/o}$ )	+	Endo opioids (Dyn, Enk, endorphin)
	Cannabis	Cannabinoid receptors ( $G_{i/o}$ )	+	Endocannabinoids (AEA, 2-AG)
<b>II</b>	Nicotine	nAChR	+	ACh
	Alcohol	GABA <sub>A</sub> R, 5-HT <sub>3</sub> R, nAChR, NMDAR		GABA
	PCP	NMDAR	-	
<b>III</b>	Psycho-stimulants	DAT, SERT, NET ( $\pm$ VMAT)	-	DA, 5-HT and NA respectively

PCP: phenylcyclidine; Dyn: dynorphin; Enk: enkephalin; AEA: anandamide; 2-AG: 2-arachidonylglycerol. + and - correspond to an agonistic or antagonistic action respectively.

Adapted from Luscher *et al.* (2006)

Class I and II drugs stimulate dopaminergic neurons firing, while class III drugs displace presynaptic DA to extracellular medium and block its uptake.

**Cannabinoids and opiates**, which belong to class I, inhibit GABAergic interneurons in the VTA by acting on their respective GPCRs, which are both coupled to  $G_{i/o}$ . This leads to a disinhibition of VTA dopaminergic neurons.

In class II, **nicotine** seems to directly activate VTA DA neurons via nAChRs stimulation. Nicotine also indirectly stimulates its presynaptic receptors on glutamatergic terminals that innervate the DAergic cells. **Alcohol** acts on several targets, including GABA ionotropic  $GABA_A$  receptor. The stimulation of  $GABA_A$ R results in inhibition of GABAergic terminals in the VTA. In turn VTA dopamine neurons are disinhibited.

Class III comprises **psychostimulants (amphetamine, cocaine, ecstasy)**, which all inhibit biogenic amine transporters (DAT, NET and SERT). Blocking DAT results in an immediate accumulation of extracellular DA in the striatum.

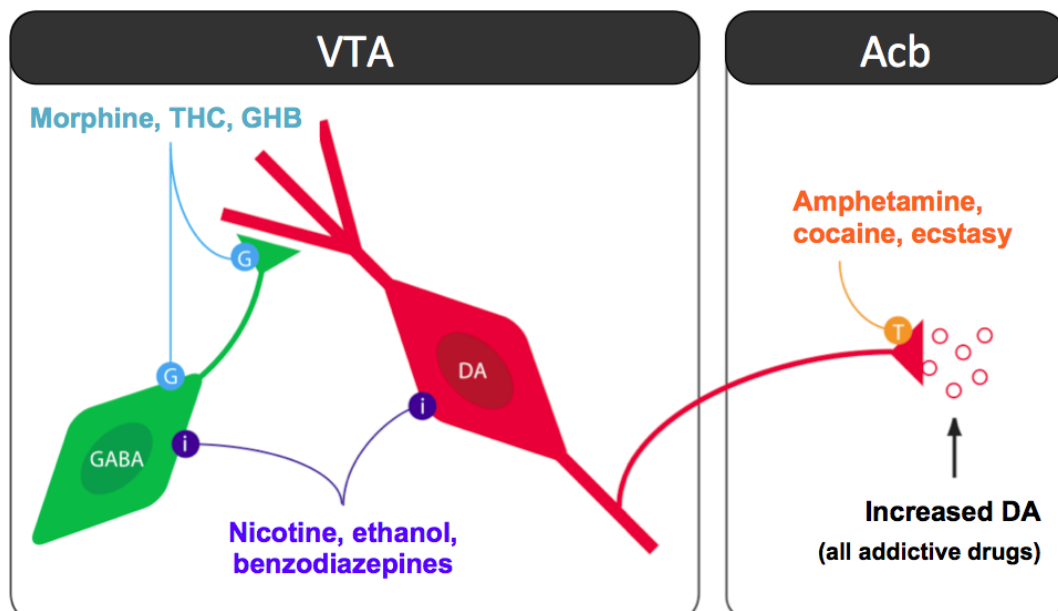


**Figure A.40: Major targets of addictive drugs**

All drugs of abuse enhance dopamine level in the nucleus accumbens (Acb). Morphine, THC and GHB are drugs that act on  $G_{i/o}$ -coupled receptors located on GABAergic INs (G, *in light blue*) and disinhibit DA neurons of the ventral tegmental area (VTA). Nicotine, ethanol and benzodiazepines modulate diverse ionotropic receptors (I, *in dark blue*) that excite or disinhibit DA neurons of the VTA. Amphetamine, cocaine and ecstasy (psychostimulants) block DA recapture in the nucleus accumbens (Acb) by acting on DA transporter (T, *in orange*).

Adapted from Luscher *et al.* (2006)

### 1.3 Drug addiction

- [Drug addiction](#)

Drugs of abuse are told to be both **rewarding**, *i.e.* they give the feeling of pleasure, and **reinforcing**, *i.e.* the intake leads to subsequent intakes.

**Drug addiction** is defined as a brain disease characterized by a repetitive and escalating drug intake despite harmful consequences. According to the fifth edition of

Diagnostic and Statistical Manual of Mental Disorders (DSM- 5), substance use is considered as being pathological when at least three of the following criteria are fulfilled within a 12- month period:

- **Tolerance:** the effect of a given dose of drug is decreased
- **Withdrawal:** there is a physiological lack for the drug, alleviated by a new intake
- **Taken more/longer** than intended
- **Desire/unsuccessful effort to quit use**
- **Great deal of time** taken by activities involved in use (e.g. process to get drugs)
- **Use despite knowledge of problems** associated with use
- **Important activities given up** because of use
- Recurrent use resulting in a **failure to fulfill important role obligation**
- Recurrent use resulting in **physically hazardous behavior** (e.g. driving)
- Continued use despite recurrent **social problems** associated with use
- **Craving** for the substance

(From DSM- 5', 2013)

Drug intake does not always go hand in hand with substance use disorder. It was estimated that only 15% of individuals (humans or animals) that experience drug develop addiction. Vulnerable individuals will be very susceptible to relapse after a period of withdrawal (Deroche-Gamonet *et al.* 2004).

According to World Health Organization, at least 15.3 million persons suffer from drug use disorders. Recent estimates are that in 2008, 155 to 250 million people, or 3.5% to 5.7% of the world's population aged 15-64, used psychoactive substances such as cannabis, amphetamines, cocaine, opioids, and non-prescribed psychoactive medication. The use of psychoactive substances causes significant health and social problems. It is also a major health issue because it represents a 2%-expenditure item of the GDP in countries that have measured it.

In animal models, addiction to drugs can be assessed by a battery of tests, which dissect the liking (hedonic component) from the wanting (goal- directed behavior) and from the compulsion (intake by habits).

It is notable that apart from psychoactive drugs, other items such as gambling, gaming or sex stimulate the same neuronal circuits and are fully recognized as addictive behaviors. Additionally, it is important to highlight the fact that simultaneous or concurrent use of two or more psychoactive substances is a commonplace (Meyerhoff 2017). So the notion of polysubstance use (PSU) should gain momentum in research. PSU is accompanied by cerebral changes differing from those observed with a single substance of interest, or from additive effects of several drugs. Therefore, it is crucial to gain insight into what happens in PSU to find effective treatment for addiction.

- Behavioral sensitization & tolerance

**Sensitization** is defined as an enhancement of the behavioral response to repeated drug exposure. This phenomenon occurs in psychostimulant drug abusers and can be induced in animals by giving multiple injections of drug at a given dose. It can either manifest itself through the repeated injections, or appear after a period of withdrawal. The effects are usually persistent after the last drug administration, thus mimicking long-term sensitivity to drugs observed in human addicts (Robinson and Becker 1986).

On the other hand, **tolerance** translates the decline in the effect produced by a substance upon multiple exposures. To maintain the initial drug effect, the dose must be increased. Tolerance to alcohol is a well-known example (Abraham et al. 2017).

- Switch from goal-directed behavior to habits

In addicts, drug experience is indissociable from the context of intake. Therefore, re-exposure to the drug is a way to relapse. But re-exposure to environmental cues can also lead to the same outcome. Cues and experience share the same neurocircuitry and underlying molecular mechanisms (Luscher 2016, Dong et al. 2017).

Acute drug exposure leads to activation of Acb to encode reward, but also of hippocampus and amygdala in the associative part of the process. It was demonstrated in humans and animals that re-exposure to the drug will expand the initial pattern of activation by including other brain regions, such as the dorsal striatum and neocortex (Koob 2005). This switch from ventral to dorsal striatum activation with repeated drug exposure translates the behavioral switch from early goal-directed behavior (GDB) to late compulsive behavior that turns out to be a drug-taking habit. Investigations proposed that within the dorsal striatum, the caudal DMS is responsible for GDB and the rostral DLS for habits. Transition between GDB and habits happens after repeated exposures (Everitt et al. 2013). This can be specifically assessed in **operant conditioning tasks**. The animal has to perform an action (e.g. lever press) to get a reward (e.g. food pellet) while a sensory stimulus (e.g. light) indicates that the reward is available. After the behavioral instatement, the reward is devaluated. In other words unlimited amount of the reward is provided before the training sessions. If the animal keeps on operating the action to get the reward, even when devaluated, this means its behavior has become habitual (Rossi and Yin 2012). Molecular changes underlie the transition from GDB to habits. Prolonged drug administration produces an enhanced DAergic tone, and electrophysiological and structural changes in the DLS (Everitt et al. 2013).

Interestingly, animals that self-administrate drugs with intermittent punishment (*i.e.* they sometimes receive mild electric footshock instead of drug) stop seeking it if they

had a short history with the drug, but about 15-20% of animals with extended history keep taking the drug in a compulsive manner (Everitt *et al.* 2013).

- Reward network in drug addiction

Current circuit-specific investigations try to elucidate the encoding of the different neural components of addictive behaviors. Thanks to optogenetics and chemogenetics, specific pathways of the reward system can be selectively activated / inhibited (Luscher 2016). By this mean, it has been possible to draw some provisional conclusions:

- The mesolimbic DAergic pathway (VTA → Acb) determines the plasticity critical for setting up and maintaining drug addiction.
- The cortico-accumbal glutamatergic pathway (mPFC → Acb) participates in the modulation of decision-making and goal-directed behaviors such as seeking and consuming substances or activities associated with reward, and provides the “executive control” required for planning and performing actions to obtain reward.
- The amygdalo-accumbal glutamatergic pathway (BLA → Acb) mediates behaviors associated with positive or negative valence. It is necessary for the expression of addiction-like behaviors and reinforcement learning, and represents the “emotional control”.
- The hippocampo-accumbal glutamatergic pathway (vHc → AcbSh) provides contextual information regarding the affective valence of location in space and previous experience generated from emotional learning. It represents the “spatial control”.

Two pathways seem to be effective to inhibit the progression of addiction: the striatopallidal pathway and the projections from the infralimbic cortex to the AcbSh. Thanks to different conditional tools, it was demonstrated that, similar to the motor outcome, striatonigral and striatopallidal neurons of the vStr display antagonistic roles (reinforcing or inhibiting respectively) in the control of reward behavior and drug sensitization (for review, see Ena *et al.* 2011).

#### **1.4 Molecular basis of drug addiction**

All addictive substances have the ability to hijack the dopaminergic system. They increase DA extracellular levels in the Acb. The acquisition and maintenance of addiction-like behaviors arise from molecular and cellular adaptations of striatal circuits. These changes underlie the lasting nature of the addictive phenotype.

- Intracellular signaling

After the increase of striatal DA, D<sub>1</sub>R- expressing neurons are preferentially recruited, with a concomitant glutamate / DA signaling. D<sub>1</sub>R stimulation recruits G<sub>αs/olf</sub> and leads to intracellular phosphorylation signaling cascades. These cascades involve both PKA and extracellular-regulated kinases 1 and 2 (ERK1/2; Figure A.41; Valjent *et al.* (2006), Bertran-Gonzalez *et al.* (2008), Gangarossa *et al.* (2013)). ERK activation requires the concomitant stimulation of D<sub>1</sub>R and NMDAR (Valjent *et al.* 2005).

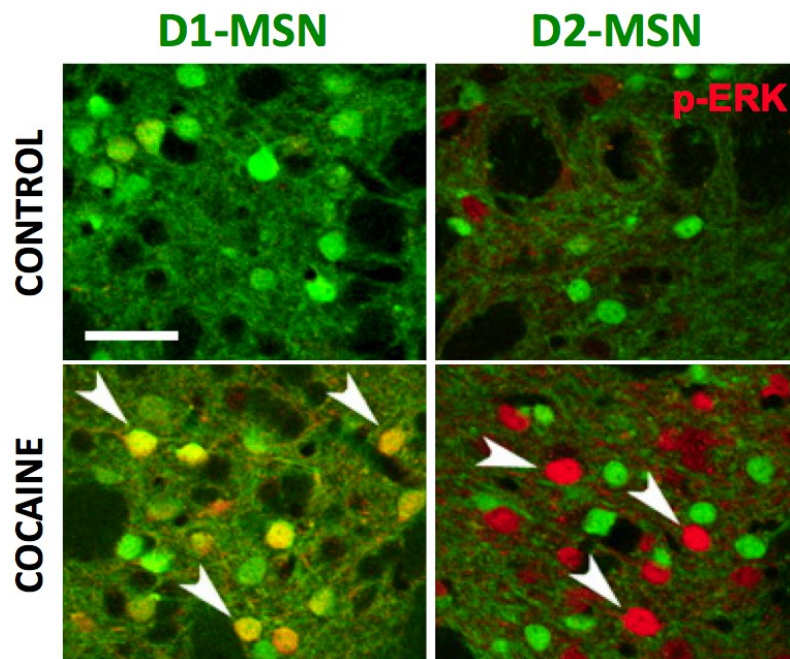


**Figure A.41: ERK activation in D1- and D2- MSNs following acute cocaine**

ERK activation (*red*) occurs exclusively in striatal D<sub>1</sub>R- expressing (*green*, **right panel**) and not in D<sub>2</sub>R- expressing neurons (*green*, **left panel**) after an acute injection of cocaine (20 mg/kg). *Arrowheads* indicate p-ERK-ir in MSNs. *Scale bar* = 40  $\mu$ m.

Adapted from Bertran-Gonzalez *et al.* (2008)

These cascades result in the phosphorylation of inactive cytoplasmic transcription factors, which will be imported in the nucleus. Activated transcription factors then activate the transcription of immediate early genes (IEG) in the striatum, with a drug-specific pattern (Graybiel *et al.* 1990). Drug-induced IEG products can themselves form transcription factors to induce “later-onset gene” expression. These late-onset genes are the ultimate regulators of the postsynaptic neuron (Figure A.42).

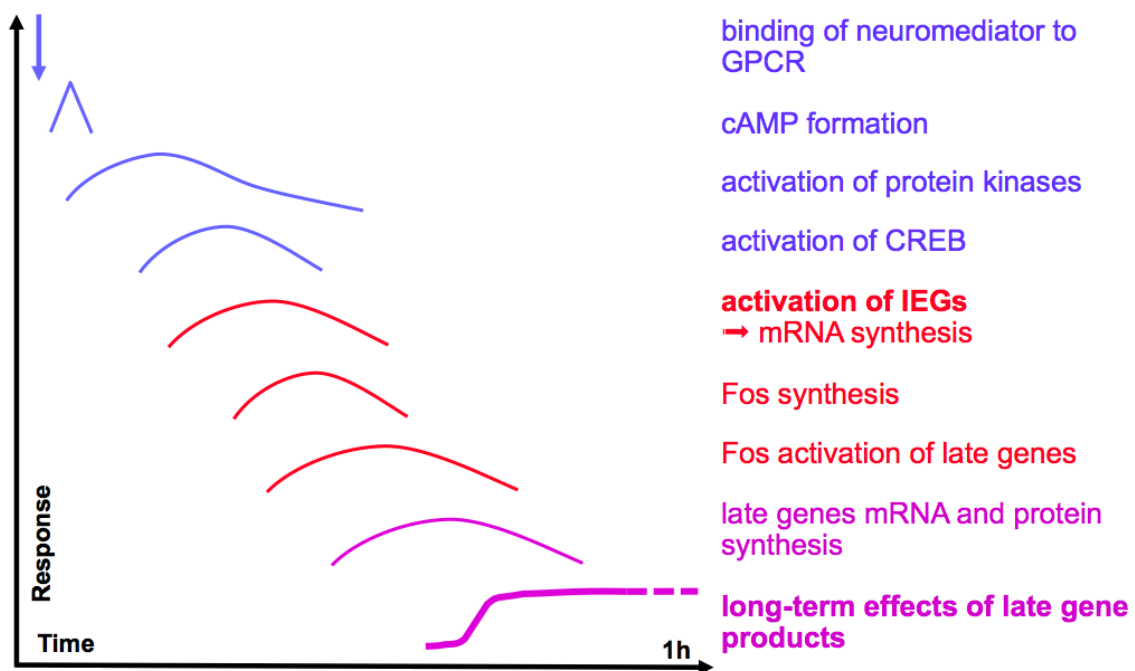


**Figure A.42: IEG activation cascade time-course**

Adapted from Stahl, Essential psychopharmacology

For example, ERK1/2 activates MSK1 (mitogen and stress-activated protein kinase-1). This ultimately causes deep adjustments in cells by activating transcription factors such as CREB or Fos and modifying histone H3 (Brami-Cherrier *et al.* 2009).

Another important protein recruited upon D<sub>1</sub>R activation through the action of PKA is DARPP-32 (Greengard 2001). In D1-MSNs, drug exposure promotes DARPP-32-pThr34 form, which maintains PKA active while inhibiting PP-1. On the other hand, in D2-MSNs, DARPP-32-pThr75 is favored, leading to PP-1 activation (Lobo and Nestler 2011). In D1-MSNs, phosphorylation of Ser97 is essential for DARPP-32 nuclear accumulation and targeting of histone H3 (for review, see Ena *et al.* 2011).

IEGs induced by drugs include *cFos*, *FosB*, *Zif268*. For instance, FOS family transcription factors associate with JUN family transcription factors to form a complex called activator protein 1 (AP1; Hope *et al.* (1994)). AP1 will activate the transcription of other genes. Acute drug exposure induces *FosB* in D1-MSNs. In contrast, chronic exposure induces  $\Delta$ FosB, which is a stable product of the *FosB* gene generated by alternative splicing, in the Acb and dStr. Natural rewards also induce  $\Delta$ FosB accumulation in D1-MSNs (Lobo *et al.* 2013). This exceptional stability of  $\Delta$ FosB could account for the persistence of drug-induced changes even after weeks of withdrawal (Robison and Nestler 2011).

- Epigenetic changes

Repeated drug exposure yields epigenetic changes. These are stable changes in gene expression that do not involve modification of DNA sequence. Epigenetic changes mainly consist in covalent modification of genes (such as methylation) or chromatin modification. DNA is like a pearl necklace, with the beads being more or less tightened. These pearls correspond to nucleosomes, which are octamers of histones (H2A, H2A, H3, H4 repeated two times), and around which DNA is wrapped. Histones N-termini are available for post-translational modifications (phosphorylation, methylation and acetylation) that will determine DNA level of compaction. The looser DNA is, the more active transcriptional activity occurs. Histone H3 plays a crucial role in chromatin remodeling upon drug exposure. In D1-MSNs, phosphorylation of H3 on Ser10 by MSK-1 leads to chromatin decondensation, thereby allowing transcription factors to access DNA and increasing the expression of specific IEGs. An additional effect is obtained by demethylation of H3 Lys9 residue that disinhibits gene repression (Brami-Cherrier *et al.* 2009, Robison *et al.* 2011).

- Synaptic plasticity

Addictive drugs affect synaptic transmission. Psychostimulants enhance excitatory transmission at corticostriatal synapses after withdrawal. There is a down-regulation of GLT-1, an astrocytic transporter for glutamate, which results in glutamate overflow (Fischer-Smith *et al.* 2012). Furthermore, NMDARs and AMPARs are redistributed at the plasmalemma (van Huijstee and Mansvelder 2014). GluA2-lacking AMPARs that are calcium-permeable, and GluN2B-containing NMDARs that are less desensitizing, appear. Together, the two previous changes result in an increased AMPAR/NMDAR ratio, making synapses more responsive to glutamate. Along with this, presynaptic mGluR2, which would decrease glutamate release probability, are downregulated, resulting in an increase of extracellular glutamate. Together, these changes result in the strengthening of glutamatergic transmission (Russo *et al.* 2010, van Huijstee *et al.* 2014).

- Morphological changes

The ability of experience to alter dendritic tree structure is considered to be the primary mechanism by which past experience influences subsequent behaviors. This process is called structural plasticity.

In the striatum, the dendritic tree of MSNs receives various inputs. The proximal dendrites are innervated by local inputs. Extrinsic afferents preferentially contact the distal dendrites. Cortical glutamatergic projections form asymmetric synapses on spine heads, whereas spine shafts and necks are contacted by DA fibers that form symmetric synapses (Smith *et al.* 1990).

One form of drug-induced synaptic plasticity involves alterations of the density of dendritic branching and dendritic spines in the Acb. After psychostimulant exposure, there is a rapid strong formation of new spines on MSNs, especially in the AcbSh (Kochman *et al.* 2006, Dos Santos *et al.* 2017). On the other hand, opiates decrease the number of spines in the Acb (Russo *et al.* 2010). These changes depend on the duration of drug exposure and withdrawal time. They reflect the reorganization of synapses on MSNs (Anderson and Self 2017). Exposure to psychostimulants preferentially enhances the spine density and the number of branches on distal dendrites (Li *et al.* 2003). This reflects the increased connectivity between the striatum and its afferent structures.

These changes in connectivity have been related to the activity of MNK1 (mitogen-activated protein kinase interacting kinase-1),  $\Delta$ FosB and downstream-induced genes such as genes involved in dendritic spine architecture (*e.g.* activity-regulated cytoskeleton-associated protein (ARC); Russo *et al.* (2010)).

Other factors such as an enriched environment have the ability to induce the formation of new spines. Interestingly, pre-exposure to psychostimulants limits this structural plasticity in neocortex and Acb. This could explain the cognitive deficits associated with drug abuse (Kolb *et al.* 2003).

### **1.5 Role of VGLUT3 in addiction**

VGLUT3 is massively expressed by CINs in the striatum. These neurons are centrally involved in reward behaviors, and release both glutamate and acetylcholine. Toxin-mediated CIN ablation leads to an increased sensitivity to short-term (acute injection) and long-term (conditioned place preference, CPP) effects of cocaine (Hikida *et al.* 2001). On the other hand, conditional VAcHT knockout in the CINs (Drd2-Cre::VAcHT<sup>LoxP/LoxP</sup>) that have lost the ability to release acetylcholine show minimal alteration of their behavioral response to cocaine (Guzman *et al.* 2011). Thus, it could be inferred that the reward-related phenotypes observed in CIN-KO could be due to a signalling with glutamate (Higley *et al.* 2011). Therefore, the implication of VGLUT3 was assessed in reward and addiction by using VGLUT3<sup>-/-</sup> mice (Sakae *et al.* 2015).

Relatively to WT, VGLUT3<sup>-/-</sup> mice have an increased locomotion in response to an acute injection of cocaine (10 mg/kg). This increase remains stable through repeated drug injections. This is in contrast with control littermates that show the typical increase of locomotion corresponding to locomotor sensitization (Figure A.43).

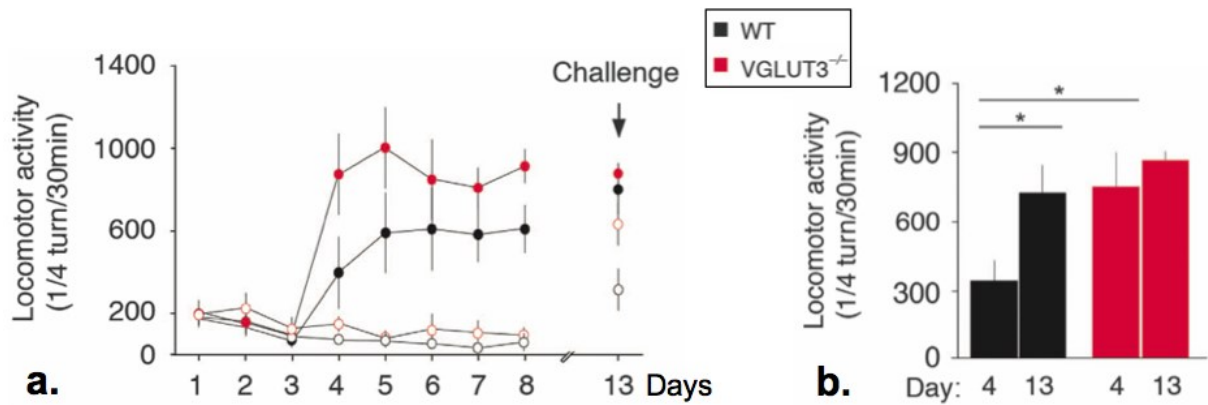


**Figure A.43: Locomotor sensitization to cocaine in VGLUT3<sup>-/-</sup> mice**

**a.** While control mice (*in black*) show an enhanced hyperlocomotion in response to repeated administration of cocaine, VGLUT3<sup>-/-</sup> mice (*in red*) respond very strongly and this response is not further increased. **b.** VGLUT3<sup>-/-</sup> mice have a pre-sensitization to cocaine while WT littermates display a classical sensitization.

From Sakae *et al.* (2015)

They are also more sensitive to the rewarding effects of cocaine in CPP and self-administration experiments. In the self-administration paradigm, VGLUT3<sup>-/-</sup> mice show an increased motivation to obtain the drug and are more vulnerable to cue-induced relapse. Together, these results show that VGLUT3<sup>-/-</sup> mice are more vulnerable to the effects of cocaine.

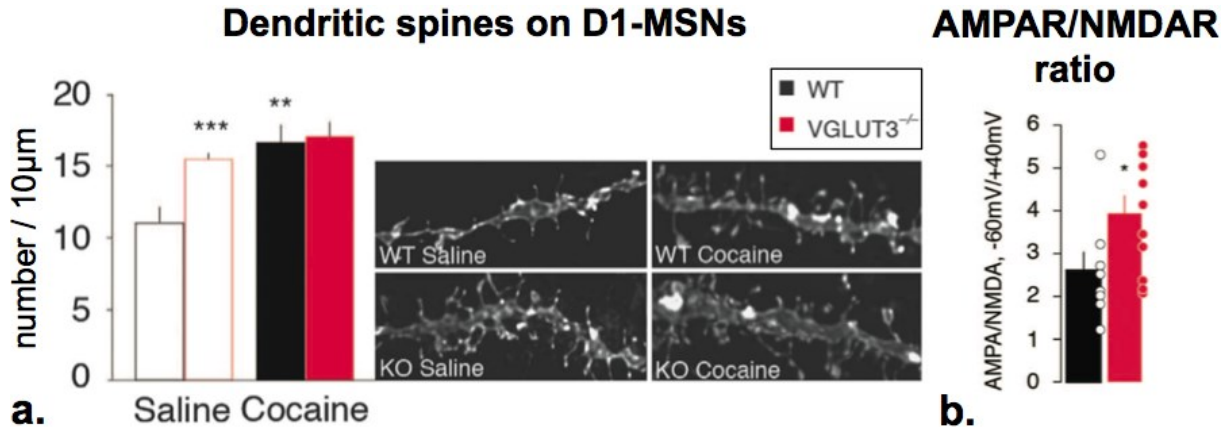


**Figure A.44: D1-MSNs characteristics in VGLUT3<sup>-/-</sup> mice**

**a.** VGLUT3<sup>-/-</sup> mice (*in red*) have a constitutive elevated number of dendritic spines on D1-MSNs. This number is not further increased by cocaine treatment, unlike control mice (*in black*). **b.** The AMPAR/NMDAR ratio is higher in VGLUT3<sup>-/-</sup> mice, suggesting that synapses are more responsive.

Adapted from Sakae *et al.* (2015)

VGLUT3<sup>-/-</sup> mice show several adaptations of the striatal circuits. They have a marked increase of dopamine release in the Acb (Divito *et al.* 2015, Sakae *et al.* 2015). On the other hand, DA efflux is decreased in the Acb of mice lacking VACHT (Sakae *et al.* 2015). Thus CINs exert a bidirectional regulation of DA efflux. Interestingly, glutamate released by the CINs negatively regulates DA release by acting on mGluR2/3. VGLUT3<sup>-/-</sup> mice

also have an increase of D<sub>1</sub>R level specifically in the Acb. Moreover, the number of dendritic spines and the AMPAR/NMDAR ratio of D1-MSNs, and phospho-ERK are constitutively higher in the Acb of VGLUT3<sup>-/-</sup> mice (Figure A.44).

These results point toward reinforced DA and glutamatergic transmissions on D1-MSNs in VGLUT3<sup>-/-</sup> mice (Sakae *et al.* 2015).

In summary, the following model was proposed to explain the morphological and electrophysiological changes observed in VGLUT3<sup>-/-</sup> mice (Figure A.45).

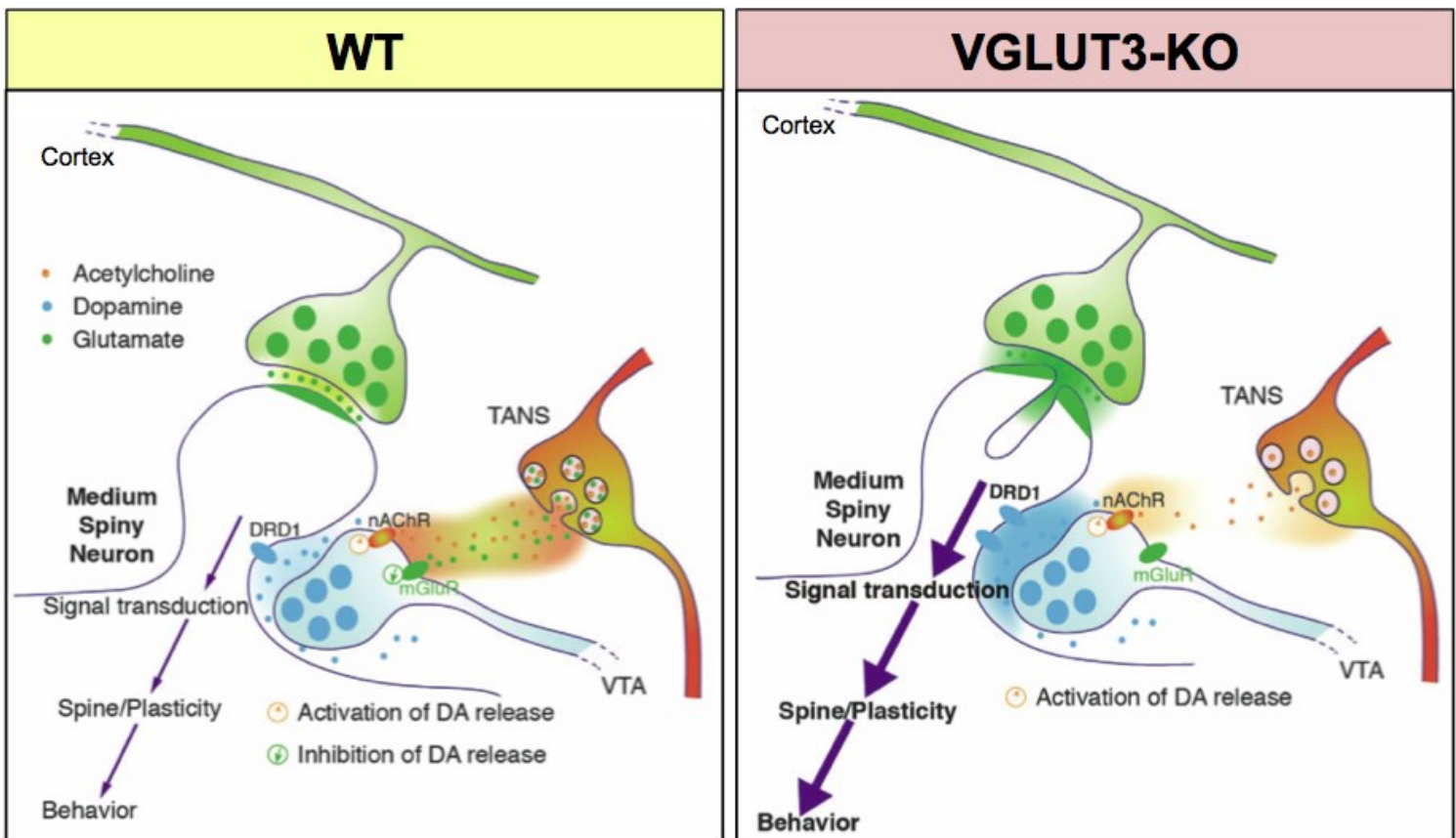


**Figure A.45: Dual regulation of DA efflux by ACh and Glu from CINs in the Acb**

CINs express VACHT and VGLUT3 and therefore co-release ACh and glutamate. These two co-transmitters exert opposing effects on DA release. In wild-type (WT) mice (**left panel**) DA efflux is stimulated by ACh through nicotinic ACh receptors (nAChRs), and inhibited by VGLUT3-dependent glutamate through metabotropic glutamate receptors (mGluR2/3) most likely located on DA terminals. In VGLUT3<sup>-/-</sup> mice (**right panel**), the mGluR-driven inhibition is lost and therefore DA efflux is markedly enhanced. Consequently the D<sub>1</sub>R signaling cascade is overactivated, and dendritic spine density (without modification of the number of excitatory terminals) and cortico-striatal glutamatergic activity are increased, leading to augmented sensitivity to the rewarding properties of cocaine.

Adapted from Sakae *et al.* (2015)

## 1.6 Amphetamine

Amphetamine (contraction of  $\alpha$ -methyl-phenethyl-amine) was first synthesized in 1887. It was initially commercialized under the name Bensedrine and used to treat a wide range of medical conditions: including chronic pain, low blood pressure, narcolepsy or else obesity. Until 1939, amphetamine was available without prescription. Its addictive potential was not fully recognized until the mid-sixties (Sulzer 2011).

Amphetamine (AMPH = 'speed') has some popular derivatives: methamphetamine (METH = 'ice') and 3,4- methylenedioxymethamphetamine (MDMA = 'ecstasy') that share a phenylethylamine core structure. AMPH and METH have the same effects in terms of pharmacokinetics and DA increase-potential in the dStr. However, METH is more effective at increasing DA levels in the Acb of rats. Methylphenidate, an AMPH derivative, is widely used to treat attention deficit disorder and narcolepsy. Clinical administration of METH or AMPH yields a cerebral concentration of 5 to 10  $\mu\text{M}$ , while off- label use may result in hundreds of  $\mu\text{M}$  (Sulzer 2011).

Amphetamine use often goes along with the intake of marijuana and alcohol. This PSU leads to a decrease of the ventromedial PFC and insula volume. After long periods of abstinence, other morphometric alterations are seen, for example the increase of pallidal and striatal volumes (Meyerhoff 2017). According to the World Health Organization, amphetamine- type stimulants are the second most commonly used psychoactive drugs worldwide after cannabis (Figure A.46).

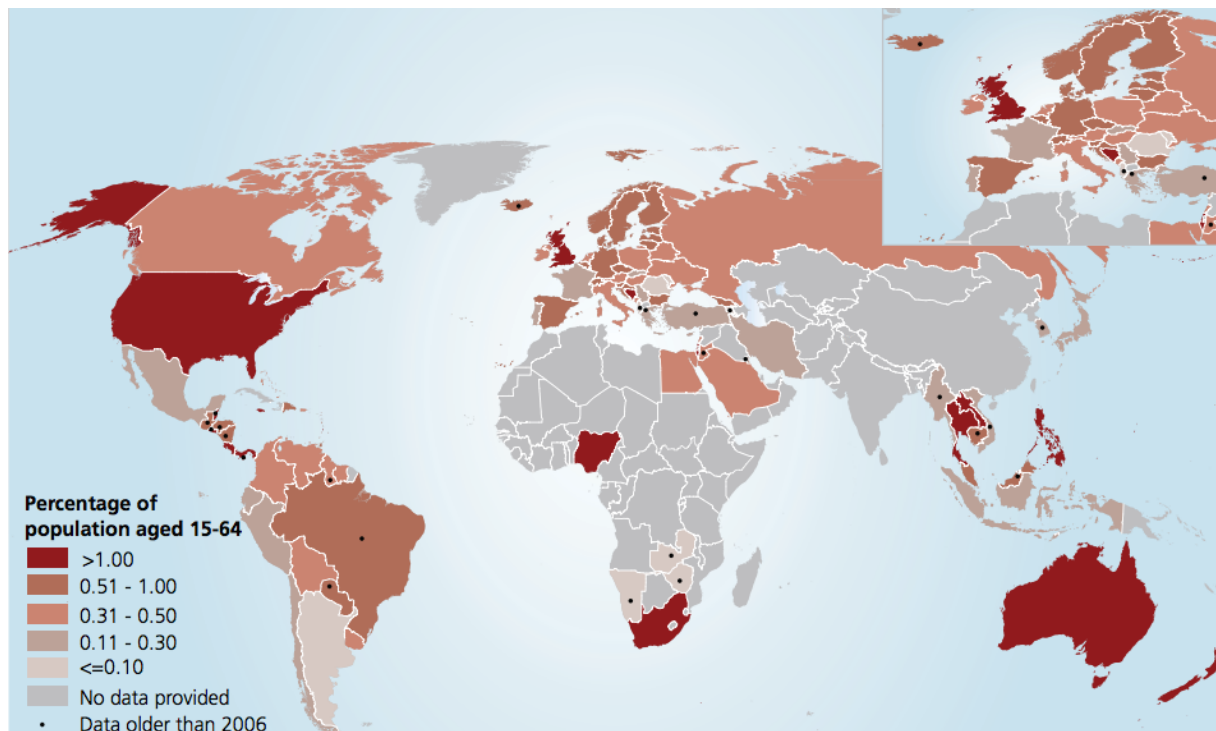


**Figure A.46: Prevalence of amphetamine- type stimulants (excluding ecstasy) in 2010**

Source: World Drug Report 2012, World Health Organization

- Specific mode of action of amphetamine

Amphetamine and its derivatives have the ability to elevate synaptic monoamine concentrations in the striatum, in particular in the AcbSh with a two-fold increase compared to the CPU (Di Chiara *et al.* 1993). Amphetamine binds to DAT, SERT and NET. Unlike cocaine that blocks these transporters, AMPH and derivatives reverse the activity of these transporters. In addition, amphetamine has the same effect on VMAT2 (Luscher *et al.* 2006, Sulzer 2011).

At basal state, the tonic firing of DAergic neurons provides a constant supply of DA that is carried in the cell by DAT. Once in the cytosol, DA is loaded into SVs by VMAT2. Tyrosine hydroxylase (TH) is the rate-limiting enzyme for the multi-step synthesis of DA (Figure A.15), while monoamine oxidase (MAO) is responsible for its catalysis into DOPAC.

The molecular mechanisms of amphetamine-induced VMAT2- and DAT-mediated reverse transports are still a matter of debate (Figure A.47). Reverse transport is thought to involve the uptake of amphetamine by the transporters and its passive diffusion through the membrane. The “weak-base hypothesis” states that the accumulation of AMPH within SVs depletes vesicular stores of dopamine by dissipating the proton gradient (Sulzer 2011). Thereby, AMPH elevates cytosolic dopamine concentration and renders DA available for reverse transport by DAT. Additionally, AMPH activates TH and inhibits MAO, leading to an increased production of DA at the same time (Sulzer 2011).

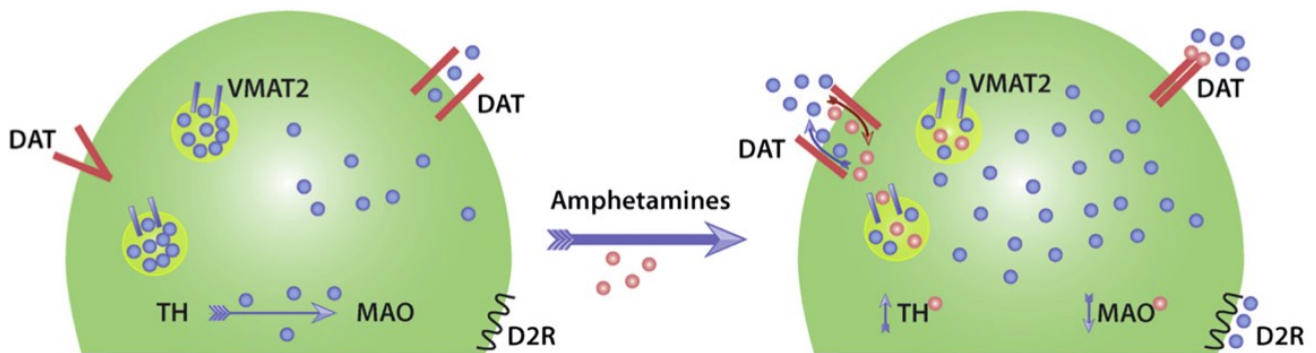


**Figure A.47: Amphetamine modes of action**

**Left side:** DA transporter (DAT) mediates extracellular DA influx to the cytosol. DA is then accumulated in SVs via the vesicular monoamine transporter (VMAT2) to very high levels. Tyrosine hydroxylase (TH) synthesizes the DA precursor L- DOPA, while monoamine oxidase (MAO) is responsible for its degradation. **Right side:** Amphetamine is a substrate for DAT and acts to favor release via the reverse transport of cytosolic DA. Once in the cytosol, amphetamine acts at several levels to increase cytosolic DA, thereby providing additional substrate for DAT reverse transport, by i) activating TH, ii) inhibiting MAO and iii) redistributing vesicular DA to the cytosol, probably by VMAT2 inhibition and/or reversal.

From Sulzer (2011)

Sustained extracellular levels of DA promote the development of drug addiction. Even an acute exposure to amphetamine yields deep and rapid changes thanks to IEG expression. With amphetamine, this activation is disproportionately increased in the striosomes compared to the matrix compartment, specifically in D1-MSNs (Graybiel *et al.* 1990). This striosome-to-matrix gene induction ratio directly depends on CINs (Saka *et al.* 2002).

Amphetamine, like other psychostimulants, preferentially acts on the vStr. At low doses (0-3 mg/kg), it produces a hyperlocomotion by acting preferentially on the Acb (Di Chiara *et al.* 1988, Drevets *et al.* 1999). On the other hand, high doses will also activate dStr and drive stereotypies. Therefore, amphetamine has a biphasic effect (Yates *et al.* 2007, Hadamitzky *et al.* 2012).

## 2. Dorsal striatum defects

### 2.1 Parkinson's disease

- Etiology of Parkinson's disease

Parkinson's disease (PD) is a neurodegenerative disorder characterized by a triad of symptoms: bradykinesia (difficulty to initiate and slowing of movement), muscle rigidity and resting tremor. In this hypo-kinetic pathology, dopamine-containing neurons of the SNc degenerate (Figure A.48a). This leads to a progressive caudo-rostral DAergic denervation of the dStr. In the early phases, the putamen (sensorimotor part of the Str) is mainly affected, leading to execution defects of voluntary movements; later, the degeneration progresses toward the caudate nucleus.

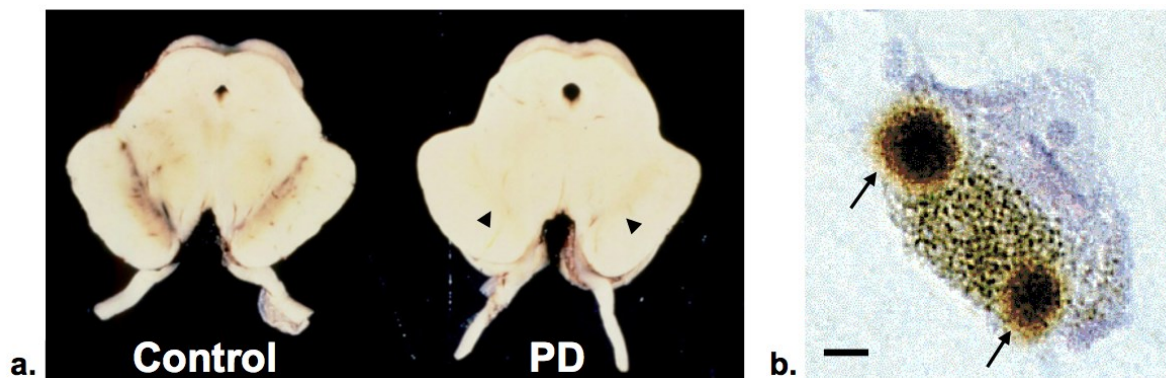


**Figure A.48: Anatomical and cellular defects in human PD**

**a.** Cross-sections of human midbrain in a healthy individual (**left**) and in a patient with PD (**right**). There is a specific loss of pigmentation corresponding to neuromelanin-producing DAergic neurons in SNc (*arrowhead*) in human PD compared to control. From Marcus and Jacobson (2003)  
**b.** DAergic pigmented neurons of the SNc present  $\alpha$ -synuclein-containing cytoplasmic aggregates corresponding to Lewy Bodies (*arrow*). Scale bar = 8  $\mu$ m. From Spillantini *et al.* (1997)

The etiology of PD is very complex and this disorder seems to be primarily sporadic. However, it has been demonstrated that neuronal degeneration is linked to cellular defects. Among those, there is the formation of large cytoplasmic inclusions known as Lewy bodies, which contain high levels of  $\alpha$ -synuclein aggregates (Figure A.48b; Spillantini, 1997 #1010@@author-year). This provokes mitochondrial dysfunctions along with oxidative stress in DAergic neurons (Dias *et al.* 2013). The primary damage is worsened by microglial activation and autoimmune responses that accelerate cell apoptosis by production of nitric oxide and subsequently of  $\alpha$ -synuclein nitration (Koshimori *et al.* 2015).

Apart from local defects in the DAergic nuclei of BG, major distal changes occur in the striatum. PD results in an imbalanced signaling in the BG where the striatopallidal pathway is favored compared to the direct pathway, resulting in the motor deficits associated with PD (Albin *et al.* 1989). Moreover, DA depletion biases direct-pathway MSNs towards LTD and indirect-pathway MSNs towards LTP at glutamatergic synapses following hypo-activation of D<sub>1</sub>R and D<sub>2</sub>R (Gerfen *et al.* 2011). There is also an imbalance between striosomal and matricial compartments (Crittenden *et al.* 2011). Enkephalin is globally upregulated, translating the stimulation of the indirect pathway, with no alteration of the Dynorphin, which is the marker of direct MSNs. In addition, opioid receptors  $\mu$  and  $\delta$  are specifically downregulated in the striosomes, in a compensatory manner (Figure A.49; Koizumi *et al.* (2013)).

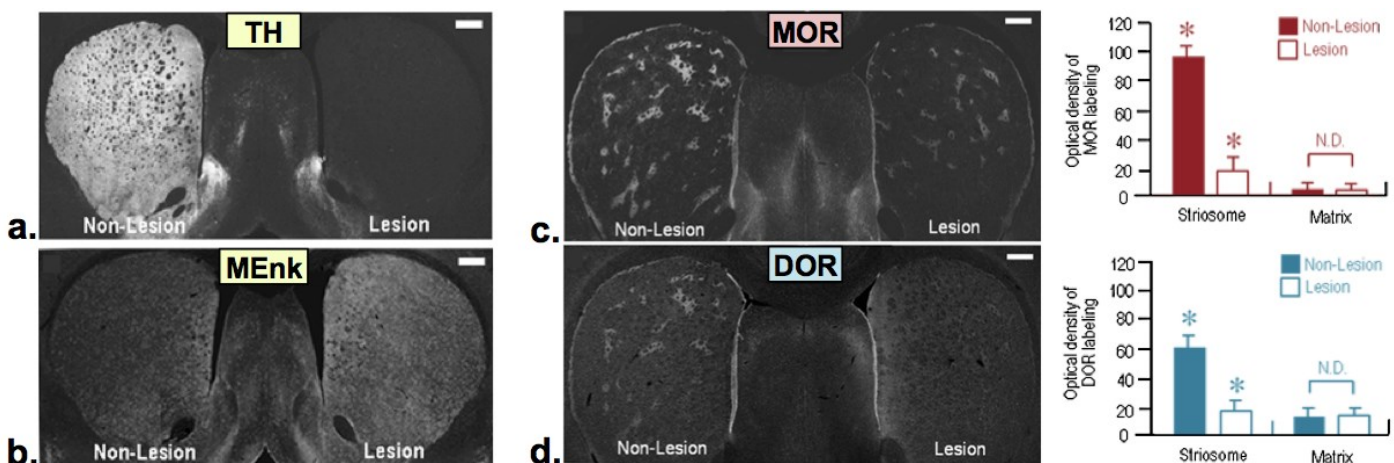


**Figure A.49: Enkephalin and opioid receptors expression in toxin-induced parkinsonism**

**a.** Rats unilaterally injected with 6-OHDA in the SNc have a massive loss of DAergic innervation in the Str, as visualized by TH-ir. **b.** The endogenous opioid met-enkephalin (MENk) is upregulated in the whole Str after DA depletion. **c.**  $\mu$ -opioid receptor (MOR), usually enriched in striosomes, is specifically downregulated in this compartment in the lesioned side. **d.**  $\delta$  opioid receptor (DOR) is expressed in both compartments, but is enriched in striosomes. DOR is specifically downregulated in striosomes of the lesioned side. Scale bars = 500  $\mu$ m.

Adapted from Koizumi *et al.* (2013)

- Animal models of Parkinson's disease

It is very difficult to find models that phenocopy PD, because SNc DAergic neurons loss is probably not the only feature of this pathology. Therefore, a combination of different approaches may be necessary to study the PD progressive neurodegeneration (Blesa and Przedborski 2014).

### **Toxin- based models**

The aim of this model is to eliminate SNc DAergic neurons of the SNc, by the mean of intranigral or intrastriatal neurotoxin injection. The most commonly used toxins are 6- hydroxydopamine (6- OHDA) or 1- methyl- 4- phenyl-1,2,3,6- tetrahydropyridine (MPTP). Rats are resistant to MPTP. These two compounds are uptaken into DA neurons by DAT - directly for 6- OHDA, and indirectly for MPTP that is first transformed into 1- methyl- 4- phenylpyridinium (MPP+) by glial cells. Once in the cell, they will interfere with the mitochondrial oxidative phosphorylation chain and generate reactive oxygen species (ROS) that, in term, will cause cell apoptosis (Chaudhry *et al.* 2008).

Usually, the experimenter proceeds to a unilateral lesion in order to use the unlesioned side as a control for normal DAergic innervation, by checking TH level. After the lesion, at basal state, the lesioned side is hypodopaminergic and the unlesioned side is dominant; therefore, the animal presents spontaneous ipsiversive rotations. Moreover, because of this hypodopaminergy, DA receptors become hypersensitive on the lesioned side. Thus, DAergic stimulation with a DA receptor agonist such as apomorphine leads to a stronger activation of the striatonigral pathway on DA-depleted side, resulting in contralateral rotations (Pycock 1980). The extent to which the animal turns reflects the success of the surgery. Another reason for using unilateral lesion is that bilateral ones lead to aphagia and adipsia, which interfere with the study of parkinsonism.

Other neurotoxins are also used to induce DAergic cell death, such as rotenone, paraquat, or the amphetamine- type psychostimulants methamphetamine and MDMA. Rotenone, which is a pesticide, is very useful because it can be administered by intraperitoneal route; repeated daily systemic administration of rotenone leads a specific nigral dopaminergic defect, accompanied by the formation of Lewy Bodies, which reproduces human PD features. This toxin is highly toxic in rats, but does work in mouse models (Blesa *et al.* 2014). MDMA mainly acts on the serotonergic system but also on the dopaminergic system with a greater trophism for dopaminergic inputs to the striosomes relative to the surrounding matrix (Luscher *et al.* 2006, Crittenden *et al.* 2011).

### **Genetic models**

Several causal mutations have been identified in familial forms of PD. Transgenic mouse models with the same defects are useful to understand the molecular mechanisms involved in the pathology. However, they fail to reproduce the final neuropathological

defects of PD since they do not yield DAergic neuron loss. These mutations affect proteins involved in mitochondrial function, mitophagy, ubiquitination or ROS production (Blesa *et al.* 2014).

### **AAV- based models**

To understand the molecular basis of PD, another approach consists in the delivery of  $\alpha$ -synuclein thanks to a rAAV- $\alpha$ -synuclein injection in the SNc (Volpicelli-Daley *et al.* 2016). This technique allows the formation of  $\alpha$ -synuclein inclusions, and recapitulates many of the features found in PD (neuron loss, inclusions with biochemical and morphologic features similar to Lewy bodies, spread of pathology throughout the brain and defects in motor behaviors). The AAV-based model is more and more used to understand PD.

- [Therapies for Parkinson's disease in human](#)

Many avenues are explored for treating PD (Smith *et al.* 2012). They mainly consist in providing a new source of DA. This is always followed by motor side-effects that are treated with other drugs. Here, we will present a few.

### **Dopatherapy & other drug therapies**

Because PD results in dopaminergic denervation, one therapy consists in compensating DA depletion by oral administration of its metabolic precursor L-3,4-dihydroxyphenylalanine (L- DOPA or levodopa; Figure A.15) together with a peripheral decarboxylase inhibitor. Indeed, unlike DA, L- DOPA crosses brain blood barrier to be metabolized in the brain. It is either transformed by the residual DA neurons, or by other neurons that have the necessary enzymatic array. For example, another biogenic amine neuron such as the serotonergic neuron can uptake L- DOPA thanks to SERT. DA is then metabolized by the DOPA decarboxylase (also known as aromatic L-amino acid decarboxylase), and internalized in SVs by VMAT2.

In early phases of dopatherapy, L- DOPA can efficiently relieve (and even suppress for some patients) the motor symptoms of PD. For this reason, it is referred to as the honeymoon phase. However, in later phases when DA depletion becomes more severe, some other undesirable involuntary movements appear, known as L- DOPA- induced dyskinesia (Smith *et al.* 2012). At this stage, each drug intake is followed by swings in DA extracellular concentration, which is usually maintained constant thanks to the continuing concerted action of DAT and the autoreceptor D<sub>2</sub>R present on DAergic terminals. The treatment must be curtailed for this reason.

Several other avenues are explored in the treatment of PD. The adjunction of D<sub>2</sub>R agonists could suppress the undesired movements by stimulating the indirect pathway. As mentioned earlier, D1- and D2- MSNs express adenosine receptors. Adenosine and

dopamine exert opposing effects on BG. Adenosine receptors antagonistic coupling to cAMP-cascade propels them as novel targets to treat PD. The use of **specific A<sub>2A</sub>R antagonists** could normalize motor dysfunctions observed in patients (Armentero *et al.* 2011).

In both 6-OHDA-lesioned animals and PD patients, it was demonstrated that corticostriatal **glutamate neurotransmission** is hyperactive (Calabresi *et al.* 2000). The NMDAR antagonist amantadine is efficient at reducing LID and is used as an add-on to L-DOPA in PD patients (Hallett and Standaert 2004). Likewise, the mGluR5 antagonist mavoglurant improves LID (Rascol *et al.* 2014).

It has been demonstrated that the **cholinergic system** is also involved in parkinsonism, because of the striatal ACh/DA balance. In PD, striatal ACh level is increased. This is a direct result of DA depletion, which prevents activation of D<sub>2</sub>R on CINs; these receptors would normally inhibit ACh release (DeBoer *et al.* 1996). On top of that, the activity of M<sub>4</sub>R on CIN is also decreased because of intracellular coupling, which yields a self-disinhibition of ACh release (Ding *et al.* 2006). Indeed, studies have shown that nicotine (nAChR agonist) has a neuroprotective effect against striatal damage. The  $\alpha 6\beta 2^*$  heteromer (\* meaning that other subunits may be involved in this heteromer) is a target of particular relevance because its distribution is fairly restricted to the nigrostriatal dopaminergic system and a few other catecholaminergic systems. Anticholinergic drugs targeting mAChRs are also used as complements to L-DOPA treatment (Quik *et al.* 2007).

Once dopaminergic neurons have degenerated, **serotonergic neurons** overtake their role because they have the ability to convert L-DOPA to DA and to load it in SVs through VMAT2. Thus, they can store both 5-HT and DA in SVs. However, exocytic DA is poorly regulated because of the lack of DAT; it was hypothesized that this contributes to LID. In 6-OHDA models, 5-HT striatal levels are decreased, showing that these two transmitters compete for synaptic uptake (Figure A.50). Serotonergic agonists for 5-HT<sub>1A</sub>R and 5-HT<sub>1B</sub>R are efficient at decreasing LID in a synergistic way. Indeed, these two receptors act as autoreceptors (in the somatodendritic and axonal domains respectively) and downregulate 5-HT neurons firing and subsequently exogenous DA release (Carta *et al.* 2008).

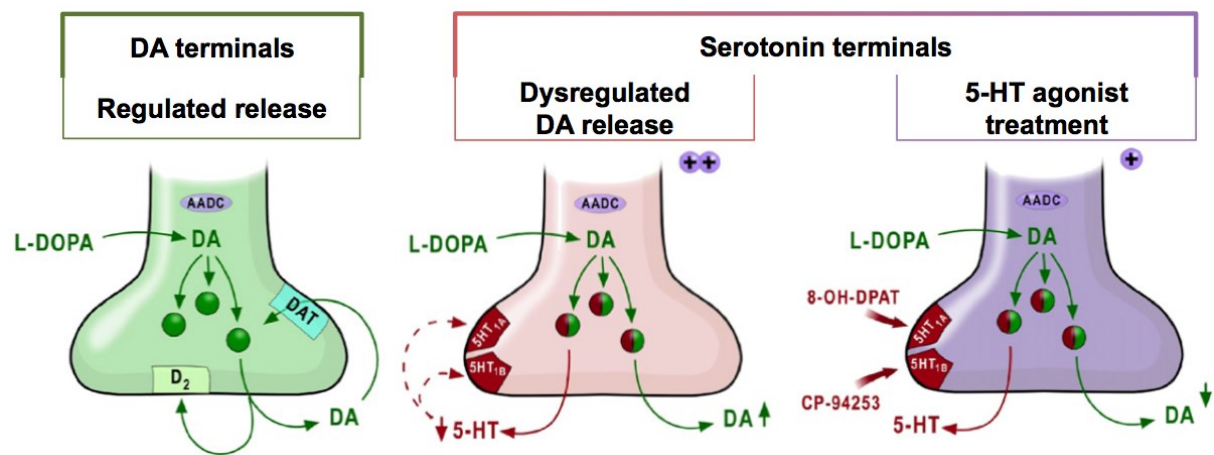


**Figure A.50: Presynaptic model of 5-HT-mediated LID**

**Left panel:** At early stages of PD, spared striatal DA terminals sustain the therapeutic effect of L-DOPA. L-DOPA is taken up by the DA terminals, stored into SVs and released in an activity-dependent manner. Extracellular DA levels are regulated by auto-regulatory feedback mechanisms mediated by D2 autoreceptors and the DA transporter present on DA terminals. **Middle panel:** As neurodegeneration progresses, fewer and fewer DA terminals will remain to mediate L-DOPA conversion and the serotonin terminals will come to play a major role. However, due to the lack of normal auto-regulatory feedback control and concomitant hyper-activation of serotonin terminals caused by depletion of endogenous serotonin by DA accumulating in the SVs, DA released from serotonin terminals will be poorly regulated, resulting in uncontrolled, excessive swings in DA release. The imbalance between the capacity of the serotonin terminals to release L-DOPA-derived DA, and the inability of the same neurons to provide a feedback control mechanism to regulate the level of the neurotransmitter in the synaptic cleft, would be the driving force in the induction of dyskinesia. **Right panel:** According to this model, 5-HT<sub>1A</sub>R and 5-HT<sub>1B</sub>R agonists, particularly in combination, completely suppress L-DOPA-induced abnormal movements in 6-OHDA-lesioned rats by dampening DA synaptic levels to a more physiological range. Note that for simplicity 5-HT<sub>1A</sub>Rs are positioned at the terminal level, but are indeed located at the level of the cell body of 5-HT neurons.

Adapted from Carta *et al.* (2008)

### Cell replacement therapy

To counterbalance the DAergic cell loss in PD patients, surgical procedures consisting in grafting dopaminergic cells in the putamen have been tested. The use of fetal dopaminergic cells allows a strong reinnervation of the striatum and these cells can survive for the life of the patient. This is accompanied by motor benefits that allow a stop of medical therapy for years (Kordower and Olanow 2016).

### Deep brain stimulation

Deep brain stimulation (DBS) is a method requiring a surgical procedure where a brain pacemaker is implanted in a given cerebral structure to stimulate it. It is a reversible technique, unlike invasive ablation surgeries. Subthalamic nucleus (major) and GPi (minor) are two structures targeted in DBS treatment of PD. They relieve some of PD motor symptoms and allow a lowering of medication (Morin *et al.* 2014).

## 2.2 Obsessive-compulsive disorders

We mentioned earlier how chronic treatment with drugs of abuse induces a compulsive behavioral pattern. This has been inferred to rely on the connectivity between orbitofrontal cortex and striatum (Everitt *et al.* 2013).

Obsessive-compulsive disorder (OCD) is a psychological disease characterized by repetitive, distressing thoughts accompanied by repetitive behaviors that relieve distress (Kim *et al.* 2013). It is associated with a hyperactivity of the OFC and with decreased D<sub>2</sub>R levels in the striatum. Several approaches are used to relieve OCDs. They can be treated with the administration of selective serotonin reuptake inhibitors (SSRI) with D<sub>2</sub>R antagonists as an add-on. For severe forms of OCDs, DBS in the ventral striatum have proven to be a successful approach.

Other disorders are related to stereotypies, such as autism spectrum disorder (ASD) or Tourette's syndrome, but will not be detailed here.

## 3. Stereotypies

### 3.1 Definition and general considerations

Stereotypies consist in purposeless, repetitive and restricted involuntary movements. They can be found in pathological states such as OCD, PD with dopatherapy or Tourette's syndrome. Drugs that enhance dopaminergic signaling can also artificially induce them.

In the sixties, it was noticed that specific pharmacological drugs such as amphetamine and apomorphine induce repetitive behaviors in animals (Fog *et al.* 1967, Randrup and Munkvad 1967, 1967). Both of these drugs act on the dopaminergic system. Therefore, these observations pointed toward a central role of BG and more specifically of the striatum in mediating these responses. *In situ* striatal injections of dopamine or dopaminergic agonists induce stereotypies (Ungerstedt *et al.* 1969). Additionally, lesions of the dorsal striatum prevent the induction of stereotypies by amphetamine without impairing the locomotor response (Kelly *et al.* 1975). The involvement of cortical structures in stereotypies was demonstrated with intrastriatal administration of NMDA (Karler *et al.* 1994), or intracortical enhancement of corticostriatal projections with D<sub>2</sub>R antagonists (Karler *et al.* 1998).

Altogether, these results settled down the central involvement of BG in stereotypies. Numerous experiments built up the theory of an imbalanced activity along the direct and indirect pathways. This imbalance is characterized by a relative increase in the nigrostriatal tone. Manipulations disinhibiting thalamocortical projections induce stereotypy. In contrast, the ones increasing the inhibitory tone in the thalamus attenuate stereotypies. For example, a recent study showed that optogenetic activation of the

striatonigral direct pathway is able to induce motor stereotypies (grooming, nose-poking in a hole and rearing) by manipulating the afferents to the ventromedial SNr, which are thought to arise from the striatal part innervated by the orbitofrontal cortex (Bouchekioua *et al.* 2017).

## **3.2 Animal models to elicit stereotypies**

### **3.2.1 L- DOPA- induced dyskinesia**

As presented above, PD is characterized by the loss of DAergic neurons from the SNc and a replacement treatment consists in levodopa oral administration. This supply of DA metabolic precursor leads to the production of debilitating movements at later stages, called **L- DOPA- induced dyskinesia (LID)**.

Based on the toxin- induced model of PD, there is a pharmacological procedure to produce LID in animal. After the unilateral neurotoxin- mediated DAergic loss, animals are treated with levodopa to mimic the process of dopatherapy and the LID that go with it. The treatment produces abnormal turning and movements, which can be assessed with abnormal involuntary movement (AIM) scales. These movements display dystonic or hyperkinetic features observed in axial and orofacial muscles (Morin *et al.* 2014).

The **AIMs rating scale** is constituted of three categories, each corresponding to a topographical area of the body: (1) limb dyskinesia characterized by repetitive and rhythmic movements or dystonic posturing of the forelimb on the side contralateral to the lesion; (2) axial dyskinesia characterized by lateral flexion and axial rotation / torsion affecting the neck and the upper trunk toward the side contralateral to the lesion; and (3) orolingual dyskinesia affecting the orofacial musculature including chewing movements, tongue protrusions and jaw tremor. Each category is scored based on a severity scale.

### **3.2.1 Drug- induced stereotypies**

An important feature of psychostimulants systemic administration is its ability to elicit a dose-dependent stimulation of the locomotor activity. At higher doses this locomotor outcome gets tainted with the emergence of idiosyncratic motor behaviors referred to as stereotypies (Figure A.51a). One way of producing stereotypies is by repeated injections of a low dose, or injection of a high dose of psychostimulants, *e.g.* amphetamine or cocaine. We will specifically focus on the effects of D-amphetamine, and refer to this phenomenon as **drug- induced stereotypies (DISs)** hereafter.

In rodents, while low doses of amphetamine preferentially affect glutamatergic connections in the medial AcbSh and enhance locomotion, higher doses activate DAergic transmission across the striatum, and particular in the dorsal part. This results in

progressively more focused stereotypic behaviors, culminating in continuous purposeless oral activities such as licking, gnawing, and chewing (Di Chiara *et al.* 1988, Drevets *et al.* 1999, Yates *et al.* 2007, Hadamitzky *et al.* 2012). These behaviors are prone to sensitization, since they exhibit a more rapid onset and a greater intensity upon repeated drug exposures (Hadamitzky *et al.* 2012). However, even at low doses, the hyperlocomotion induced by amphetamine appears to be patterned and perseverative (Schiørring 1979), feature also found in human addicts (the subject will walk along the same path aimlessly and repeatedly). This shift from locomotion to stereotypies has been extensively studied over the years (Russell and Pihl 1978, Yates *et al.* 2007).

D- amphetamine at high dose leads to a multiphasic response, as described by Schiørring:

- “The **“prephase”**, from injection of drug until all items of behavior (except sniffing, licking, and biting with head movements) [are] decreased to zero;
- The **“stereotypy phase”**, when only sniffing, licking, and biting with head movements [persist] and locomotion [is] absent, except for sporadic examples of backward locomotion;
- And the **“after phase”**, when the normal behavior items [reappear] successively, generally in the same order of their disappearance in the prephase., (Figure A.51b; Schiørring (1979)).

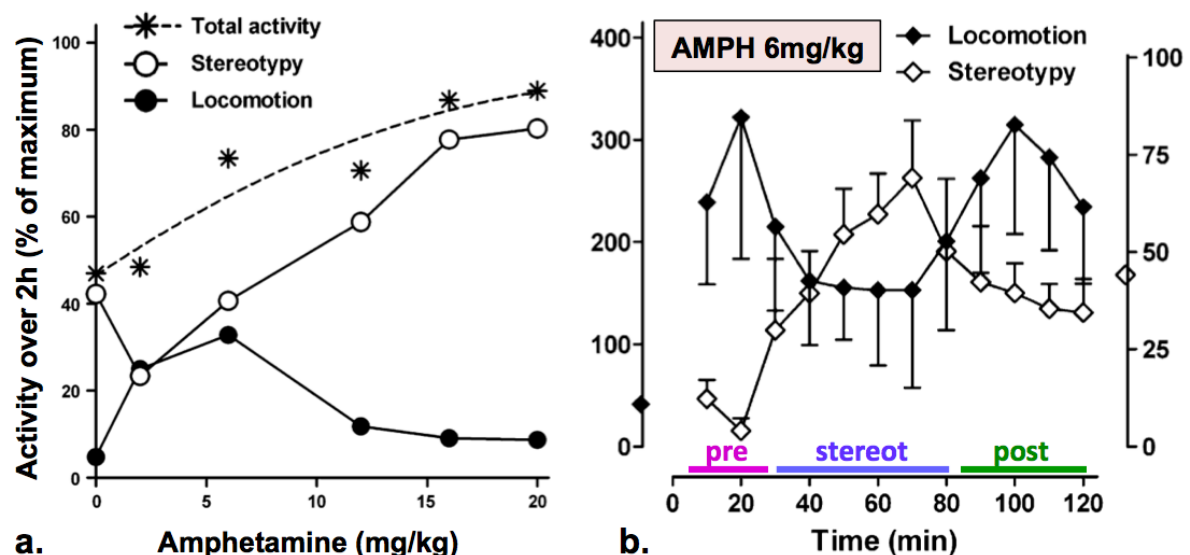


**Figure A.51: Amphetamine biphasic effect on locomotion and stereotypies**

**a.** Low doses of amphetamine mainly drive locomotion in C57/BL6 mice, while increasing doses result in a potentiation of stereotypies and a decrease of locomotion. **b.** At 6 mg/kg, mice show a typical multiphasic response, where the pre- and post-phases have high levels of locomotor activity and no stereotypy, while the stereotypy phase has low locomotion. Locomotor and stereotypic activities mirror each other.

Adapted from Yates *et al.* (2007)

### 3.3 Functional and biochemical correlates of stereotypies

- [Dopamine/acetylcholine imbalance in DISs](#)

Striatum plays a central role in the expression of stereotypies. It was inferred stereotypies onset would rely on the DA / ACh balance in this structure, and more precisely on the dorsal part of the striatum. Indeed, it was demonstrated that specific lesion of DAergic striatonigral pathway prevents DISs (Iversen *et al.* 1975). Likewise, dorsal striatum lesions (Kelly *et al.* 1975) or application of DA antagonist in the dStr yield the same result. More recently, a potential role for an imbalance between the medial prefrontal cortex and the sensorimotor component of the BG was inferred, as repeated cocaine would activate PFC without altering dStr signaling (Aliane *et al.* 2009).

During the time-course of stereotypies, there is a strong increase of DA release in the dStr, which remains constant until the wash-out of this behavior. On the contrary, ACh levels are inversely correlated to the intensity of the stereotypies (Aliane *et al.* 2011). It was demonstrated that DA released by nigrostriatal projections acts on D<sub>2</sub>R that activate GIRKs (potassium channels) leading to a rapid inhibition of CINs (DeBoer *et al.* 1996, Chuhma *et al.* 2014). This corresponds to the pause of CINs firing observed in the striatum in response to a salient cue (Morris *et al.* 2004). In their study, Aliane *et al.* proposed that ACh has the ability to arrest motor stereotypies. Indeed, application of D<sub>2</sub>R antagonist or mAChR antagonist would shorten or prolong the motor stereotypies respectively. Therefore, they proposed a mechanism where DA would inhibit ACh release, and an unknown mechanism would alleviate this inhibition to stimulate MSNs carrying mAChR (Aliane *et al.* 2011). Based on these observations, there is an ongoing clinical trial on children with ASD with the AChE inhibitor donepezil (Peter *et al.* 2017).

- [Biochemical correlates in LIDs](#)

For both LID and DISs, reports tend to link stereotypy severity to an imbalance between striosomal and matrix compartment activation in the DLS: **the stronger the striosomal activation, the more severe the stereotypies**. The increased striosome-to-matrix activity ratio is a common feature of several brain disorders, such as Huntington's disease, Parkinson's disease or drug addiction. It is more generally correlated with hyper-responsivity to psychomotor stimulants (Crittenden *et al.* 2011). This corresponds to a preferential activation of IEGs in the striosomal compartment (Saka *et al.* 2002).

It is believed that LID is due to a hyper-responsivity of MSNs to DA, in a compensatory mechanism to tackle the DAergic denervation. D<sub>1</sub>R stimulation seems to be essential for the development of LID: 6-OHDA-lesioned mice lacking D<sub>1</sub>R barely present LID after L-DOPA treatment, while D<sub>2</sub>R-KO mice display control levels of LID (Darmopil *et al.* 2009). With different models, it was demonstrated that a compartmental

imbalance appears, with a striosomal overactivation of D1-MSNs correlated with LID severity. This is imputable to an increased transduction of two D<sub>1</sub>R signaling cascades (PKA and ERK1/2), as inhibition of ERK1/2 or mTOR, but also of PKA or DARPP32-pThr34 and up/downstream targets alleviates LID (for review, refer to Crittenden *et al.* 2011, Murer and Moratalla 2011). ERK1/2 seems to be important during the early onset of LID, while its maintenance relies on overactivation of PKA/DARPP-32, and both result in an overexpression of IEGs. In line with this, compartmental imbalance has also been reported for two ERK1/2 regulators, namely calcium-diacylglycerol-guanine nucleotide exchange factor (CaDAG-GEF) in a rat LID model (Crittenden *et al.* 2009). GEFs are proteins that activate GTPases by exchanging the GDP they carry for a GTP, e.g. the Ras superfamily. CaDAG-GEFI, which is matrix-enriched, activates Rap1/2, and CaDAG-GEFII that is striosome-enriched activates Ras. In this study, it was reported that matricial CaDAG-GEFI was down-regulated while striosomal CaDAG-GEFII was up-regulated, suggesting an overactivation of ERK pathway in the striosomes. Plus, the extent to which their level was modified could reflect the severity of abnormal motor responses evoked by the L-DOPA treatment (Figure A.52; Crittenden *et al.* (2009)).

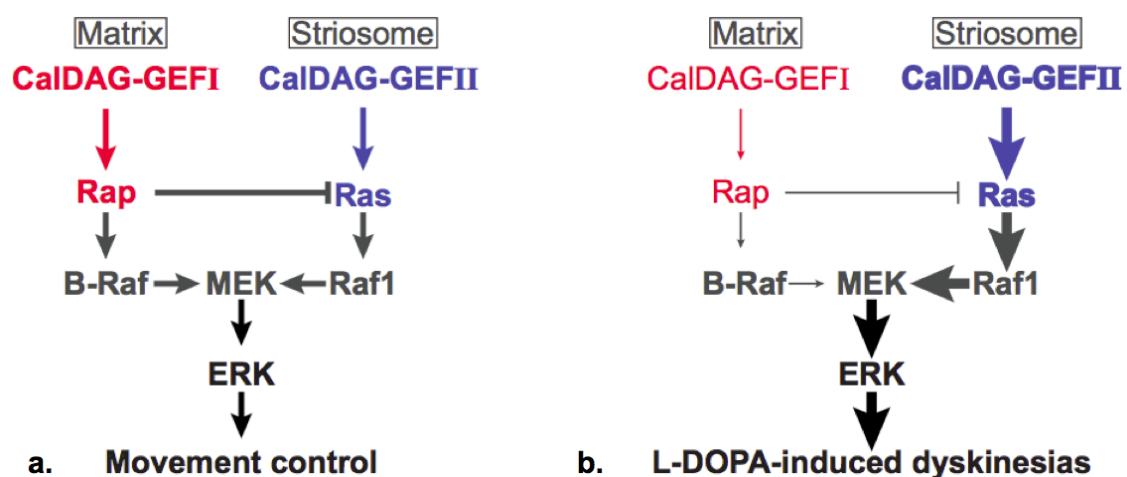


**Figure A.52: Model of CaDAG-GEFs striatal signaling to ERK in LID**

**a.** In the normal striatum, a balance between striatal compartments yield to movement control. **b.** In a model of LID, the overexpression of CaDAG-GEFII in striosomes leads to an overactivation of ERK signaling in D1-MSNs and yield to an increased level of dyskinesia.

From Crittenden *et al.* (2009)

As for LID, Crittenden *et al.* demonstrated that CaDAG-GEFs intervene in abnormal movements induced by amphetamine. Knock-out mice for CaDAG-GEFI show increased stereotypies in response to D-amphetamine (Crittenden *et al.* 2009).

Very interestingly,  $\Delta$ FosB, a truncated form of the iEG *FosB*, highly accumulates in D1-MSNs with repeated injections of amphetamine, and also with L-DOPA-treated PD models. This isoform is stable and maintained to high levels a long after disruption of

drug treatment. Its level is directly correlated to the severity of dyskinesia (Murer *et al.* 2011). Another example of compartmental imbalance is that opioid receptors are differentially regulated upon DA depletion (Figure A.49), and it was demonstrated that inhibition of the striosomal-enriched MOR leads to a reduction of LID (Koprach *et al.* 2011).

Earlier, we discussed the role of CINs and ACh / DA in DISs. This balance is also involved in LID. Striatal cholinergic tone is enhanced in LID, even if the number of CIN is not altered (Gangarossa *et al.* 2016). While acute L-DOPA induces the activation of MSNs via ERK phosphorylation, repeated L-DOPA treatment shifts this activation toward CINs (Ding *et al.* 2011). Their basal firing rate and DA-evoked responses are then enhanced, and this increased excitability is mediated by ERK activation. Thus, inhibition of ERK or application of muscarinic antagonists improve LID (Ding *et al.* 2011). More evidences support the idea of LID as a result of an enhanced striatal cholinergic tone. CIN neurotoxic ablation (Won *et al.* 2014) and CIN optogenetic inhibition (Ztaou *et al.* 2016) both reduce LID. On the other hand, optogenetic activation of CINs either improves (with long stimulation, both nAChR- and mAChR-dependent) or worsens them (with brief pulse, mAChR-dependent; Bordia *et al.* (2016)). It has been proposed beneficial effects observed with prolonged CINs optogenetic stimulation comes from the desensitization of nAChRs. Indeed, treatment with nAChR agonists also decreases LID up to 50% (Bordia *et al.* 2010). Both M<sub>1</sub>R (expressed by D1- and D2-MSNs) and M<sub>4</sub>R blockade (expressed post-synaptically by D1-MSNs and pre-synaptically by CINs) alleviate the motor abnormalities observed in parkinsonian models, as their specific antagonists applied locally in the dorsal striatum decrease LID. The effect observed with M<sub>4</sub>R is imputable to D1-MSNs (Ztaou *et al.* 2016).

Together, these studies demonstrate common neural basis in the abnormal movements found in pathological states such as Parkinson's disease or artificially drug-induced stereotypies. The circuit involved is localized in the dorsal part of the striatum, and CINs play a major role in this phenotype. The classical model of imbalance between direct » indirect pathways can thus be inflated with an imbalance between striosomal » matricial compartments.

### **3.4 Methods to assess drug-induced stereotypies**

Stereotypies are subtle locomotor loops that can be triggered by high psychostimulant doses. They are difficult to assess since this score is empirical, and based on a subjective rating by the experimenter. It is crucial that the experimenter remains blind to the treatment, so that there is less chance of biasing the score attributed to each mouse.

For a given mouse strain of same age and sex, not only according to the psychostimulant used and to its dose, but also to the experimental environment (homecage  $\pm$  litter) and time of day, stereotypies will express in different ways. For instance, it is well known that high doses of cocaine (> 20 mg/kg) trigger limb stereotypies such as excessive rearing. Amphetamine will preferentially lead to orofacial stereotypies (Randrup *et al.* 1967, Randrup *et al.* 1975).

Currently, the only way to assess stereotypies is by manual scoring. However, this rating technique is hardly reproducible between experimenters because one may consider that some behavior is very intense while one other may rate it as mild, based on the comparison between the groups observed. Therefore, stereotypy scoring would be greatly improved if it were automated, by video tracking and software analysis. The difficulty resides in that stereotypies are natural behaviors that are repeated with abnormal patterns, so parameters defined to discriminate between what is 'normal' and what is stereotypic would be difficult. Moreover, there are some subtle kinds of stereotypies triggered by D- amphetamine, displayed as jaw or tongue movements and biting, which would be more difficult to record. The manual scoring omits some important aspects of behavior occurrence, such as the frequency or the duration of each episode. For those reasons, it would be very interesting to develop a tool to perform this kind of analysis.

The most common stereotypy rating scale is based on Creese & Iversen's work, see Table A.6 (Creese and Iversen 1975). This scale was initially used to assess the effects of D- amphetamine 1.5 mg/kg on adult male Wistar rats.

**Table A.6: Creese & Iversen stereotypy rating scale**

<b>CREESE &amp; IVERSEN (1975)</b>	
<b>0</b>	Asleep or stationary
<b>1</b>	Active
<b>2</b>	Predominantly active but with bursts of stereotyped sniffing or rearing
<b>3</b>	Stereotyped activity such as sniffing along a fixed path in the cage
<b>4</b>	Stereotyped sniffing or rearing maintained in one location
<b>5</b>	Stereotyped behavior in one location with bursts of licking
<b>6</b>	Continual gnawing or licking of the cage bars

### 3.5 Role of VGLUT3 in LID

As discussed earlier, CINs play a central role in the development of LID. These neurons accumulate and release glutamate along with acetylcholine. Therefore, it was inferred that glutamate released from CINs could participate in the development of LID (Divito *et al.* 2015, Gangarossa *et al.* 2016).

In one study, Gangarossa *et al.* used either VGLUT3<sup>-/-</sup> mice or mice lacking VAcHT in the CINs (Drd2-Cre::VAcHT<sup>LoxP/LoxP</sup> referred to as cKO-VAcHT; Gangarossa *et al.* (2016)). DA depletion led to an upregulation of VAcHT and VGLUT3. The lack of VGLUT3 alleviated LID (Figure A.53a), along with a decreased striatal signaling (normalization of ERK/mTOR and rpS6 signaling compared to LID animal). On the other hand, LID was globally unchanged in cKO-VAcHT mice, even if the AIMs score was increased in these mice during the treatment, probably because of compensatory mechanisms (Figure A.53b). The authors proposed that glutamate released from CINs, rather than ACh, could contribute to the development of LID (Gangarossa *et al.* 2016). Indeed, it was already demonstrated that glutamate modulates DA release by acting on mGluRs (Sakae *et al.* 2015). Antagonists for mGluR5 improve motor deficits observed in PD rat models (Breyse *et al.* 2002). Therefore, the authors suggested that mGluR5 might be the preferential target of CIN-released glutamate (Gangarossa *et al.* 2016).

Divito *et al.*, in agreement with the previous study, found that VGLUT3<sup>-/-</sup> mice have decreased LID. Using another conditional model (ChAT-IRES-Cre::VGLUT3<sup>LoxP/LoxP</sup> referred to as cKO-ChAT), they found that LID was slightly decreased in cKO-ChAT (Divito *et al.* 2015).

Together, these results demonstrate that VGLUT3 is involved in mediating LID. As set forth by the two studies, this contribution could stem from another source than CINs.

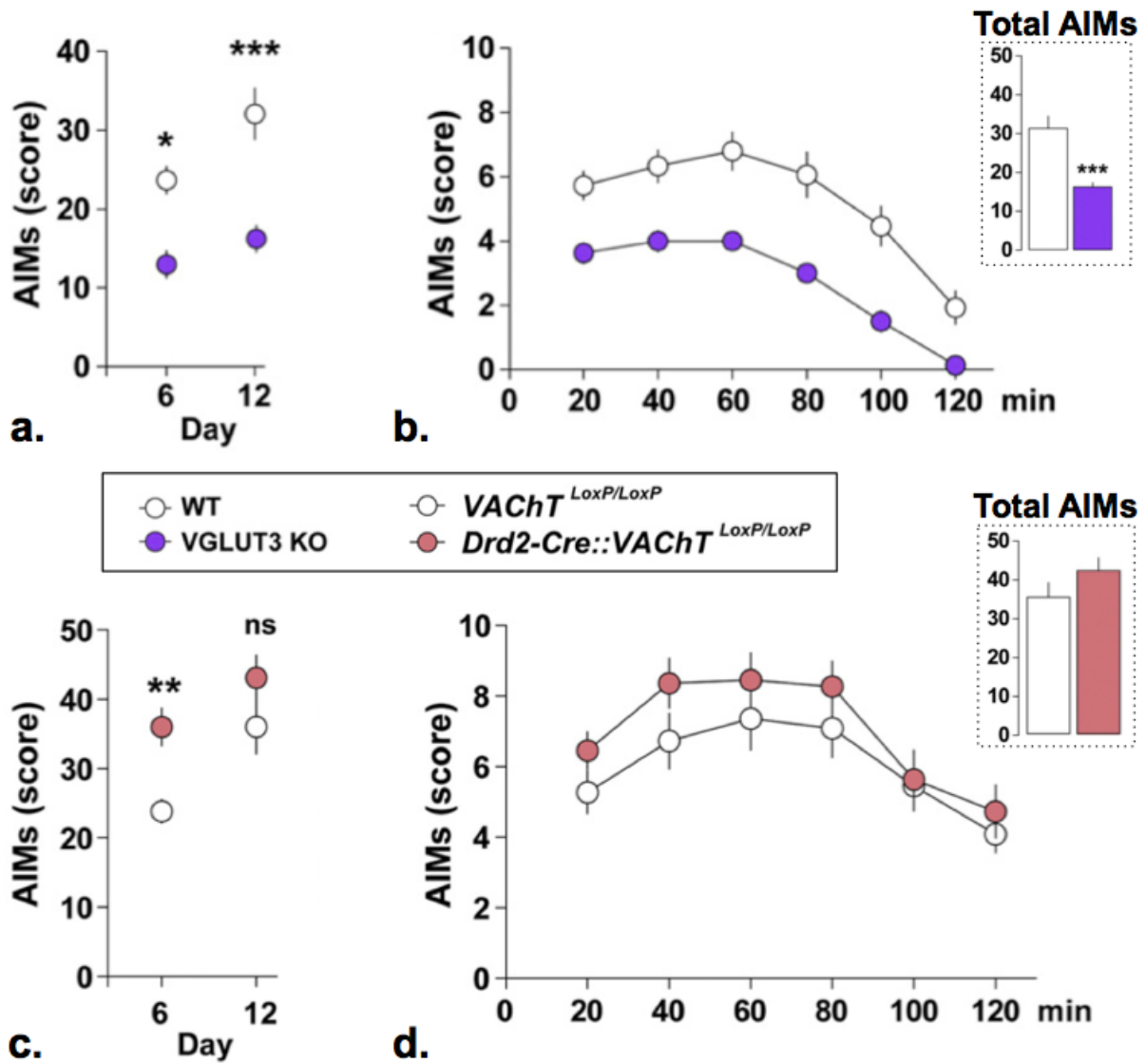


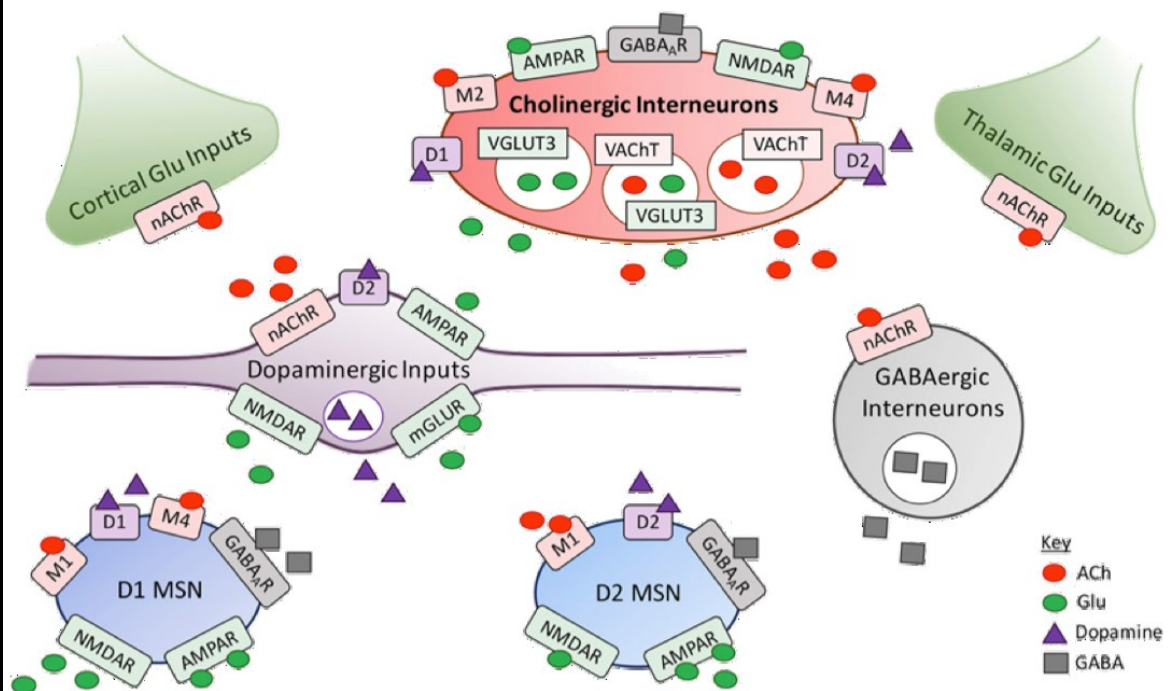
**Figure A.53: LID in VGLUT3<sup>-/-</sup> and Drd2-Cre::VACHT<sup>LoxP/LoxP</sup>**

LID is attenuated in VGLUT3<sup>-/-</sup> mice (**top panel, in purple**) while it is unchanged in Drd2-Cre::VACHT<sup>LoxP/LoxP</sup> (**bottom panel, in red**). **a** and **c** represent the cumulative score of total AIMs at day 6 and day 12 of L-DOPA treatment after unilateral 6-OHDA lesion. **b** and **d** represent the time-course of total AIMs following the last L-DOPA injection (day 12) and the cumulative score of total AIMs (*inset*).

Adapted from Gangarossa *et al.* (2016)

Dopamine is a central regulator of striatal activity. Dysfunctions related to DA mesolimbic and mesocortical projections affect drug-related behaviors, such as excessive drug intake or development of psychosis. DA nigrostriatal projections provide a regulation of motor-related loops and compulsive behaviors, and are affected in disorders such as Parkinson's disease (PD) or obsessive-compulsive disorders. Drugs of abuse hijack the dopaminergic system and artificially enhance DA levels.

The dyskinesia found in pathological states such as PD and drug-induced stereotypies share common neural basis. Both rely on an overactivation of the striosomes compared to the surrounding matrix.



From Kljatic *et al.* (2017)

Cholinergic interneurons are local regulators of striatal activity, and they modulate the dopaminergic transmission. Their activity is altered in PD and in chronic drug intake.

# PROBLEMATIC

## GENERAL CONTEXT

VGLUT3<sup>-/-</sup> mice demonstrate a wide range of pleiotropic phenotypes, such as increased anxiety, deafness or hypersensitivity to pain (Seal *et al.* 2008, Seal *et al.* 2009, Amilhon *et al.* 2010). Among these phenotypes, VGLUT3<sup>-/-</sup> mice present constitutive hallmarks of addiction to cocaine. In VGLUT3<sup>-/-</sup> mice, DA release is increased in the Acb, along with an overactivation of the direct pathway. The number of dendritic spines on D1-MSNs is constitutively elevated, as well as the AMPAR/NMDAR ratio (Sakae *et al.* 2015).

VGLUT3 is expressed by all cholinergic interneurons (CINs) where it enhances cholinergic tone by a mechanism referred to as vesicular synergy (Gras *et al.* 2008). This cell population plays a critical role in the modulation of striatal inputs, including cortical and subcortical glutamatergic inputs, and midbrain DAergic inputs (Lim *et al.* 2014). There is a tight DA / ACh balance in the striatum, where DA inhibits cholinergic tone by acting on presynaptic D<sub>2</sub>R, while ACh increases DAergic tone by acting on presynaptic nicotinic acetylcholine receptors (DeBoer *et al.* 1996, Threlfell *et al.* 2012). Recently, it was demonstrated that not only does VGLUT3 regulate ACh tone, but that glutamate released from CINs also participates to the regulation of DA release by acting on inhibitory presynaptic mGluRs (Sakae *et al.* 2015).

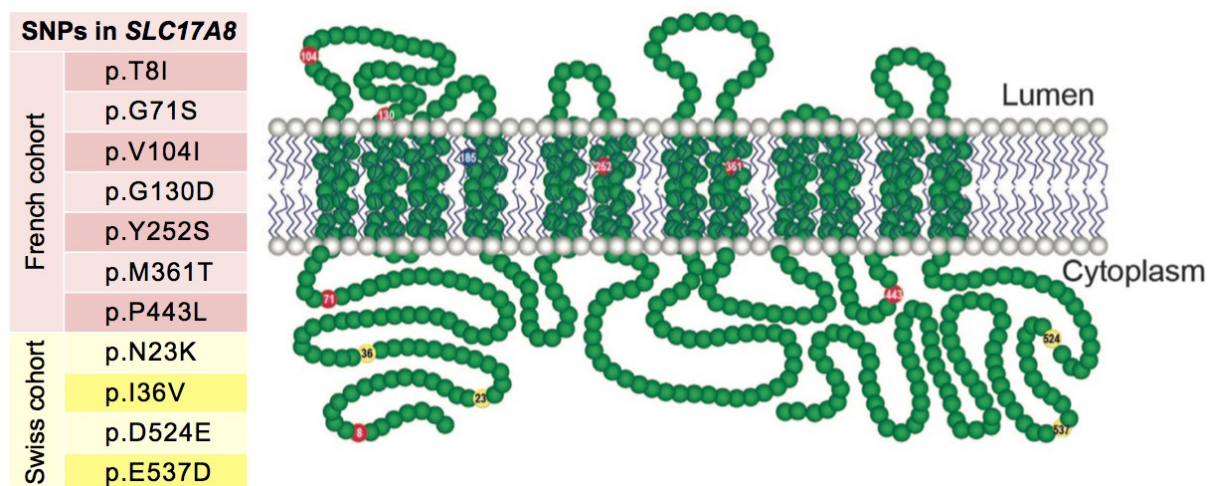


**Figure A.54: VGLUT3 mutations in humans with severe drug abuse**

Several punctual mutations were identified in *SLC17A8*, the gene encoding VGLUT3, in human polyaddicts. Seven independent SNPs were identified in a French cohort of 230 patients (*in red*) and four other SNPs were found in a Swiss cohort of 265 patients (*in yellow*).

Adapted from Sakae *et al.* (2015)

Because of the obvious contribution of VGLUT3 in the response to cocaine in mice, it was suspected that this protein could also be involved in mediating the response to drugs of abuse in humans (human and mouse VGLUT3 share more than 90 % amino acids identity). Indeed, a study conducted on human polyaddicts highlighted the existence of several SNPs in *SLC17A8*, the gene encoding VGLUT3 (Figure A.54; Sakae *et al.* (2015)). These results place VGLUT3 as a regulator of drug abuse, in both mice and humans.

We have discussed the role of CINs in modulating the rewarding effects of drugs. Their ablation enhances vulnerability to cocaine, but this effect is imputable to the glutamate they release rather than the acetylcholine. Indeed, genetic deletion of VACHT, the vesicular transporter for acetylcholine, has a little impact on cocaine sensitivity (Hikida *et al.* 2003, Guzman *et al.* 2011, Sakae *et al.* 2015).

CINs are also involved in the regulation of abnormal movements, such as L- DOPA- induced dyskinesia (LID). Optogenetic experiments show that inhibition of CINs decreases LID whereas their activation exacerbates LID (Ding *et al.* 2011, Won *et al.* 2014, Bordia *et al.* 2016). Different studies tried to identify the involvement of acetylcholine and glutamate released from CINs in LID or drug- induced dyskinesia (Aliane *et al.* 2011, Crittenden *et al.* 2014, Divito *et al.* 2015, Gangarossa *et al.* 2016). Concordant studies demonstrated that VGLUT3 null mice are more resistant to LID, suggesting that glutamate released from CINs could be responsible for this phenotype (Divito *et al.* 2015, Gangarossa *et al.* 2016). However, selective deletion of VGLUT3 in CINs does not reproduce the resistance to LID (Divito *et al.* 2015). On the other hand, the contribution of acetylcholine to the development of LID or drug- induced dyskinesia is still a matter of debate. One study reported that acetylcholine in the dorsal striatum is necessary to arrest cocaine- induced stereotypies while another stated that increased striatal cholinergic tone (VACHT overexpressing mice) exacerbates amphetamine- induced stereotypies (Aliane *et al.* 2011, Crittenden *et al.* 2014).

## **PROBLEMATIC**

VGLUT3 plays an essential role in mediating cocaine's rewarding effects. This protein also appears as a factor of susceptibility of drug abuse in human addicts. Therefore, we investigated if this effect could be extended to other drugs. During my PhD, I addressed the role of VGLUT3 in the behavioral effects of another psychostimulant, amphetamine. I assessed the amphetamine- induced locomotion and stereotypies in behavioral sensitization paradigms in mice lacking VGLUT3 in the whole brain.

In the striatum VGLUT3 is present in cholinergic and serotonergic fibers. I tried to evaluate the contribution of these two different VGLUT3- positive neurotransmitter systems in mediating the behavioral effects of amphetamine. I used a Cre- lox- based

genetic approach consisting in crossing VGLUT3<sup>LoxP/LoxP</sup> mice with serotonergic- or cholinergic- specific Cre- expressing lines.

VGLUT3 null mice present major alterations in the accumbal neuronal circuitry, which supposedly underlie the hyper- responsivity to cocaine. I also tried to knockdown VGLUT3 specifically in the Acb. This knockdown was obtained by infusing Cre- expressing AAV viruses in the nucleus accumbens of VGLUT3<sup>LoxP/LoxP</sup> to assess the behavioral response to cocaine.

## **MAJOR FINDINGS**

With my work, I demonstrated that unlike cocaine, amphetamine at low doses produces a locomotor sensitization in VGLUT3 null mice. The amphetamine- induced hyperlocomotion is greater in these mice compared to control siblings, suggesting that VGLUT3<sup>-/-</sup> mice are indeed more sensitive to drugs.

Higher doses of amphetamine elicit abnormal movements in the form of stereotypies. With these doses I observed that VGLUT null mice hyperlocomotion is doubled compared to WT mice. Furthermore, VGLUT3<sup>-/-</sup> mice lacking are particularly resistant to stereotypies.

The study of conditional knockouts for VGLUT3 ruled out a contribution of the VGLUT3- positive serotonergic system in the phenotypes observed in VGLUT3 null mice. However, the VGLUT3- positive cholinergic system contributes to the amphetamine- induced stereotypies.

In another part of my work, I proceeded to VGLUT3 accumbal knockdown. Preliminary results indicate a negative correlation between the residual accumbal level of VGLUT3 and the extent of cocaine- induced hyperlocomotion.

These results offer new insights into the role of VGLUT3 in mediating drug- related behaviors. They also place VGLUT3 as an interesting target not only for drug abuse, but also for abnormal movements.



# MATERIALS AND METHODS

## 1. Animal models

All animal care and experiments were conducted in accordance with the European Communities Council Directive for the Care and the Use of Laboratory Animals (86/809/EEC), in compliance with the *Ministère de l'Agriculture et de la Forêt, Service Vétérinaire de la Santé et de la Protection Animale* (authorization number 01482.01 from ethics committee Darwin #5). All efforts were made to minimize the number of animals used in the course of the study and to ensure their well-being. The animals were housed in groups of 2-5 per cage, in a temperature-controlled room ( $21 \pm 2^\circ\text{C}$ ) with a 12:12-h dark/light cycle (lights on 7:30 a.m. to 7:30 p.m.). Water and food were provided *ad libitum*.

### 1.1 VGLUT3<sup>-/-</sup>

VGLUT3<sup>-/-</sup> are mice that constitutively lack VGLUT3 in the whole body. These mice were generated by the *Institut Clinique de la Souris* (Strasbourg, France) by homologous recombination in embryonic stem cells (129/Sv). They have been backcrossed on a C57BL/6J background for more than 12 generations. In the mutant, the exon 2 is replaced with an FRT-flanked neomycin resistance cassette that creates a STOP codon in frame with exon 1 (Figure B.1a), and results in a null mutation (Gras *et al.* 2008). Mice are genotyped with the primers listed in Table B.1 (Figure B.1b).

**Table B.1: Primers for VGLUT3<sup>-/-</sup> PCR**

Primer	Sequence	Primers	Band size	Allele
P1	5' – GTG TGA CAT GAA GCC TGG ACT GTT C – 3'	P1 x P3	<b>278 bp</b>	<b>WT</b>
P2	5' – GAA GGG TGA GAA CAG AGT ACC TAC – 3'	P2 x P3	<b>604 bp</b>	<b>KO</b>
P3	5' – AGC AGA CTG AAG CGT CTC CAT GGT G – 3'			

Apart from being deaf, VGLUT3<sup>-/-</sup> have no major defects (normal weight, size, fertility and life span; Gras *et al.* (2008)). As shown in Figure B.1c, these mice have no residual VGLUT3 protein or mRNA in the striatum.

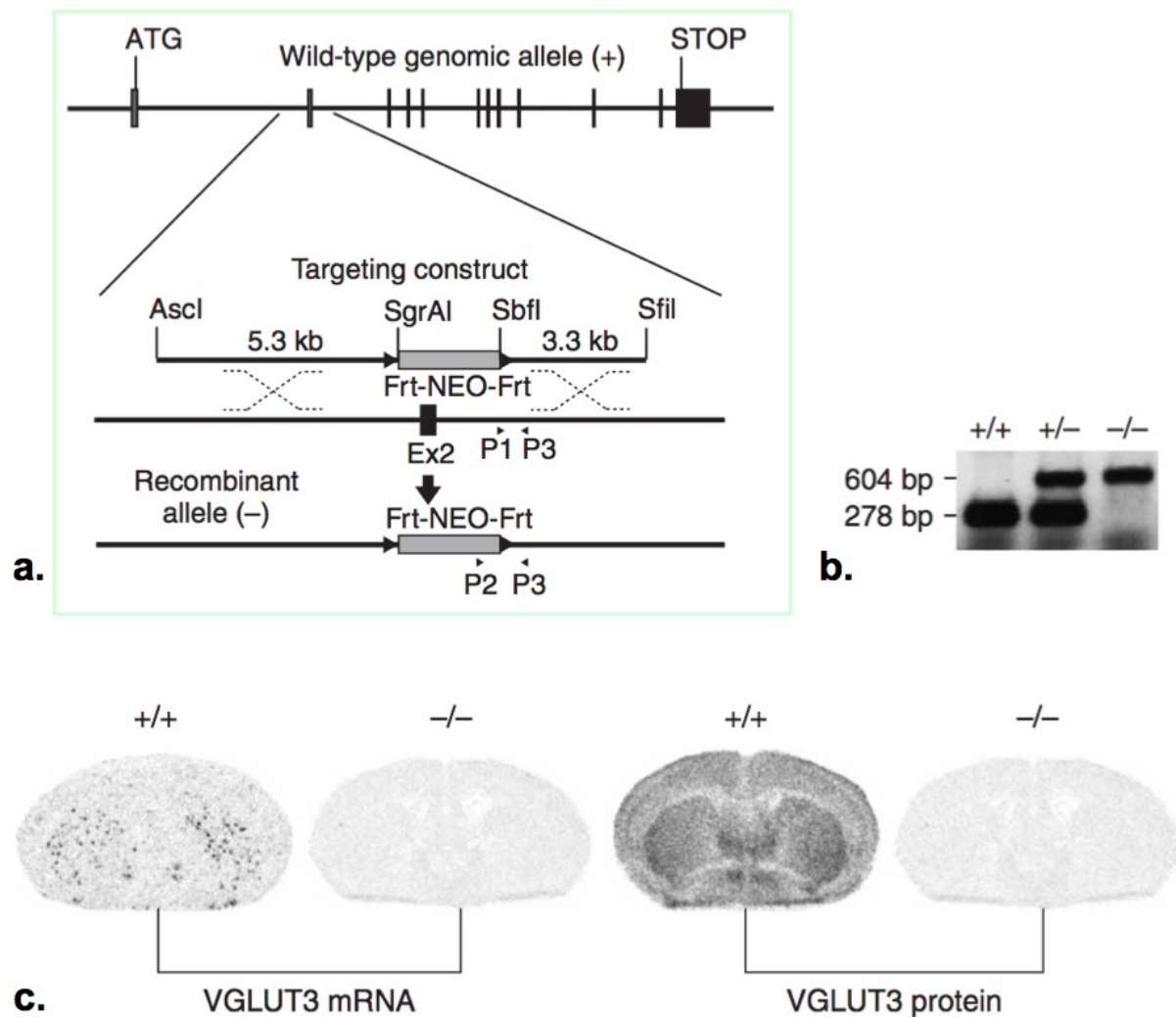


**Figure B.1: VGLUT3<sup>-/-</sup> construct**

**a.** The targeting strategy consists in replacing exon 2 of *Vglut3* gene with a neomycin (NEO) cassette. **b.** Genotyping of VGLUT3 by PCR with a three-primer-based protocol (P1-3). **c.** The effect of the mutation on the expression of VGLUT3 in the striatum is assessed by ISH (**left**) and immunohistochemistry (**right**). VGLUT3 mRNA and protein are totally absent in knockout mice (-/-) compared to wild-types (+/+).

Adapted from Gras *et al.* (2008)

## 1.2 VGLUT3<sup>LoxP/LoxP</sup>

VGLUT3<sup>LoxP/LoxP</sup> mice carry two LoxP sites in their coding sequence. Using appropriate tools, this floxed sequence can be excised by the Cre recombinase (Cre-Lox system), resulting in a premature STOP codon and therefore to the absence of the protein (Nagy 2000).

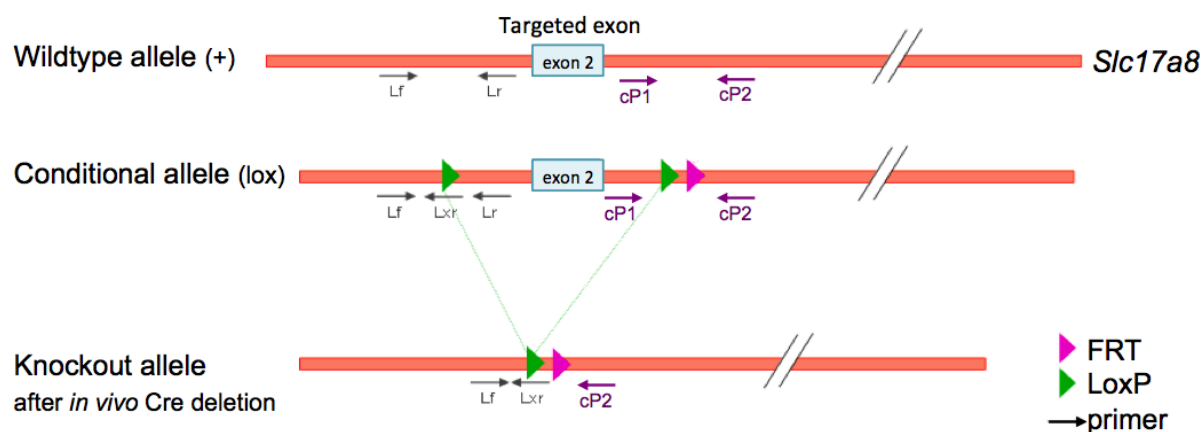


**Figure B.2: VGLUT3<sup>LoxP/LoxP</sup> construct**

As for VGLUT3<sup>-/-</sup>, VGLUT3<sup>LoxP/LoxP</sup> mice were generated by the *Institut Clinique de la Souris*. They have been backcrossed on a C57BL/6N background for 2 generations. In these mice, the exon 2 of *SLC17A8* gene is floxed (Figure B.2). Mice are genotyped by PCR with the primers presented in Table B.2.

**Table B.2: Primers for VGLUT3<sup>LoxP/LoxP</sup> PCR**

Primer	Sequence	Band size	Allele
cP1	5' – TTG TGA AAA AGC AAA CAG AGC CAT TC – 3'	277 bp	WT
cP2	5' – TGT CTG AGC CAT CAC TTT CTC TGG AAA – 3'	382 bp	Lox

### 1.3 VGLUT3 conditional knock-out: genetic approach

In order to understand the contribution of the different VGLUT3-positive neurotransmitter systems in the brain, we crossed VGLUT3<sup>LoxP/LoxP</sup> mice with different cell-specific Cre-expressing lines. For all the breedings, we make sure there is only one allele with the Cre recombinase.

The breeding strategy is as follows (Figure B.3). We maintain the founder line, called Cre line, by incrossing Cre/+ with +/+ mice. With their F0 offspring, we form the 1<sup>st</sup> breeding by crossing the Cre/+ males with homozygous VGLUT3<sup>LoxP/LoxP</sup> females from the VGLUT3 Lox line. Then the F1 (Cre/+; VGLUT3<sup>LoxP/+</sup>) males are mated with heterozygous VGLUT3<sup>LoxP/+</sup> females from the VGLUT3 Lox line to form the 2<sup>nd</sup> breeding. This breeding generates the animals used for experiments. We systematically compare the double mutant mice, called conditional knock-out (cKO), to the control that do not carry the Cre allele (+/+; VGLUT3<sup>LoxP/LoxP</sup>).

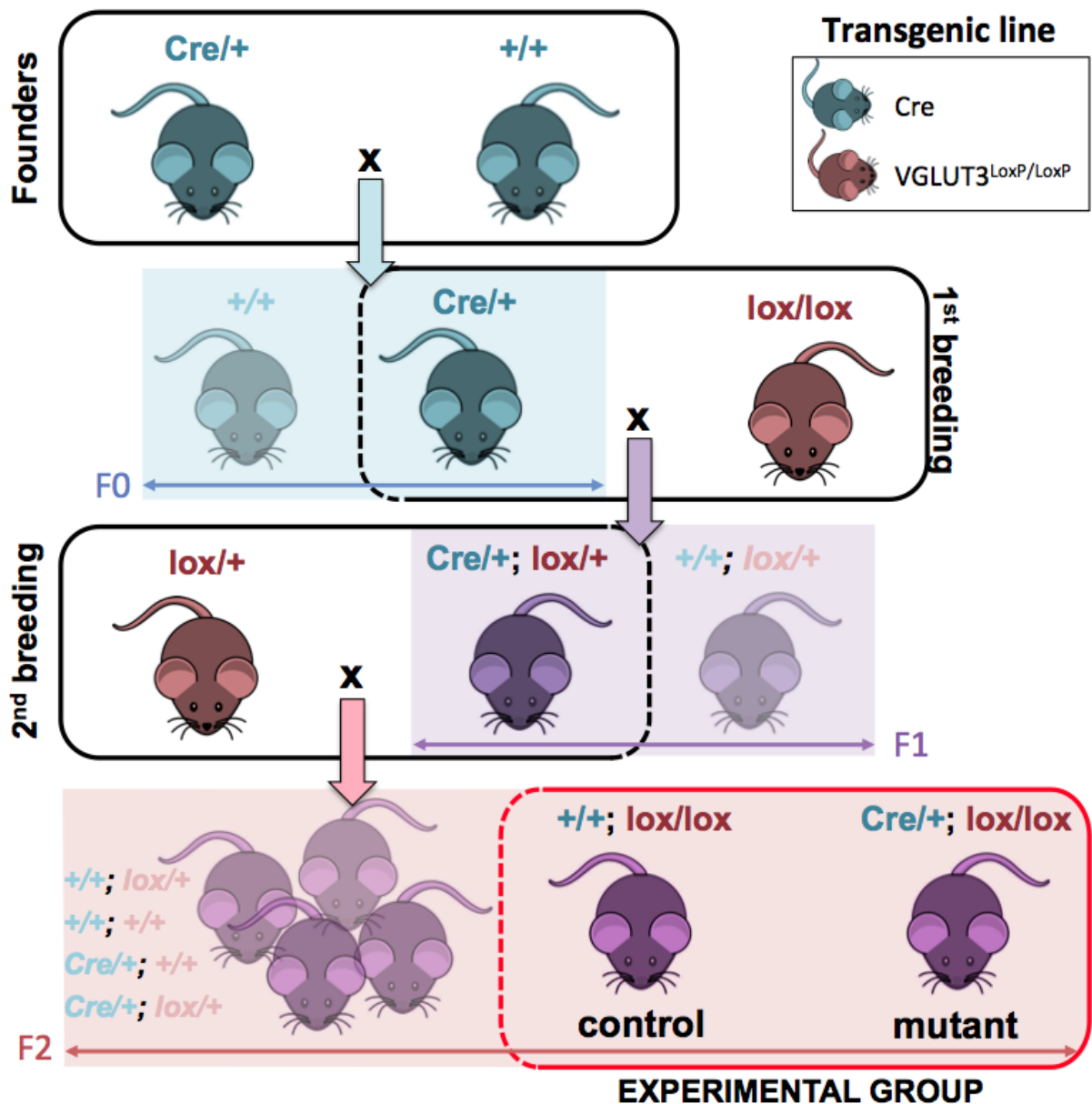


**Figure B.3: VGLUT3 conditional knock-out breeding strategy**

The breeding is done in 3 steps. First, we produce heterozygous  $Cre/+$  animals. These mice are crossed with homozygous  $VGLUT3^{LoxP/LoxP}$  and constitute the 1<sup>st</sup> breeding. The double heterozygous ( $Cre/+; VGLUT3^{LoxP/+}$ ) are then crossed with heterozygous  $VGLUT3^{LoxP/+}$  from the VGLUT3 Lox line and constitute the 2<sup>nd</sup> breeding. A fraction of the resulting animals will be included in the experimental group: controls are ( $+/+; VGLUT3^{LoxP/LoxP}$ ) and conditional knock-outs are ( $Cre/+; VGLUT3^{LoxP/LoxP}$ ). The faded animals represent littermates that are not used in our protocols. The plain color squares represent the offspring from the crossing positioned right above. The black boxes represent the crossings, and the red box is the experimental group.

### 1.3.1 SERT-Cre conditional knock-out

In order to specifically remove VGLUT3 in the serotonergic system, we crossed our  $VGLUT3^{LoxP/LoxP}$  mice with the SERT-Cre line generated by Zhuang *et al.* (Zhuang *et al.* 2005). This line is currently commercialized by Jackson Laboratory under the name

B6.129(Cg)-*Slc6a4*<sup>tm1(cree)Xz</sup>/J (stock number 014554), and has been backcrossed to C57BL/6J for more than 10 generations by the donating lab.

The SERT-Cre is a "knock-in" allele: the exon 2 of the *Slc6a4* gene (SERT) is replaced by the Cre recombinase. The inserted cassette contains the Cre recombinase coding sequence with a nuclear localization signal and the neomycin-resistance gene flanked by FRT sites. Therefore, the inserted transgene disrupts one copy of the SERT gene that leads to specific failure of serotonin uptake and clearance in homozygous SERT-Cre mice, even if still viable and fertile (Sanders *et al.* 2007). Yet, we only use heterozygous in our crossings, and they are no known phenotypes for these mice.

The F2 animals are genotyped with 2 different PCRs, one for the Lox allele (Table B.2) and the other for the Cre allele (Table B.3).

**Table B.3: Primers for SERT-Cre PCR**

Primer	Sequence	Primers	Band size	Genotype
Cre <sub>rev</sub>	5' – GAA CGA ACC TGG TCG AAA TCA G – 3'	Comm x WT	<b>380 bp</b>	<b>WT</b>
WT <sub>rev</sub>	5' – GGC ACT AAC CTC CAC CAT TCT G – 3'	Comm x Cre	<b>500 bp</b>	<b>CRE</b>
Comm <sub>forw</sub>	5' – CAT CCG CAC CAC TGA CTG ACC A – 3'			

### 1.3.2 ChAT-IRES-Cre conditional knock-out

To investigate the role of VGLUT3-positive cholinergic neurons in the brain, we bred out VGLUT3<sup>LoxP/LoxP</sup> mice with a cholinergic-Cre-expressing line: ChAT-IRES-Cre (B6.129S6-*Chat*<sup>tm2(cree)Lowl</sup>/J, stock number 006410, Jackson Laboratory). In this line, an "IRES-Cre" sequence is inserted downstream of the stop codon. The endogenous ChAT gene promoter controls the Cre expression, with the IRES (internal ribosome entry sequence) providing Cre an independent transcript from ChAT mRNA. Thus, ChAT gene expression is unaffected and mice have normal levels of ACh. Cre recombinase activity is reported in all cholinergic neurons.

F2 animals are genotyped with 2 different PCRs, one for the Lox allele (Table B.2) and the other for the Cre allele (Table B.3). As for SERT-Cre, breedings are designed so that there is just one or no copy of Cre in the animals. We have two different PCRs for the Cre allele. The first is the "universal Cre PCR" that gives either one band if the animal carries the Cre allele and no band if the animal is WT (Table B.4). The other PCR was developed for the ChAT-IRES-Cre line, and gives two bands if the animal carries a copy of Cre allele, or one band if the animal is WT (Table B.5).

**Table B.4: Primers for universal Cre PCR**

Primer	Sequence	Band size	Genotype
Cre <sub>up</sub>	5'- GAT CTC CGG TAT TGA AAC TCC AGC -3'	no band	WT
WT <sub>down</sub>	5'- GCT AAA CAT GCT TCA TCG TCG G -3'	650 bp	CRE

**Table B.5: Primers for ChAT-Cre PCR**

Primer	Sequence	Primers	Band size	Genotype
Cre <sub>forw</sub>	5' – CCT TCT ATC GCC TTC TTG ACG – 3'	Comm x WT	280 bp	WT
WT <sub>forw</sub>	5' – GTT TGC AGA AGC GGT GGG – 3'	Comm x Cre	360 bp	CRE
Comm <sub>rev</sub>	5' – AGA TAG ATA ATG AGA GGC TC – 3'			

## 1.4 VGLUT3 conditional knock-out: viral approach

In order to understand the local contribution of VGLUT3 in the nucleus accumbens without the developmental contribution of the protein, we used a viral approach. VGLUT3<sup>LoxP/LoxP</sup> mice are injected in the nucleus accumbens with an adeno-associated virus expressing the Cre recombinase. VGLUT3 will be invalidated in all cells, but only the ones that express the protein VGLUT3 will be affected. Thus, this technique allows a specific removal of VGLUT3 in the cholinergic interneurons, which all co-express it (Gras *et al.* 2002).

### 1.4.1 Surgical procedure

Two weeks prior to the stereotaxic surgery, animals are transferred to the behavioral facility. For the surgery, they are deeply anesthetized with a mix of ketamine: xylazine (10: 1 mg/mL in NaCl .9%, i.p. injection 0.08 mL/10 g body weight), then placed on a stereotaxic frame with a digital monitoring (Model 900 Small Animal Stereotaxic Instrument, Kopf, TUJUNGA, CA, USA) thanks to the two ear bars and the tooth bar. The body temperature is maintained with a heating plate, and the eyes are moistened with an ophthalmic moisturizing ointment. Before incising the scalp, local anesthesia is performed by application of lidocaine chlorhydrate (5 mg/mL in NaCl .9%).

Once the scalp opened, the skull is positioned flat by checking that lambda and bregma (cranial plate sutures) are at the same height, as well as two points on both lateral sides of the bregma. Then, the skull is bilaterally drilled at the appropriate coordinates (bregma = 0) to target the **nucleus accumbens**, according to Paxinos & Franklin brain atlas:

Antero-posterior	Medio-lateral	Dorso-ventral
+16.0mm	±7.5mm	-43.0mm

The injection set-up we use has a two-syringes holder connected to a pump that controls the flow, and both sides are injected simultaneously (Phymep, Paris, France). The two needles are separated with a custom-made spacer (here, 15 mm).

Once the needles placed, we wait 3 min, and then proceed to the injection, with 400 nL virus per side (detailed in the next paragraph) and an 80 nL.min<sup>-1</sup> flow. When the infusion is over, we wait for another 5' and then slowly pull up the needles. Then we clip the skin and monitor the animal's recovery. Following the surgery, we administrate Carprofen, a nonsteroidal anti-inflammatory drug, in the drinking water of the animals (0.1 mg/mL) for one week. After 8 weeks, the animals are used for behavior, with a one-week-period of handling before the start of experiments.

### 1.4.2 Cre-expressing virus

To inactivate VGLUT3, we infuse VGLUT3<sup>LoxP/LoxP</sup> mice with a virus expressing the Cre recombinase fused with GFP so to be able to visualize the injection site (mutant mice). The control mice are VGLUT3<sup>LoxP/LoxP</sup> injected with a virus expressing GFP without the Cre recombinase.

These viruses are recombinant adeno-associated viruses (AAV) that are nonpathogenic human parvovirus. They contain a single-stranded DNA that expresses the Cre recombinase under the control of a specific promotor. They also carry a WPRE sequence (Woodchuck hepatitis virus posttranscriptional regulatory element) that enhances the transgene expression by creating a tertiary structure.

The two viruses are solubilized in DMEM. They are provided by UPenn (Penn Vector Core in the Gene Therapy Program of the University of Pennsylvania, USA) and are presented in Table B.6.

**Table B.6: List of viruses used**

Virus	Lot	Titer (GC/mL)	Yield (GC)	Mouse
<b>AAV2.hSyn.HI.eGFP-Cre.WPRE.SV40</b>	V4640MI-S	2.93e13	2.637e13	mutant
<b>AAV2.hSyn.eGFP.WPRE.bGH</b>	V4641MI-S	1.13e13	1.356e13	control

## 2. Behavioral experiments

The animals used for behavior were housed in groups of 2-5 per cage. We always designed crossings to produce both wild-type and mutant mice as mixed littermates. All the animals used in the following experiments are males aged 2-4 months. They are genotyped at birth, and transferred to the stabulation room of the behavioral facility when 8-weeks-aged. After one week, they are habituated to handling for minimum

5 days prior to the first experiment. Except for the spontaneous locomotor activity, all tests presented below started between 8:00 and 8:30 a.m.

For the behavioral analysis, the animals were randomly allocated to the experimental groups, and the investigator was blind to genotypes during experimental procedures. Animals were excluded from the experimental data analysis only when their results were detected as outliers using Grubb's test (GraphPad Prism Software, La Jolla, CA, USA).

The tests presented below respect the chronologic order in which they were performed. Prior to each experiments, and each day of experiment, the animals were placed in the room at least 15- 20 min before the start of the test, to let them acclimatize to the new room.

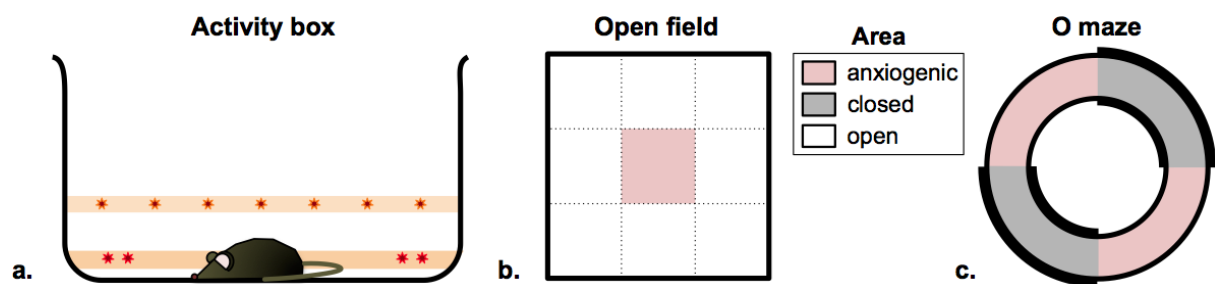


**Figure B.4: Set- ups used for behavior**

**a.** Side view of the activity box apparatus. **b.** and **c.** View from above of the open field (**b**) and the O maze (**c**).

## 2.1 Spontaneous locomotor activity

The aim of this test is to check the basal activity level of the mouse.

To do so, each animal is individually placed in a Plexiglas activity box (L 24 x w 15 x h 25 cm), as depicted on Figure B.4a. In this set-up, 2 sets of horizontal infrared photocell beams located 15 mm above the floor of the enclosure along the long axis (2 in the front, 2 in the back) give a measurement of the horizontal activity (number of back & forth). Another set of beams located 30 mm above the floor provides a measurement of the vertical activity (number of rearings). The box is closed with another box placed upside- down as a lid. Each box is connected to a computer by an interface (Imetronic, Pessac, France). We put some new bedding and hydrogel in each box at the beginning of the experiment. The light is set to ~ 50 lux to match the conditions of stabulation, and respects the light- on/off hours (light on: 7:30 a.m.- 7:30 p.m.). Spontaneous locomotion is measured in 60- min intervals over 24 h starting 10:30 a.m., in order to record mouse activity during a whole circadian cycle.

## **2.2 Anxiety tests**

### **2.2.1 Open field**

The open field (OF) gives a measure of anxiety. It consists in a white Perspex arena (42 x 42 x 26 cm) located in a 45-lux-illuminated room (Figure B.4b). The area is virtually divided in 9 squares, and the central square represents the most anxiogenic zone of the OF. Indeed, mice tend to stay close to walls to remain under cover.

The animal is individually placed in the OF periphery at the beginning of the test (white area on Figure B.4b). Its horizontal activity is video-tracked from above during the 10 minutes of test and then analyzed with the ANY-maze<sup>®</sup> software (<http://www.anymaze.co.uk/>). Between each mouse, the area is cleaned with ethanol 20 % and then dried.

### **2.2.2 O maze**

The O maze test provides another measure of anxiety, and is more anxiogenic than the OF. It is an elevated O-shaped maze where 2 quarters have walls and the 2 remaining ones do not and thus correspond to the anxiogenic zone (Figure B.4c). The light is set so that there is a 10-lux-intensity in the middle of the open arms. The area is 47 cm-diameter and 52 cm-height and the band on which the mouse circulates is 7 cm-wide. Each session lasts 10 minutes, and the mouse is individually placed in the middle of a closed arm. The video-tracking is performed from above and analyzed with ANY-maze<sup>®</sup> software. Between each mouse, the area is cleaned with ethanol 20 % and then dried.

## **2.3 Behavioral sensitizations**

Behavioral sensitization is the enhancement of a behavioral output for a given drug dose with intermittent repeated injections.

After the animals transfer to the behavioral facility, mice would be habituated to handling for minimum 5 days, then to contention for minimum 3 days and to injections for minimum 3 days before the start of sensitization. We did either sensitization to amphetamine in the activity boxes described above, or sensitization to cocaine in another apparatus called cyclotron. In the two sets of experiments, mice were individually tested, but recorded simultaneously in separate activity boxes and could not see the other animals. The first day, they would be placed in their activity box with fresh bedding. They were systematically put back in the same activity box each day of the experiment, so that the environment would be familiar and non-hostile when they would receive the first injection of drug, because of another animal odor.

### 2.3.1 Behavioral sensitization to amphetamine

The sensitization to amphetamine was performed in the activity boxes described previously (Figure B.4a), according to the experimental procedure depicted on Figure B.5.

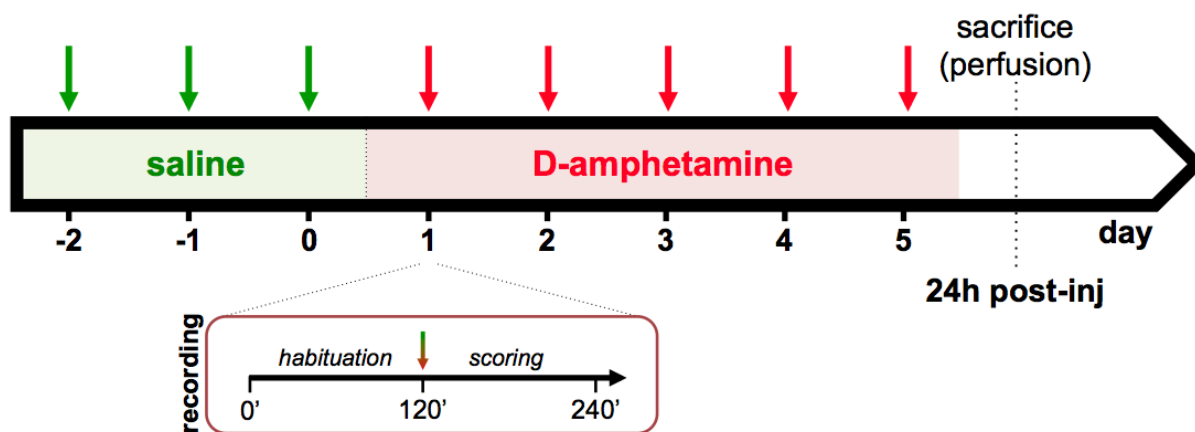


**Figure B.5: Protocol for behavioral sensitization to amphetamine**

The behavioral sensitization had 2 phases: the habituation and the sensitization. The former phase consisted in a daily i.p. injection of saline (NaCl .9%) for 3 days, and the latter phase was done with a daily i.p. injection of amphetamine for 5 consecutive days. Each day, the animal would be placed in the box for 2 hours to reach a minimal level of activity. Then it would be taken out of the box, injected intraperitoneally, and placed back in the cage. The resulting activity would be recorded for the remaining 90 min. The integrality of the 3.5 hours was analyzed for the horizontal (number of back & forth) and vertical (number of rearings) activities in 5-min time bins. As for spontaneous activity, data were recorded through an interface designed by Imetronic.

24 hours after the last injection, animals were deeply anesthetized and perfused.

### 2.3.2 Locomotor sensitization to cocaine

We also performed sensitization to cocaine 10 mg/kg. Instead of using activity boxes, we did the experiment in cyclotron (Imetronic, Pessac, France). In this set-up, each mouse is placed in a circular corridor (4.5- cm width, 17- cm external diameter) bearing 4 infrared beams placed at 90° angles. A software gives a measure of the locomotor activity as the number of ¼ turns, *i.e.* the consecutive interruption of two adjacent beams.

We used a protocol similar to the one for amphetamine sensitization, except that after the 3 saline injections and the 5 consecutive injections of drug, the animal would have a withdrawal period of 5 days, and a last challenge injection of cocaine 10 mg/kg (Figure B.6). Each day, the animal would be placed for two hours in the cyclotron, then

injected with the appropriate solution, and placed back to assess the locomotion for two additional hours. 24 hours after the last injection, the animals sacrificed by cervical dislocation and their dissected brain would be freshly frozen.

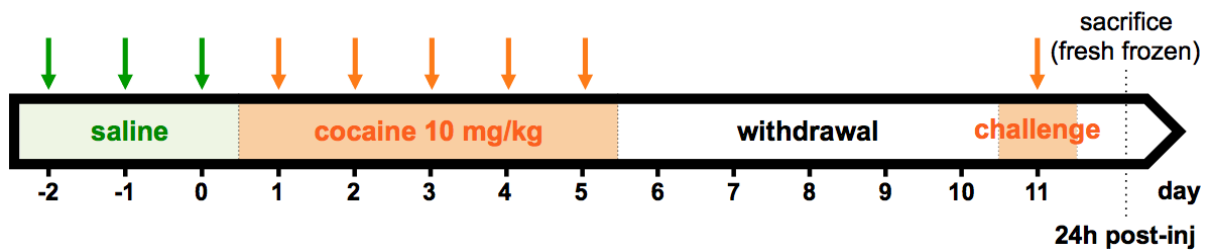


**Figure B.6: Protocol for behavioral sensitization to cocaine**

## 2.4 Stereotypy scoring

As discussed in the introduction, low dose of amphetamine stimulates locomotion while higher doses also yield stereotypies, which consist in motor responses that are repetitive, invariant, and seemingly without purpose or goal. Thus, during behavioral sensitization with amphetamine 5 mg/kg, the stereotypies were manually scored for the 90-minute-period following drug injection.

The scoring was performed blindly to the genotype by the experimenter, by directly watching the animal starting five minutes after drug injection. Each animal was sequentially observed for 45" every 10'. Two different scales were used.

After several pilot experiments conducted on C56BL/6 mice injected intraperitoneally with 5 mg/kg of D- amphetamine, we were able to determine the behavioral repertoire displayed by the mice in our experimental conditions: animal bred in groups of 2-5, but tested individually in a novel environment with fresh bedding at the start of the experiment, yet considered as familiar when the amphetamine injections started. It was a prerequisite to do so, because stereotypies rating scales are meant for assessing stereotypies in a given set-up, for a given animal model with a specific drug. For example, as described thoroughly by Russell & Pihl, novelty plays a major role on the stereotypic output (Russell *et al.* 1978). The more familiar the environment is, the stronger stereotypies will express. Therefore, novelty highly reduces the occurrence of stereotypies.

### 2.4.1 Categorical scoring

To be able to precisely assess the behavior of our mice, we first used an objective methodological approach. The protocol consisted in an observational time-sampling procedure over the course of the behavioral testing period (Kelley 2001). For each time bin, the experimenter would note the presence or absence of a given behavior (0 or 1). Then, it was possible to summate the score of all items for each time bin, and also to

assess the frequency of a given behavior by looking at the temporal evolution of the behavior through time.

Because we had determined the behavioral repertoire during pilot experiments, we modified the scale proposed by Kelley to include all the behavioral categories displayed by our mice in our experimental conditions, as presented in Table B.7 (Kelley 2001). The categories that are modified are indicated with the appropriate key in the table afterwards.

**Table B.7: Categorical scoring of stereotypies**

<b>Category</b>	<b>Description</b>
<b>Still</b>	Asleep or lying still with eyes open but no movement
<b>Locomotion</b>	Movement from one side of the cage to another
<b>Groom / Taffy pull •</b>	Head or body grooming / Repetitive, tremorous paw- to- mouth movement
<b>Rear</b>	Rearing on hind legs
<b>Head- up sniff</b>	Continuous sniffing (>5 sec), with head/snout directed towards top of cage
<b>Head- down sniff</b>	Continuous sniffing (>5 sec), with head/snout directed towards floor of cage
<b>Mouth movements / Licking •</b>	Non- specific oral movements, tongue protrusion, air / wall licking
<b>Bite #</b>	Biting the bedding
<b>Head- down sniff/paw •</b>	Continuous snout movements towards flank / Paw movements directed through floor of cage
<b>Head sway</b>	Rhythmic lateral swaying of head
<b>Head bob</b>	Rhythmic vertical head bobbing
<b>Turn ∞</b>	Perseverative turn in a corner of the cage

•, regrouping of 2 categories; ∞, added category; #, modified category

Adapted from Kelley (2001)

We describe many categories in Table B.7. Yet, most of the time, responses consisted in sniffing and oral stereotypies. Rearing was anecdotic. On the other hand, head movements were present in all mice, especially head bobbing. We had to regroup some categories as shown in Table B.7, because it was difficult to discriminate between two items closely related in mice (small animals), while it is probably possible in rats (where even jaw tremor can be assessed). As for locomotion, it was purely informative because the activity box software directly monitored locomotor activities.

At first, we thought that this was the most objective way to rate stereotypies, because the outcome is binary: 1, the behavioral item is present, 0 the behavioral item is absent. But we faced two problems with this. The first problem was that it did not take into account the intensity of the behavior. The second, major one was that with repeated injections, the behavioral repertoire would drastically narrow down, often to only one or two behavioral items (most often biting ± sniffing) that would be maintained during the whole time bin. This would correspond to a score of 1 or 2, which would not reflect at all the severity of the behavior. Thus, we kept using the categorial scoring as an informative and complementary rating to the rating scale presented in the next paragraph. And instead of using a binary rating, we shaded the scale by attributing a score of 0/.25/.5/.75/1.

### 2.4.2 Rating- scale- based scoring of general stereotypies

The “traditional” way for assessing stereotypies is by using rating scales, which implies that the displayed behavioral repertoire is a continuum. The scale commonly used is based on Creese & Iversen work, initially developed to quantify stereotypies induced by psychostimulants (Table A.6; Creese and Iversen (1973)). We decided to use a scoring system based on the one proposed by Costall *et al.*, developed for 5 mg/kg amphetamine i.p. injection in rats (Costall *et al.* 1972), and closely related to Creese & Iversen rating scale (Table A.6).

**Table B.8: Rating scale for general stereotypies**

Score	Description
0	Asleep or stationary
1	Active
2	Constant exploratory activity with discontinuous sniffing
3	Continuous sniffing with periodic exploratory activity
4	Continuous sniffing, discontinuous biting, gnawing or licking with very brief periods of locomotor activity
5	Continuous biting, gnawing or licking with a residual locomotor activity
6	Continuous biting, gnawing or licking without locomotor activity

### 2.4.3 Rating- scale- based scoring of orofacial stereotypies

Because amphetamine specifically elicits oral- based stereotypies (Creese *et al.* 1975), we also assessed orofacial stereotypies based on another scale, as described in Table B.9.

**Table B.9: Rating scale for orofacial stereotypies**

Score	Description
0	No orofacial stereotypy
1	Continuous sniffing with bursts of orofacial licking or biting
2	Continuous licking or biting with locomotion
3	Continuous biting in a restricted area $\pm$ bursts of licking
4	Continuous biting without locomotion

### **3. Drug treatments**

Mice were weighted 2 days prior to the beginning drug injections. Drugs were administered intraperitoneally in a volume of 0.1 mL/10 g body weight (0.3 mL for a mouse weighting 30 g), and control injections consisted in an equivalent volume of the drug vehicle (0.9% NaCl).

**Cocaine:** Cocaine chlorhydrate (Cooper, Melun, France) was dissolved in a saline solution (0.9% NaCl w/v) and prepared at 1 mg/mL for a final concentration of 10 mg/kg per mouse.

**Amphetamine:** D- amphetamine sulfate (Sigma, Steinheim, Germany) was dissolved in a saline solution (0.9% NaCl) and prepared at 0.1/ 0.3/ 0.5 mg/mL for a final concentration of 1/ 3/ 5 mg/kg per mouse.

### **4. Anatomical studies by immunohistochemistry**

#### **4.1 Immunofluorescence**

##### **4.1.1 Conditional knock- outs validation: VGLUT3, VAcHT and 5- HT**

To validate the loss of VGLUT3 protein in the different neurotransmitter systems in the double mutant mice (ChAT- IRES- Cre::LoxP/LoxP and SERT- Cre::LoxP/LoxP), we did immunofluorescence experiments with antibodies directed against VGLUT3, VAcHT and 5- HT. We used 2 controls (VGLUT3<sup>LoxP/LoxP</sup>) and 2 double- mutant males for each mouse line.

Animals were deeply anesthetized with pentobarbital sodium (0.1 mL/10 g body weight, then rapidly perfused intracardially with paraformaldehyde (PFA) 4% prepared in ice- cold phosphate- buffered saline (PBS). The volume of PFA was 50 mL/mouse, with a flow of  $\sim$  16 mL/min. The perfusion needed to be rapid, *i.e.* start maximum 2' after the anesthesia, to prevent cerebral 5- HT degradation. Brains were dissected, post- fixed in

the same fixative for 24 h at 4°C, rinsed 3 times with PBS. Coronal sections (30 µm) were cut using a vibratome then stored at 4°C in PBS with 0.01% sodium azide until use.

Immunofluorescence was performed on free-floating sections as follows. Slices were washed 3 times in 1x PBS for 10', then incubated with a gelatine blocking buffer (0.2% gelatine - triton 0.25% prepared in PBS) for 3 x 15 min at room temperature (RT). Next, sections were incubated overnight (ON) at 4°C with the appropriate primary antibodies: VGLUT3 rabbit antiserum (1:2'000, Synaptic Systems, catalog ref. 135–203), serotonin rat monoclonal antiserum (1:50, Millipore Bioscience Research Reagents, catalog ref. AB12) and home-made VAcHT guinea pig antiserum (1:4'000). The next day, sections were washed 3 times in PBS for 10', then incubated 2 h at RT with the secondary antibodies: anti-rabbit, anti-rat and anti-guinea pig IgGs coupled to Alexa Fluor 488, Cy5 and Alexa Fluor 555 respectively (1:2'000; Invitrogen). Slices were mounted on glass slides with Fluoromount-G (Southern-Biotech). Images were acquired using a fluorescent microscope equipped with an ApoTome module (Axiovert 200M; Carl Zeiss) and processed using ImageJ software.

#### **4.1.2 ΔFosB immunofluorescence**

In order to understand the underlying mechanisms of our behavioral studies, we performed IF against ΔFosB, a marker of activation that is induced by repeated drug injections.

24 h after the last drug injection, animals were deeply anesthetized with pentobarbital sodium (0.05 mL/10 g body weight (0.15 mL for a mouse weighting 30 g)) then perfused intracardially with paraformaldehyde PFA 1.5% prepared in ice-cold phosphate buffer (PB). The volume of PFA was 45 mL/mouse, with a flow of ~15 mL/min. Brains were dissected, and cut in half. One half was post-fixed in the same fixative for 1 h at 4°C, rinsed 3 times with PB and then stored in PB- azide 0.01% (protocol for dendritic spines diolistic labeling). The other half was post-fixed with PFA 4% in PBS for 24 h at 4°C, then rinsed 3 times with PBS. Coronal sections (30 µm) were cut using a vibratome then stored at 4°C in PBS with 0.01% sodium azide until use.

Immunofluorescence was performed on free-floating sections as follows. Slices were washed 3 x 10' in 1x PBS, then incubated with a donkey serum blocking buffer (3% normal donkey serum- triton 0.1% prepared in 1x PBS) for 45 min at RT. Next, sections were incubated ON at 4°C with the appropriate primary antibodies: FosB rabbit antiserum (1:1'000, Santa Cruz, catalog ref. sc- 48) and home-made VAcHT guinea pig antiserum (1:4'000). The next day, sections were washed 3 times in 1x PBS for 10', then incubated with the secondary antibodies for 2 h at RT: anti-rabbit and anti-guinea pig IgGs coupled to Alexa Fluor 555 and Alexa Fluor 488 (1:1'000; Invitrogen). Slices were

mounted on glass slides with Fluoromount-G. Images were acquired using a Confocal Laser Scanning Microscope (Leica TCS SP5 AOBS, Leica Microsystems, Mannheim, Germany) equipped with a 63x, 1.4 NA oil immersion objective with the pixel size set to 60 nm and a z-step of 130 nm. Images were deconvoluted using a Maximum Likelihood Estimation algorithm with Huygens 3.6 software (Scientific Volume Imaging, Hilversum, plugin for ImageJ).

## **4.2 Immunoautoradiography**

To validate the conditional knock-outs (both genetic and viral approaches), we checked VGLUT3 levels by immunoautoradiography (IAR) experiments.

Mice were decapitated, their brain frozen by immersion in isopentane chilled at - 30°C with dry ice, and then stored at - 80°C. Serial coronal sections (14 µm- thick) were then cut at - 20°C using a cryostat (CM 3050S, Leica), and mounted onto "Superfrost® plus" slides (Thermo scientific), then stored at - 80°C. Immunoautoradiography experiments were performed on these fresh frozen brain sections as follows.

Brain slices were taken out of the - 80°C until completely dry, then post- fixed with PFA 4% in 1x PBS for 15' at RT. Next, the slices were washed 3 x 10' with 1x PBS under agitation, then incubated with the blocking buffer (BSA 3%, NaI 1 mM, normal goat serum 1%, sodium azide 0.02%) for 1 h at RT. Later, slices were incubated with VGLUT3 rabbit polyclonal antiserum (1:20'000, Synaptic Systems) ON at 4°C. The next day, they were washed 3 x 10' with 1x PBS, and then incubated with the secondary anti-rabbit [<sup>125</sup>I]-IgG antibodies (PerkinElmer). Sections were washed in PBS, rapidly rinsed in water, dried, and exposed to X-ray films (Biomax MR, Kodak) for 5 d. Standard radioactive microscaler were exposed with each film to ensure that labeling densities were in the linear range. Densitometry measurements were performed with MCID analysis software on six to eight sections for each region per mouse.

## **5. Statistics**

All statistical comparisons were performed with two-sided tests in Prism 6 (GraphPad Software, La Jolla, CA, USA).

To compare two means, we always checked if the data belonged to a normal distribution (D'Agostino & Pearson omnibus normality test). If not, we used an unpaired Mann-Whitney test (nonparametric). If yes, we used a parametric test. We verified that the compared groups have equal standard deviations, in which case we used an unpaired t test. If not, we applied the Welch's correction. We will refer to this test as t test hereafter. To study the effect of acute drug injections, we compared the area under

curve (AUC) between the two genotypes with the appropriate test; the 2- hour period preceding drug injection was not included in the analysis.

To analyze the behavioral sensitization, we systematically used two- way analysis of variance (ANOVA) with repeated-measures (time); we will refer to this test as two- way ANOVA hereafter. Saline injections were not included in the ANOVA for comparison of the cumulative effect of sensitization. Bonferroni's test for multiple comparisons *post hoc* analysis was performed when required unless otherwise indicated.

All results are expressed as mean  $\pm$  S.E.M., and differences were considered significant for  $p < .05$ . The following code was employed for significance: \* $p < .05$ ; \*\* $p < .01$ ; \*\*\* $p < .001$ ; \*\*\*\* $p < .0001$ .

## 6. Experiments color code

Here is a summary of the color and symbol codes used for the different transgenic lines and experiments that will be found across results this report.

Line	Experiment	Color code	Part
<b>VGLUT3<sup>-/-</sup></b>	AMPH 1 mg/kg		Part I
	AMPH 3 mg/kg		Part I
	AMPH 5 mg/kg		Part I
<b>SERT- Cre::VGLUT3<sup>LoxP/LoxP</sup></b>	AMPH 5 mg/kg		Part II
<b>ChAT- IRES- Cre::VGLUT3<sup>LoxP/LoxP</sup></b>	AMPH 5 mg/kg		Part II
	COC 10 mg/kg		Part II
<b>VGLUT3<sup>LoxP/LoxP</sup> AAV- injected</b>	COC 10 mg/kg		Part III

Experiment	Symbol code
<b>Locomotion</b>	●
<b>General stereotypies</b>	◆
<b>Orofacial stereotypies</b>	■
<b>Open field</b>	□
<b>O maze</b>	⊙



# RESULTS

## PART I.

### VGLUT3 FULL KNOCK- OUT AND AMPHETAMINE

#### CONTEXT

- ▶ VGLUT3<sup>-/-</sup> mice are hypersensitive to the rewarding effects of cocaine. Moreover, they have a constitutive elevated number of dendritic spines on D1- MSNs in the striatum, as well as an upregulation of D<sub>1</sub>R levels and an overactivation of p- ERK (Sakae *et al.* 2015).
- ▶ The frequency of rare mutations is increased in the gene encoding VGLUT3 in people suffering from polysubstance addictions compared to controls (Sakae *et al.* 2015).
- ▶ VGLUT3 appears as a regulator of drug abuse.

#### PROBLEMATIC

- VGLUT3 is altered in some poly- addict individuals, which suggests a broader implication of the protein in drug abuse. We wondered if the hypersensitivity of VGLUT3<sup>-/-</sup> mice to cocaine could be generalized to other drugs of abuse. Thus, we studied the effects of another psychostimulant, amphetamine on VGLUT full knock- out mice.
- ▶ We first studied the locomotor effects of low doses of amphetamine on VGLUT3<sup>-/-</sup> mice.
  - ▶ Then, we characterized the locomotor and stereotypic responses of VGLUT3 null mice to a high dose of amphetamine.

Cocaine and amphetamine are two drugs that both increase extracellular dopamine levels, but with very different molecular mechanisms. Cocaine blocks DAT and therefore inhibits reuptake of dopamine originating from neuronal activity-dependent release. Amphetamine has much more complex effects. Not only does it block dopamine reuptake, but it also depletes vesicular stores of dopamine and promotes efflux of dopamine from the intracellular compartment via the reversal of DAT and VMAT (Sulzer 2011). Therefore, amphetamine promotes a nonvesicular and neuronal activity-independent release of dopamine. Thus, release of DA is far greater with amphetamine than cocaine administration (Cagniard *et al.* 2014).

## 1. Basal characterization

### 1.1 Number of VGLUT3<sup>-/-</sup> used

To study the effects of amphetamine, we based our study on a behavioral sensitization protocol, as detailed in the Materials & Methods. After 3 days of habituation with daily i.p. saline injections, we intermittently injected a daily dose of amphetamine to our mice and recorded the resulting activity. We conducted this study with three different doses of amphetamine, a low dose that mainly stimulates locomotion (1 mg/kg), an intermediate dose (3 mg/kg) and a high dose that elicits stereotypies (5 mg/kg).

### 1.2 VGLUT3<sup>-/-</sup> mice weight

When all the animals used in our study on VGLUT3 null mice were pooled together, we observed that the weight of VGLUT3<sup>-/-</sup> mice is smaller relatively to VGLUT3<sup>+/+</sup> littermates (Figure C.1; -3.3%,  $p = .047$ , unpaired t test). However, among each experiments, unpaired t tests revealed no difference between mutants and controls (data not shown).

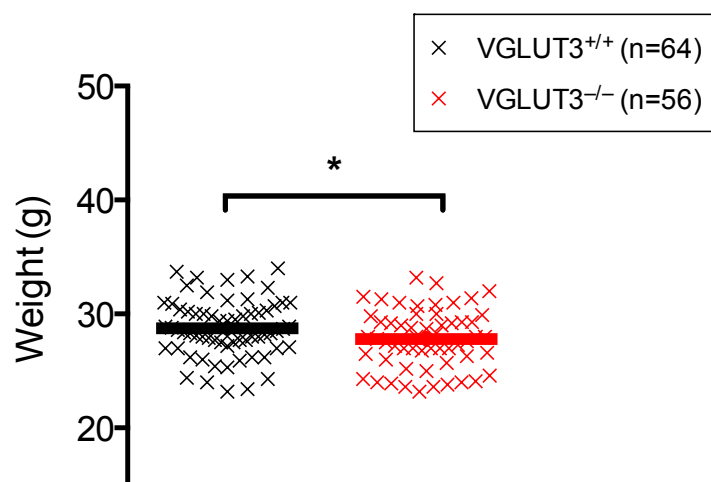


**Figure C.1: VGLUT3<sup>-/-</sup> mouse weight**

VGLUT3<sup>-/-</sup> are slightly lighter than VGLUT3<sup>+/+</sup> littermates (n = 64-56).

### 1.3 Spontaneous locomotion

Our behavioral sensitization protocol consisted in repeated exposures to saline, then to amphetamine in a given environment. Each day, the animal was placed in the activity box 2 h prior to the injection. The spontaneous locomotion was analyzed in this environment during the habituation phase of the sensitization protocol, when mice are still naive to the drug (Figure C.2). As previously described (Gras *et al.* 2008), we confirmed that VGLUT3<sup>-/-</sup> mice have an increased spontaneous locomotor activity compared to WT littermates, both horizontally (two-way ANOVA, effect of genotype,  $F_{1,112} = 7.442$ ,  $p = .007$ ; Bonferroni's post test  $p = .005$  for saline 2), and vertically (two-way ANOVA, effect of genotype,  $F_{1,111} = 5.255$ ,  $p = .024$ ; Bonferroni's post test  $p = .014$  for saline 2; Gras *et al.* (2008)). However, there was no interaction time x genotype in the two-way ANOVA realized for horizontal and vertical activities, which demonstrates that VGLUT3<sup>-/-</sup> mice and WT do habituate similarly to the environment.

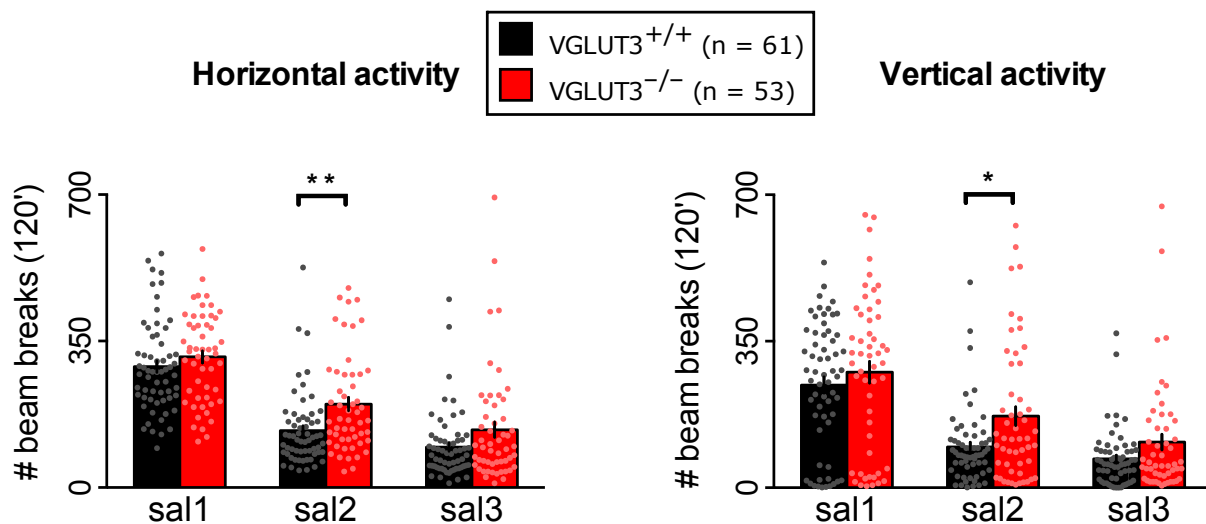


**Figure C.2: VGLUT3<sup>-/-</sup> mice spontaneous activity**

VGLUT3<sup>-/-</sup> mice (red bars) have a slightly higher spontaneous locomotor activity compared to WT littermates (black bars;  $n = 61-53$ ).

## 2. VGLUT3<sup>-/-</sup> and amphetamine 1 mg/kg

We then investigated the effects of AMPH on locomotion in VGLUT3<sup>-/-</sup> mice and WT mice at low doses, in a behavioral sensitization paradigm.

### 2.1 Acute injection of amphetamine 1 mg/kg

We looked at the effect of an acute injection of AMPH 1 mg/kg.

The first injection of amphetamine (called acute injection), elicited a hyperlocomotion that did not significantly differ from the third saline injection (SAL3) in terms of horizontal activity (Figure C.3a; two-way ANOVA, effect of time,  $p > 0.8$  between SAL3 and AMPH1). The vertical activity was significantly decreased between the third saline

injection and AMPH1 (Figure C.3d; two-way ANOVA, effect of time,  $F_{1,21} = 4.344$ ,  $p = .049$ ). When comparing SAL3 to AMPH1, we also found that there was an effect of genotype in both horizontal and vertical activities. VGLUT3<sup>-/-</sup> mice locomotion was higher than control mice (Figure C.3a and d; two-way ANOVA, effect of genotype,  $F_{1,21} = 9.275$ ,  $p = .006$  for horizontal activity;  $F_{1,21} = 11.52$ ,  $p = .003$  for vertical activity).

The hyperlocomotion induced by the acute AMPH 1mg/kg injection was higher in VGLUT3<sup>-/-</sup> mice compared to WT mice by comparing the area under curve (AUC) during the 90' post-injection (Figure C.3a, inset: WT  $6.273 \pm 1.479$  vs. mutant  $20.92 \pm 5.535$  beam breaks, Mann-Whitney test,  $p = .005$  for horizontal activity; Figure C.3d, inset: WT  $4.727 \pm 1.253$  vs. mutant  $15.62 \pm 3.449$  beam breaks, unpaired t test with Welch's correction,  $p = .010$  for vertical activity).

## 2.1 Repeated injections of amphetamine 1 mg/kg

We kept injecting mice daily with AMPH 1 mg/kg during 5 days. The effect of repeated injections was studied by comparing the cumulative locomotion during the 90-minute-period following each injection. This protocol produced a significant locomotor sensitization (Figure C.3b, two-way ANOVA, effect of time,  $F_{4,84} = 3.729$ ,  $p = .008$  for horizontal activity; Figure C.3e,  $F_{4,88} = 1.369$ ,  $p = 0.251$  not significant for vertical activity) with no difference between genotypes (Figure C.3b, two-way ANOVA, effect of genotype,  $F_{1,21} = 2.107$ ,  $p = 0.161$  for horizontal activity; Figure C.3e,  $F_{1,22} = 1.366$ ,  $p = 0.255$  for vertical activity). The temporal course of the horizontal activity for each day of injection is presented in the Appendices section (Figure E.1).

We also compared the first day (AMPH1) to the last day (AMPH5) of AMPH injection to look at the overall sensitization effect in our protocol (Figure C.3c and f). We found a strong effect of time for horizontal activity (Figure C.3c; two-way ANOVA,  $F_{1,21} = 44.05$ ,  $p < .001$ ; post test  $p < .001$  for WT,  $p = .031$  for mutant) and a tendency for the vertical activity (Figure C.3f; two-way ANOVA,  $F_{1,22} = 3.548$ ,  $p = .073$ ; post test  $p > .05$  for WT and mutant). This demonstrated that both mutant and WT sensitized to AMPH 1 mg/kg. This result was surprising since we previously reported the lack of sensitization to cocaine (COC) 10 mg/kg in null mice (Sakae *et al.* 2015). However, there was no effect of genotype in the horizontal and vertical activities (two-way ANOVA,  $F_{1,21} = 0.532$ ,  $p = 0.474$  and  $F_{1,22} = 1.859$ ,  $p = 0.187$  respectively).

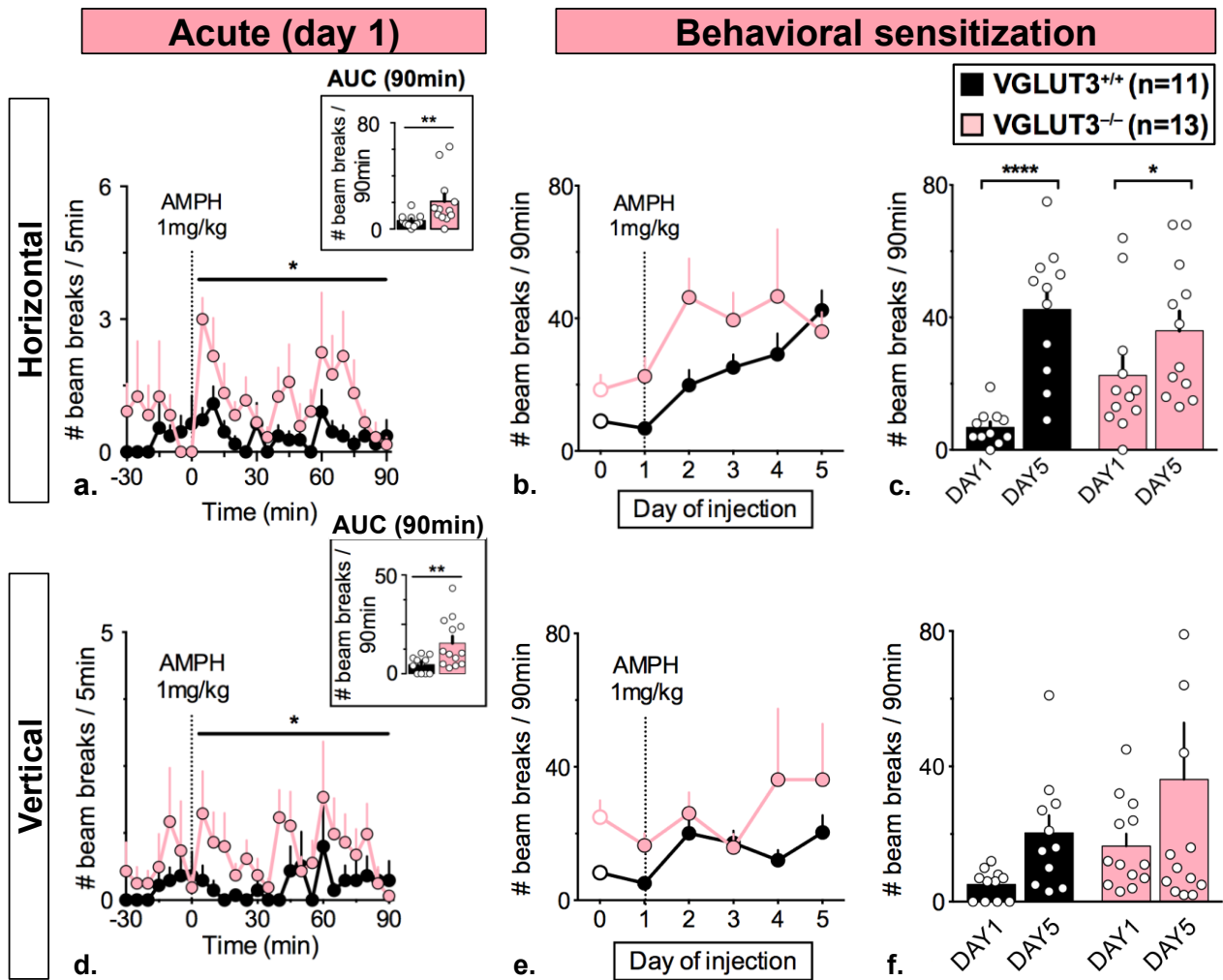


**Figure C.3: VGLUT3<sup>-/-</sup> locomotor sensitization to AMPH 1 mg/kg**

Effect of acute (**a** and **d**, left panel) and repeated injections (right panel) of AMPH 1mg/kg on horizontal (**top panel**, number of back & forth) and vertical activities (**bottom panel**, number of rearings) in VGLUT3<sup>-/-</sup> mice. **a** and **d** represent the time course of the acute response to AMPH, during the 30' preceding the injection, until 90' post-injection. The insets correspond to the areas under curve between t = 0 and t = 90 min. **b** and **e** represent the cumulative locomotion during the 90' post-injection for the 3<sup>rd</sup> day of saline (day 0) and the five injections of AMPH (day 1- 5). **c** and **f** represent the cumulative locomotion during the 90' post-injection for the 1<sup>st</sup> day (AMPH1) and the last day of AMPH (AMPH5).

**a.** and **d.** VGLUT3 null mice display higher horizontal (**a**) and vertical (**d**) activities in response to an acute injection of AMPH 1 mg/kg. **b.** and **c.** Both WT and mutant mice have a locomotor sensitization to AMPH 1 mg/kg. **e.** and **f.** The vertical activity does not sensitize and does not differ between genotypes (n = 11-13).

In summary VGLUT3<sup>-/-</sup> mice do sensitize to AMPH 1 mg/kg, unlike what was previously reported with cocaine. This locomotor sensitization is similar to that of control mice. However, VGLUT3<sup>-/-</sup> mice sensitization is slightly higher than the one observed in WT mice.

### **3. VGLUT3<sup>-/-</sup> and amphetamine 3 mg/kg**

With the same paradigm, we then investigated the effects of an intermediate dose of AMPH, 3 mg/kg, which mainly stimulates locomotion.

#### **3.1 Acute injection of amphetamine 3 mg/kg**

Unlike the lower dose, the acute injection of AMPH 3 mg/kg elicited a strong response compared to the saline injection (two-way ANOVA, effect of time,  $F_{1,39} = 48.93$ ,  $p < .001$  for horizontal activity between SAL3 and AMPH1;  $F_{1,41} = 40.99$ ,  $p < .001$  for vertical activity). During the acute injection of AMPH 3 mg/kg, both control and mutant mice displayed a bell-shaped horizontal hyperlocomotion that started right after the injection and culminated at 45 min post-injection. Drug effects washed out slowly until 90 min post-injection (Figure C.4a). The vertical locomotion was also enhanced, but with a very different profile. Following the injection, vertical activity regularly increased until reaching a maximal level around 75 min post-injection (Figure C.4d). A comparison between WT and mutant mice AUC for the first day of injection revealed no difference between the two groups (Figure C.4a, inset: WT  $226.8 \pm 34.5$  and mutant  $267.6 \pm 67.67$  beam breaks, Mann-Whitney test,  $p > 0.999$  for horizontal activity; Figure C.4d, inset: WT  $97.78 \pm 14.47$  and mutant  $77.33 \pm 15.66$  beam breaks, Mann-Whitney test,  $p = 0.455$  for vertical activity).

In conclusion, VGLUT3<sup>-/-</sup> and VGLUT3<sup>+/+</sup> mice respond similarly to an acute injection of AMPH 3 mg/kg.

#### **3.1 Repeated injections of amphetamine 3 mg/kg**

We then investigated the effects of repeated exposures to AMPH 3 mg/kg on VGLUT3<sup>-/-</sup> mice. From the 2<sup>nd</sup> day of injection, we found a differential response in the horizontal activity between mutant and control mice. VGLUT3<sup>-/-</sup> mice showed a higher hyperlocomotion than WT mice (Figure C.4b; two-way ANOVA, effect of time,  $F_{4,156} = 59.42$ ,  $p < .001$ , effect of genotype,  $F_{1,39} = 8.466$ ,  $p = .006$ , interaction  $F_{4,156} = 3.611$ ,  $p = .008$ ). The vertical activity did not vary between genotypes (Figure C.4e;  $F_{1,40} = 0.141$ ,  $p = 0.709$ ) but there was an effect of time ( $F_{4,160} = 2.449$ ,  $p = .048$ ).

We then compared the locomotion between AMPH1 and AMPH5 (Figure C.4c and f). Both VGLUT3<sup>-/-</sup> and VGLUT3<sup>+/+</sup> mice displayed locomotor sensitization for the horizontal activity (Figure C.4c; effect of time,  $F_{1,39} = 76.81$ ,  $p < .001$ , effect of genotype,  $F_{1,39} = 8.423$ ,  $p = .006$ , interaction time x genotype  $F_{1,39} = 5.421$ ,  $p = .025$ ; post test between AMPH1 and AMPH5 for both genotypes  $p < .001$ ). The horizontal locomotion was not significantly different between WT and mutant mice at AMPH1, but it was greater for mutants at AMPH5 (Figure C.4c; post test between WT and mutant at AMPH5  $p < .001$ ).

VGLUT3<sup>-/-</sup> mice displayed a 1.5-fold increased response compared to WT mice (WT 659.2 ± 52.85 and mutant 1008 ± 120.3 beam breaks). There was no effect of time or genotype on the vertical locomotion (Figure C.4f). The temporal course of the horizontal activity for each day of injection is presented in the Appendices section (Figure E.2).

Once more, surprisingly there is a locomotor sensitization of VGLUT3<sup>-/-</sup> mice at AMPH 3 mg/kg. In addition, VGLUT3<sup>-/-</sup> mice display a stronger response than VGLUT3<sup>+/+</sup> mice.

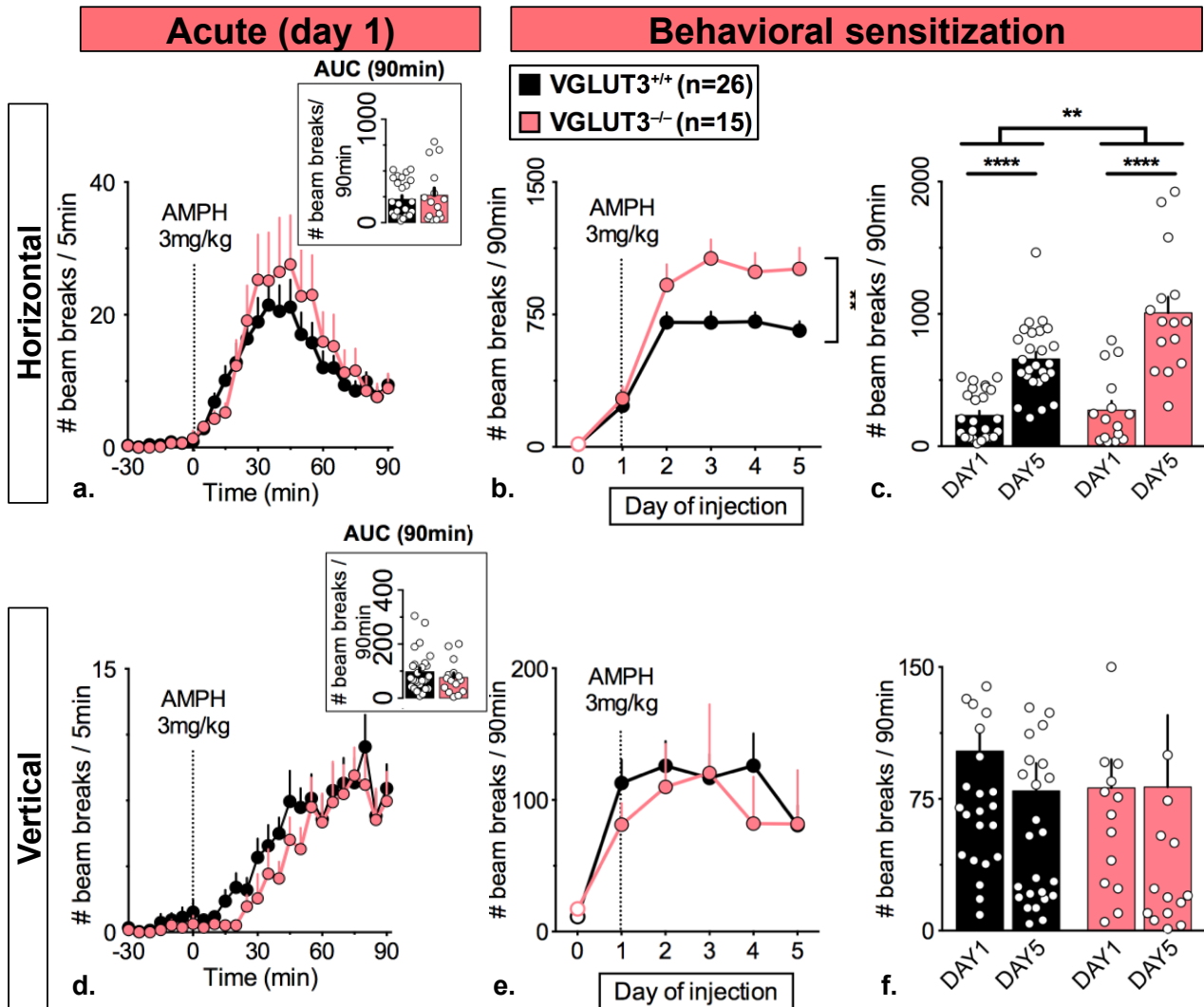


**Figure C.4: VGLUT3<sup>-/-</sup> locomotor sensitization to AMPH 3 mg/kg**

Legend similar to that of Figure C.3.

**a.** and **d.** WT and mutant mice display similar levels of horizontal and vertical AMPH-induced hyperlocomotion. **b.** The cumulative horizontal activity increases across trials and is higher in VGLUT3 null mice. **c.** The horizontal activity appears sensitized by comparing the first (AMPH1) to the last day of injection (AMPH5), and is higher in mutant mice. **e.** and **f.** On the other hand, the cumulative vertical activity remains stable across sessions and does not differ between genotypes (n = 26-15).

## **4. VGLUT3<sup>-/-</sup> and amphetamine 5 mg/kg**

VGLUT3<sup>-/-</sup> mice are more resistant to LID (Divito *et al.* 2015, Gangarossa *et al.* 2016). We wondered if this result could be transposed to another form of abnormal movements: amphetamine-induced stereotypies. To answer this question, we chose to use a higher dose of amphetamine (5 mg/kg) with the same behavioral sensitization protocol. This dose has been previously described to elicit both hyperlocomotion and stereotypies (Yates *et al.* 2007, Singh *et al.* 2012). We characterized the locomotion and stereotypies on the same batches of mice treated with AMPH 5 mg/kg. During this experiment, we also included mutant and WT animals only injected with saline during the whole time-course of the experiment to have an additional control.

### **4.1 Effect on locomotion**

#### **4.1.1 Acute injection of amphetamine 5 mg/kg**

As for AMPH 3 mg/kg, AMPH 5 mg/kg elicited a strong locomotor activation in both WT and mutant mice compared to saline (two-way ANOVA, effect of time,  $F_{1,20} = 30.95$ ,  $p < .001$  for horizontal activity between SAL3 and AMPH1;  $F_{1,21} = 24.22$ ,  $p < .001$  for vertical activity). Following the acute injection of AMPH 5 mg/kg, both groups displayed a substantial hyperlocomotion that reached a plateau 30 min after the injection and lasted ~ 1 hour. The saline-injected groups only had a residual activity (Figure C.5a). The horizontal activity of VGLUT3<sup>-/-</sup> mice was two times higher compared to WT littermates (Figure C.5a, inset: t test,  $p < .001$ ; WT  $608.3 \pm 99.36$  and mutant  $1366 \pm 136.3$  beam breaks). The temporal course of the horizontal activity for each day of injection is presented in the Appendices section (Figure E.3).

The vertical locomotion had a profile similar to AMPH 3 mg/kg, with a constant increase starting 30 min post-injection (Figure C.5d). There was no difference between genotypes, even though VGLUT3<sup>-/-</sup> mice displayed higher levels of vertical activity (Figure C.5d, inset: t test with Welch's correction,  $p = .113$ , WT  $54.78 \pm 11.14$  and mutant  $87.36 \pm 16.62$  beam breaks). On the other hand, animals injected with saline displayed a vertical activity during 30 min and then started to sleep.

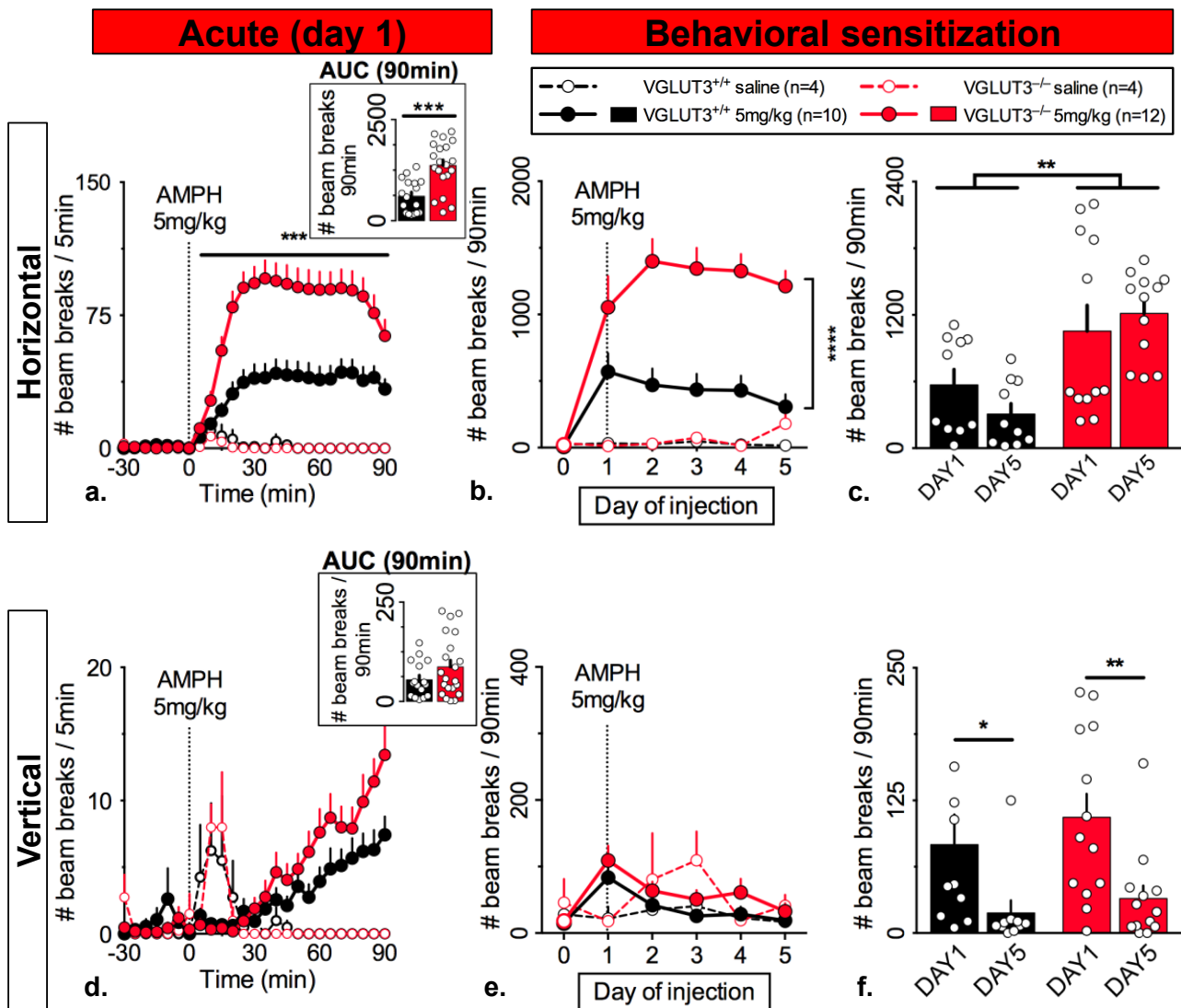


**Figure C.5: VGLUT3<sup>-/-</sup> locomotor sensitization to AMPH 5 mg/kg**

Legend similar to that of Figure C.3.

**a.** WT mice display a rapid and plateau-shaped hyperlocomotion in response to AMPH 5 mg/kg. Mutant mice have a two-fold hyperlocomotion compared to controls. **b.** The cumulative horizontal activity reveals that the two-fold increase of VGLUT3<sup>-/-</sup> horizontal activity is maintained during all sessions. **c.** At 5 mg/kg, there is no potentiation of the horizontal activity between the first (AMPH1) and last injection (AMPH5). **d.** WT and mutant mice display similar vertical activation in response to the acute injection of AMPH 5 mg/kg, with a late onset and a constant increase. **e.** The cumulative vertical activity does not differ between genotypes. **f.** The cumulative vertical activity significantly decreases between AMPH1 and AMPH5, but does not differ between genotypes (n = 10-12 for AMPH, n = 4-4 for SAL).

Overall, VGLUT3<sup>-/-</sup> mice have a two-fold hyperlocomotion compared to WT mice in response to an acute injection of AMPH 5 mg/kg.

#### 4.1.2 Repeated injections of amphetamine 5 mg/kg

We then explored the effects of repeated injections of AMPH 5 mg/kg on VGLUT3<sup>-/-</sup> mice. When comparing the five days of injections, we found an important differential of the cumulative horizontal activity between VGLUT3<sup>-/-</sup> and WT mice. Mutant mice

responded several times stronger than controls (Figure C.5b; two-way ANOVA, effect of genotype,  $F_{1, 20} = 20.29$ ,  $p < .001$ ). There was no effect of time in the response, which was globally unchanged across trials (Figure C.5b; two-way ANOVA, effect of time,  $F_{4, 84} = 1.448$ ,  $p = 0.226$ ). The saline group only displayed a residual locomotion during the 5 days of injection. In terms of vertical activity, we found no difference between genotypes. However we observed a constant decrease of the vertical activity across trials, until almost abolished (Figure C.5e; two-way ANOVA, effect of time,  $F_{4, 84} = 12.12$ ,  $p < .001$ , no effect of genotype,  $F_{1, 20} = 1.471$ ,  $p = 0.239$ ).

We also compared the first day to the last day of injection, and found no effect of time on the horizontal activity (Figure C.5c; two-way ANOVA, no effect of time,  $F_{1, 20} = 0.176$ ,  $p = 0.680$ ). We noticed a strong decrease of the vertical activity (Figure C.5f; two-way ANOVA, effect of time,  $F_{1, 21} = 19.53$ ,  $p < .001$ ). The only difference between WT and mutant mice for the horizontal activity was between AMPH1 and AMPH5 (Figure C.5c; two-way ANOVA, effect of genotype,  $F_{1, 20} = 13.08$ ,  $p = .002$ ).

In conclusion, AMPH 5 mg/kg produces a substantial enhanced hyperlocomotion in VGLUT3<sup>-/-</sup> compared to VGLUT3<sup>+/+</sup> that translates into a differential horizontal activity. Vertical activity decreases across trials and does not differ between mutant and control mice.

## 4.2 Effect on stereotypies

AMPH at higher doses has the ability to elicit abnormal movements. Therefore, we assessed stereotypies in VGLUT3<sup>-/-</sup> mice in the same behavioral sensitization protocol. We investigated general stereotypies, based on the scale described in Table B.8. Amphetamine effects have been widely explored since the seventies. This drug has the particularity to stimulate orofacial stereotypies (Creese *et al.* 1975). Therefore, we also assessed the orofacial stereotypies separately, with a finer scale as described in Table B.9.

As for locomotion, stereotypy is a behavior that is sensitized with repeated drug exposures. This is reflected by the increased intensity of stereotypies and a decreased onset across trials (Robinson *et al.* 1986).

### 4.2.1 General stereotypies

In our sensitization protocol, we rated stereotypies during the 90-minute period following each injection. We sequentially observed mice and attributed a score between 0 (asleep or stationary) and 6 (continuous biting, gnawing or licking without locomotor activity) according to the severity of stereotypies. In our experimental conditions (C57BL/6 mouse, 5 mg/kg D- amphetamine i.p.), we observed a different kinetics from the one previously described, with the phases being shortened (Schierring 1979).

Indeed, during the acute injection of amphetamine, locomotion started to increase after 5 to 10 minutes, and this phase lasted 10 to 20 minutes. But rapidly, we observed the start of the stereotypy phase, which lasted ~70 to 80 minutes, with the climax of stereotypies around 20 minutes after the beginning of the phase. Animals received a daily injection of D- amphetamine for 5 days. The kinetics evolved along the trials: each day, the onset of stereotypies was more precocious. The duration of this phase lengthened until it reached the whole scoring period during the last trial. Notably, through trials, the intensity of stereotypies increased so much that most animals showed no residual locomotion during the last session.

By comparing the kinetics of stereotypy across time for each day of injection, we found that VGLUT3<sup>-/-</sup> mice displayed significantly less stereotypies than WT littermates (Figure C.6a; two-way ANOVA, effect of genotype, day 1,  $F_{1,11} = 14.58$  and  $p = .003$ , day 2,  $F_{1,11} = 9.176$  and  $p = .012$ , day 3,  $F_{1,26} = 20.22$  and  $p < .001$ , day 4,  $F_{1,26} = 12.18$  and  $p = .002$ , day 5,  $F_{1,26} = 9.379$  and  $p = .005$ ). We then compared the maximum stereotypy score and the median stereotypy score for each day of injection (Figure C.6b and c). We found that both maximum (Figure C.6b; two-way ANOVA, effect of time,  $F_{4,104} = 6.639$ ,  $p < .001$ , effect of genotype,  $F_{1,26} = 11.50$ ,  $p = .002$ ) and median stereotypy scores (Figure C.6c; two-way ANOVA, effect of time,  $F_{4,104} = 12.74$ ,  $p < .001$ , effect of genotype,  $F_{1,26} = 18.41$ ,  $p < .001$ , interaction time x genotype,  $F_{4,104} = 2.856$ ,  $p = .027$ ) increased across sessions and that VGLUT3<sup>-/-</sup> mice exhibited less stereotypies than WT mice. These stereotypies were also less intense.

To verify the overall effect of injections on stereotypies, we compared the median stereotypy score between AMPH1 and AMPH5. We found that WT, but not mutant mice, exhibited a statistically significant stereotypic sensitization (Figure C.6d; two-way ANOVA, effect of time,  $F_{1,26} = 28.23$ ,  $p < .001$ ; post test between AMPH1 and AMPH5,  $p < .001$  for WT,  $p = .071$  for mutant). Moreover, VGLUT3<sup>-/-</sup> mice had a lower median stereotypy score compared to WT littermates (effect of genotype,  $F_{1,26} = 10.75$ ,  $p = .003$ , interaction time x genotype,  $F_{4,104} = 4.751$ ,  $p = .039$ ).

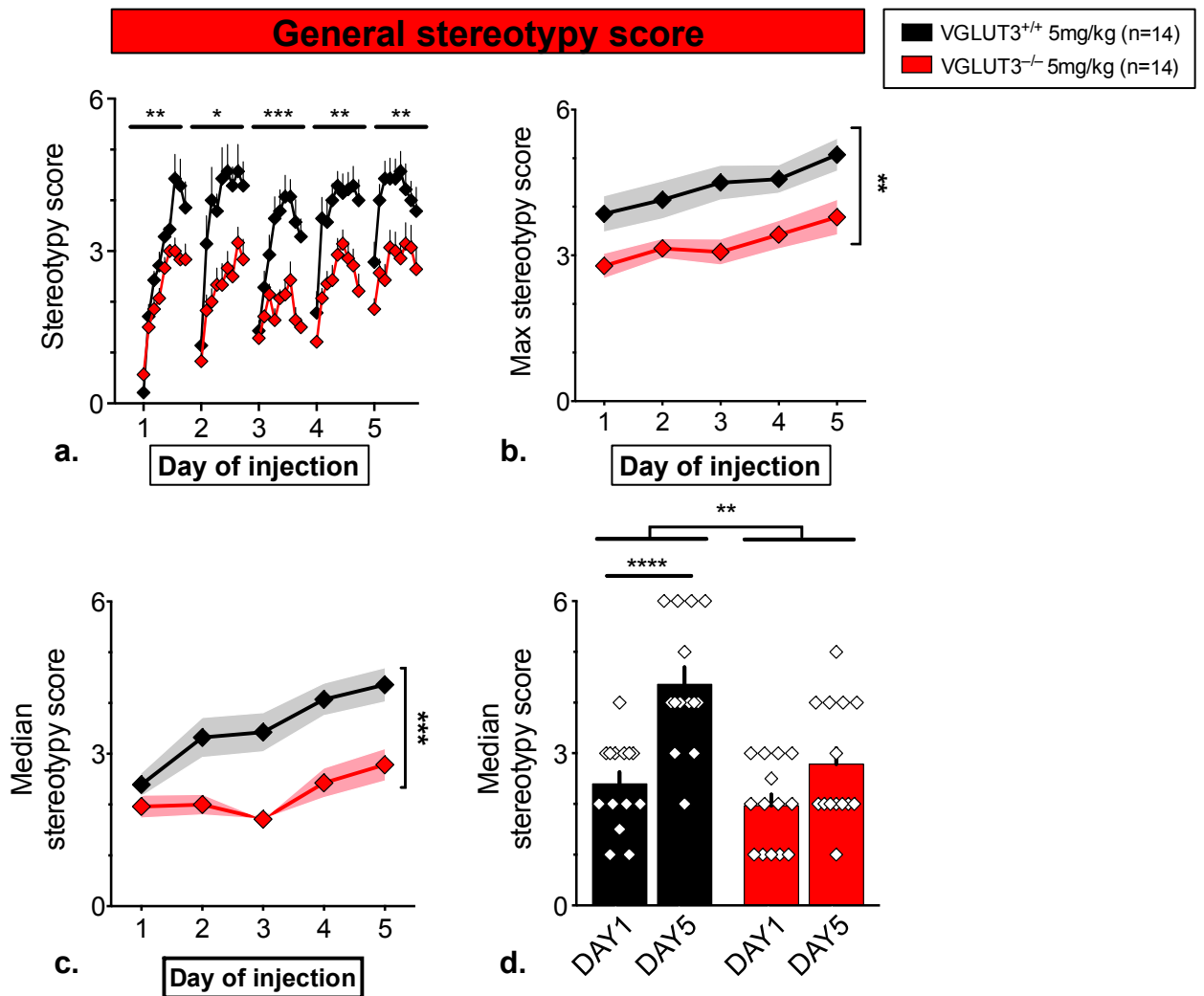


**Figure C.6: VGLUT3<sup>-/-</sup> general stereotypies with AMPH 5 mg/kg**

**a.** Temporal course of general stereotypies for the 5 days of injection (1 to 5), during each 90- min- period following drug injection, every 10- min time bins. **b.** Maximum stereotypy score observed during each day of injection. **c.** Median stereotypy score observed during each day of injection. **d.** Comparison of the median stereotypy score between the 1<sup>st</sup> (AMPH1) and the last injection (AMPH5).

**a.** After each AMPH injection, the level of stereotypies increases and becomes maximal around 35 min post-injection. VGLUT3<sup>-/-</sup> mice display less stereotypies than WT littermates. **b.** and **c.** The maximal stereotypy score of WT mice for each session is systematically higher than mutants. **d.** General stereotypies do sensitize between AMPH1 and AMPH5 in control mice, but not in VGLUT3 null mice (n = 14-14).

Overall, mice lacking VGLUT3 are more resistant to amphetamine- induced stereotypies and do not display stereotypy sensitization to AMPH 5 mg/kg.

#### 4.2.2 Orofacial stereotypies

During the experiments, some mice would display orofacial stereotypies while others would not. An alternative rating scale specific for orofacial stereotypies was thus used (Table B.9). This scale ranged from 0 (no orofacial stereotypy) to 4 (continuous cob bedding biting without locomotion). The score was attributed blindly by re- analyzing the

combination of the categorical and rating scales we used during our experiments, as detailed in Materials & Methods.

When looking at the effect of daily AMPH 5 mg/kg injections on orofacial stereotypies, we found that VGLUT3<sup>-/-</sup> mice displayed systematically lower orofacial stereotypies compared to WT littermates (Figure C.7a; two-way ANOVA, effect of genotype, day 1,  $F_{1,11} = 4.931$  and  $p = .048$ , day 2,  $F_{1,11} = 4.585$  and  $p = .056$ , day 3,  $F_{1,26} = 7.037$  and  $p = .013$ , day 4,  $F_{1,26} = 5.05$  and  $p = .033$ , day 5,  $F_{1,26} = 6.905$  and  $p = .014$ ). We also compared the maximum (Figure C.7b; two-way ANOVA, effect of genotype,  $F_{1,26} = 10.77$  and  $p = .003$ ) and median orofacial stereotypy scores (Figure C.7c; two-way ANOVA, effect of genotype,  $F_{1,26} = 6.587$  and  $p = .016$ ) between WT and mutant mice, and found that VGLUT3<sup>-/-</sup> mice had lower orofacial stereotypy levels than control mice. Moreover, as for general stereotypies, orofacial stereotypies got more intense across sessions (two-way ANOVA, effect of time,  $F_{4,104} = 5.886$ ,  $p < .001$  for maximal orofacial stereotypy score, and  $F_{4,104} = 6.436$ ,  $p < .001$  for median orofacial stereotypy score).

When comparing AMPH1 to AMPH5, we found that indeed, VGLUT3<sup>-/-</sup> displayed less orofacial stereotypies than WT littermates (Figure C.7d; two-way ANOVA, effect of genotype,  $F_{1,26} = 6.933$ ,  $p = .014$ , effect of time,  $F_{1,26} = 15.60$ ,  $p < .001$ , interaction time x genotype  $F_{1,26} = 6.933$ ,  $p = .014$ ; post test between AMPH1 and AMPH5,  $p < .001$  for WT,  $p = 0.721$  for mutant).

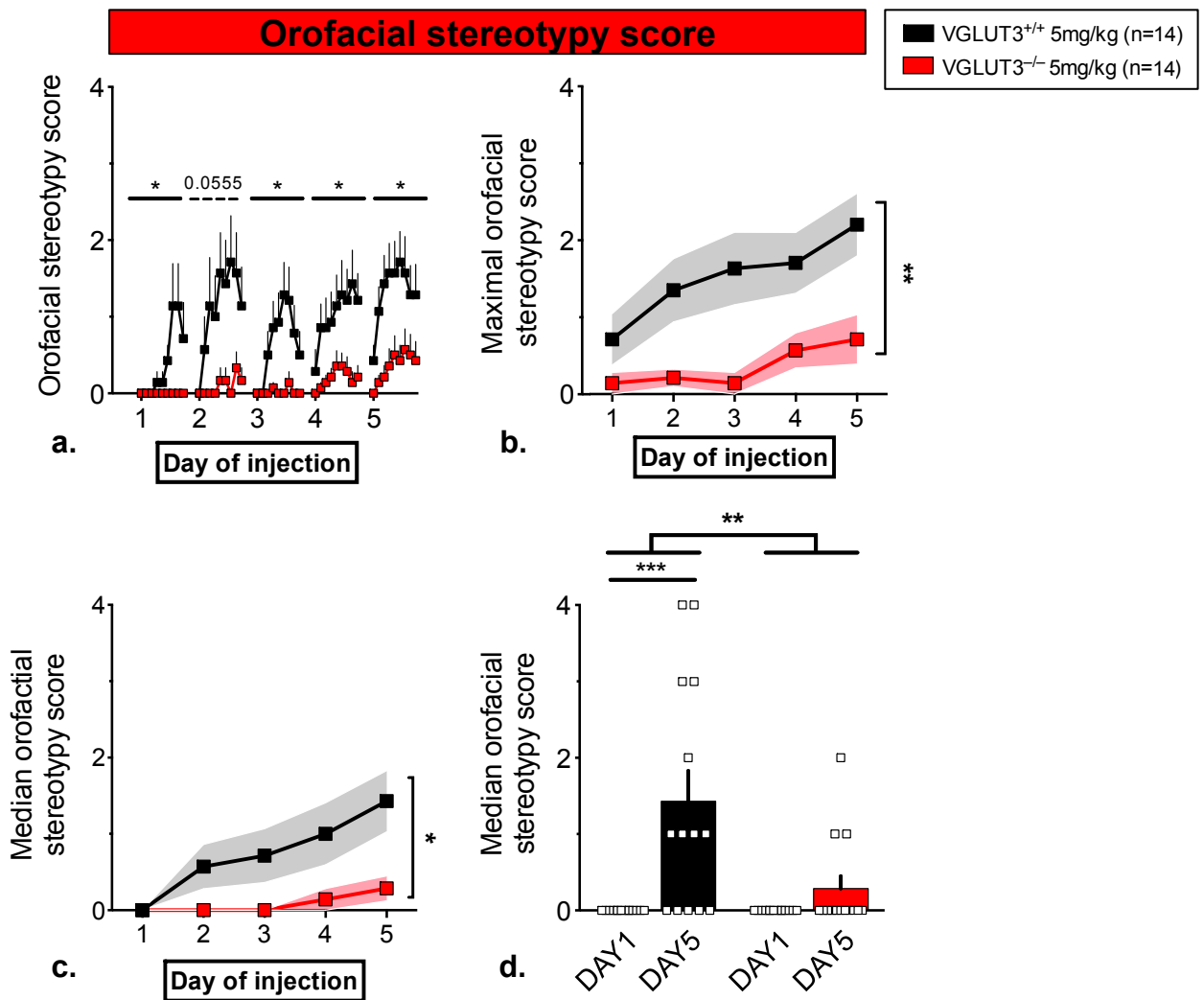


**Figure C.7: VGLUT3<sup>-/-</sup> orofacial stereotypies with AMPH 5 mg/kg**

**a.** Temporal course of orofacial stereotypies for the 5 days of injection (1 to 5), during each 90- min- period following drug injection, every 10-min time bins. **b.** Maximal orofacial stereotypy score during each day of injection. **c.** Median orofacial stereotypy score observed during each day of injection. **d.** Comparison of the median orofacial stereotypy score between the 1<sup>st</sup> (AMPH1) and the last injection (AMPH5).

**a.** After each AMPH injection, WT mice display orofacial stereotypies, while VGLUT3 knockouts barely present any. **b.** and **c.** The maximal stereotypy score of WT mice for each session is systematically higher than mutants. **d.** General orofacial stereotypies do sensitize between AMPH1 and AMPH5, but VGLUT3 null mice display less orofacial stereotypy than WT siblings (n = 14-14).

These results demonstrate that VGLUT3<sup>-/-</sup> mice have less orofacial stereotypies than VGLUT3<sup>+/+</sup> mice. Moreover, they do display no sensitization for orofacial stereotypies.

## 5. Discussion

Mice constitutively lacking VGLUT3 have a marked increased sensitivity to cocaine (Sakae *et al.* 2015). Interestingly these mutant mice do not sensitize to cocaine (10 mg/kg). They also demonstrate an increased drug intake and drug seeking, and an exacerbated motivation for cocaine in a self- administration paradigm. This intake would

be “rational”, meaning that mice would not compulsively try to administrate the drug when it is not available, suggesting that the actions of VGLUT3 null mice are guided by reward (goal- directed behaviors) rather than by habits and compulsion.

All these behavioral characteristics have been related to the accumbal basal changes present in VGLUT3 null mice. They have an increased accumbal DA release and an overactivation of the mesolimbic pathway. Indeed, D<sub>1</sub>R- expressing MSNs present a constitutive elevated number of dendritic spines, as well as an increased number of D<sub>1</sub>R and an increased AMPAR/NMDAR ratio. This could have explained the fact that VGLUT3<sup>-/-</sup> respond to lower doses of cocaine in CPP and that they are pre- sensitized to cocaine. Cocaine is known to induce such changes in WT mice, which underlie the long- lasting effects of the drug and explain the behavioral sensitization observed with repeated administrations of drug (Russo *et al.* 2010). Intriguingly, cocaine treatment does not enhance the number of spines in mice constitutively lacking VGLUT3, even if D<sub>1</sub>R downstream signalling cascade is activated (the striatal levels of phospho- ERK are identical between WT and mutants after sensitization to cocaine 10 mg/kg; Sakae *et al.* (2015)).

Because the sequencing of *SLC17A8* revealed punctual mutations of VGLUT3 in human addicts with polysubstance abuse, we wondered if VGLUT3 null mice would also present the same responses to other drugs of abuse. Since these mice have basal accumbal alterations, we postulated that they should be pre- sensitized to substances other than cocaine. We chose to investigate the effects of another psychostimulant that also directly enhances extracellular dopamine levels: D- amphetamine.

Surprisingly we found that at low doses:

- i) The acute injection of amphetamine results in the same level of hyperlocomotion in VGLUT3<sup>-/-</sup> mice and WT mice.
  - ii) Repeated administrations of amphetamine elicit locomotor sensitization in VGLUT3<sup>-/-</sup> mice.
- Low doses of amphetamine induce similar locomotor activation in VGLUT3<sup>-/-</sup> mice and WT mice.

The acute injection of two low doses of amphetamine (1 and 3 mg/kg) induced similar levels of locomotor activation in both WT and VGLUT3-null mice. This result was quite unexpected, since the postulate for cocaine pre- sensitization of VGLUT3 mutant relied on a constitutively enhanced DA release and a hyper- responsivity of the D<sub>1</sub>- pathway. In view of the results described above, it seems that amphetamine action could be

independent of this CIN- mediated modulation of DA release (Figure C.8). This result suggests that the model proposed by Sakae *et al.* (2015) is incomplete.

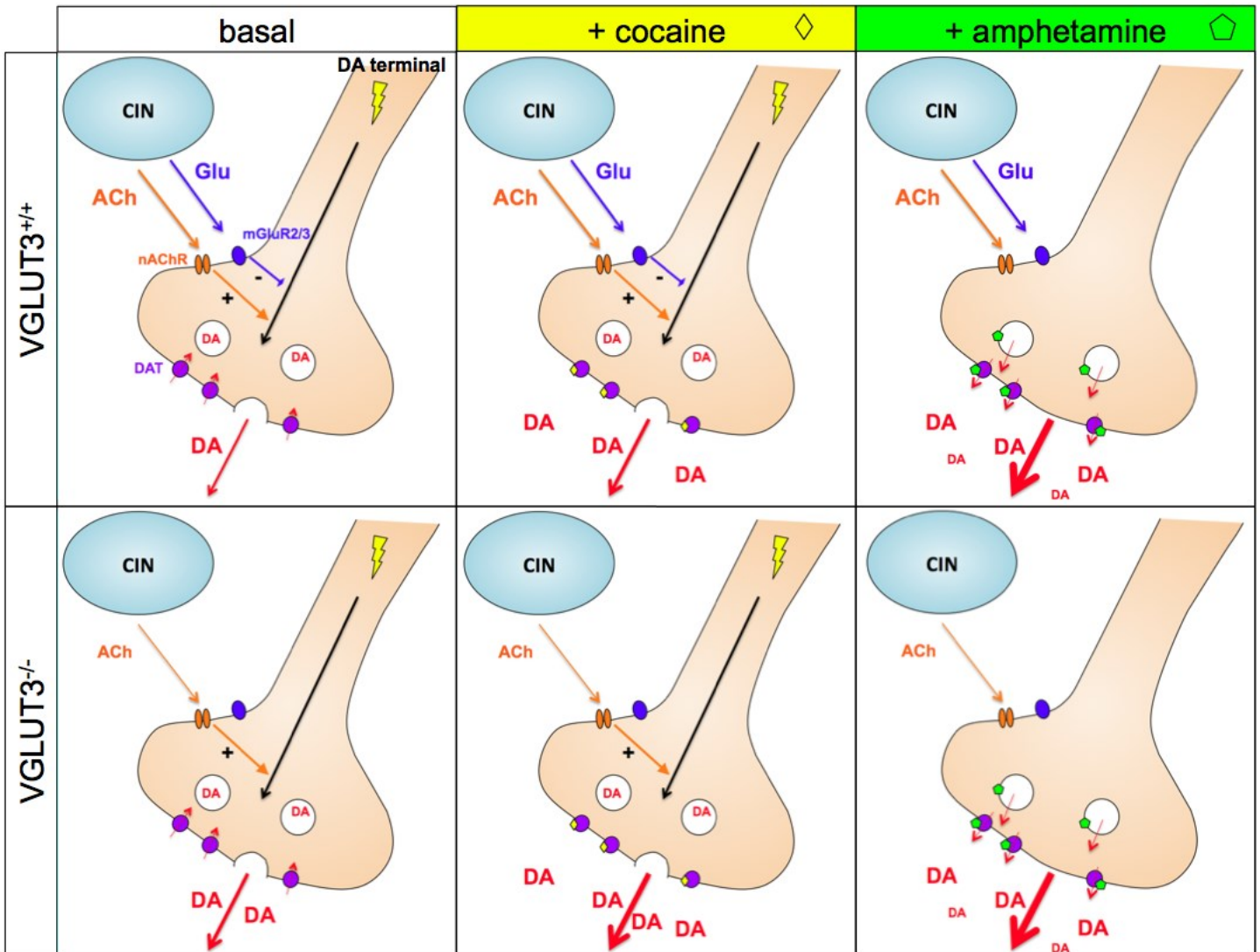


**Figure C.8: Model of cocaine and amphetamine action in VGLUT3<sup>-/-</sup> mice**

**Left panel:** At basal state, CINs exert a dual opposite regulation of DA release in the striatum. Glutamate inhibits DA release by acting on presynaptic mGluR2/3 (*in blue*), while ACh favors it by gating presynaptic nAChRs (*in orange*). In VGLUT3 null mice, despite the decreased ACh release, there is no negative feedforward exerted by CIN- released glutamate, which results in an enhancement of extracellular DA levels.

**Middle panel:** The administration of cocaine (*in yellow*) results in increased extracellular DA levels upon inhibition of the plasmalemmal transporter DAT (*in purple*). This is time- locked with a pre- existing synaptic release of DA. Because VGLUT<sup>-/-</sup> mice already have doubled the amount of DA release upon stimulation of the terminal, cocaine induces an exacerbated increase of extracellular DA compared to WT.

**Right panel:** The administration of amphetamine (*in green*), on the other hand, needs no prior neuronal discharge to release DA. It reverses both DAT and the vesicular DA transporter VMAT2, which results in a massive non- vesicular extracellular release of DA. This release is probably in the same range in WT and mutant mice.

Indeed, amphetamine has the particularity of depleting DAergic terminals from their intracellular DA stores in an activity- independent manner. In contrast, cocaine acts by preventing the reuptake of neuronal activity- dependent DA release. Therefore,

amphetamine administration yields greater levels of extracellular DA compared to cocaine, even if it has been evidenced that not all of this DA is functional (Darracq *et al.* 1998, Darracq *et al.* 2001). Therefore amphetamine could shunt the presynaptic modulation of DA release exerted by CINs. This could explain why WT and mutant mice present the same amphetamine- induced hyperlocomotion with a low dose.

- [Repeated administrations of amphetamine elicit locomotor sensitization in VGLUT3<sup>-/-</sup> mice.](#)

VGLUT3<sup>-/-</sup> mice do sensitize to amphetamine. We even observe a higher sensitization in the mutant compared to control littermates. This means that amphetamine-induced morphological or synaptic plasticity must occur in VGLUT3<sup>-/-</sup> mice. Yet, it was demonstrated that in the case of cocaine, structural plasticity is not involved in null mice (same number of dendritic spines after chronic cocaine), despite the activation of the D1- mediated molecular cascade (increase of phospho- ERK levels in the Acb and dStr similar to that of WT mice in response to acute cocaine 10 mg/kg; Sakae *et al.* (2015)).

In WT animals, both cocaine and amphetamine yield an increased number of dendritic spines on MSNs in the Acb and CPu, in particular in distal dendritic fields that mainly receive distal projections (Li *et al.* 2003). The number of spines is also increased on the apical dendrites of pyramidal cells in the prefrontal cortex (Robinson and Kolb 2004). Moreover, dendritic morphological plasticity disappears when behavioral sensitization disappears (Kolb *et al.* 2003). Amphetamine yields a massive DA release compared to cocaine. Consequently, the resulting downstream events could diverge between the two drugs. Given the presence of AMPH- induced locomotor sensitization in VGLUT3 null mice, it cannot be excluded that structural plasticity of MSNs (lacking in the case of COC) would be triggered by AMPH. It is also likely that the phenomenon underlying amphetamine sensitization results from changes in distal regions such as the prefrontal cortex.

These hypotheses will have to be tested by evaluating the number of dendritic spines by diolistic labeling (Heck *et al.* 2015). It should be noted that some drugs decrease spine complexity, such as alcohol and opiates, but an increased synaptic strength maintains an overall reinforced transmission (Russo *et al.* 2010). Therefore it cannot be excluded that even if the number of spines is not modified by the AMPH treatment, some other changes such as surface receptor expression or intracellular cascades could be altered.

Amphetamine is a potent monoamine releaser that acts on DAT, NET and SERT (Sulzer 2011). Consequently, it can naturally be inferred that the serotonergic and noradrenergic systems contribute to the phenotypes we observe in response to AMPH. Despite its strong influence on the serotonergic transmission, cocaine does not seem to

participate in NET and SERT blockade in the ventral striatum (White *et al.* 1998, Budygin *et al.* 2002). On the other hand, *in vivo* studies revealed that amphetamine yields enhanced striatal serotonergic levels when administered at doses higher than 2 mg/kg (Kuczenski and Segal 1989, Salomon *et al.* 2006). Serotonin has been linked to drug response (Salomon *et al.* 2007). Thus, is the case of AMPH 3 mg/kg, the serotonergic component might come into play in the observed response.

It also appears that the role of the noradrenergic system has largely been underestimated in the vast number of studies regarding the effects of psychostimulants. Several studies reported that NA is necessary to mediate amphetamine-induced hyperlocomotion (Darracq *et al.* 1998, Pascoli *et al.* 2005, Salomon *et al.* 2006). For example, the blockade of adrenergic receptors in the prefrontal cortex efficiently prevents amphetamine-induced hyperlocomotion even if DA levels are increased in the Acb (Darracq *et al.* 1998). This means that some of the phenotypes we observe in VGLUT3 null mice may be imputable to the action of amphetamine on the release of noradrenaline.

To specifically test the contribution of serotonergic and noradrenergic systems, we could use an alternative pharmacological agent to amphetamine, venlafaxine, a dual 5-HT/NA reuptake inhibitor. These two systems regulate each other via  $\alpha_{1b}$ -AR and 5-HT<sub>2A</sub>R, but amphetamine treatment has proved to abolish this coupling by differentially modulating pyramidal neurons that project to the striatum (Salomon *et al.* 2006).

- [VGLUT3 null mice are more resistant to AMPH-induced stereotypies.](#)

Higher doses of amphetamine elicit stereotypies in rodents (Creese *et al.* 1975). These repetitive behaviors rely on an abnormal functioning of loop circuits interconnecting the frontal cortex to the dorsal part of the striatum (Langen *et al.* 2011). Chronic administration of amphetamine induces the activation of D1-MSNs in the dorsal striatum, especially in the dorsolateral part (Graybiel *et al.* 2000). This loop is altered in several pathologies, such as obsessive-compulsive disorders or Tourette's syndrome, but also in drug addicts with stereotypies (Crittenden *et al.* 2011).

It has been proposed that in response to drug injection, the behavioral outcome is a competition between ambulation and stereotypies. Ambulation relies on the ventral striatum while stereotypies are related to the dorsal striatum activation (Bickerdike *et al.* 1997). Both acute and chronic injections of amphetamine, cocaine or DA receptor agonists result in the expression of treatment-specific IEGs (*e.g.* Fos, JunB, Fra) in the dStr, with predominance in the striosomal compartment (Graybiel *et al.* 1990, Canales and Graybiel 2000, Saka *et al.* 2002). Interestingly, the amount by which the activation of striosomes exceeds the activation in the matrix (ISMP) is a strong predictor of motor

stereotypies severity (Canales *et al.* 2000). Drugs of abuse have the ability to elevate accumbal DA levels (Di Chiara *et al.* 1988). This activates loops that favor actions and reward. All these circuits are topographically organized, and subsequently the repeated injections of drug will progressively recruit more dorsal loops, first in the DMS when the behavior is guided by the reward, and later in the DLS when it becomes habitual (Everitt *et al.* 2013). As a functional correlate, it was demonstrated that repeated exposure to psychostimulants enhances the number of spines on MSNs in the DLS while their density decreases in the DMS (Jedynak *et al.* 2007).

In our study, repeated injections of AMPH 5 mg/kg induced stereotypies. They mainly consisted in sniffing and orofacial actions and became more severe across injections. We observed no stereotypical sensitization in VGLUT3<sup>-/-</sup> mice, and their stereotypies were weaker than controls, especially the orofacial ones. Orofacial stereotypies are attributed to the ventromedial subregion of the striatum (Kelley and Delfs 1994).

Locomotion and stereotypies are two striato-nigro-thalamo-cortical loops in competition. We propose that repeated injections of amphetamine preferentially recruit the stereotypy loop in WT mice, as previously described (Iversen 1975). In contrast, a relative hyperactivation of the locomotor loop must be favored in VGLUT3<sup>-/-</sup> mice.

In our team in Montreal, DA efflux was estimated in the striatal subcompartments of VGLUT3<sup>-/-</sup> mice using *in vivo* voltammetry. Interestingly, the study revealed that DA levels were increased in the DMS of mutant mice compared to WT. In contrast, these levels were similar between genotypes in the DLS, as depicted on Figure C.9 (Mathieu Favier, unpublished results). These are the first data to support our working hypothesis. DA levels in VGLUT3 null mice fit the hypothesis according to which these mice would be more resistant to stereotypies: the ventral and dorsomedial striata would be preferentially activated by amphetamine. This result is also consistent with the cocaine self-administration experiment conducted on VGLUT3<sup>-/-</sup>, which revealed that mice would administrate more drug but also stop seeking it when it is not available, suggesting an enhanced motivation without compulsion. In other words, VGLUT3 null mice seem to remain in a goal-directed scheme.

However, to address the question of psychostimulants striatal effects, one should consider the compartmental organization of striatum rather than the classical regional one, *i.e.* matrix / striosome instead of vStr / DMS / DLS. Indeed, psychostimulants induce the expression of IEGs predominantly in D1-MSNs located in striosomes (Graybiel *et al.* 2000, Saka *et al.* 2002, Crittenden *et al.* 2011, Biever *et al.* 2016). This striosomal predominance of IEGs has been described in another pathological situation: L-DOPA treatment in DA-depleted animals and patients (Graybiel *et al.* 2000, Crittenden *et al.* 2009, Crittenden *et al.* 2011, Murer *et al.* 2011). Therefore, the resistance to

AMPH- induced stereotypies can be paralleled by the L- DOPA- induced dyskinesia- resistance reported in two recent studies (Divito *et al.* 2015, Gangarossa *et al.* 2016).

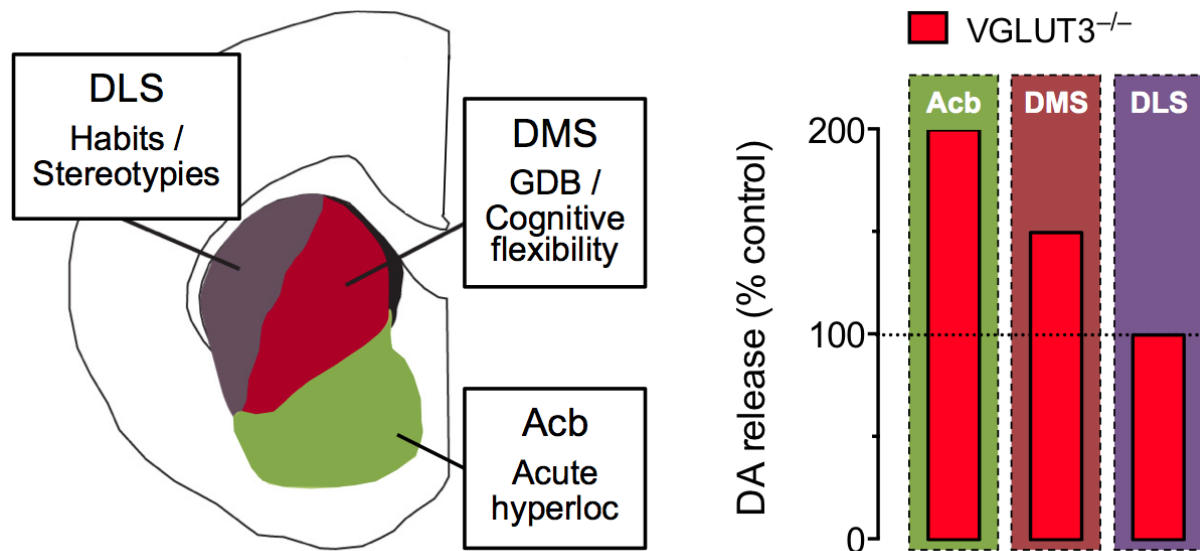


**Figure C.9: Striatal evoked dopamine levels in VGLUT3<sup>-/-</sup> mice**

**Left panel:** The initial stages of the development of drug dependence are thought to involve the limbic cortical and limbic striatal regions, where DA modulation of the nucleus accumbens (Acb) pathway alters stimulus- response and reward associations by affecting the motivational and emotional salience of a drug. Continued drug exposure recruits the dorsomedial striatum (DMS) to execute goal-directed behaviors (GDB) and cognitive flexibility with regards to drug seeking and drug taking. With further drug use, there is an additional activation of the dorsolateral striatum (DLS) such that drug use shifts from goal-directed to progressively more automatic and habitual behavior. Amphetamine facilitates the development of habits. **Right panel:** VGLUT3 null mice have double the amount of DA released in the Acb after K<sup>+</sup>-induced DA efflux, while this level is 1.5- fold high than controls in the DMS and equivalent in the DLS.

Adapted from data kindly provided by Mathieu Favier

In line with these results, we make three assumptions.

- 1) VGLUT3-null mice should be less prone to the development of habits.
- 2) The dendritic spine density on MSNs should be higher in WT mice compared to knockouts.
- 3) Neurons in striosomes should have decreased levels of IEGs in null mice (ERK1/2, CaIDAG- GEFII,  $\Delta$ FosB), and more generally in the dStr.

We are currently testing this last hypothesis by  $\Delta$ FosB immunostaining (see Materials & Methods), which is specifically expressed upon chronic drug treatment (Lobo *et al.* 2013). Repeated injections preferentially activate D1- MSNs rather than D2- MSNs, and CINs also express  $\Delta$ FosB with this regimen. Disruption of CINs prevents the preferential gene induction in striosomes (Saka *et al.* 2002)

## **CONCLUSION**

**In the behavioral sensitization protocol we used, we found that amphetamine, unlike cocaine, leads to a locomotor sensitization at low dose in VGLUT3<sup>-/-</sup> mice. Moreover, mutant mice seem to be more sensitive to the amphetamine- induced hyperlocomotion.**

**At a high dose, we revealed that VGLUT3<sup>-/-</sup> mice are more resistant to stereotypies, especially the orofacial ones.**



## **PART II.**

# **CONTRIBUTION OF VGLUT3- POSITIVE SYSTEMS IN THE RESPONSE TO AMPHETAMINE**

### **CONTEXT**

- ▶ **VGLUT3 is mainly expressed by “non- glutamatergic” neurons. These neurons are cholinergic, serotonergic or GABAergic.**
- ▶ **VGLUT3<sup>-/-</sup> mice are hypersensitive to the rewarding effects of cocaine. They are also more sensitive to the amphetamine- induced hyperlocomotion but less prone to stereotypies.**
- ▶ **The dorsal striatum is a central structure in the development of stereotypies.**

### **PROBLEMATIC**

**VGLUT3<sup>-/-</sup> mice are more resistant to amphetamine- induced stereotypies. Given the central involvement of the striatum in this effect, we wondered if the different striatal sources of VGLUT3 could account for the phenotypes we found with the full knock- out.**

**To understand the contribution of VGLUT3- positive neurotransmitter systems, we studied the effects of amphetamine in two conditional knock- out mice models.**

- ▶ **To deplete the striatum from the exogenous source of VGLUT3, we used SERT- Cre::VGLUT3<sup>LoxP/LoxP</sup> mice.**
- ▶ **To remove the local source of VGLUT3 in the cholinergic interneurons, we used ChAT- IRES- Cre::VGLUT3<sup>LoxP/LoxP</sup> mice.**

## 1. The VGLUT3- positive serotonergic drive of the striatum

In the striatum VGLUT3 is found in ACh and 5-HT fibers. In order to understand the involvement of the VGLUT3-positive serotonergic system in the AMPH-induced hyperlocomotion and AMPH-induced stereotypies, SERT-Cre mice were crossed with VGLUT3<sup>LoxP/LoxP</sup> to specifically remove VGLUT3 in the serotonergic neurons. As a result, the targeted neurons have two phenotypes: loss of glutamate release, and decrease of 5-HT release because of the lack of vesicular synergy. We will refer to these double mutants as cKO-VGLUT3<sub>5-HT</sub> thereafter. In this study, we compared SERT<sup>Cre/+</sup>::VGLUT3<sup>LoxP/LoxP</sup> mice with SERT<sup>+/+</sup>::VGLUT3<sup>LoxP/LoxP</sup> as control siblings

### 1.1 Anatomical characterization of cKO-VGLUT3<sub>5-HT</sub>

The newly generated transgenic mice were validated by immunoautoradiography (IAR). We quantified the remaining levels of VGLUT3 in the cerebral structures of interest. This characterization was partly done by our team in Montreal (Figure C.10).

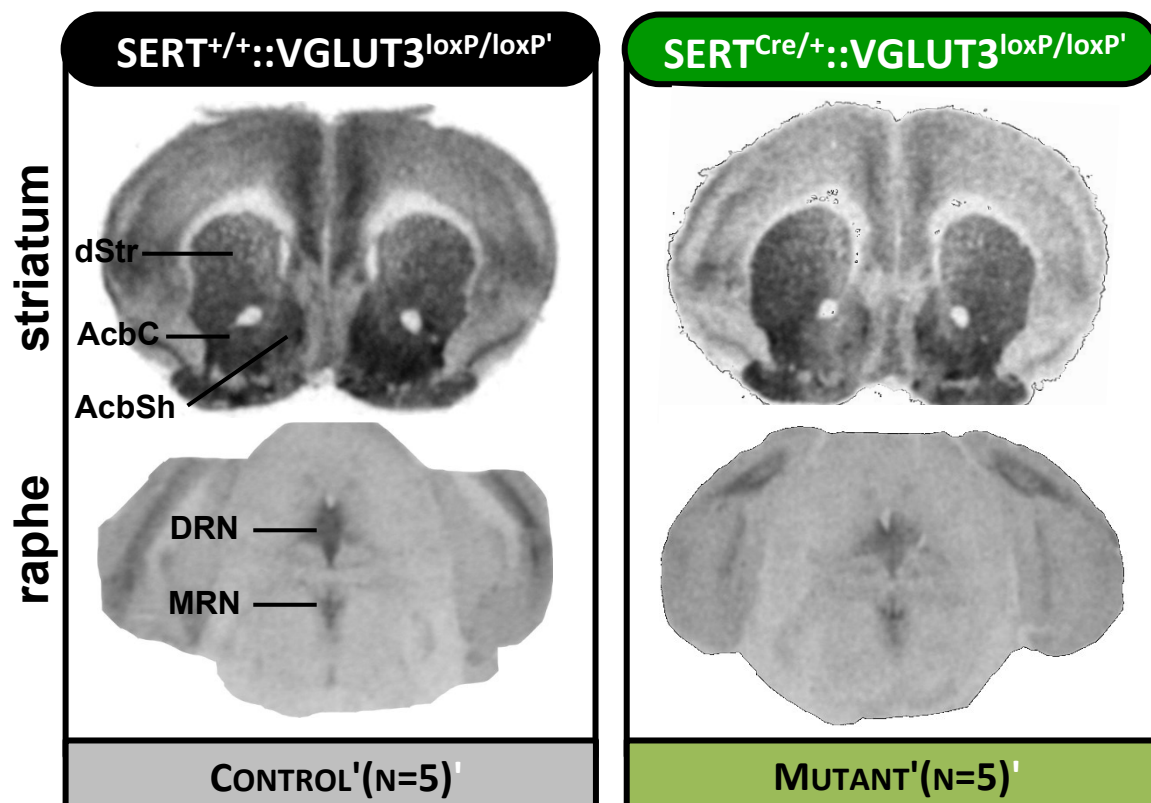


**Figure C.10: Immunoautoradiography for VGLUT3 in cKO-VGLUT3<sub>5-HT</sub> mice**

**Top panel:** coronal section at striatal level. **Bottom panel:** coronal section at raphe nuclei level. VGLUT3 is decreased in the striatum, in particular in the shell part of the nucleus accumbens (AcbSh) and the median and dorsal raphe nuclei (MRN and DRN) in mutant mice compared to control littermates (n = 5-5).

We observed a 30% decrease of VGLUT3 levels in the dorsal and median raphe nuclei. This is consistent with the neural composition of raphe nuclei, where three equal populations can be distinguished: pure VGLUT3- positive neurons, mixed VGLUT3 / 5- HT neurons, and pure 5- HT neurons (Hioki *et al.* 2010). The 30% decrease we observe in cKO-VGLUT3<sub>5-HT</sub> mice corresponds to the loss of VGLUT3 in mixed VGLUT3 / 5- HT neurons.

In the striatum, VGLUT3 levels were diminished from 15% in the AcbSh and by only 2- 3%, in the AcbC and the dorsal striatum. This is consistent with previous data suggesting a ~ 15% colocalization between VGLUT3 and 5- HT in the accumbens (Sakae *et al.* 2015). Thus, VGLUT3-positive serotonergic fibers preferentially project to the nucleus accumbens shell rather than the dorsal striatum.

## 1.2 Behavioral characterization of cKO-VGLUT3<sub>5-HT</sub>

### 1.2.1 Weight

We found similar body weights in cKO-VGLUT3<sub>5-HT</sub> mice and controls (Figure C.11; Mann- Whitney,  $p = 0.484$ , control  $31.63 \pm 1.4$  g and mutant  $30.14 \pm 1.28$  g).

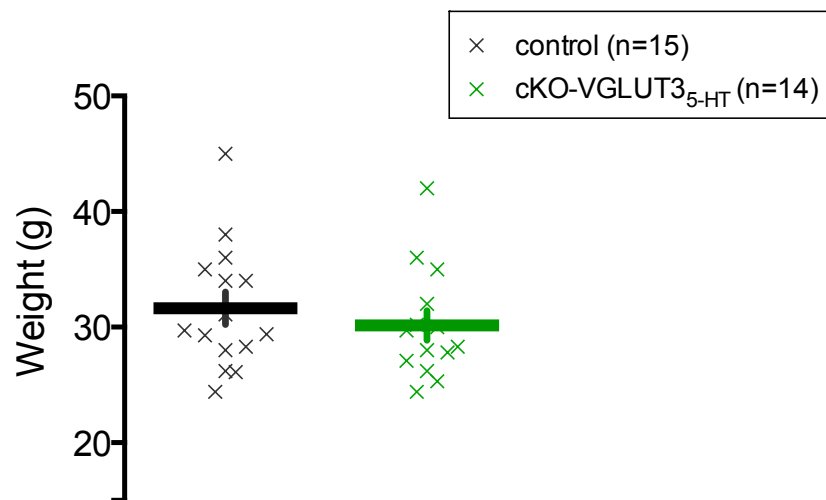


**Figure C.11: cKO-VGLUT3<sub>5-HT</sub> mice weight**

cKO-VGLUT3<sub>5-HT</sub> and age- matched control littermates have the same weight ( $n = 15-14$ ).

### 1.2.2 Basal locomotion

We assessed the basal locomotion of the mutant line by recording the spontaneous activity during 24 consecutive hours, as described in Materials & Methods (Figure B.4a). Several mice batches were pooled together, by a collaborative work with another PhD student, Fiona Henderson.

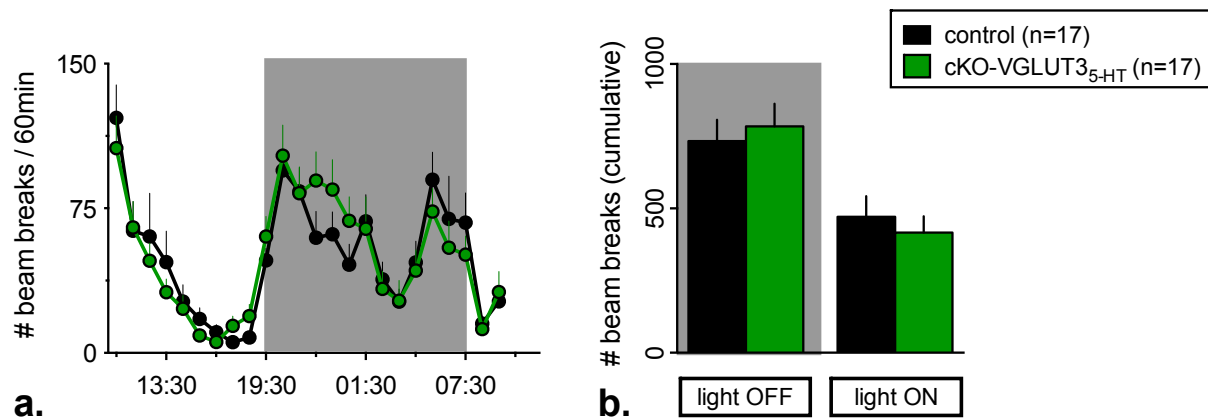


**Figure C.12: cKO-VGLUT3<sub>5-HT</sub> circadian locomotor activity**

**a.** Temporal course of the horizontal activity during 24 hours, from 10:30 a.m. to 10:30 a.m. the next day. cKO-VGLUT3<sub>5-HT</sub> (*in green*) and control siblings (*in black*) have a similar basal locomotion. The light- off period is represented by the *grey rectangle* (7:30 p.m.-7:30 a.m.). **b.** Cumulative locomotion during the light- off period (**left bars**, represented by the *grey rectangle*) and the light- on period (**right bars**). The cumulative locomotion during the light- off and the light- on phases does not differ between control and mutant mice (n = 17-17).

The time course of the horizontal activity revealed no difference of locomotion between cKO-VGLUT3<sub>5-HT</sub> and control littermates (Figure C.12a; two-way ANOVA, no effect of genotype,  $F_{1,30} < .001$ ,  $p = 0.98$ , effect of time,  $F_{23,690} = 14.94$ ,  $p < .001$ ). We also compared the cumulative locomotion during the light- off period, which corresponds to the active period of the animals. We found no difference between genotypes (Figure C.12b; t test,  $p = 0.646$ , control  $733.1 \pm 73.67$  and mutant  $783.4 \pm 78.45$  beam breaks). Likewise, there was no difference between cKO-VGLUT3<sub>5-HT</sub> and control siblings during the light- on phase (Figure C.12b; t test,  $p = 0.548$ , control  $470.9 \pm 71.46$  and mutant  $416.1 \pm 56.65$  beam breaks).

These results show that the specific ablation of VGLUT3 in 5-HT neurons does not disrupt the spontaneous locomotor activity of cKO-VGLUT3<sub>5-HT</sub> mice.

### 1.2.3 Anxiety tests

Serotonin is a neuromodulator of mood and is involved in stress and depression. Classical antidepressant drugs often belong to the SSRI family, and their goal is to increase the serotonergic tone. Thus, we explored if cKO-VGLUT3<sub>5-HT</sub> mutants could present anxiety- like phenotypes in two set- ups: the open field (OF) and the O maze (Figure B.4b and c). Fiona Henderson performed these experiments.

- Open field

Mice were individually placed in the OF for 10 minutes. cKO-VGLUT3<sub>5-HT</sub> mice spent as much time as control littermates in the central area, which corresponds to the most

anxiogenic zone (Figure C.13a; t test,  $p = 0.386$ ). Control mice spent  $3.97 \pm 0.9 \%$ , while cKO- SERT spent  $5.07 \pm 0.79 \%$  of time in the central zone (data not shown).

When looking at the distance travelled in the central area, mutant mice displayed a non- significantly different response compared to control siblings (Figure C.13b; t test,  $p = 0.229$ ).

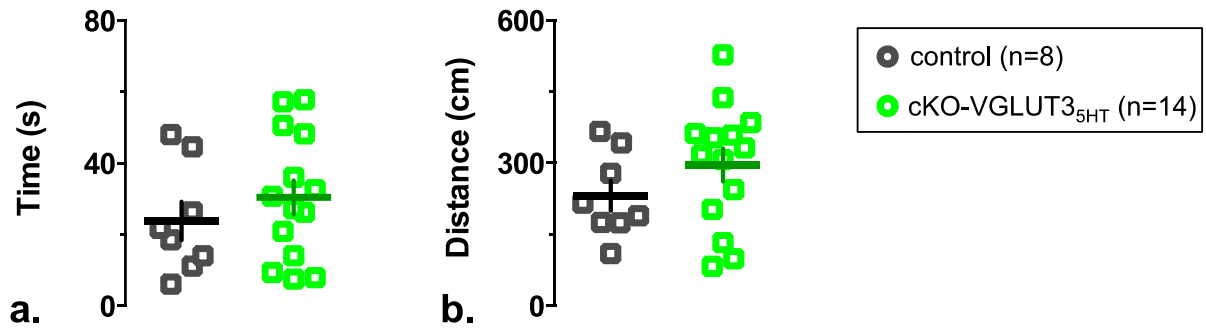


**Figure C.13: cKO-VGLUT3<sub>5HT</sub> anxiety levels in the open field test**

**a.** The time spent in the anxiogenic central zone does not differ significantly between cKO-VGLUT3<sub>5HT</sub> (*in green*) and control littermates (*in black*). **b.** cKO-VGLUT3<sub>5HT</sub> mice have a tendency to travel less in the central zone ( $n = 8-14$ ).

- O maze

We then assessed the anxiety levels in the O maze for 10 minutes. We found no difference in the time and distance spent in the open arms of the maze (anxiogenic zone) between cKO-VGLUT3<sub>5HT</sub> and control mice (Figure C.14a, Mann-Whitney for the time spent,  $p = 0.585$ ; Figure C.14b, Mann-Whitney for the distance travelled,  $p = 0.454$ ).

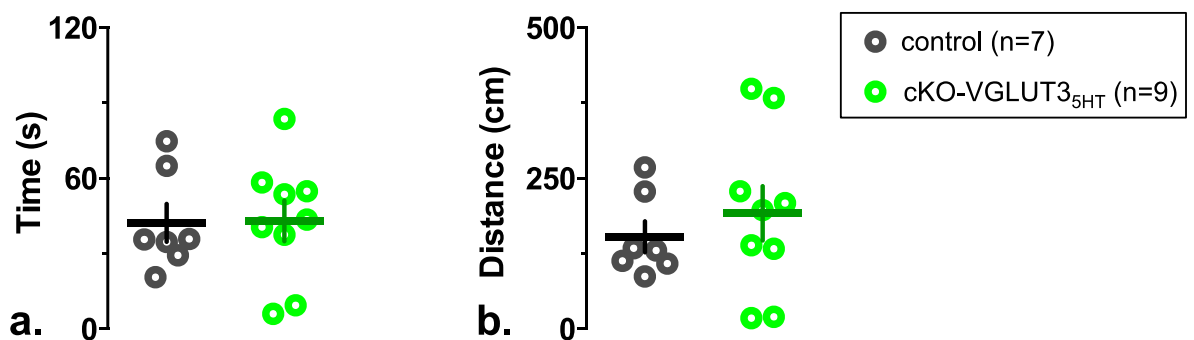


**Figure C.14: cKO-VGLUT3<sub>5HT</sub> anxiety levels in the O maze test**

**a.** The time spent in the anxiogenic open arms does not differ significantly between cKO-VGLUT3<sub>5HT</sub> (*in green*) and control littermates (*in black*). **b.** cKO-VGLUT3<sub>5HT</sub> travel as much as control mice in the open arms ( $n = 7-9$ ).

Together, the open field and O maze test seem to indicate that constitutive invalidation of VGLUT3 in serotonergic neurons does not affect anxiety levels of cKO-VGLUT3<sub>5HT</sub> mice.

### 1.2.4 Spontaneous locomotion before sensitization

We assessed the horizontal and vertical locomotion during the 2 h preceding each day of saline injections in the locomotor sensitization protocol. By proceeding to two-way ANOVAs for the horizontal and vertical locomotor activities, we found no interaction time x genotype, indicating that animals do habituate the same way to their activity box.

By comparing the differential horizontal response during sessions, we found no difference between cKO-VGLUT3<sub>5-HT</sub> and control siblings (Figure C.15, left panel; two-way ANOVA, effect of time,  $F_{2,48} = 26.68$ ,  $p < .001$ , no effect of genotype,  $F_{1,24} = 0.654$ ,  $p = .427$ ). Likewise, the vertical activity did not differ between genotypes (Figure C.15, right panel; two-way ANOVA, effect of time,  $F_{2,42} = 24.22$ ,  $p < .001$ , no effect of genotype,  $F_{1,21} = 0.1803$ ,  $p = 0.675$ ).

In line with the spontaneous activity recorded during 24 h (Figure C.12), cKO-VGLUT3<sub>5-HT</sub> and control littermates displayed similar levels of locomotion during the 3 days of habituation of the locomotor sensitization.

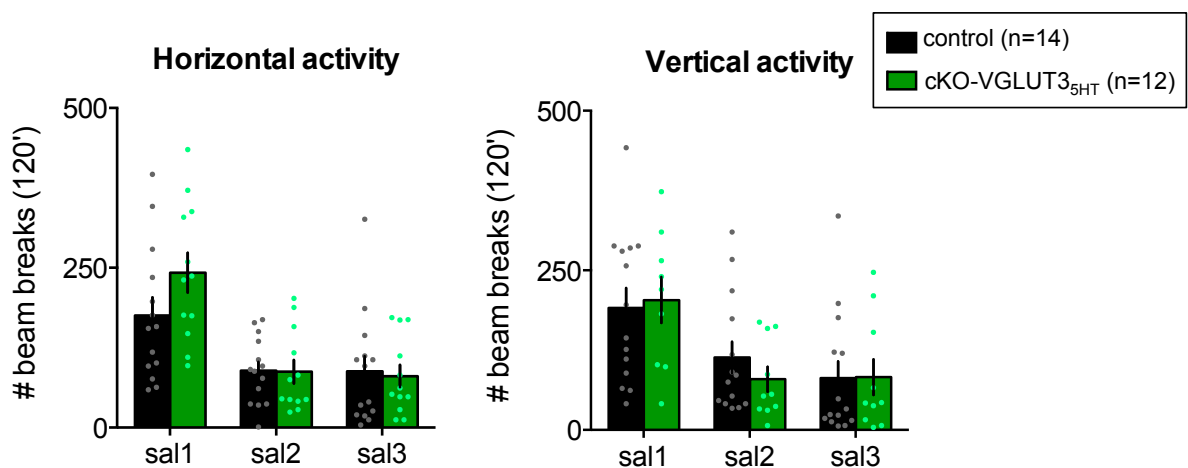


**Figure C.15: cKO-VGLUT3<sub>5-HT</sub> spontaneous activity**

cKO-VGLUT3<sub>5-HT</sub> and control littermates have the same levels of horizontal and vertical activity, and habituate to their new environment similarly ( $n = 14-12$ ).

## 1.3 cKO-VGLUT3<sub>5-HT</sub> and amphetamine 5 mg/kg

### 1.3.1 Effect on locomotion

In order to understand the contribution of the VGLUT3- positive serotonergic, we performed a behavioral sensitization to amphetamine 5 mg/kg on cKO-VGLUT3<sub>5-HT</sub>, as described before.

- [Acute injection of amphetamine 5 mg/kg](#)

We first analyzed mice response to an acute injection of AMPH 5 mg/kg. We found that acute AMPH 5 mg/kg yields a strong hyperlocomotion compared to the last saline

injection (horizontal activity: two-way ANOVA, effect of time,  $F_{1,17} = 59.86$ ,  $p < .001$ , no effect of genotype,  $F_{1,17} = 1.725$ ,  $p = 0.207$ ; vertical activity: two-way ANOVA, effect of time,  $F_{1,17} = 4.645$ ,  $p = .046$ , no effect of genotype,  $F_{1,17} = 0.023$ ,  $p = 0.882$ ). This hyperlocomotion was similar in mutant and control mice (Figure C.16a and d). The horizontal activity increased until becoming maximal around 30 min post-injection, and then slowly decreased, with a similar profile for control and mutant animals (Figure C.16a, inset: Mann-Whitney,  $p = 0.645$ ; control  $590.2 \pm 108.6$  and mutant  $689.2 \pm 127.4$  beam breaks). The vertical activity slowly rose after the injection and constantly increased but did not differ between groups (Figure C.16d, inset: Mann-Whitney,  $p = 0.643$ ; WT  $46.2 \pm 16.12$  and mutant  $37.28 \pm 21.42$  beam breaks). Animals injected with saline only displayed a residual activity (two-way ANOVA, no effect of genotype between cKO-VGLUT3<sub>5-HT</sub> and control injected with saline,  $F_{1,4} = 1.417$ ,  $p = 0.3$ ).

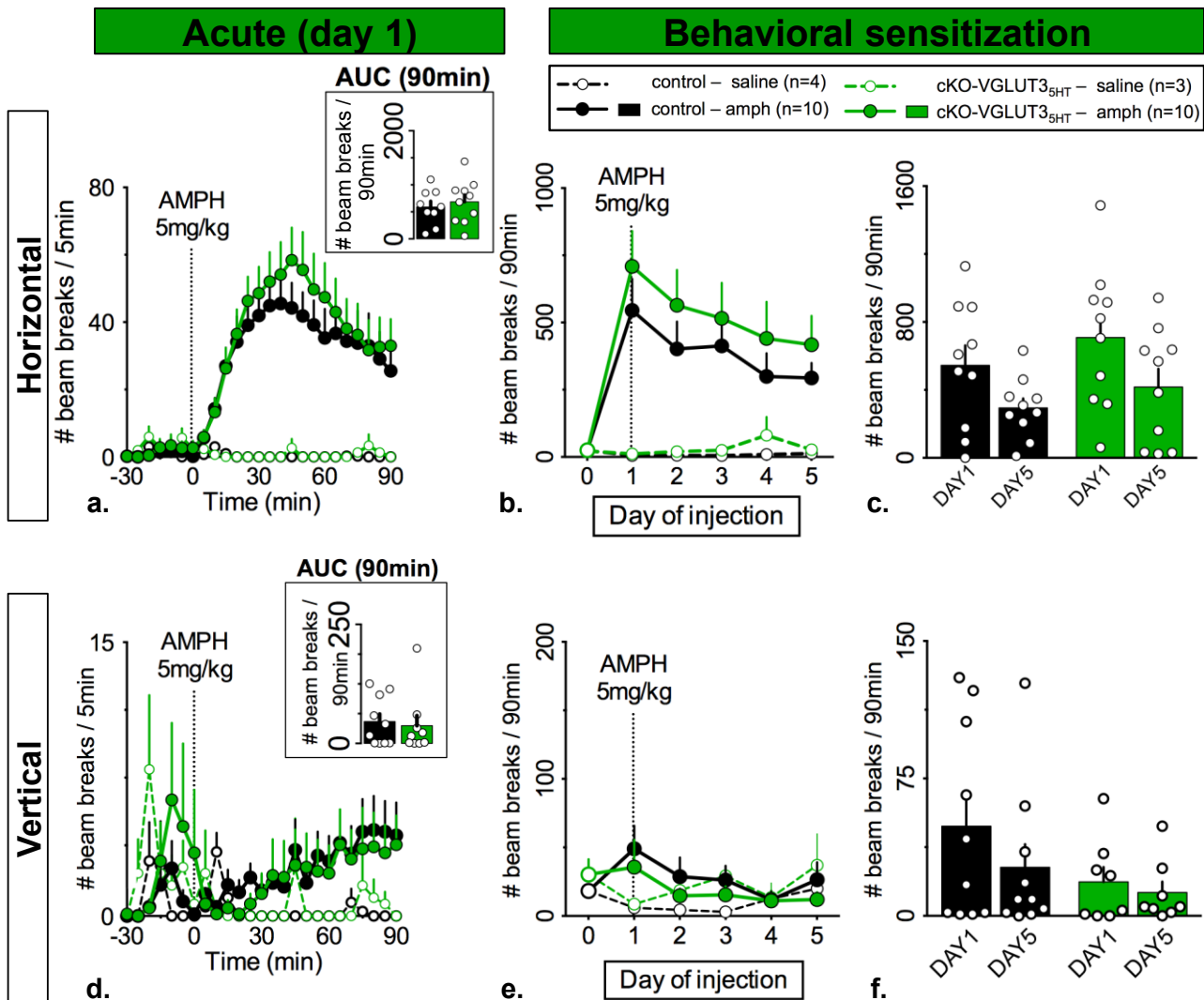


**Figure C.16: cKO-VGLUT3<sub>5-HT</sub> locomotor sensitization to AMPH 5 mg/kg**

Legend similar to that of Figure C.3

**a.** and **d.** Control and mutant mice display similar levels of horizontal and vertical AMPH-induced hyperlocomotion. **b.** The cumulative horizontal activity decreases across trials and is similar in the two groups. **c.** The horizontal activity appears decreased between the first (AMPH1) and the last injection (AMPH5), and is similar in cKO-VGLUT3<sub>5-HT</sub> and controls. **e.** and **f.** Likewise, the cumulative vertical activity remains stable across sessions and does not differ between genotypes (n = 10-10 for AMPH, n = 4-3 for SAL).

Thus cKO-VGLUT3<sub>5-HT</sub> and control littermates respond similarly to an acute injection of AMPH 5 mg/kg.

- Repeated injections of amphetamine 5 mg/kg

We next compared the effects of repeated injections of AMPH 5 mg/kg on cKO-VGLUT3<sub>5-HT</sub> and control siblings. The horizontal activity decreased across trials with no difference between genotypes (Figure C.16b; two-way ANOVA, effect of time,  $F_{4,72} = 3.894$ ,  $p = .006$ , no effect of genotype,  $F_{1,18} = 1.243$ ,  $p = 0.28$ ). Animals injected with saline only displayed a residual locomotion during trials. The vertical activity also decreased across trials, but did not differ between cKO-VGLUT3<sub>5-HT</sub> and their controls (Figure C.16e; two-way ANOVA, effect of time,  $F_{4,68} = 4.961$ ,  $p = .001$ , no effect of genotype,  $F_{1,17} = 0.496$ ,  $p = 0.491$ ), or between treatment (two-way ANOVA between controls injected with saline or amphetamine, no effect of treatment,  $F_{1,11} = 0.814$ ,  $p = 0.386$ ; two-way ANOVA between cKO-VGLUT3<sub>5-HT</sub> injected with saline or amphetamine, no effect of treatment,  $F_{1,10} = 0.894$ ,  $p = 0.367$ ). The temporal course of the horizontal activity for each day of injection is presented in the Appendices section (Figure E.4).

We then compared the first day (AMPH1) to the last day of injection (AMPH5), and found that both horizontal and vertical activity decreased (Figure C.16c: two-way ANOVA, effect of time,  $F_{1,18} = 6.327$ ,  $p = .022$  for horizontal activity; Figure C.16f: two-way ANOVA, effect of time,  $F_{1,16} = 5.971$ ,  $p = .027$  for vertical activity). However, we found no difference between cKO-VGLUT3<sub>5-HT</sub> and control littermates (two-way ANOVA, no effect of genotype,  $F_{1,18} = 1.838$ ,  $p = 0.192$  for horizontal activity; no effect of genotype,  $F_{1,16} = 1.693$ ,  $p = 0.212$  for vertical activity).

In conclusion, cKO-VGLUT3<sub>5-HT</sub> locomotor response is similar to control littermates in response to repeated injections of AMPH 5 mg/kg.

### **1.3.2 Effect on stereotypies**

We also investigated the stereotypic response of cKO-VGLUT3<sub>5-HT</sub> mice during repeated injections of AMPH 5 mg/kg.

- General stereotypies

During each day of injection, cKO-VGLUT3<sub>5-HT</sub> and control littermates displayed similar stereotypy levels (Figure C.17a; two-way ANOVA for each day of injection, no effect of

genotype). The maximal and median stereotypy scores revealed no difference between genotypes (Figure C.17b; two-way ANOVA for the maximal stereotypy score, no effect of genotype,  $F_{1,18} = 0.783$ ,  $p = 0.388$ ; Figure C.17c; two-way ANOVA for the median stereotypy score, no effect of genotype,  $F_{1,18} = 0.147$ ,  $p = 0.706$ ) but the scores increased across trials (two-way ANOVA for the maximal stereotypy score, effect of time  $F_{4,72} = 18.47$ ,  $p < .001$ ; two-way ANOVA for the maximal stereotypy score, effect of time  $F_{4,72} = 19.13$ ,  $p < .001$ ).

The comparison of general stereotypies between AMPH1 and AMPH5 demonstrated a clear sensitization of stereotypies with no difference between genotypes (Figure C.17d; two-way ANOVA, effect of time,  $F_{1,18} = 42.03$ ,  $p < .001$ , no effect of genotype,  $F_{1,18} = 0.134$ ,  $p = 0.719$ ).

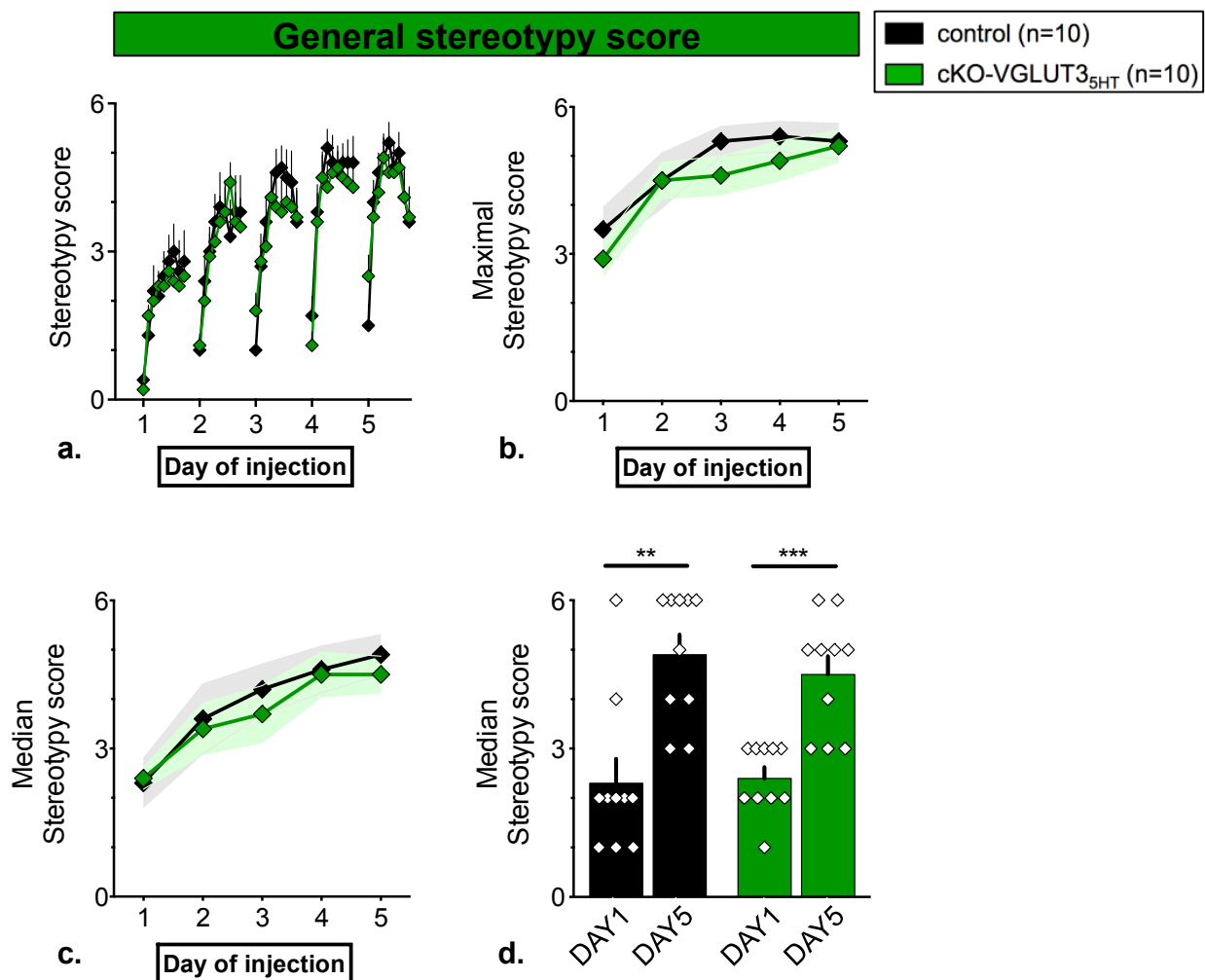


**Figure C.17: cKO-VGLUT3<sub>5-HT</sub> general stereotypies with AMPH 5 mg/kg**

Legend similar to that of Figure C.6

**a.** After each AMPH injection, the level of stereotypies increases and becomes maximal around 35 min post-injection. cKO-VGLUT3<sub>5-HT</sub> display similar stereotypy levels than control littermates. **b.** and **c.** The maximal and mean stereotypy scores of cKO-VGLUT3<sub>5-HT</sub> and control mice do not differ between genotypes. **d.** General stereotypies do sensitize between AMPH1 and AMPH5, but there is no difference between genotypes ( $n = 10-10$ ).

These results show that cKO-VGLUT3<sup>5-HT</sup> and control littermates have a similar stereotypic sensitization.

- Orofacial stereotypies

We then focused on orofacial stereotypies. Likewise, we found no difference between the two genotypes (Figure C.18a; two-way ANOVA for each day of injection, no effect of genotype).

By studying maximal and median orofacial stereotypy scores, we observed an increase of the scores across trials (Figure C.18b, two-way ANOVA for the maximal stereotypy score, effect of time,  $F_{4, 72} = 10.82$ ,  $p < .001$ ; Figure C.18c, two-way ANOVA for the median stereotypy score, effect of time,  $F_{4, 72} = 13.43$ ,  $p < .001$ ), but no significant difference between cKO-VGLUT3<sup>5-HT</sup> and control littermates (two-way ANOVA for the maximal stereotypy score, no effect of genotype,  $F_{1, 18} = 1.105$ ,  $p = 0.307$ ; two-way ANOVA for the median stereotypy score, no effect of genotype,  $F_{1, 18} = 1.633$ ,  $p = 0.437$ ).

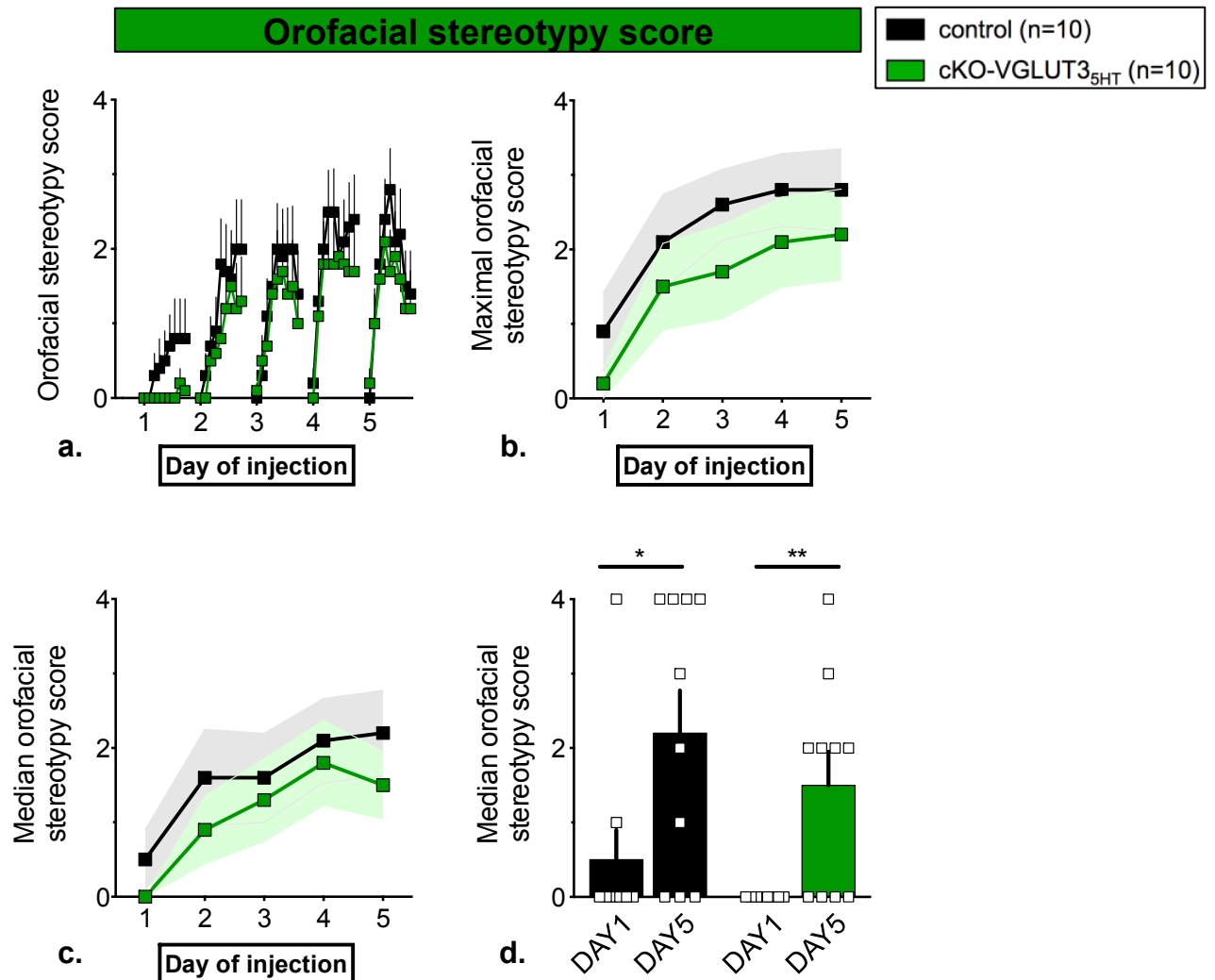


**Figure C.18: cKO-VGLUT3<sub>5-HT</sub> orofacial stereotypies with AMPH 5 mg/kg**

Legend similar to that of Figure C.7

**a.** After each AMPH injection, the level of orofacial stereotypies increases and becomes maximal around 35 min post-injection. cKO-VGLUT3<sub>5-HT</sub> display similar orofacial stereotypy levels than control littermates. **b.** and **c.** The maximal and mean stereotypy scores reveal no difference in the response between cKO-VGLUT3<sub>5-HT</sub> and control mice. **d.** Orofacial stereotypies do sensitize between AMPH1 and AMPH5, but there is no difference between genotypes (n = 10-10).

The comparison between AMPH1 and AMPH5 confirmed that orofacial stereotypies sensitized, with no difference between genotypes (Figure C.18d; two-way ANOVA, effect of time,  $F_{1, 18} = 20.66$ ,  $p < .001$ , no effect of genotype,  $F_{1, 18} = 1.608$ ,  $p = 0.221$ ).

To summarize, deletion of VGLUT3 specifically in 5-HT neurons does not modify acute or chronic effects of amphetamine. Thus, the phenotype we observe in VGLUT3<sup>-/-</sup> does not seem to involve VGLUT3- positive serotonergic fibers.

## **2. The VGLUT3- positive cholinergic drive of the striatum**

We also investigated the role of the VGLUT3- positive cholinergic component in amphetamine-induced phenotypes. Specific deletion of VGLUT3 in CINs was obtained by

crossing ChAT- IRES- Cre and VGLUT3<sup>LoxP/LoxP</sup> mice. We will refer to these double mutants as cKO-VGLUT3<sub>ACh</sub> thereafter.

## 2.1 Anatomical characterization of cKO-VGLUT3<sub>ACh</sub>

The double transgenic line was characterized in our lab in Montreal by IAR (Figure C.19).

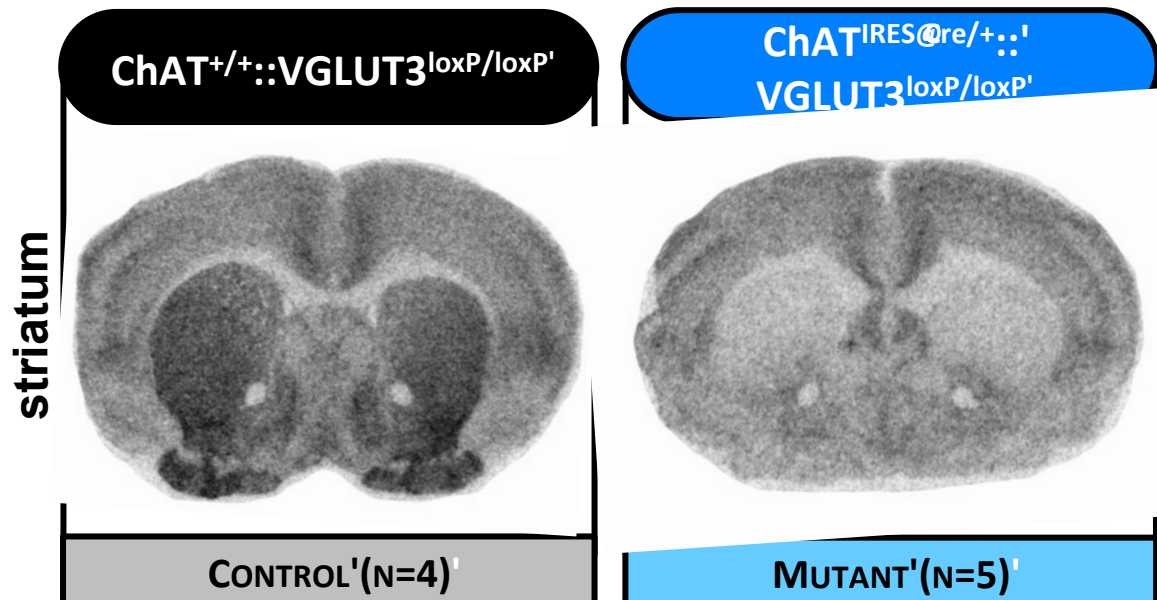


**Figure C.19: Immunohistochemistry for VGLUT3 in cKO-VGLUT3<sub>ACh</sub> mice (n = 5-5)**  
VGLUT3 is almost completely absent in the dorsal striatum of mutant mice, and its level is two-times decreased in the ventral striatum compared to control littermates (n = 4-5).

This experiment revealed a massive loss of VGLUT3 in the striatum of  $\sim 50\%$  in the nucleus accumbens and  $\sim 95\%$  in the dorsal striatum. This is consistent with the fact that all cholinergic interneurons of the striatum coexpress VGLUT3. This result also corresponds to the distribution of cholinergic neurons in the striatum, which are more numerous and have a higher density in the dorsal striatum (Matamales *et al.* 2016).

As shown in Figure C.10, VGLUT3-positive 5-HT fibers are relatively abundant in the Acb and are spared in this mutant. This also raises the question that maybe pure VGLUT3-positive projections may target the Acb.

## 2.2 Behavioral characterization of cKO-VGLUT3<sub>ACh</sub>

We performed a basal characterization of the mice weight, spontaneous locomotion and anxiety levels of cKO-VGLUT3<sub>ACh</sub> mice.

### 2.2.1 Weight

The average weight of cKO-VGLUT3<sub>ACh</sub> was  $25.56 \pm 0.734$  g. Age-related control littermates weight was  $25.19 \pm 0.761$  g (Figure C.20). Therefore the average weight did not differ between mutant and control mice (t test,  $p = 0.733$ ).

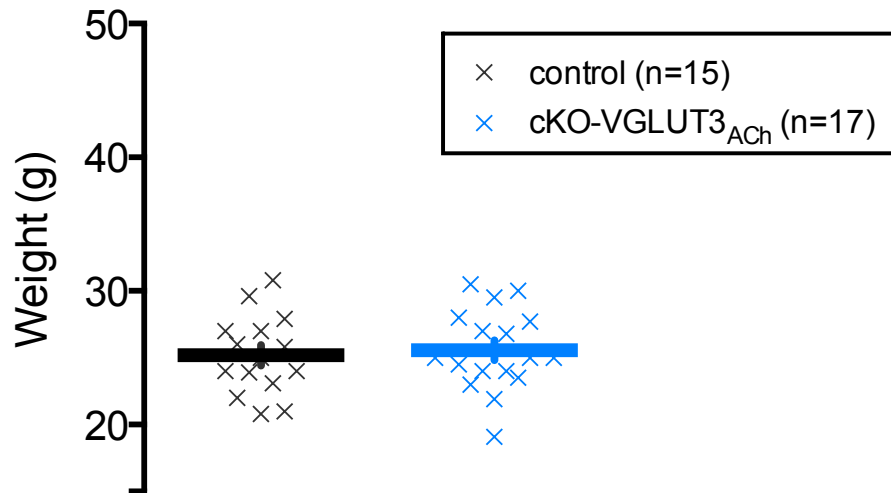


**Figure C.20: cKO-VGLUT3<sub>ACh</sub> mice weight**

cKO-VGLUT3<sub>ACh</sub> and age- matched control littermates have the same weight (n = 15-17).

### 2.2.2 Basal locomotion

We then assessed the spontaneous horizontal and vertical activities. Mice were placed individually in activity boxes at 10:30 a.m. and their locomotion was recorded during 24 h.

The horizontal activity did not significantly differ between cKO-VGLUT3<sub>ACh</sub> mice and control littermates (Figure C.21a; two-way ANOVA, effect of time,  $F_{23, 460} = 11.34$ ,  $p < .001$ , no effect of genotype,  $F_{1, 20} = 0.243$ ,  $p = 0.628$ ). The cumulative locomotion between genotypes during the whole light- off period (active period) and during the light- on period was evaluated (Figure C.21b). The cumulative horizontal activity was similar between genotypes (t test for the light- off period,  $p = 0.534$ , control  $911.3 \pm 138.4$  vs. mutant  $1074 \pm 209.6$  beam breaks; Mann- Whitney for the light- on period,  $p = 0.273$ , control  $310.8 \pm 73.5$  vs. mutant  $444.5 \pm 87.74$  beam breaks).

For the vertical activity, cKO- VGLUT3<sub>ACh</sub> mice had a trend for an greater activity compared to controls (Figure C.21c; two-way ANOVA, effect of time,  $F_{23, 437} = 11.67$ ,  $p < .001$ , no effect of genotype,  $F_{1, 19} = 1.195$ ,  $p = 0.288$ ). By separating the cumulative activity in light- on/off components, we found a strong tendency visible at night (Figure C.21d; Mann- Whitney for the light- off period,  $p = .098$ , control  $752.1 \pm 148.4$  vs. mutant  $1080 \pm 184.5$  beam breaks; Mann- Whitney for the light- on period,  $p = 0.575$ , control  $373.5 \pm 76.29$  vs. mutant  $387.6 \pm 76.48$  beam breaks).

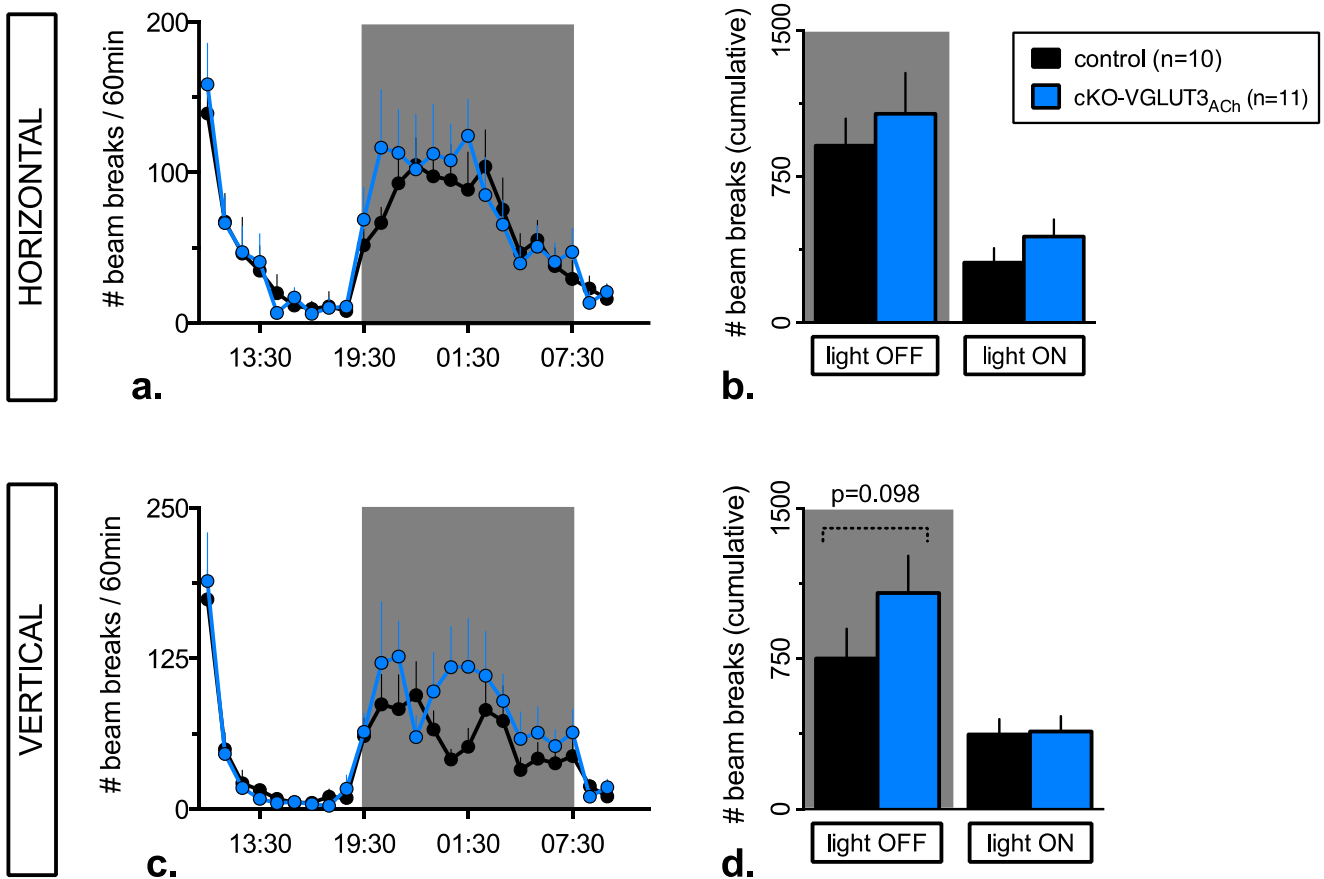


**Figure C.21: cKO-VGLUT3<sub>ACh</sub> circadian locomotor activity**

**Top panel: horizontal activity**

**a.** The temporal course of the horizontal activity during 24 hours shows that cKO-VGLUT3<sub>ACh</sub> (*in blue*) and control siblings (*in black*) have a similar basal locomotion. The light- off period is represented by the *grey rectangle* (7:30 p.m.-7:30 a.m.). **b.** The cumulative locomotion during the light- off and the light- on phases does not differ between control and mutant mice.

**Bottom panel: vertical activity**

**a.** The temporal course of the vertical activity shows that cKO-VGLUT3<sub>ACh</sub> have a trend for more rearings during the night. **b.** The cumulative locomotion during the light- off confirms a strong tendency for an increased vertical activity of cKO-VGLUT3<sub>ACh</sub> mice during the light- off phase but no difference when lights are- on (n = 10-11).

These results indicate that the invalidation of VGLUT3 in the cholinergic neurons only has very limited effects.

**2.2.3 Anxiety tests**

We then assessed anxiety levels of cKO-VGLUT3<sub>ACh</sub> mice with the open field and O maze as described before, over 10 min sessions.

- Open field

We tracked the time and distance that mice spent in the anxiogenic central zone of the open field. We found that cKO-VGLUT3<sub>ACh</sub> mice had a non- significant tendency to spend less time in the central zone (Figure C.22a; Mann- Whitney, p = 0.184, control

25.70 ± 4.745 s vs. mutant 15.35 ± 5.619 s). This corresponded to a 4.283 ± 0.791 % of time spent in the central zone for control mice and 2.558 ± 0.937 % for mutant mice.

There was no difference in the distance travelled in the central zone between genotypes (Figure C.22b; t test,  $p = 0.379$ , control 181.7 ± 30.98 cm vs. mutant 137.5 ± 38.71 cm).

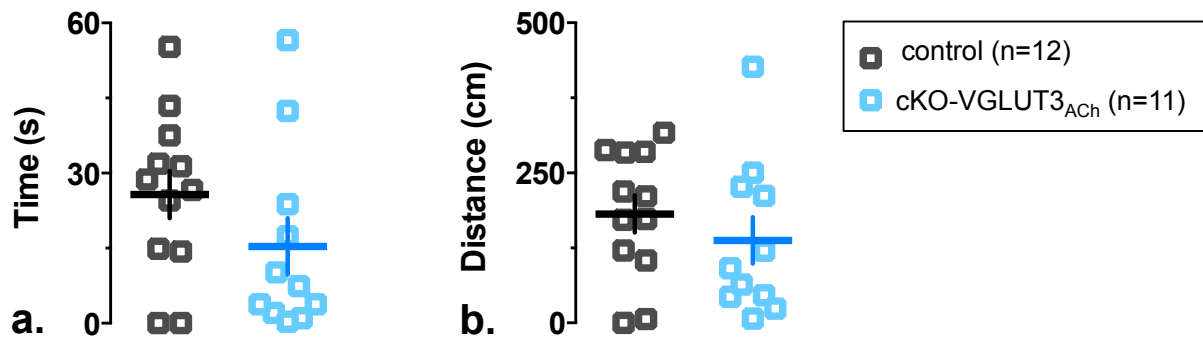


**Figure C.22: cKO-VGLUT3<sub>ACh</sub> anxiety levels in the open field test**

cKO-VGLUT3<sub>ACh</sub> have a non-significant trend towards less time and travel spent in the anxiogenic zone of the open field compared to control siblings ( $n = 12-11$ ).

- O maze

We then assessed the anxiety level in the O maze test. We found that cKO-VGLUT3<sub>ACh</sub> mice had a tendency to spend less time in the anxiogenic open arms compared to control littermates (Figure C.23a; t test,  $p = 0.334$ , control 139.7 ± 17.47 s and mutant 114 ± 19.21 s). cKO-VGLUT3<sub>ACh</sub> mice spent 19 ± 3.2 % of time in the open arms, while control siblings spent 23.28 ± 2.911 %. There was no difference in the distance travelled in the open arms (Figure C.23b; t test,  $p = 0.968$ , control 442 ± 55.72 cm and mutant 446.6 ± 102.8 cm).

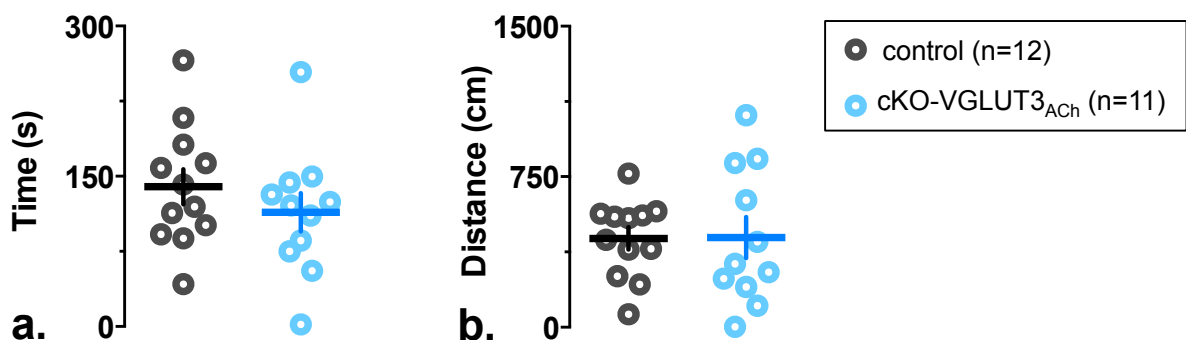


**Figure C.23: cKO-VGLUT3<sub>ACh</sub> anxiety levels in the O maze test**

cKO-VGLUT3<sub>ACh</sub> spend as much time and travel as much as control littermates in the anxiogenic zone of the O maze ( $n = 12-11$ ).

As a summary, cKO-VGLUT3<sub>ACh</sub> mice do not display a strong anxiety-related phenotype.

## 2.2.4 Spontaneous locomotion before sensitization

To assess the ability of cKO-VGLUT3<sub>ACh</sub> mice to adapt to a new environment, we analyzed the 2 h- period of habituation during the 3 first days of the sensitization protocol.

As for cKO-VGLUT3<sub>5-HT</sub> mice, we found no difference in the ability of cKO-VGLUT3<sub>ACh</sub> mice to adapt to the activity box compared to control siblings (two-way ANOVA, no interaction time x genotype for horizontal or vertical activities).

We also compared the horizontal and vertical activity between genotypes, and again, found no effect of genotype (Figure C.24, left panel: two-way ANOVA for the horizontal activity, effect of time,  $F_{2, 58} = 27.07$ ,  $p < .001$ , no effect of genotype,  $F_{1, 29} = 3,356e-5$ ,  $p = .995$ ; Figure C.24, right panel: two-way ANOVA for the vertical activity, effect of time,  $F_{2, 56} = 27.05$ ,  $p < .001$ , no effect of genotype,  $F_{1, 28} = 0.242$ ,  $p = .627$ ).

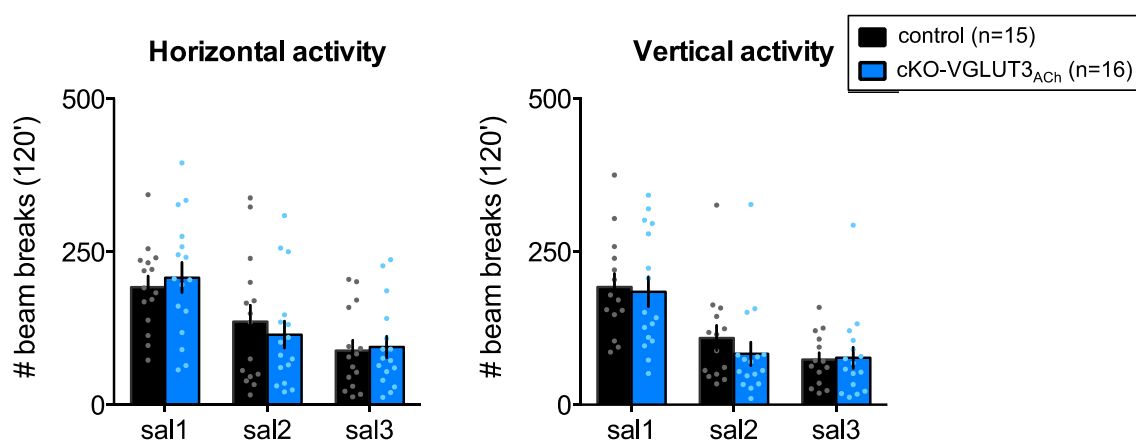


**Figure C.24: cKO-VGLUT3<sub>ACh</sub> spontaneous activity**

cKO-VGLUT3<sub>ACh</sub> and control littermates have the same levels of horizontal and vertical activity, and habituate to their new environment similarly (n = 15-16).

To summarize, we found that cKO-VGLUT3<sub>ACh</sub> and control littermates have the same levels of locomotion in a new environment during a short period of the light- on period, and they habituate the same way to this environment.

## 2.3 cKO-VGLUT3<sub>ACh</sub> and amphetamine 5 mg/kg

### 2.3.1 Effect on locomotion

Because of the critical role of CINs in the DA / ACh striatal balance, we explored with much care the effects of CIN- specific VGLUT3 loss in the response to amphetamine. We performed a behavioral sensitization to AMPH 5 mg/kg.

- Acute injection of amphetamine 5 mg/kg

The injection of AMPH 5 mg/kg produced a strong horizontal hyperlocomotion compared to the last injection of saline in both groups (two-way ANOVA between SAL3 and AMPH1, effect of time,  $F_{1, 21} = 122.7$ ,  $p < .001$ , no effect of genotype,  $F_{1, 21} = 2.16$ ,  $p = 0.156$ ). This activity culminated around 30 min post-injection and slowly decayed (Figure C.25a). cKO-VGLUT3<sup>ACh</sup> mice had a greater horizontal locomotor response than control littermates, but this effect did not reach statistical difference (Figure C.25a, inset: unpaired t test for AUCs,  $p = 0.16$ , control  $881.3 \pm 116.4$  and mutant  $1139 \pm 133.7$ ). We also found a strong vertical activity compared to the last saline injection (two-way ANOVA between saline 3 and AMPH1, effect of time,  $F_{1, 20} = 25.48$ ,  $p < .001$ , no effect of genotype,  $F_{1, 20} = 2.505$ ,  $p = 0.129$ ), which slowly rose starting the injection of AMPH 5 mg/kg (Figure C.25d). As for the horizontal activity, cKO-VGLUT3<sup>ACh</sup> mice showed a greater vertical locomotion than control siblings, but this effect did not reach statistical difference (Figure C.25d, inset: unpaired t test with Welch's correction for AUCs,  $p = 0.117$ , control  $48.91 \pm 9.8$  and mutant  $95.23 \pm 25.78$  beam breaks).

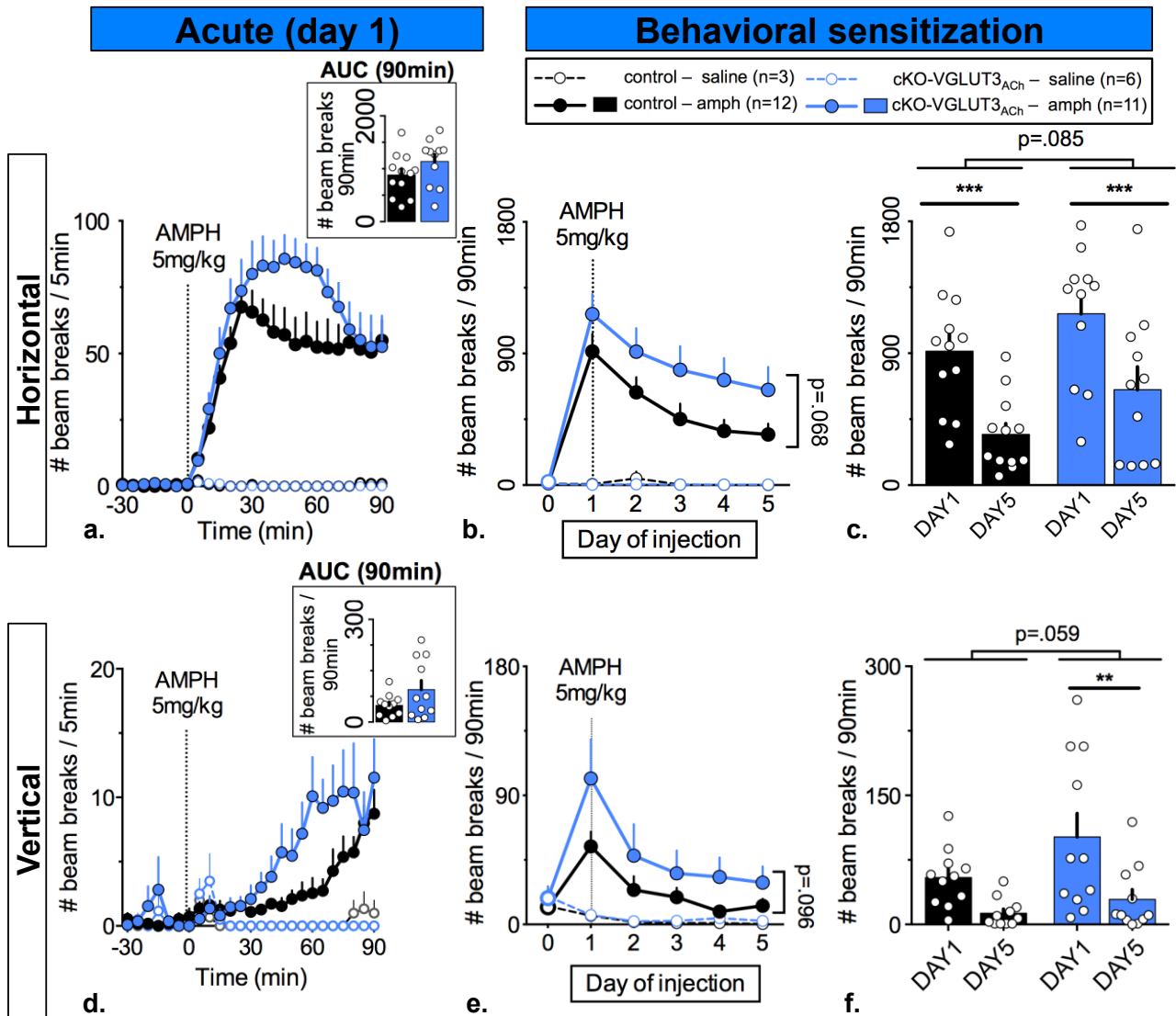


**Figure C.25: cKO-VGLUT3<sub>ACh</sub> locomotor sensitization to AMPH 5 mg/kg**

Legend similar to that of Figure C.3

**a.** and **d.** cKO-VGLUT3<sub>ACh</sub> mice present a non-significant increase of horizontal and vertical AMPH-induced hyperlocomotions compared to control littermates. **b.** The cumulative horizontal activity decreases across trials and cKO-VGLUT3<sub>ACh</sub> display a trend for higher horizontal activity. **c.** The horizontal activity appears decreased between the first (AMPH1) and the last injection (AMPH5), and is lower in cKO-VGLUT3<sub>ACh</sub>. **e.** Likewise, the cumulative vertical decreases across sessions and cKO-VGLUT3<sub>ACh</sub> mice display a trend for increased vertical activity. **f.** The vertical activity appears decreased between the first (AMPH1) and the last injection (AMPH5), and is lower in cKO-VGLUT3<sub>ACh</sub> (n = 12-11 for AMPH, n = 3-6 for SAL).

- Repeated injections of amphetamine 5 mg/kg

We then studied the effects of repeated injections of AMPH 5 mg/kg on locomotion. We found that both horizontal and vertical activities decreased across sessions (Figure C.25b; two-way ANOVA for horizontal activity, effect of time,  $F_{4,84} = 23.68$ ,  $p < .001$ ; Figure C.25e; two-way ANOVA for vertical activity, effect of time,  $F_{4,80} = 9.333$ ,  $p < .001$ ). AMPH-injected cKO-VGLUT3<sub>ACh</sub> mice showed a trend toward enhanced horizontal and vertical locomotor responses. However, this increase failed to

reach statistical significance (two-way ANOVA for horizontal activity, no effect of genotype,  $F_{1,21} = 3.678$ ,  $p = .068$ ; two-way ANOVA for vertical activity, no effect of genotype,  $F_{1,20} = 3.043$ ,  $p = .096$ ). The temporal course of the horizontal activity for each day of injection is presented in the Appendices section (Figure E.5).

We also compared the first to the last injection of AMPH 5 mg/kg, and confirmed that the horizontal activity decreased, with a trend for a greater locomotion in cKO-VGLUT3<sub>ACh</sub> compared to control littermates (Figure C.25c; two-way ANOVA, effect of time,  $F_{1,21} = 44.07$ ,  $p < .001$ , no effect of genotype,  $F_{1,21} = 3.275$ ,  $p = .085$ ). Similarly, the vertical activity decreased between AMPH1 and AMPH5, with a tendency for greater activation in cKO-VGLUT3<sub>ACh</sub> mice (Figure C.25f; two-way ANOVA, effect of time,  $F_{1,20} = 13.06$ ,  $p = .002$ , no effect of genotype,  $F_{1,20} = 4.013$ ,  $p = .059$ ).

Together, these results demonstrate that cKO-VGLUT3<sub>ACh</sub> mice develop a trend toward greater locomotor responses that does not reach statistical significance. However, this hyperactivity is far from the levels observed with VGLUT3<sup>-/-</sup> mice.

### 2.3.2 Effect on stereotypies

We then focused on the effects of AMPH 5 mg/kg on stereotypies.

- General stereotypies

We first assessed general stereotypies. We observed that cKO-VGLUT3<sub>ACh</sub> mice presented a trend for less general stereotypies than control siblings (Figure C.26a; two-way ANOVA for the daily temporal courses, effect of genotype: day 1,  $F_{1,21} = 5.528$ ,  $p = .029$ ; day 2,  $F_{1,21} = 2.323$ ,  $p = 0.142$ ; day 3,  $F_{1,21} = 1.605$ ,  $p = 0.219$ ; day 4,  $F_{1,21} = 1.866$ ,  $p = 0.186$ ; day 5,  $F_{1,21} = 0.735$ ,  $p = 0.401$ ).

We also studied the daily maximal stereotypy score. We found that this score increased across sessions, and that cKO-VGLUT3<sub>ACh</sub> mice had lower levels of stereotypies than control littermates (Figure C.26b; two-way ANOVA, effect of time,  $F_{4,84} = 25.51$ ,  $p < .001$ , effect of genotype,  $F_{1,21} = 4.465$ ,  $p = .047$ ). We also compared the daily median stereotypy scores. We found an increase of the median scores across sessions, and non-statistically significant decreased levels of general stereotypies in cKO-VGLUT3<sub>ACh</sub> mice (Figure C.26c; two-way ANOVA, effect of time,  $F_{4,84} = 21.41$ ,  $p < .001$ , effect of genotype,  $F_{1,21} = 3.887$ ,  $p = .062$ ).

Finally, we compared the median stereotypy scores between AMPH1 and AMPH5 (Figure C.26d). We confirmed a stereotypic sensitization (two-way ANOVA, effect of time,  $F_{1,21} = 50.67$ ,  $p < .001$ ) and a significant decrease of stereotypies in cKO-VGLUT3<sub>ACh</sub> mice (effect of genotype,  $F_{1,21} = 4.797$ ,  $p = .04$ ).

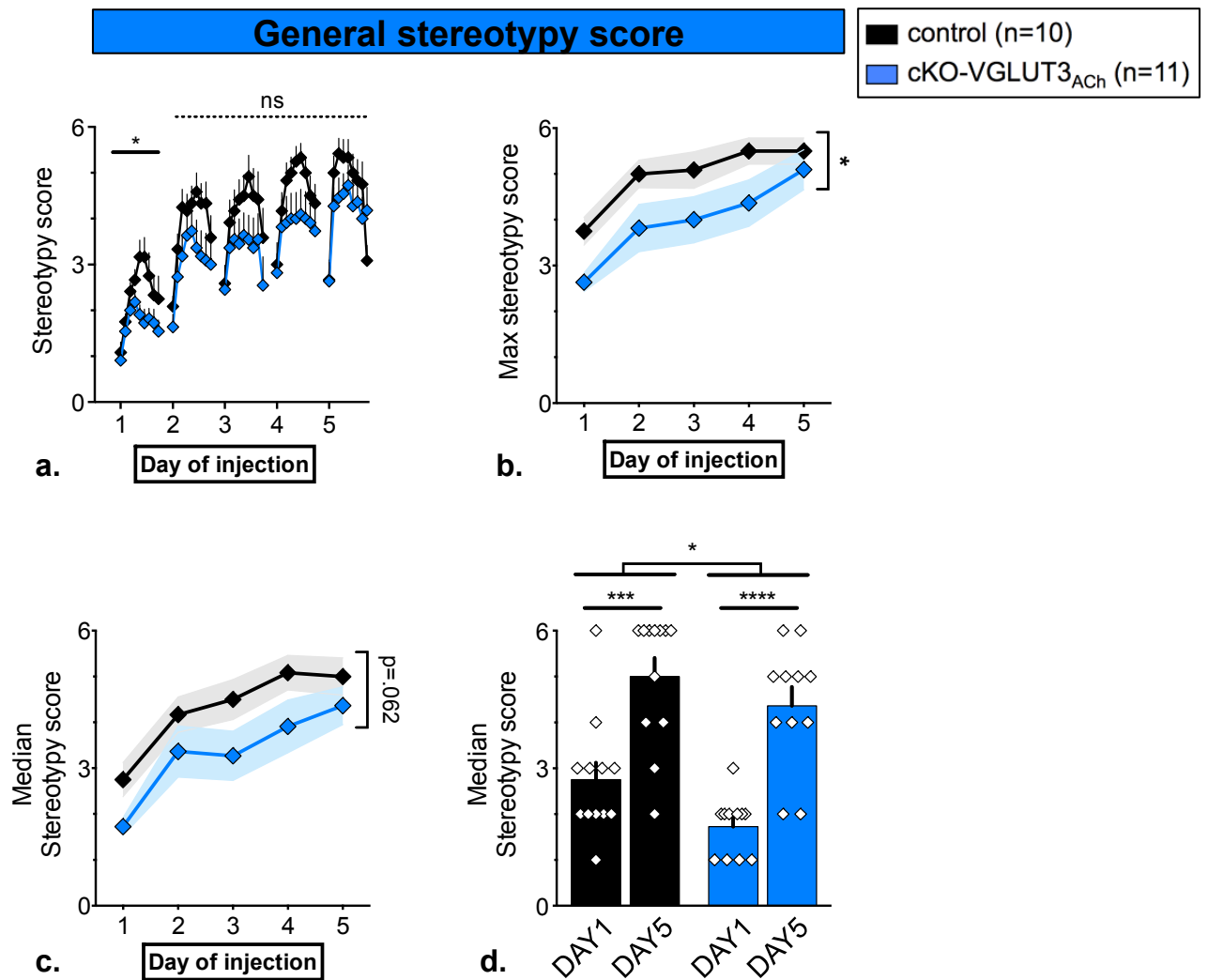


**Figure C.26: cKO-VGLUT3<sub>ACh</sub> general stereotypies with AMPH 5 mg/kg**

Legend similar to that of Figure C.6

**a.** After each AMPH injection, the level of stereotypies increases and becomes maximal around 35 min post-injection. cKO-VGLUT3<sub>ACh</sub> mice systematically have a tendency for decreased stereotypy levels compared to control littermates. **b.** and **c.** The maximal and mean stereotypy scores reveal that cKO-VGLUT3<sub>ACh</sub> mice have lower levels of stereotypies compared to control siblings. **d.** General stereotypies do sensitize between AMPH1 and AMPH5, and cKO-VGLUT3<sub>ACh</sub> stereotypies are lowered compared to control mice (n = 10-11).

- Orofacial stereotypies

We then focused on orofacial stereotypies. The daily temporal course revealed no difference between cKO-VGLUT3<sub>ACh</sub> mice and control siblings (Figure C.27a; two-way ANOVA for the daily temporal courses, effect of genotype: day 1,  $F_{1,21} = 2.193$ ,  $p = 0.154$ ; day 2,  $F_{1,21} = 0.435$ ,  $p = 0.517$ ; day 3,  $F_{1,21} = 0.952$ ,  $p = 0.34$ ; day 4,  $F_{1,21} = 1.017$ ,  $p = 0.325$ ; day 5,  $F_{1,21} = 0.736$ ,  $p = 0.401$ ).

The daily maximal orofacial stereotypy score increased across trials with a trend for lower levels in cKO-VGLUT3<sub>ACh</sub> mice compared to controls (Figure C.27b; two-way ANOVA, effect of time,  $F_{4,84} = 21.7$ ,  $p < .001$ , no effect of genotype,  $F_{1,21} = 2.434$ ,

$p = 0.134$ ). With the daily median stereotypy score, we also observed an increase across sessions. No significant difference was found between the two genotypes (Figure C.27c; two-way ANOVA, effect of time,  $F_{4, 84} = 13.75$ ,  $p < .001$ , no effect of genotype,  $F_{1, 21} = 1.385$ ,  $p = 0.253$ ).

In order to estimate the overall effect of the treatment on median orofacial stereotypy scores, we compared the response at AMPH1 and AMPH5 (Figure C.27d). We found that orofacial stereotypies sensitized to a similar extent between genotypes (two-way ANOVA, effect of time,  $F_{1, 21} = 22.73$ ,  $p < .001$ , no effect of genotype,  $F_{1, 21} = 1.233$ ,  $p = 0.28$ ).

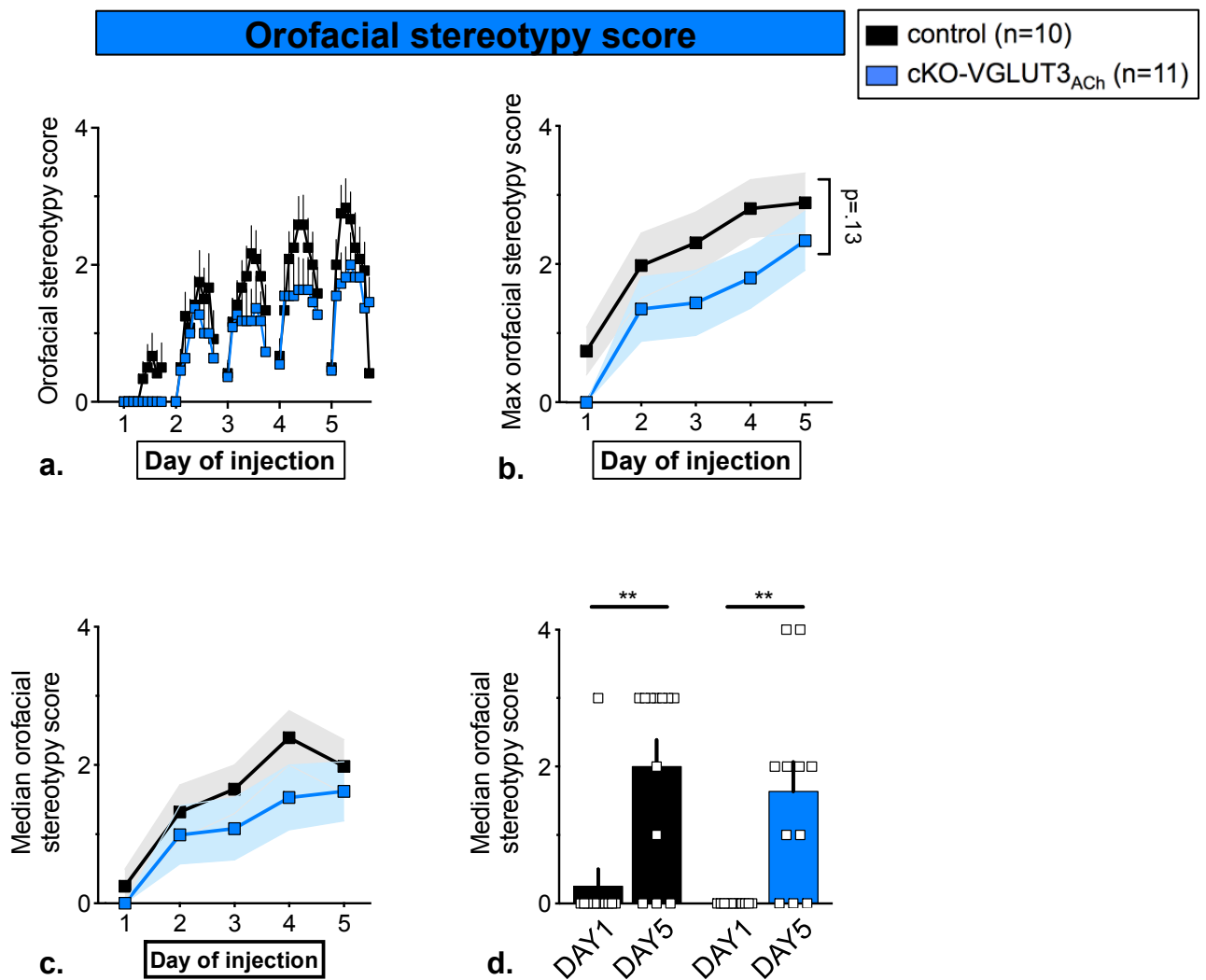


**Figure C.27: cKO-VGLUT3<sub>ACh</sub> orofacial stereotypies with AMPH 5 mg/kg**

Legend similar to that of Figure C.7

**a.** After each AMPH injection, the level of orofacial stereotypies increases and becomes maximal around 35 min post-injection. cKO-VGLUT3<sub>ACh</sub> mice have a tendency for decreased orofacial stereotypy levels compared to control littermates. **b.** and **c.** The maximal and mean stereotypy scores reveal a trend for decreased orofacial stereotypies for cKO-VGLUT3<sub>ACh</sub> compared to control mice. **d.** Orofacial stereotypies do sensitize between AMPH1 and AMPH5, but there is no difference between genotypes (n = 10-11).

In summary, cKO-VGLUT3<sub>ACh</sub> mice show trends for higher levels of locomotion and lower levels of general stereotypies compared to control littermates. The orofacial stereotypies are only slightly impacted.

The major finding of this part of our work is that deletion of VGLUT3 in CINs does not phenocopy results obtained with the constitutive knockouts.

## 2.4 cKO-VGLUT3<sub>ACh</sub> and cocaine 10 mg/kg

Cocaine and amphetamine have different modes of action. Thus, we assessed the effect of cocaine 10 mg/kg on cKO-VGLUT3<sub>ACh</sub> mice. Diana Sakae performed this pilot experiment in our team in Montreal (Figure C.28b).

The acute injection of COC 10 mg/kg produced the same hyperlocomotion in cKO-VGLUT3<sub>ACh</sub> and control mice (Figure C.28b; Mann-Whitney for AUC during the 90 min post-injection,  $p = 0.429$ , control  $966.9 \pm 350.8$  and mutant  $1179 \pm 270.9$  cm). Usually, an acute injection of COC 10 mg/kg would produce a sharp hyperlocomotion: rise right after the injection, maximal effect 5-10 min after the injection, and rapid wash-out to become almost null 30-45 min post-injection. In our pilot experiment, both cKO-VGLUT3<sub>ACh</sub> and control mice had a COC-induced hyperlocomotion different from the classical profile.

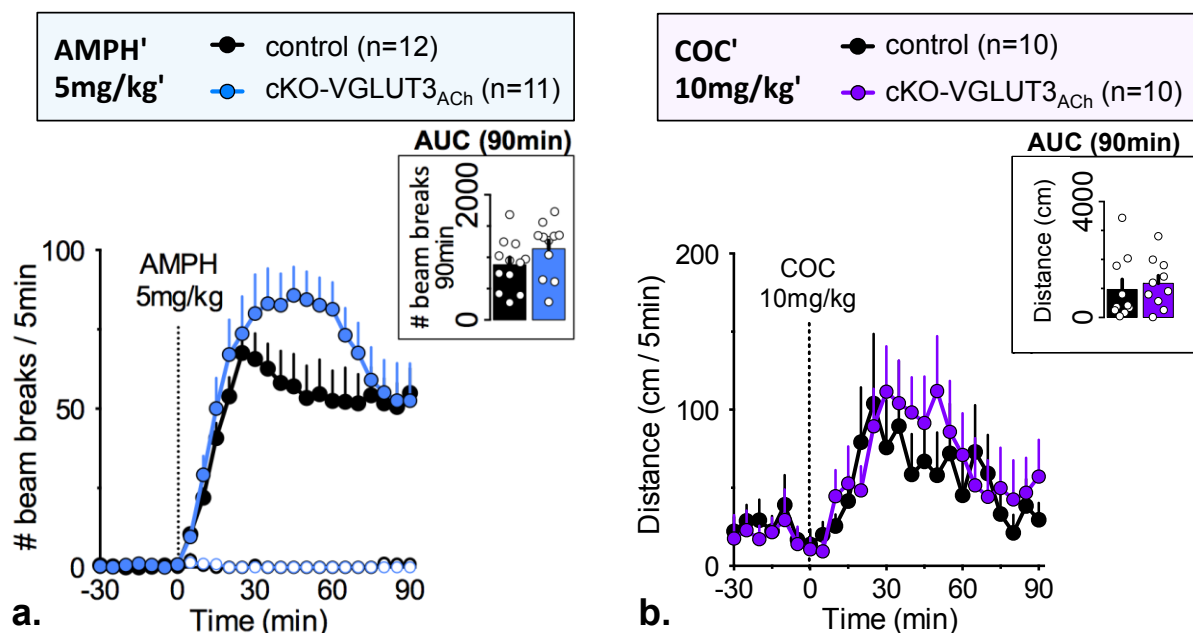


**Figure C.28: cKO-VGLUT3<sub>ACh</sub> locomotor response to acute AMPH 5 mg/kg or COC 10 mg/kg**

**a.** cKO-VGLUT3<sub>ACh</sub> mice have a slightly higher hyperlocomotion in response to amphetamine 5 mg/kg compared to controls. **b.** In response to an acute injection of cocaine 10 mg/kg, cKO-VGLUT3<sub>ACh</sub> and control mice respond similarly ( $n = 12-11$  for AMPH,  $n = 10-10$  for COC).

For both the acute injection of cocaine (Figure C.28b) and amphetamine (Figure C.28a), cKO-VGLUT3<sub>ACh</sub> mice response is very different from VGLUT3<sup>-/-</sup>, which

display a locomotor activation twice as big as their control siblings (Sakae *et al.* (2015) and Figure C.5).

### 3. Discussion

At least two sources of VGLUT3 are involved in the striatal circuitry (Figure C.29). The major source is local and provided by CINs that all express VGLUT3 along with VACHT (Gras *et al.* 2002, Schafer *et al.* 2002, Herzog *et al.* 2004, Gras *et al.* 2008). The distal source of VGLUT3 stems from the serotonergic projections, which do partly co-express SERT, and preferentially innervate the ventral striatum (Vertes 1991, Gras *et al.* 2002, Gagnon *et al.* 2014, Sakae *et al.* 2015, Voisin *et al.* 2016).

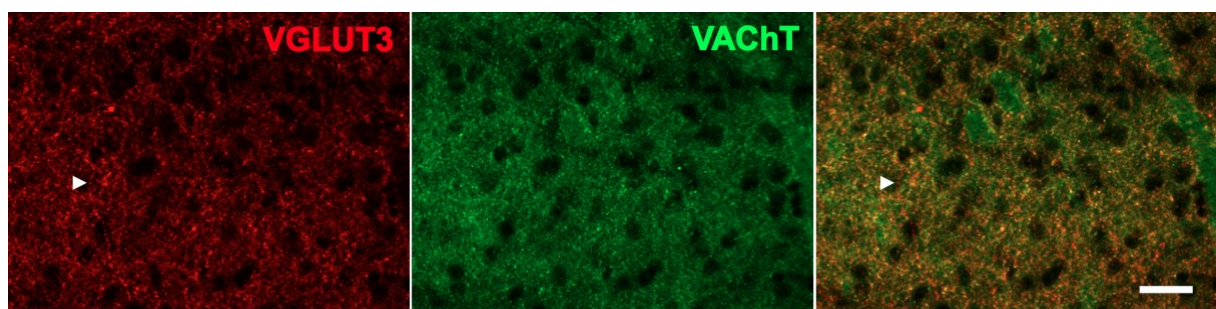


**Figure C.29: VGLUT3 striatal expression in cholinergic interneurons and 5-HT fibers**

VGLUT3 (*in red*) is co-expressed with VACHT (*in green*) in the cholinergic interneurons of the striatum. A minor source of VGLUT3 comes from the dorsal raphe serotonergic projections (one putative 5-HT fiber is indicated by the *white arrowhead*). *Scale bar = 100  $\mu$ m.*

In VGLUT3<sup>-/-</sup> mice, we previously reported a marked increase of cocaine effect on locomotor activity (Gras *et al.* 2008, Sakae *et al.* 2015). Here we show that amphetamine as well dramatically increases locomotor activity of VGLUT3-null mice. In addition we report for the first time that VGLUT3<sup>-/-</sup> mice are more resistant to amphetamine-induced stereotypies. In this part of my PhD project, I tried to dissect the contribution of each of the two sources of VGLUT3-positive fibers in the striatum. The acute and chronic effect of amphetamine were analyzed in mice lacking VGLUT3 in either 5-HT (cKO-VGLUT3<sub>5-HT</sub>) or ACh (cKO-VGLUT3<sub>ACh</sub>) striatal fibers. Surprisingly, none of the two specific conditional knockouts phenocopied the constitutive knockout.

- The VGLUT3-positive serotonergic system is not involved in AMPH-induced behaviors

Serotonin is a key regulator of mood and anxiety. One of the major anxiolytic / antidepressant treatments consist in increasing extracellular levels of serotonin by inhibiting 5-HT reuptake (SSRI) to counterbalance its decreased levels found in these disorders (Renoir *et al.* 2012)

In the **anxiety tests**, cKO-VGLUT3<sub>5-HT</sub> mice displayed similar anxiety levels than controls. This result is quite surprising, since VGLUT3 null mice display robust anxiety-like phenotypes (Amilhon *et al.* 2010). Amilhon *et al.* proposed that VGLUT3 null mice would display higher levels of anxiety because of a decreased serotonergic tone as a result of the loss of vesicular synergy (Amilhon *et al.* 2010). Thus, it was expected that mice lacking VGLUT3 in the serotonergic system would present increased anxiety behaviors. However, that was not the case.

One explanation for the anxiety levels found in VGLUT3<sup>-/-</sup> mice is a regulation by VGLUT3- positive GABAergic interneurons. Indeed, GABA is involved in anxiety, and benzodiazepines, which are GABA<sub>A</sub> receptor agonists, are widely used as anxiolytics (Tallman *et al.* 1980). Another explanation is that purely glutamatergic VGLUT3- positive neurons from raphe nuclei are responsible for the enhanced anxiety observed in VGLUT3 null mice. The purely VGLUT3- positive neuronal population of the brainstem have not been characterized yet, but our laboratory is currently developing approaches based on a VGLUT3- Cre expressing line.

After the basal characterization of the line, we studied the **effects of AMPH 5 mg/kg on cKO-VGLUT3<sub>5-HT</sub> mice**. We found no difference in terms of locomotion and stereotypy neither during the acute nor the following repeated injections of amphetamine. Therefore a straightforward interpretation of this negative finding would be that the VGLUT3- positive serotonergic system is not involved in the effects of amphetamine. Since amphetamine hyperlocomotor and sensitizing effects require functional 5- HT<sub>2A</sub>R (Salomon *et al.* 2006), we could have expected a difference in the response of cKO- VGLUT3<sub>5-HT</sub> mice since they have a decreased serotonergic tone (Amilhon *et al.* 2010). However, that was not the case, probably because the AMPH masks this depression by inhibiting SERT.

- **The VGLUT3- positive cholinergic system contributes to AMPH- induced behaviors**

To understand the role of the glutamate released by CINs, we produced VGLUT3 conditional knock- outs in cholinergic neurons. Two cerebral structures contain mixed VAcH/VGLUT3 populations: CINs of the striatum, and basal forebrain, a structure that provides the main cholinergic innervation of the cerebral cortex. In the basal forebrain, VGLUT3 is expressed by a population of cholinergic neurons - mainly from the ventral pallidum and the *nucleus basalis* of Meynert - that project to the basolateral amygdala (BLA; Nickerson Poulin *et al.* (2006)). Because of the central involvement of BLA in the encoding of emotions, in particular the aversive memory, our team recently explored cKO-VGLUT3<sub>ACh</sub> mice response in fear conditioning, but found no difference in the elementary and contextual memories, along with similar extinction levels compared to controls (Nida Chabbah, unpublished data).

VGLUT3 null mice have a basal hyperlocomotion, which can be rescued by the systemic administration of donepezil, an AChE inhibitor (Gras *et al.* 2008, Divito *et al.* 2015). Additionally, CIN ablation yields same levels of hyperlocomotion (Kitabatake *et al.* 2003), but specific removal of VAcHT and thus of ACh from CINs does not affect locomotion (Guzman *et al.* 2011). This suggests that the hyperlocomotor phenotype is imputable to the glutamate released by CINs.

For the basal locomotion of cKO-VGLUT3<sub>ACh</sub> mice, we found a slight hyperlocomotion during the dark phase. These experiments were also conducted in our team in Montreal, and they found a significant hyperlocomotion at night (+ ~ 20%). These data provide additional evidence that VGLUT3 in CINs is responsible for the basal locomotor activity modulation.

Numerous studies place CINs as key modulators of striatal DAergic transmission. The acute injection of AMPH 5 mg/kg resulted in a slightly higher AMPH-induced hyperlocomotion in cKO-VGLUT3<sub>ACh</sub> mice, suggesting that glutamate released by CINs may play a role in the response to AMPH. However, this AMPH-induced hyperlocomotion was dramatically smaller (+ 30%) than the one observed in VGLUT3<sup>-/-</sup> mice (+ 125%). Preliminary results with COC 10 mg/kg comforted this observation. These results cripple the proposed mechanism to explain VGLUT3<sup>-/-</sup> hyperlocomotion by Sakae *et al.* (2015), according to which the hyperlocomotion is imputable to the loss of a presynaptic CIN-originating glutamatergic break on DAergic transmission. Further studies need to be conducted to solve this discrepancy.

We also explored the AMPH-induced stereotypies with repeated injections of AMPH 5 mg/kg. We found that mice lacking VGLUT3 in the cholinergic system present less stereotypies than control littermates. This result strongly suggests that the stereotypic resistance found in VGLUT3 null mice is at least partly due to the VGLUT3-positive cholinergic fibers in the striatum. This result is in line with the observations of Gangarossa *et al.* (2016) and Divito *et al.* (2015), where LID was explored. Both studies reported that LID is attenuated in VGLUT3<sup>-/-</sup> mice.

Gangarossa *et al.* studied LID in mice lacking VAcHT in CINs (Drd2- Cre::VAcHT<sup>LoxP/LoxP</sup>). They found that these mice have normal or enhanced level of abnormal movements. Reciprocally, Divito *et al.* found that mice lacking VGLUT3 in the cholinergic neurons (ChAT- IRES- Cre::VGLUT3<sup>LoxP/LoxP</sup>) present less LID.

Together, these results strongly support the idea that glutamate released by CINs participate in the abnormal movements observed with repeated injections of drugs or L- DOPA in DA-depleted animals. It has been previously demonstrated that CINs do

participate to LID, since their selective ablation or silencing relieve the dyskinesia severity (Ding *et al.* 2011, Won *et al.* 2014).

To further support this idea, evoked DA striatal levels of mice lacking either VGLUT3 (cKO-VGLUT3<sub>ACh</sub>) or VACHT (cKO-VACHT<sub>ACh</sub>) in the cholinergic interneurons were assessed in our team in Montreal (Mathieu Favier, unpublished data). This experiment indicated that DA levels are not homogenous in the different striatal subregions of cKO-VGLUT3<sub>ACh</sub> or cKO-VACHT<sub>ACh</sub> mice (Figure C.30). DA release is increased in the DMS of cKO-VGLUT3<sub>ACh</sub> (+ 40 %). In contrast, DA release is decreased in the DMS (- 40 %) and in the Acb (- 50 %) of cKO-VACHT<sub>ACh</sub> mice. Interestingly, DA release is not affected in the DLS by deletion of VACHT or VGLUT3. The DA level in the Acb of mice lacking VGLUT3 has not been assessed yet, but we predict that it should mirror the level found in mice lacking VACHT (+ 50 %). The levels of K<sup>+</sup>-evoked DA release are consistent with the fact that ACh stimulates DA release (Cachope *et al.* 2012, Threlfell *et al.* 2012), and that CINs are more active in the DLS and less active in the vStr (Matamales *et al.* 2016).

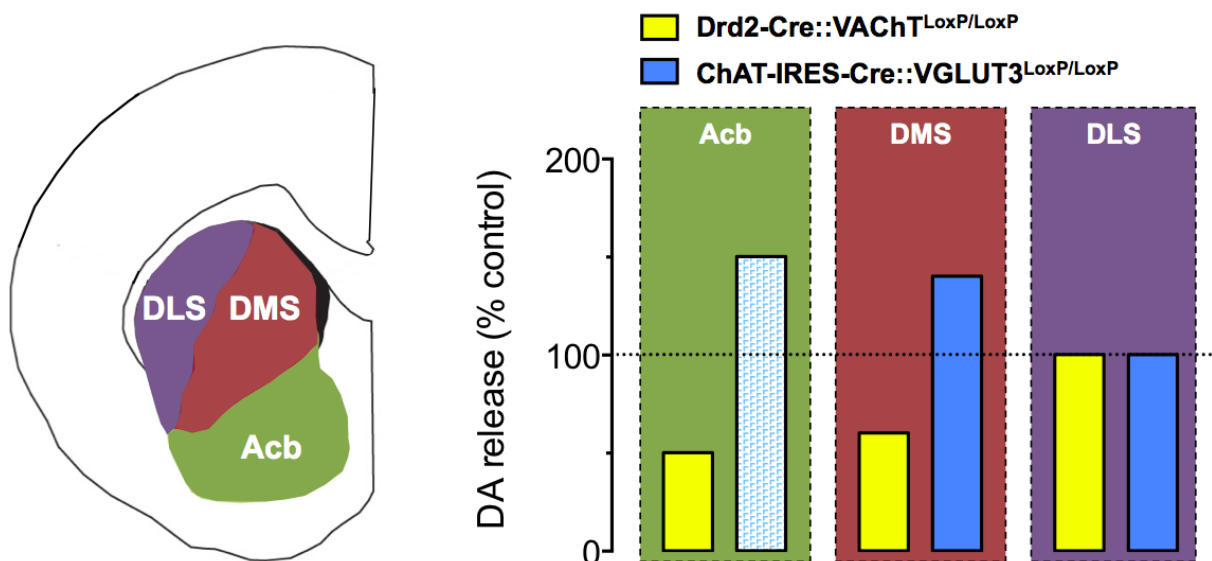


**Figure C.30: Striatal evoked dopamine levels in mice lacking VGLUT3 or VACHT in CINs**

**Left panel:** The nucleus accumbens (Acb), dorsomedial (DMS) and dorsolateral striatum (DLS) are three subregions of the striatum mediating different phases of drug dependence (see Figure C.9). **Right panel:** Mice lacking VGLUT3 in the cholinergic system (*in blue*) have increased level of DA in the DMS and putatively in the Acb (*dotted blue bar*). Mice lacking VACHT in the CINs (*in yellow*) display decreased evoked DA release in the Acb and DMS. None of the mice have alteration of DA levels in the DLS.

Adapted from data kindly provided by Mathieu Favier

The proposed mechanism of competition between locomotion and stereotypies is consistent with data obtained with cKO-VGLUT3<sub>ACh</sub>. Because they have higher levels of DA in the Acb, AMPH preferentially stimulates locomotion rather than stereotypies. Thus, it can be inferred that mice lacking VACHT in CINs should have a hypoactive vStr

compared to the dStr. Consequently AMPH should produce more intense stereotypies than in WT mice.

The results obtained with cKO-VGLUT3<sub>ACh</sub> raise several questions. We confirm the involvement of glutamate released from CINs in drug- induced abnormal movements, in line with (Divito *et al.* 2015). However, other studies have attributed this phenotype to the acetylcholine released by CINs (Aliane *et al.* 2011, Crittenden *et al.* 2014, Crittenden *et al.* 2017). This discrepancy requires careful investigation. AMPH study on mice lacking VAcHT (Drd2-Cre::VGLUT3<sup>LoxP/LoxP</sup>) will provide more answers to this question. Another puzzling information is that cKO-VGLUT3<sub>ACh</sub> mice do not display a two- fold hyperlocomotion in response to AMPH 5 mg/kg, unlike the effect obtained with VGLUT3 null mice.

Table C.1 summarizes the phenotypes observed regarding the role of CINs.

**Table C.1: CIN- related phenotypes**

Strategy	DA release (Acb)	Locomotion	Drug response	6- OHDA dyskinesia	L- DOPA- dyskinesia	Drug-induced stereotypies
VGLUT3 <sup>-/-</sup>	↑ <sup>2</sup> ↑ (night) <sup>3</sup>	↑ <sup>1, 2, 6</sup> ↑ (night) <sup>3</sup>	↑ <sup>1, 2, 6</sup>	= <sup>4</sup> ↓ <sup>3</sup>	↓ <sup>3, 4</sup>	↓ <sup>6</sup>
ChAT- IRES- Cre:: VGLUT3 <sup>LoxP/LoxP</sup>	= <sup>3</sup>	= <sup>3, 6</sup>	= <sup>6</sup>	= <sup>3</sup>	↓? <sup>6</sup>	↓ <sup>6</sup>
Drd2- Cre:: VAcHT <sup>LoxP/LoxP</sup>	↓ <sup>2</sup>	= <sup>5</sup>	= <sup>5</sup>	= <sup>4</sup>	↑? <sup>4</sup>	NA
CIN targeting	NA	NA	NA	NA	↓ <sup>7, 8</sup>	NA

**1, Gras *et al.* (2008); 2, Sakae *et al.* (2015); 3, Divito *et al.* (2015); 4, Gangarossa *et al.* (2016); 5, Guzman *et al.* (2011); 6, present study; 7, Won *et al.* (2014); 8, Won *et al.* (2014).**

- Why do VGLUT3 null mice display an enhanced drug- induced hyperlocomotion?

The resistance to amphetamine- induced stereotypies observed in VGLUT3 null mice is mildly present in cKO-VGLUT3<sub>ACh</sub> mice. Likewise, we do not reproduce their two- fold hyperlocomotion in none of the two double mutants. This last result paves the way for different hypothesis.

First, it cannot be excluded that some developmental compensation may occur in the models we used. Indeed, we did not test if markers for other neurotransmission systems were altered in our conditional knockouts. Then, it is possible that the hyperlocomotor phenotype present in VGLUT3<sup>-/-</sup> is the result of a synergistic role of the VGLUT3- positive cholinergic and serotonergic systems. To test this hypothesis, we could produce triple mutant mice lacking VGLUT3 in both systems (ChAT- IRES- CRE::SERT- CRE::VGLUT3<sup>LoxP/LoxP</sup>). Alternatively, we could combine a genetic approach with an RNA interference intervention, for example by injecting shRNA against VGLUT3 in the striatum

of SERT- CRE:: $VGLUT3^{LoxP/LoxP}$ . A direct interplay between these two systems is likely to occur since serotonin modulates the activity of CINs (Virk *et al.* 2016).

As we proposed for the anxiety- like phenotypes observed in  $VGLUT3$  null mice, it is also possible that the purely glutamatergic  $VGLUT3$ - positive circuit is involved in the drug- induced hyperlocomotion. To date, there is no knowledge of the role of these projections. It is suspected that they play a role in the rewarding effects of drugs by projecting on the VTA (Qi *et al.* 2014).

- [What about the other  \$VGLUT3\$ - positive systems?](#)

To complete our study, it would have been interesting to dissect the **role of the  $VGLUT3$ - positive GABAergic system**. Indeed, subpopulation of  $CB_1R$  /  $CCK$ - positive GABAergic interneurons express  $VGLUT3$  in the cortex and hippocampus. Yet, both the hippocampus and PFC send projections to the nucleus accumbens, and cortical projections to the striatum modulate the response to drugs (Pascoli *et al.* 2005, Aliane *et al.* 2009, Robison *et al.* 2011).

We produced the  $VIAAT$ - Cre:: $VGLUT3^{LoxP/LoxP}$  ( $cKO$ - $VGLUT3_{GABA}$ ) double mutants to remove the GABAergic source of  $VGLUT3$ . Their anatomical characterization revealed some unsuspected results. We found a substantial decrease of  $VGLUT3$  in the striatum (Figure C.31), in the dStr ( $\sim$  - 55%) and in the Acb ( $\sim$  - 20%). This observation prevented a clean interpretation of our finding with the mutant line.

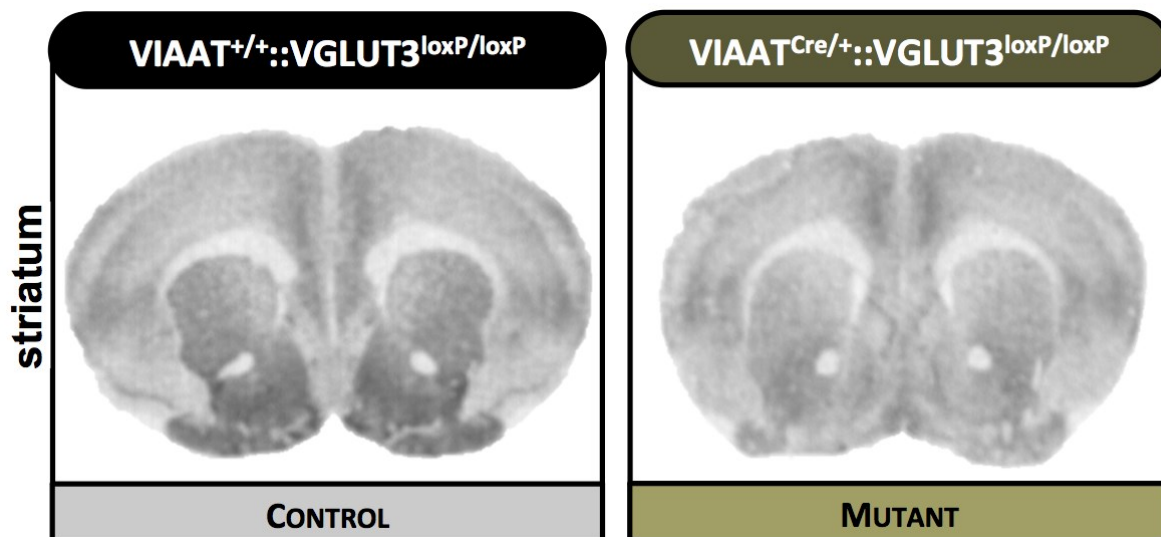


**Figure C.31: Immunohistochemistry for  $VGLUT3$  in  $cKO$ - $VGLUT3_{GABA}$  mice**  
 $VGLUT3$  levels are highly decreased in the striatum in  $cKO$ - $VGLUT3_{GABA}$  mice.

In the adulthood, GABAergic populations of the striatum do not express  $VGLUT3$ . This means that a fraction of striatal cholinergic neurons have a “double- origin” and

transiently express VIAAT during development. Indeed, CINs mainly derive from the medial ganglionic eminence and co-express the transcription factor Nkx2.1 (Marin *et al.* 2000). It has been proposed that all these progenitor cells would express Lhx6 and acquire a GABAergic identity by default. Later, the additional expression of Lhx8 by a fraction of these cells would provide the cholinergic fate (Allaway and Machold 2017).

## **CONCLUSION**

**High dose of amphetamine produces a two-fold locomotor activation in VGLUT3 null mice. The absence of VGLUT3 reduces AMPH-induced stereotypies.**

**Mice lacking VGLUT3 in the serotonergic system display similar levels of locomotion and stereotypies.**

**On the other hand, mice lacking VGLUT3 in CINs display attenuated stereotypies. Their locomotion is similar to the control mice.**

**Therefore, conditional deletion of VGLUT3 in 5-HT or ACh fibers only partially mimics the constitutive deletion of VGLUT3.**



## **PART III.**

# **STUDY OF THE ROLE OF VGLUT3 IN THE NUCLEUS ACCUMBENS IN THE RESPONSE TO COCAINE**

### **CONTEXT**

- ▶ The constitutive invalidation of VGLUT3 (VGLUT3<sup>-/-</sup> mice) leads to a hypersensitivity to the rewarding effects of cocaine.
- ▶ There are major morphological and functional changes in the nucleus accumbens of VGLUT3<sup>-/-</sup> mice.
- ▶ Nucleus accumbens is a central structure for the response to drugs, including cocaine.

### **PROBLEMATIC**

VGLUT3<sup>-/-</sup> mice are more sensitive to cocaine than controls. Given the central involvement of nucleus accumbens in this response, we wondered if the accumbal source of VGLUT3 could be responsible for the phenotypes we found with the full knock-out.

Thus, we studied the effects of cocaine in a conditional accumbal knock-out model.

- ▶ To remove VGLUT3 from the nucleus accumbens, we stereotaxically injected a Cre-expressing virus in VGLUT3<sup>LoxP/LoxP</sup> mice.

## 1. Development of viral injections

### 1.1 Choice of virus

To proceed to VGLUT3 knockdown in the nucleus accumbens (Acb), we injected VGLUT3<sup>LoxP/LoxP</sup> mice with different Cre- expressing viruses to determine which serotype works better in our hands. Viruses were unilaterally injected (with a volume of 500 nL) to use the non- injected side as a control for VGLUT3 basal level. Each virus was tested in two mice: one was sacrificed at 4 weeks post- injection, and the other at 6 weeks post- injection. We quantified the residual protein level in the injected side by IAR directed against VGLUT3 (Figure C.32).

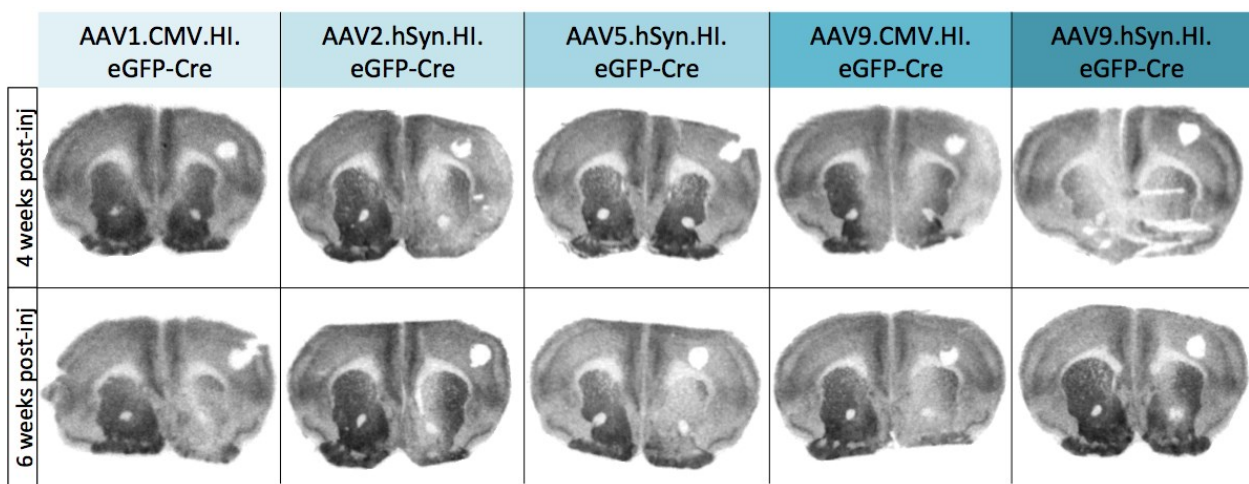


**Figure C.32: Determination of the virus and time post- injection for a VGLUT3 accumbal depletion**

Mice were unilaterally injected (side materialized by a cortical punch) in the nucleus accumbens with different virus strains and sacrificed at 4 or 6 weeks post- injection. VGLUT3 levels were visualized by IAR.

The percentage of decrease corresponding to each time- point and virus is reported in Table C.2.

**Table C.2: Percentage of VGLUT3 decrease after unilateral viral injection**

Virus	AAV1.CMV.HI eGFP- Cre		AAV2.hSyn.HI eGFP- Cre		AAV5.CMV.HI eGFP- Cre		AAV9.hSyn.HI eGFP- Cre		AAV9.CMV.HI eGFP- Cre		
	4	6	4	6	4	6	4	6	4	6	
Weeks post- injection											
Area	Acb	24	70	67	30	14	44	ND	15	ND	57
	AcbSh	- 4	52	67	43	3	49	ND	28	ND	50
	AcbC	0	62	69	63	2	54	ND	67	ND	57
	CPu	- 5	14	29	- 5	0	32	ND	17	ND	16

We found that several virus serotypes produced a strong decrease in the Acb. We decided to use a serotype that:

- produces a decrease visible at 4 weeks post- injection;
- does not diffuse much (knockdown specific for Acb);
- has not been described as being retrograde;
- has a preferential tropism for neurons rather than glial cells.

The selected serotype for the subsequent experiments was the **AAV2.hSyn.HI.eGFP- Cre**, which expresses the Cre recombinase under control of the neuron- specific promoter human synapsin (hSyn) and is mainly anterograde (Kugler *et al.* 2003, Ciesielska *et al.* 2011). Indeed, the human cytomegalovirus promoter (CMV) has a tropism for neurons but mainly for glial cells (Kugler *et al.* 2003).

We confirmed VGLUT3 knockdown at 6 weeks post- injection by immunofluorescence directed against VGLUT3 on the same slices postfixed with methanol (Figure C.33). We used a VGLUT3<sup>+/+</sup> animal as a control, and found that VGLUT3<sup>LoxP/LoxP</sup> animals injected with the control AAV2.hSyn.eGFP.WPRE.bGH virus (AAV- GFP) had similar levels of VGLUT3 in the Acb. On the other hand, animals injected with the Cre- expressing virus AAV2.hSyn.HI.eGFP-Cre.WPRE.SV40 (AAV- Cre) had almost no residual expression of VGLUT3 in the terminals.

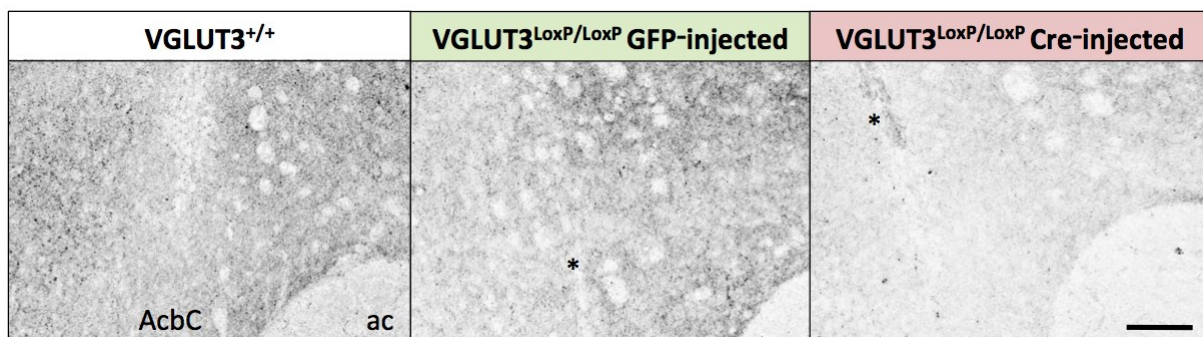


**Figure C.33: Immunofluorescence against VGLUT3 in the Acb after AAV injection**

At 6 weeks post- injection, VGLUT3<sup>LoxP/LoxP</sup> animals stereotactically injected with a GFP- expressing virus in the nucleus accumbens (Acb) have no loss of VGLUT3 in the core part (AcbC; **middle panel**) compared to VGLUT3<sup>+/+</sup> mice (**left panel**). On the other hand, VGLUT3<sup>LoxP/LoxP</sup> animals injected with a Cre- expressing virus in the Acb have a drastic decrease of VGLUT3 (**right panel**). ac: anterior commissure. *Scale bar = 200 μm.*

## 1.2 Experimental groups

To generate the experimental groups, we bilaterally injected VGLUT3<sup>LoxP/LoxP</sup> males aged 6 weeks with the AAV- GFP (controls) or the AAV- Cre (mutants) with a volume of 400 nL on each side (AP +1.6, ML ± 0.75, DV - 4.3 cm). After 8 weeks, we proceeded to

behavioral experiments on these mice. For these experiments, we used a total of 28 VGLUT3<sup>LoxP/LoxP</sup> mice (14 injected with AAV- GFP and 14 with AAV- Cre).

## 2. Anatomical validation

Once the experiments were conducted, we verified the expression of VGLUT3 in the stereotaxically injected mice by immunohistochemistry. We quantified VGLUT3 in the whole striatum (in red in Figure C.34), the Acb (in orange), the dStr (in yellow) to evaluate the anterograde action of the AAV. We also assessed VGLUT3 levels in the DRN (in purple) and MNR (in pink) to confirm that the AAV has no retrograde action.

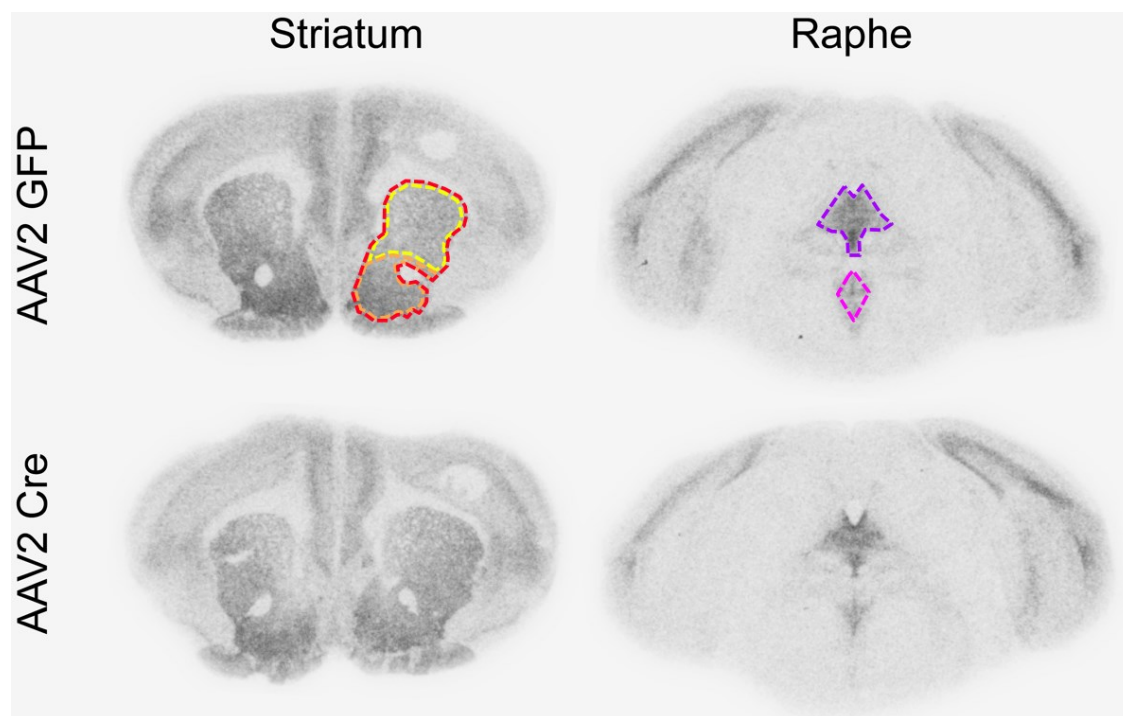


**Figure C.34: Anatomical verification of VGLUT3 level in VGLUT3<sup>LoxP/LoxP</sup> AAV- injected mice**

Striatal sections (**left panel**) and raphe sections (**right panel**) were stained for VGLUT3 by IAR. Mice injected with the AAV- Cre virus (**bottom panel**) had a slight decrease in the striatum but no difference in the raphe compared to AAV- GFP- injected mice (**top panel**).

Mice injected with the AAV- Cre had different efficiency of VGLUT3 knockdown (Figure C.35). For example, two mice had less than 50% of residual VGLUT3 in the Acb. The overall success of the surgery was limited, as the mean level of residual VGLUT3 was around 70% in the knockdown group. We expected a greater decrease.

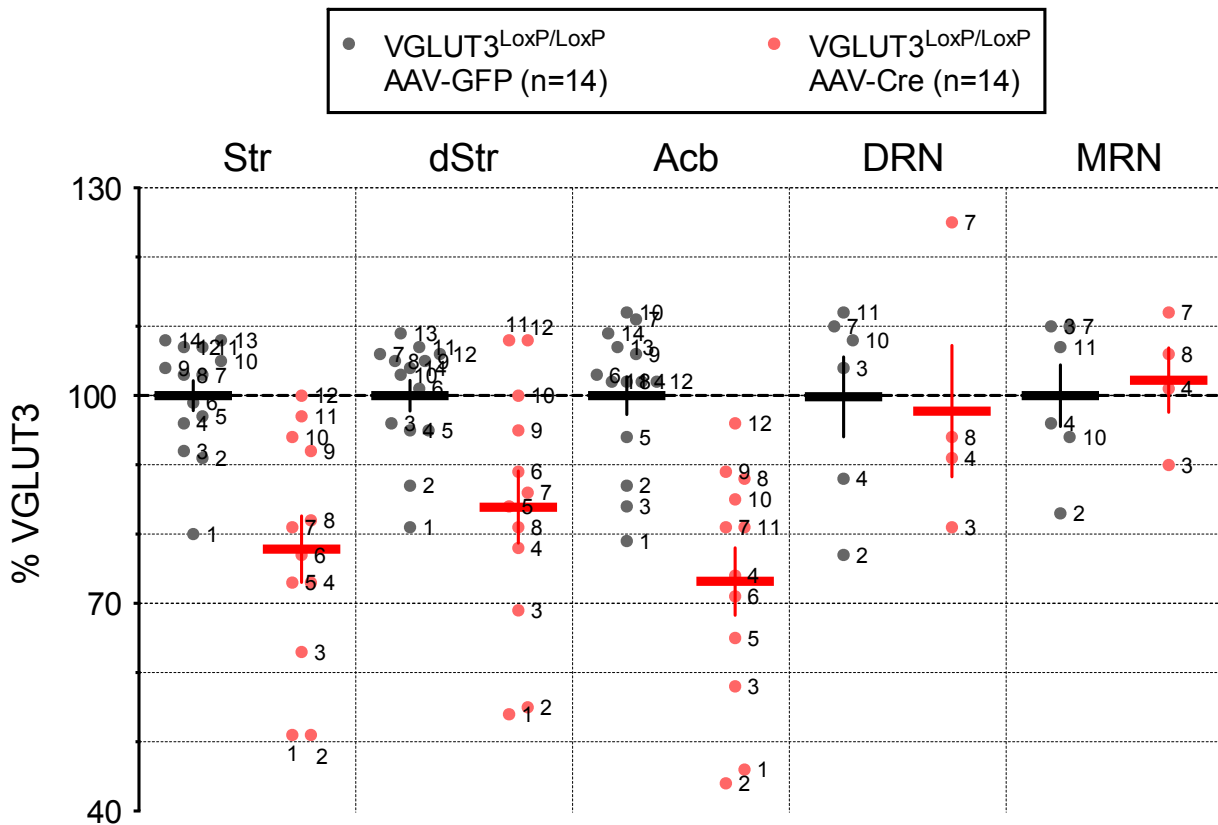


**Figure C.35: Quantification of VGLUT3 in the VGLUT3<sup>LoxP/LoxP</sup> mice injected with AAVs**

The levels of VGLUT3 were assessed in several cerebral structures and expressed as a percentage. Each *dot* represents the mean VGLUT3 level of the two hemispheres for a given mouse (*the number of the animal is indicated next to the corresponding dot*). *Horizontal bars* represent the mean VGLUT3 level of all mice pooled together. Mice injected with AAV- GFP are represented *in black*, and AAV- Cre *in red*. Str, striatum; dStr, dorsal striatum; Acb, nucleus accumbens; DRN, dorsal raphe nucleus; MNR, median raphe nucleus.

### **3. Behavioral characterization**

#### **3.1 Mice weight**

After the recovery period and the incubation time (6- 8 weeks), mice were weighted before the start of behavioral experiments. We found no difference between mice injected with AAV- GFP (controls) and with AAV- Cre (mutants; Figure C.36; t test,  $p = 0.787$ , AAV- GFP  $30.48 \pm 0.84$  g vs. AAV- Cre  $30.10 \pm 1.14$  g).

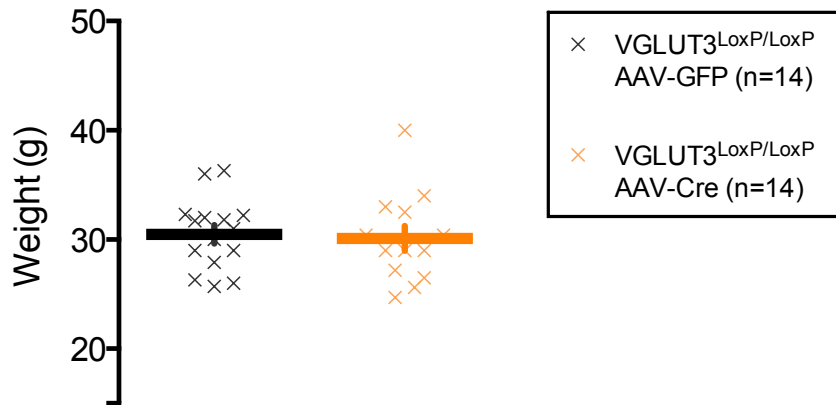


**Figure C.36: VGLUT3<sup>LoxP/LoxP</sup> AAV- injected mice weight**

Mice weight does not differ between control and mutant mice (n=14-14).

### 3.2 Basal locomotion

We first assessed the spontaneous activity of our mice during 24 h. We found no difference in the vertical activity between AAV- GFP and AAV- Cre mice (Figure C.37c; two-way ANOVA, effect of time,  $F_{23, 575} = 37.39$ ,  $p < .001$ , no effect of genotype,  $F_{1, 25} = 0.098$ ,  $p = 0.758$ ). We confirmed this result by verifying that there was no difference in the cumulative number of rearings during the light- off phase (Figure C.37d; Mann- Whitney,  $p = 0.783$ , AAV- GFP  $1431 \pm 176.3$  and AAV- Cre  $1473 \pm 153.2$  beam breaks). However, we found that AAV- Cre mice had a slightly decreased vertical activity during the light- on phase (Figure C.37d; t test,  $p = .069$ , AAV- GFP  $477.8 \pm 53.39$  vs. AAV- Cre  $353.8 \pm 35.65$  beam breaks).

On the other hand, AAV- Cre mice presented a strong tendency toward an increased horizontal locomotion at night (Figure C.37a; two-way ANOVA, effect of time,  $F_{23, 575} = 17.82$ ,  $p < .001$ , no effect of genotype,  $F_{1, 25} = 3.291$ ,  $p = .082$ , *post-hoc* test showed a difference between genotypes at 2:30, 3:30 and 4:30 a.m.). We then compared the cumulative horizontal activity and found that it was highly increased in AAV- Cre injected mice at night (Figure C.37b; Mann- Whitney,  $p = .049$ , AAV- GFP  $875.3 \pm 115.5$  vs. AAV- Cre  $1733 \pm 382.2$  beam breaks) but not significantly different during the light- on phase (Mann- Whitney,  $p = 0.151$ , AAV- GFP  $374.3 \pm 32.46$  vs. AAV- Cre  $347.1 \pm 56.16$  beam breaks).

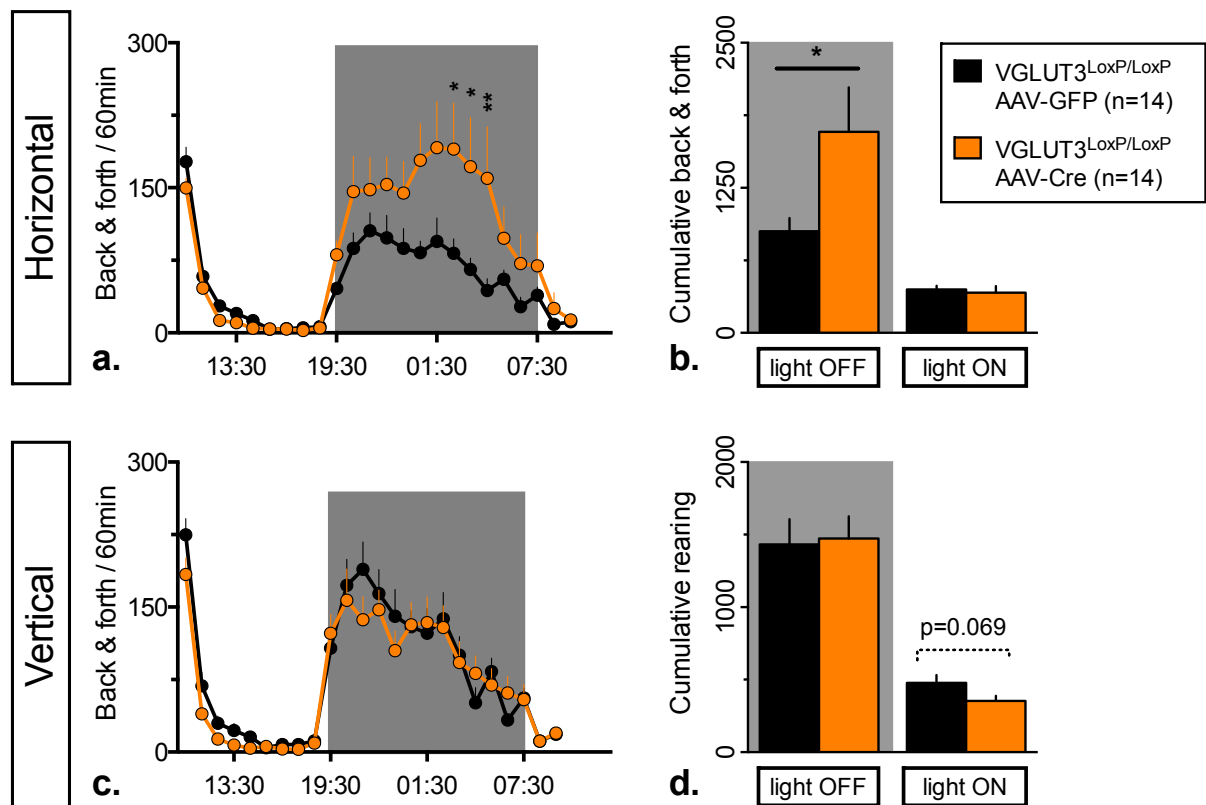


**Figure C.37: VGLUT3<sup>LoxP/LoxP</sup> AAV- injected circadian locomotor activity**

Legend similar to that of Figure C.12. VGLUT3<sup>LoxP/LoxP</sup> injected with the AAV- Cre (*in orange*) have an increased locomotion at night compared to control mice injected with AAV- GFP (*in black*).

Together, these results indicate that VGLUT3<sup>LoxP/LoxP</sup> mice injected with AAV- Cre in the nucleus accumbens have an increased locomotion at night compared to control mice.

### 3.3 Anxiety levels

We also assessed the anxiety level of stereotaxically injected mice in the open field and O maze tests.

- Open field

During 10 min sessions, we individually placed mice in an open field and tracked their locomotion. We found that AAV- Cre-injected mice had a strong trend to spend less time and travel less in the anxiogenic central zone of the open field (Figure C.38, left panel: t test,  $p = 0.112$ , control  $9.64 \pm 1.46$  s and mutant  $7 \pm 0.62$  s spent in the central zone; Figure C.38, right panel: t test,  $p = .086$ , control  $160.6 \pm 26.22$  cm and mutant  $109.4 \pm 10.14$  cm travelled in the central zone). This corresponded to  $1.601 \pm 0.24$  % of time spent in the central zone for AAV- GFP injected mice and  $1.167 \pm 0.1$  % for AAV- Cre injected mice.

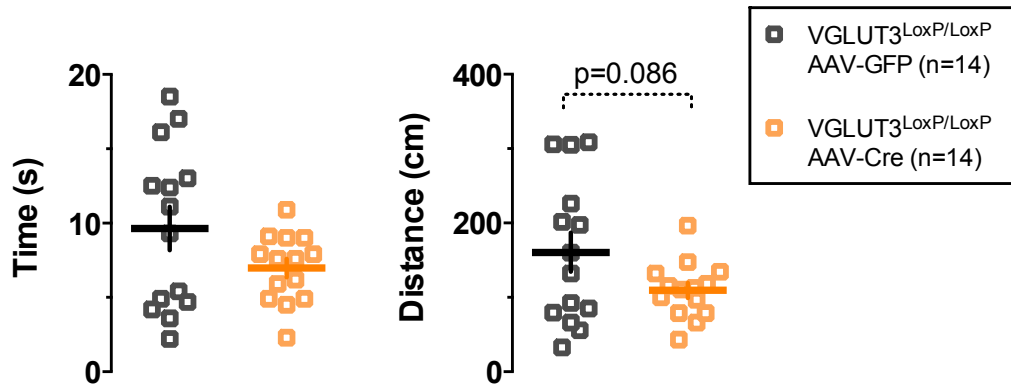


**Figure C.38: VGLUT3<sup>LoxP/LoxP</sup> AAV- injected anxiety levels in the open field test**

AAV- Cre injected mice seem to spend less time in the central zone compared to AAV- GFP mice (n = 14-14).

- O maze

We then tested mice response in the O maze during 10 min- sessions. Again, we found that AAV- Cre injected mice would spend less time in the anxiogenic zone (open arms) compared to AAV- GFP injected animals (Figure C.39, left panel; t test, p = .068, AAV- GFP 24.04 ± 2.454 s vs. AAV- Cre 16.16 ± 3.32 s spent in the open arms, which correspond respectively to 4 ± 0.409 % and 2.693 ± 0.553 % of the total time). They also travelled less in the open arms with no statistically significant difference (Figure C.39, right panel; t test, p = 0.113, AAV- GFP 205.8 ± 23.57 cm vs. AAV- Cre 140.1 ± 32.46 cm travelled in the open arms).

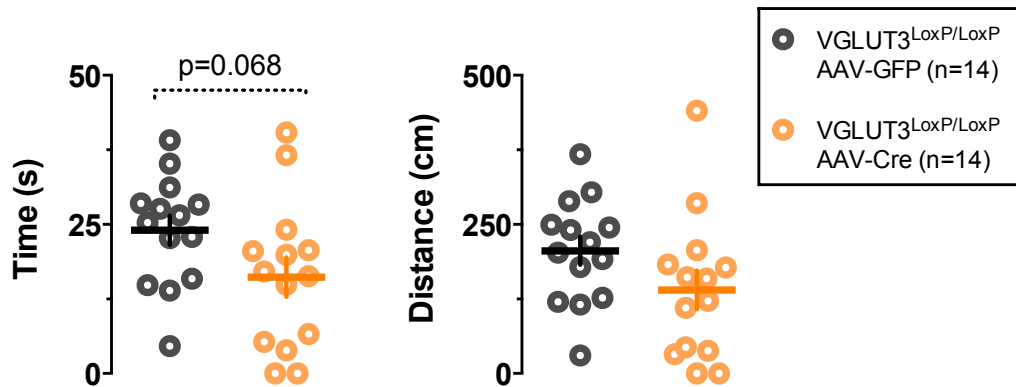


**Figure C.39: VGLUT3<sup>LoxP/LoxP</sup> AAV- injected anxiety levels in the O maze test**

AAV- Cre injected mice seem to spend less time in the open arms compared to AAV- GFP mice (n = 14-14).

In summary, VGLUT3<sup>LoxP/LoxP</sup> mice injected with the AAV- Cre in the nucleus accumbens seem slightly more anxious compared to control mice.

#### 4. Locomotor sensitization to cocaine

After the basal behavior testing, we proceeded to a locomotor sensitization protocol to cocaine 10 mg/kg. The protocol was closely related to the one used for AMPH (*cf* Materials & Methods). The set-up was the cyclotron, a bun-shaped corridor where the mouse can move. The number of ¼ turns provides a measure of the activity (locomotion). After the 5<sup>th</sup> injection, mice were withdrawn from the drug for 5 days, and then challenged with a last dose of COC 10 mg/kg.

- Acute injection of cocaine 10 mg/kg

We first assessed the locomotion in response to an acute injection of COC 10 mg/kg (Figure C.40a). This injection led to a very mild hyperlocomotion that was not significantly different from a saline injection (two-way ANOVA between SAL and COC1, no effect of time,  $F_{1,25} = .018$ ,  $p = 0.9$ , no effect of virus,  $F_{1,25} = 0.948$ ,  $p = 0.34$ ).

The response to acute COC 10 mg/kg did not differ between our two groups of mice (Figure C.40a, inset; Mann-Whitney,  $p = 0.542$ , AAV-GFP  $58.61 \pm 13.61$  vs. AAV-Cre  $45.81 \pm 9.905$  ¼ of turn).

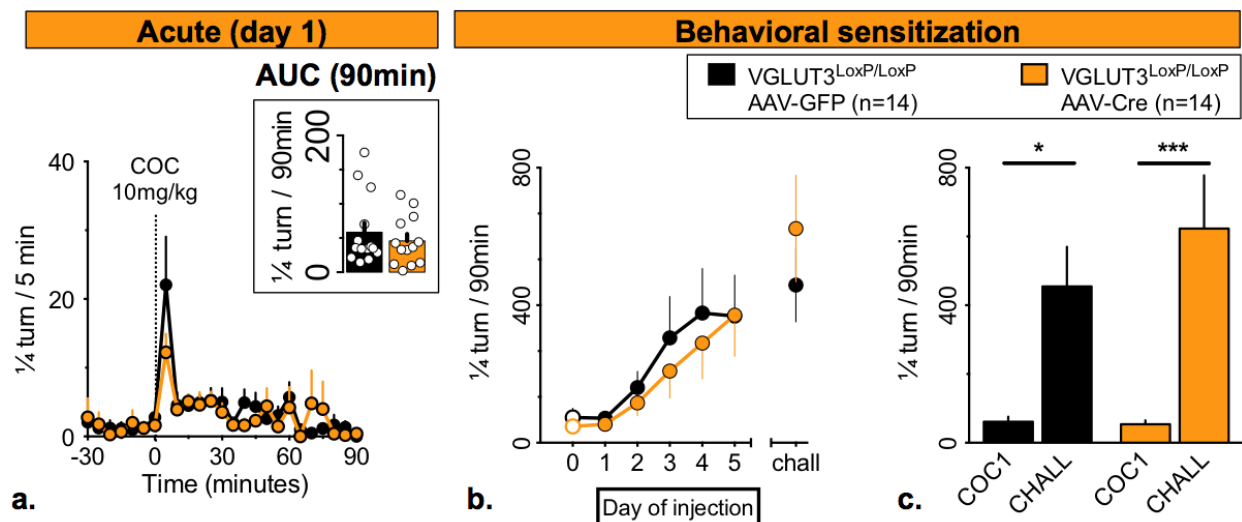


**Figure C.40: VGLUT3<sup>LoxP/LoxP</sup> AAV-injected locomotor sensitization to cocaine**

**a.** The acute injection of cocaine 10 mg/kg reveals no difference in terms of hyperlocomotion between AAV-Cre- (*in orange*) and AAV-GFP-injected mice (*in black*). **b.** Both types of virus produce the same locomotor sensitization in response to repeated injections of cocaine. **c.** The sensitization is similar for the 2 groups of mice ( $n = 14-14$ ).

- Repeated injections of cocaine 10 mg/kg

We injected mice for 4 other days with the same dose of cocaine. We observed that the cocaine-induced hyperlocomotion increased across sessions, but did not differ between AAV-GFP- and AAV-Cre-injected mice (Figure C.40b; two-way ANOVA for COC1 to COC5, effect of time,  $F_{4,100} = 11.74$ ,  $p < .001$ , no effect of virus,  $F_{1,25} = 0.201$ ,

$p = 0.658$ ). After 5 days of withdrawal, we did a challenge with COC 10 mg/kg. We confirmed that this protocol produced a strong locomotor sensitization, even though there was no difference between our two groups (Figure C.40c; two-way ANOVA between COC1 and challenge, effect of time,  $F_{1, 25} = 27.62$ ,  $p < .001$ , no effect of virus,  $F_{1, 25} = 0.588$ ,  $p = 0.45$ , *post-hoc* between COC1 and challenge,  $p = .01$  for AAV- GFP mice, and  $p < .001$  for AAV- Cre).

We also analyzed if we could find a correlation between the accumbal level of VGLUT3 and the cocaine- induced locomotion. To do so, we calculated the mean cumulative locomotion during the 90 minutes post- injection during the 6 injections of COC 10 mg/kg, and then plotted this mean activity as a function of VGLUT3 accumbal level (Figure C.41). The prediction would state that the smaller VGLUT3 accumbal level, the stronger the cocaine- induced locomotion. Indeed, we found such a profile for the AAV- Cre- injected group, but the linear regression gave a slope that was non- significantly different from zero ( $F_{1, 9} = 2.414$ ,  $p = 0.155$ ), with an  $R^2$  of 0.212. The mean locomotion has a tendency to increase for reduced levels of accumbal VGLUT3. In contrast, we found no such relation for the control group ( $F_{1, 11} = 0.41$ ,  $p = 0.535$  with a  $R^2$  of .036).

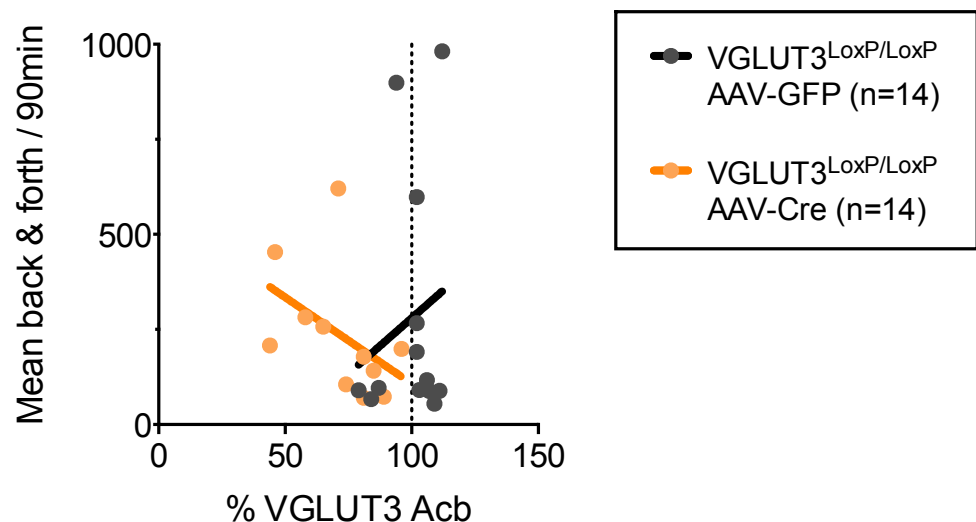


**Figure C.41: Correlation between VGLUT3 accumbal level and cocaine- induced locomotion**

There is a trend for a correlation between the level of VGLUT3 in the Acb and the mean locomotion induced by cocaine during the 6 injections of COC 10 mg/kg for the AAV- Cre- injected animals (*in orange*), but none for the control group (*in black*;  $n = 14-14$ ).

As a summary, we found no difference in terms of locomotor sensitization to cocaine between  $VGLUT3^{LoxP/LoxP}$  mice injected with the AAV- Cre (knockdown) and the ones injected with the AAV- GFP (control). However, the accumbal level of VGLUT3 seemed to be inversely correlated to the cocaine- induced locomotor outcome.

## 5. Discussion

The experiments conducted on AAV- injected animals were inconclusive. We expected to observe that mice invalidated for VGLUT3 in the Acb would have an enhanced cocaine- induced hyperlocomotion as the one observed in VGLUT3 null mice. However, the locomotor sensitization was identical in the two groups. Even if we obtain low levels of VGLUT3 knockdown in the AAV-Cre-injected mice, we find that the overall COC- induced locomotion seems to be negatively correlated to the residual VGLUT3 levels. Thus, our results do not signify that the hyper- responsivity to cocaine observed in VGLUT3<sup>-/-</sup> mice is not imputable to the accumbal source of VGLUT3. These experiments need to be replicated.

Indeed, the anatomical validation performed at the end of the experiments revealed major defects in targeting the Acb. There are several explanations for that problem.

The first one is that the stereotaxic injections were developed with a set- up with a single needle where the virus was infused manually. For the tests, we injected a volume of 500 nL, and the lesions were very widespread (Figure C.32). Therefore, we had determined that this volume should be decreased to be more specific for the Acb. On the other hand, the experimental groups were generated using a more recent set- up where two needles allow bilateral injections with a continual infusion thanks to a pump. We ordered a spacer to have a mediolateral distance of 1.5 cm between the two sites of injection. These sites were probably too medial to target the Acb, and may have produced a decrease in the medial septum instead of the striatum. Moreover, when the targeting was correct, the knockdown was not as efficient as expected. The virus volume we chose to infuse could explain this (400 nL on each side), because it may have been too small for the new set- up we used. Indeed, the virus was delivered “manually” with the old set- up, and the infused volumes were probably not accurate enough. And the targeted structure being quite large, a greater volume may have been necessary.

Another explanation could be the serotype used. Indeed, the AAV2 has a low toxicity, a tropism for neurons and majorly an anterograde action. However, given the large area we had to target, another serotype could have been more adapted, for example the AAV5 or AAV9 (Aschauer *et al.* 2013). These serotypes have been described as having an important cellular tropism in the striatum, and could have led to higher recombination rates.

To study the role of VGLUT3 in the Acb, another approach could have been used, with stereotaxic injections of shRNA directed against VGLUT3 mRNA. The experimental conditions to induce substructural striatal lesions have been developed in our laboratory in Montreal. This technique offers one advantage compared to AAV- Cre- mediated

knockdown: any kind of mouse can be used for the knockdown of VGLUT3 without the constraint of a heavy transgenic mice breeding.

### **CONCLUSION**

**The level of cocaine-induced hyperlocomotion seems to be correlated with the extent of VGLUT3 knockdown in the nucleus accumbens.**

**VGLUT3 accumbal level could account for the COC-induced hyperlocomotion observed in VGLUT3 null mice.**

# GENERAL CONCLUSION

In this work, we investigated the role of VGLUT3 in the effects of amphetamine. We first explored the effects of locomotion-stimulating doses. We found that VGLUT3 null mice displayed two-fold levels of AMPH-induced hyperlocomotion compared to WT siblings. We also found that VGLUT3<sup>-/-</sup> mice would sensitize to AMPH, unlike the previous results obtained with COC 10 mg/kg (Sakae *et al.* 2015). We suggest that these differences rely on the fact that amphetamine and cocaine have different pharmacokinetics, and propose that serotonergic and noradrenergic systems may also contribute to this outcome. We also suggest that an unforeseen plasticity could occur with AMPH, for example in the prefrontal cortex, which is part of the circuit recruited by AMPH.

We explored another motor outcome of amphetamine, by using a high dose of AMPH that induces stereotypies. We reported that VGLUT3<sup>-/-</sup> mice are particularly resistant to AMPH-induced stereotypies. This result is in line with two reports suggesting that lack of VGLUT3 protects against L-DOPA-induced dyskinesia (Divito *et al.* 2015, Gangarossa *et al.* 2016).

To unravel the contribution of the different VGLUT3-positive neurotransmitter systems in these responses, we depleted VGLUT3 in specific cell populations based on a genetic Cre-Lox approach. The removal of VGLUT3 from the serotonergic system did not interfere with AMPH-induced-hyperlocomotion and -stereotypies. Neither did it modify the basal locomotor or anxiety levels of mutant mice.

On the other hand, invalidation of VGLUT3 in the cholinergic system partly reproduced the characteristic hyperlocomotion of VGLUT3 null mice (Gras *et al.* 2008). We tested the response to AMPH 5 mg/kg, and found that AMPH-induced hyperlocomotion was slightly higher in cKO-VGLUT3<sup>ACh</sup> than control littermates, but in minimal proportions compared to the massive difference observed in VGLUT3 null mice. We thus propose that the AMPH-induced hyperlocomotion observed in the full knockout has another origin, which remains to be determined. When we assessed AMPH-induced stereotypies, we found that cKO-VGLUT3<sup>ACh</sup> displayed attenuated levels compared to control siblings. Therefore, we propose that the resistance to AMPH-induced stereotypies that we characterized in VGLUT3 null mice partly relies on the glutamate released by CINs in the striatum.

In another study, we generated VGLUT3 accumbal knockdown based on a viral approach. This study furnished first evidence for an accumbal role of VGLUT3 in the COC-induced hyperlocomotion observed in VGLUT3 null mice, as strongly suspected (Sakae *et al.* 2015).

Together, our results provide new evidence for a role of glutamate in drug-induced behaviors. It is known that CINs play a critical role in motor manifestations of Parkinson's disease, and cholinergic drugs are commonly used to treat the side effects of dopatherapy (Smith *et al.* 2012). Our work demonstrates that glutamate released by CINs also participates in these abnormal movements, and places VGLUT3 as an interesting therapeutic target to alleviate LID. To date, there is no specific agent able to specifically target one subtype of VGLUT, but development on new tools offers promising perspectives for a cell-specific targeting (Schenck *et al.* 2017).

# APPENDICES

## 1. Temporal course of AMPH injections

### 1.1 VGLUT3<sup>-/-</sup> and AMPH 1 mg/kg

During the acute injection of AMPH 1 mg/kg, VGLUT3<sup>-/-</sup> mice hyperlocomotion was higher than WT mice (Figure E.1; two-way ANOVA, effect of genotype,  $F_{1,21} = 6.636$ ,  $p = .018$ ). The horizontal activity was similar between the two genotypes during the following injections (Figure E.1; two-way ANOVA, no effect of genotype: AMPH2,  $F_{1,21} = 3.493$ ,  $p = .076$ ; AMPH3,  $F_{1,21} = 2.69$ ,  $p = .116$ ; AMPH4,  $F_{1,21} = 1.365$ ,  $p = 0.255$ ; AMPH5,  $F_{1,21} = 0.053$ ,  $p = .821$ ).

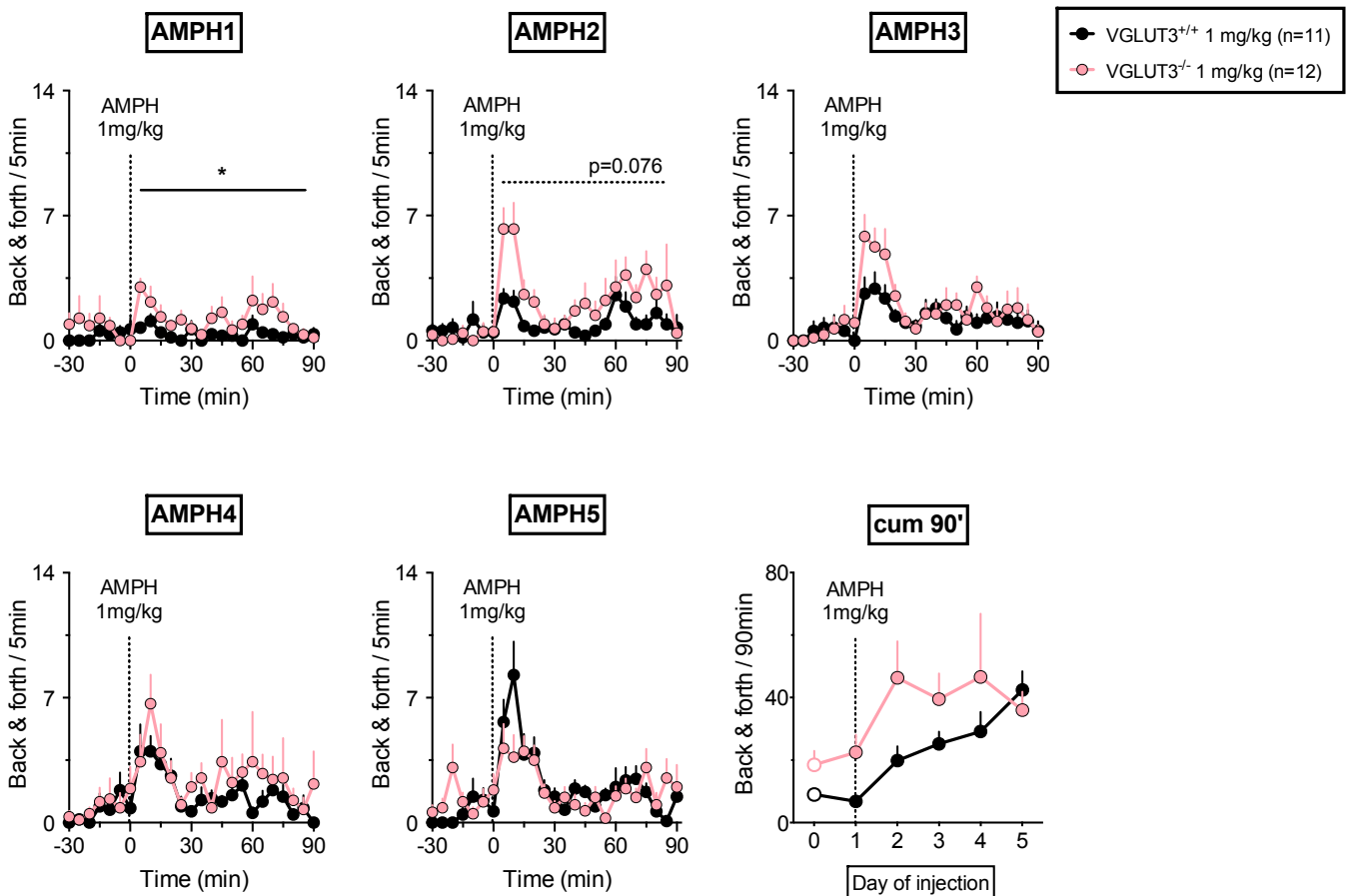


**Figure E.1: VGLUT3<sup>-/-</sup> horizontal locomotion in response to AMPH 1 mg/kg**

VGLUT3<sup>-/-</sup> mice have an enhanced horizontal activity during the acute injection of AMPH 1 mg/kg compared to WT siblings. The AMPH-induced hyperlocomotion does not differ between genotypes during the 4 other injections (n = 11-12).

## 1.2 VGLUT3<sup>-/-</sup> and AMPH 3 mg/kg

We assessed the effects of AMPH 3 mg/kg on the horizontal activity. The acute injection induced a hyperlocomotion that did not differ between VGLUT3<sup>-/-</sup> and WT mice (Figure E.2; two-way ANOVA, no effect of genotype,  $F_{1,39} = 0.352$ ,  $p = 0.557$ ). However, the following AMPH injections resulted in a greater hyperlocomotion in VGLUT3<sup>-/-</sup> mice (Figure E.2; two-way ANOVA, no effect of genotype for AMPH2,  $F_{1,39} = 3.275$ ,  $p = .074$ ). This difference became significant after the 3<sup>rd</sup> injection (Figure E.2; two-way ANOVA, effect of genotype: AMPH3,  $F_{1,39} = 9.982$ ,  $p = .003$ ; AMPH4,  $F_{1,39} = 6.93$ ,  $p = .012$ ; AMPH5,  $F_{1,39} = 9.371$ ,  $p = .004$ ).

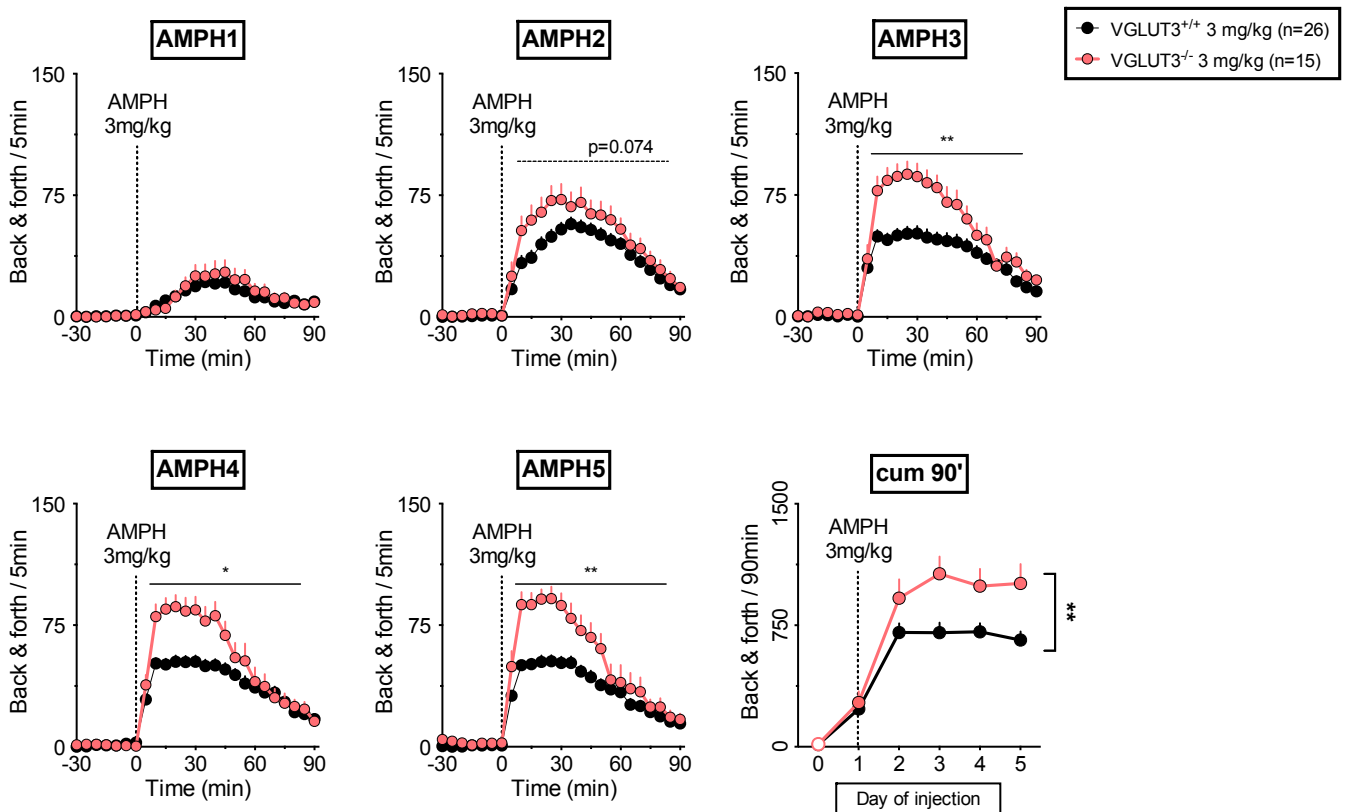


**Figure E.2: VGLUT3<sup>-/-</sup> horizontal locomotion in response to AMPH 3 mg/kg**

VGLUT3<sup>-/-</sup> mice have similar AMPH-induced hyperlocomotion at AMPH1 compared to controls. After the 2<sup>nd</sup> injection, VGLUT3<sup>-/-</sup> response becomes greater than control littermates ( $n = 26-15$ ).

### 1.3 VGLUT3<sup>-/-</sup> and AMPH 5 mg/kg

The acute injection of AMPH 5 mg/kg produced a two-fold hyperlocomotion in VGLUT3<sup>-/-</sup> mice compared to WT littermates (Figure E.3; two-way ANOVA, effect of genotype,  $F_{1,35} = 18.86$ ,  $p < .001$ ). The ratio between WT and mutant mice became even greater during the subsequent injections of AMPH (Figure E.3; two-way ANOVA, effect of genotype: AMPH2,  $F_{1,20} = 18.92$ ,  $p < .001$ ; AMPH3,  $F_{1,35} = 34.09$ ,  $p < .001$ ; AMPH4,  $F_{1,36} = 43.91$ ,  $p < .001$ ; AMPH5,  $F_{1,21} = 39.0$ ,  $p < .001$ ).

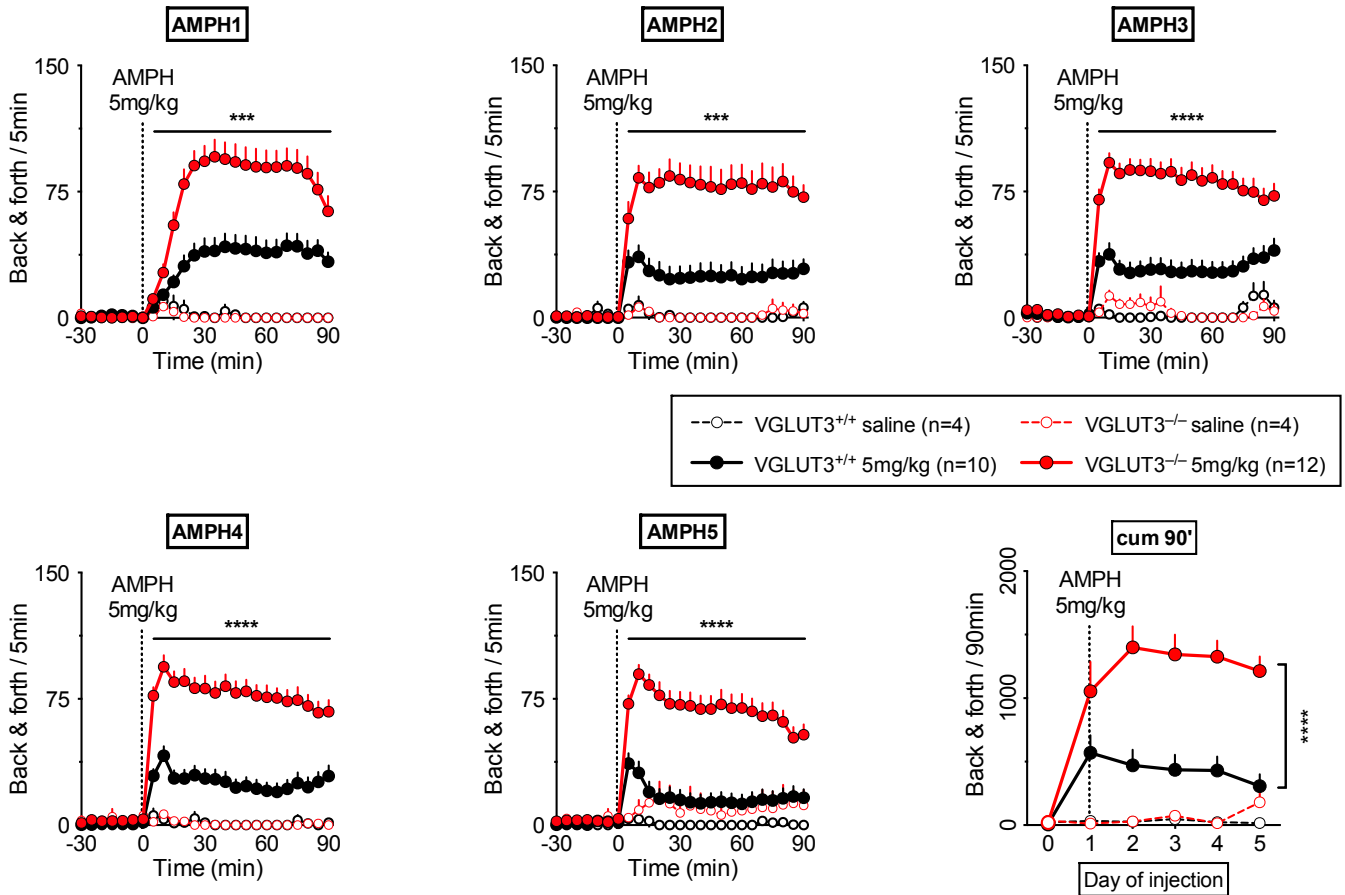


**Figure E.3: VGLUT3<sup>-/-</sup> horizontal locomotion in response to AMPH 5 mg/kg**

In response to AMPH 5 mg/kg, VGLUT3<sup>-/-</sup> horizontal activity is systematically several fold higher than WT littermates (n = 10-12 for AMPH, n = 4-4 for SAL).

## 1.4 cKO-VGLUT3<sub>5-HT</sub> and AMPH 5 mg/kg

Mice lacking VGLUT3 in the serotonergic fibers (cKO-VGLUT3<sub>5-HT</sub>) had the same locomotor response than control littermates to an acute injection of AMPH 5 mg/kg (Figure E.4; two-way ANOVA, no effect of genotype,  $F_{1,18} = 0.858$ ,  $p = 0.367$ ). This similar response was conserved during each day of injection (Figure E.4; two-way ANOVA, no effect of genotype: AMPH2,  $F_{1,18} = 0.95$ ,  $p = 0.343$ ; AMPH3,  $F_{1,18} = 0.395$ ,  $p = 0.538$ ; AMPH4,  $F_{1,18} = 0.769$ ,  $p = 0.392$ ; AMPH5,  $F_{1,18} = 1.06$ ,  $p = 0.316$ ).

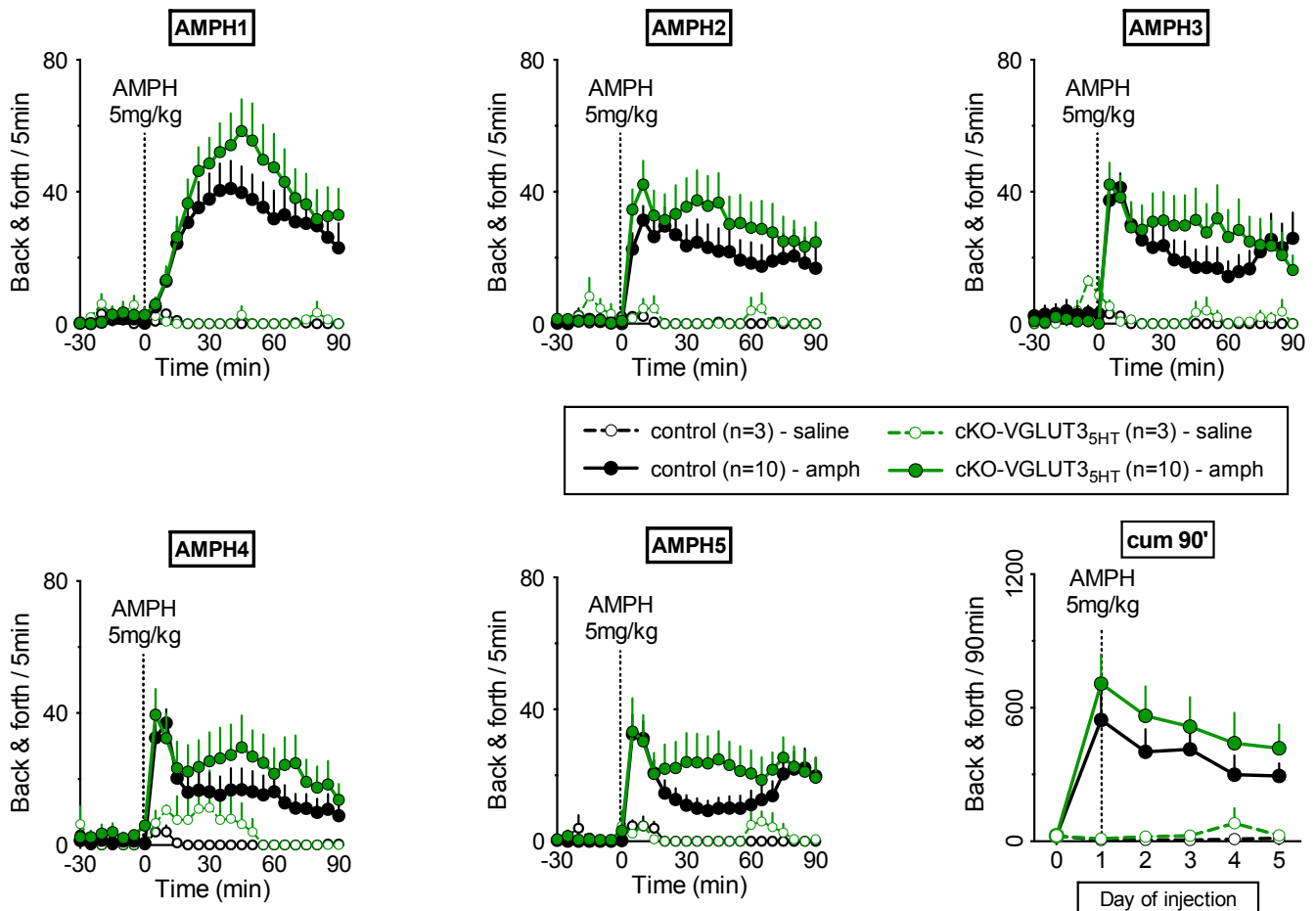


**Figure E.4: cKO-VGLUT3<sub>5-HT</sub> horizontal locomotion in response to AMPH 5 mg/kg**

During each day of injection, cKO-VGLUT3<sub>5-HT</sub> mice respond similarly to control littermates (n = 10-10 for AMPH, n = 3-3 for SAL).

## 1.5 cKO-VGLUT3<sub>ACh</sub> and AMPH 5 mg/kg

Mice lacking VGLUT3 in the cholinergic fibers (cKO-VGLUT3<sub>ACh</sub>) had a slightly non-significant enhancement of AMPH-induced locomotor response compared to control littermates in response to an acute injection of AMPH 5 mg/kg (Figure E.5; two-way ANOVA, no effect of genotype,  $F_{1,21} = 1.965$ ,  $p = 0.176$ ). This greater AMPH-induced hyperlocomotion of cKO-VGLUT3<sub>ACh</sub> mice was present during all following injections (Figure E.5; two-way ANOVA, effect of genotype: AMPH2,  $F_{1,21} = 2.198$ ,  $p = 0.153$ ; AMPH3,  $F_{1,21} = 3.197$ ,  $p = .088$ ; AMPH4,  $F_{1,21} = 4.516$ ,  $p = .046$ ; AMPH5,  $F_{1,21} = 3.306$ ,  $p = .083$ ).

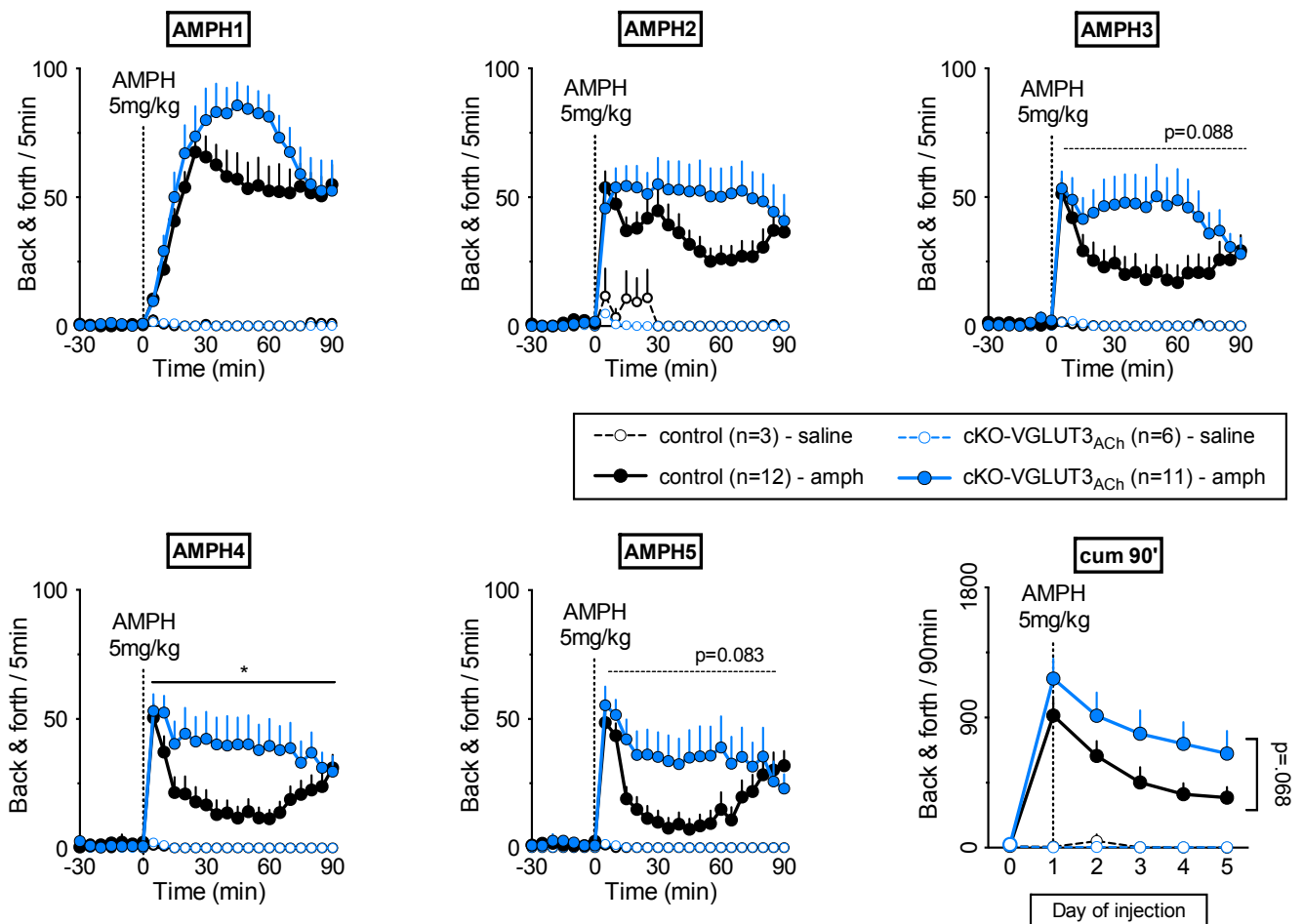


**Figure E.5: cKO-VGLUT3<sub>ACh</sub> horizontal locomotion in response to AMPH 5 mg/kg**

During each injection of AMPH, cKO-VGLUT3<sub>ACh</sub> mice displayed a trend for a greater AMPH-induced hyperlocomotion compared to control littermates ( $n = 12-11$  for AMPH,  $n = 3-6$  for SAL).

## **2. Publications**

**Journal of Neuroscience 12 April 2017, 37 (15) 4181-4199**

**Ramet L, Zimmermann J, Bersot T, Poirel O, De Gois S, Silm K, Sakae DY, Mansouri-Guilani N, Bourque MJ, Trudeau LE, Pietrancosta N, Dumas S, Bernard V, Rosenmund C, El Mestikawy S**

**“Characterization of a Human Point Mutation of VGLUT3 (p.A211V) in the Rodent Brain Suggests a Nonuniform Distribution of the Transporter in Synaptic Vesicles”**

VGLUT3 is an atypical member of the vesicular glutamate transporter family. A point mutation of VGLUT3 (VGLUT3-p.A211V) responsible for a progressive loss of hearing has been identified in humans. This mutation dramatically reduces VGLUT3 expression in terminals (~ 70%) without altering its function. Furthermore, the reduced expression levels of VGLUT3 corresponded to a decrease of the number of VGLUT3-positive vesicles at synapses. These unexpected findings challenge the vision of a uniform distribution of synaptic vesicles at synapses. Therefore, the overall activity of VGLUT3 is not proportional to the level of VGLUT3 expression. These data will be key in interpreting the role of VGLUTs in human pathologies.

# REFERENCES

- Abrahao, K. P., A. G. Salinas and D. M. Lovinger (2017). "Alcohol and the Brain: Neuronal Molecular Targets, Synapses, and Circuits." *Neuron* 96(6): 1223-1238.
- Aihara, Y., H. Mashima, H. Onda, S. Hisano, H. Kasuya, T. Hori, S. Yamada, H. Tomura, Y. Yamada, I. Inoue, I. Kojima and J. Takeda (2000). "Molecular cloning of a novel brain-type Na(+)-dependent inorganic phosphate cotransporter." *J Neurochem* 74(6): 2622-2625.
- Akil, O., R. P. Seal, K. Burke, C. Wang, A. Alemi, M. During, R. H. Edwards and L. R. Lustig (2012). "Restoration of hearing in the VGLUT3 knockout mouse using virally mediated gene therapy." *Neuron* 75(2): 283-293.
- Albin, R. L., A. B. Young and J. B. Penney (1989). "The functional anatomy of basal ganglia disorders." *Trends Neurosci* 12(10): 366-375.
- Alex, K. D. and E. A. Pehek (2007). "Pharmacologic mechanisms of serotonergic regulation of dopamine neurotransmission." *Pharmacol Ther* 113(2): 296-320.
- Alexander, G. E. (2004). "Biology of Parkinson's disease: pathogenesis and pathophysiology of a multisystem neurodegenerative disorder." *Dialogues Clin Neurosci* 6(3): 259-280.
- Aliane, V., S. Perez, Y. Bohren, J. M. Deniau and M. L. Kemel (2011). "Key role of striatal cholinergic interneurons in processes leading to arrest of motor stereotypies." *Brain* 134(Pt 1): 110-118.
- Aliane, V., S. Perez, A. Nieoullon, J. M. Deniau and M. L. Kemel (2009). "Cocaine-induced stereotypy is linked to an imbalance between the medial prefrontal and sensorimotor circuits of the basal ganglia." *Eur J Neurosci* 30(7): 1269-1279.
- Allaway, K. C. and R. Machold (2017). "Developmental specification of forebrain cholinergic neurons." *Dev Biol* 421(1): 1-7.
- Allen, T. G., F. C. Abogadie and D. A. Brown (2006). "Simultaneous release of glutamate and acetylcholine from single magnocellular "cholinergic" basal forebrain neurons." *J Neurosci* 26(5): 1588-1595.
- Almqvist, J., Y. Huang, A. Laaksonen, D. N. Wang and S. Hovmoller (2007). "Docking and homology modeling explain inhibition of the human vesicular glutamate transporters." *Protein Sci* 16(9): 1819-1829.
- Amilhon, B., E. Lopicard, T. Renoir, R. Mongeau, D. Popa, O. Poirel, S. Miot, C. Gras, A. M. Gardier, J. Gallego, M. Hamon, L. Lanfumey, B. Gasnier, B. Giros and S. El Mestikawy (2010). "VGLUT3 (vesicular glutamate transporter type 3) contribution to the regulation of serotonergic transmission and anxiety." *J Neurosci* 30(6): 2198-2210.
- Anderson, E. M. and D. W. Self (2017). "It's only a matter of time: longevity of cocaine-induced changes in dendritic spine density in the nucleus accumbens." *Curr Opin Behav Sci* 13: 117-123.
- Armentero, M. T., A. Pinna, S. Ferre, J. L. Lanciego, C. E. Muller and R. Franco (2011). "Past, present and future of A(2A) adenosine receptor antagonists in the therapy of Parkinson's disease." *Pharmacol Ther* 132(3): 280-299.
- Aschauer, D. F., S. Kreuz and S. Rumpel (2013). "Analysis of transduction efficiency, tropism and axonal transport of AAV serotypes 1, 2, 5, 6, 8 and 9 in the mouse brain." *PLoS One* 8(9): e76310.
- Association, A. P. (2013). *Diagnostic and statistical manual of mental disorders (DSM-5®)*, American Psychiatric Pub.
- Attwell, D. (2000). "Brain uptake of glutamate: food for thought." *J Nutr* 130(4S Suppl): 1023S-1025S.
- Azevedo, F. A., L. R. Carvalho, L. T. Grinberg, J. M. Farfel, R. E. Ferretti, R. E. Leite, W. Jacob Filho, R. Lent and S. Herculano-Houzel (2009). "Equal numbers of neuronal and nonneuronal cells make the human brain an isometrically scaled-up primate brain." *J Comp Neurol* 513(5): 532-541.

- Barbour, B. (2001). "An evaluation of synapse independence." *J Neurosci* 21(20): 7969-7984.
- Barbour, B. and M. Hausser (1997). "Intersynaptic diffusion of neurotransmitter." *Trends Neurosci* 20(9): 377-384.
- Bassani, S., A. Folci, J. Zapata and M. Passafaro (2013). "AMPA trafficking in synapse maturation and plasticity." *Cell Mol Life Sci* 70(23): 4411-4430.
- Beaulieu, J. M., S. Espinoza and R. R. Gainetdinov (2015). "Dopamine receptors–IUPHAR review 13." *British journal of pharmacology* 172(1): 1-23.
- Bellocchio, E. E. (2000). "Uptake of Glutamate into Synaptic Vesicles by an Inorganic Phosphate Transporter." *Science* 289(5481): 957-960.
- Bellocchio, E. E., H. Hu, A. Pohorille, J. Chan, V. M. Pickel and R. H. Edwards (1998). "The localization of the brain-specific inorganic phosphate transporter suggests a specific presynaptic role in glutamatergic transmission." *J Neurosci* 18(21): 8648-8659.
- Bernard, V., O. Laribi, A. I. Levey and B. Bloch (1998). "Subcellular redistribution of m2 muscarinic acetylcholine receptors in striatal interneurons in vivo after acute cholinergic stimulation." *J Neurosci* 18(23): 10207-10218.
- Bernard, V., C. Le Moine and B. Bloch (1991). "Striatal neurons express increased level of dopamine D2 receptor mRNA in response to haloperidol treatment: a quantitative in situ hybridization study." *Neuroscience* 45(1): 117-126.
- Bernard, V., C. Legay, J. Massoulie and B. Bloch (1995). "Anatomical analysis of the neurons expressing the acetylcholinesterase gene in the rat brain, with special reference to the striatum." *Neuroscience* 64(4): 995-1005.
- Bernard, V., E. Normand and B. Bloch (1992). "Phenotypical characterization of the rat striatal neurons expressing muscarinic receptor genes." *J Neurosci* 12(9): 3591-3600.
- Bertran-Gonzalez, J., C. Bosch, M. Maroteaux, M. Matamales, D. Herve, E. Valjent and J. A. Girault (2008). "Opposing patterns of signaling activation in dopamine D1 and D2 receptor-expressing striatal neurons in response to cocaine and haloperidol." *J Neurosci* 28(22): 5671-5685.
- Bertran-Gonzalez, J., B. C. Chieng, V. Laurent, E. Valjent and B. W. Balleine (2012). "Striatal cholinergic interneurons display activity-related phosphorylation of ribosomal protein S6." *PLoS One* 7(12): e53195.
- Bickerdike, M. J. and E. D. Abercrombie (1997). "Striatal acetylcholine release correlates with behavioral sensitization in rats withdrawn from chronic amphetamine." *J Pharmacol Exp Ther* 282(2): 818-826.
- Biever, A., J. Boubaker-Vitre, L. Cutando, I. Gracia-Rubio, M. Costa-Mattioli, E. Puighermanal and E. Valjent (2016). "Repeated Exposure to D-Amphetamine Decreases Global Protein Synthesis and Regulates the Translation of a Subset of mRNAs in the Striatum." *Front Mol Neurosci* 9: 165.
- Blesa, J. and S. Przedborski (2014). "Parkinson's disease: animal models and dopaminergic cell vulnerability." *Front Neuroanat* 8: 155.
- Blomeley, C. and E. Bracci (2005). "Excitatory effects of serotonin on rat striatal cholinergic interneurons." *J Physiol* 569(Pt 3): 715-721.
- Bolam, J. P., P. N. Izzo and A. M. Graybiel (1988). "Cellular substrate of the histochemically defined striosome/matrix system of the caudate nucleus: a combined Golgi and immunocytochemical study in cat and ferret." *Neuroscience* 24(3): 853-875.
- Bordia, T., C. Campos, J. M. McIntosh and M. Quik (2010). "Nicotinic receptor-mediated reduction in L-DOPA-induced dyskinesias may occur via desensitization." *J Pharmacol Exp Ther* 333(3): 929-938.
- Bordia, T., X. A. Perez, J. Heiss, D. Zhang and M. Quik (2016). "Optogenetic activation of striatal cholinergic interneurons regulates L-dopa-induced dyskinesias." *Neurobiol Dis* 91: 47-58.
- Bouchekioua, Y., I. Tsutsui-Kimura, H. Sano, M. Koizumi, K. F. Tanaka, K. Yoshida, Y. Kosaki, S. Watanabe and M. Mimura (2017). "Striatonigral Direct Pathway Activation is Sufficient to Induce Repetitive Behaviors." *Neurosci Res*.
- Boulland, J. L., T. Qureshi, R. P. Seal, A. Rafiki, V. Gundersen, L. H. Bergersen, R. T. Fremeau, Jr., R. H. Edwards, J. Storm-Mathisen and F. A. Chaudhry (2004). "Expression of the vesicular

glutamate transporters during development indicates the widespread corelease of multiple neurotransmitters." *J Comp Neurol* 480(3): 264-280.

Brami-Cherrier, K., E. Roze, J. A. Girault, S. Betuing and J. Caboche (2009). "Role of the ERK/MSK1 signalling pathway in chromatin remodelling and brain responses to drugs of abuse." *J Neurochem* 108(6): 1323-1335.

Breyse, N., C. Baunez, W. Spooren, F. Gasparini and M. Amalric (2002). "Chronic but not acute treatment with a metabotropic glutamate 5 receptor antagonist reverses the akinetic deficits in a rat model of parkinsonism." *J Neurosci* 22(13): 5669-5678.

Brimblecombe, K. R. and S. J. Cragg (2017). "The Striosome and Matrix Compartments of the Striatum: A Path through the Labyrinth from Neurochemistry toward Function." *ACS Chem Neurosci* 8(2): 235-242.

Brumovsky, P. R., R. P. Seal, K. H. Lundgren, K. B. Seroogy, M. Watanabe and G. F. Gebhart (2013). "Expression of vesicular glutamate transporters in sensory and autonomic neurons innervating the mouse bladder." *J Urol* 189(6): 2342-2349.

Budygin, E. A., C. E. John, Y. Mateo and S. R. Jones (2002). "Lack of cocaine effect on dopamine clearance in the core and shell of the nucleus accumbens of dopamine transporter knock-out mice." *J Neurosci* 22(10): RC222.

Burger, P. M., E. Mehl, P. L. Cameron, P. R. Maycox, M. Baumert, F. Lottspeich, P. De Camilli and R. Jahn (1989). "Synaptic vesicles immunisolated from rat cerebral cortex contain high levels of glutamate." *Neuron* 3(6): 715-720.

Cachope, R., Y. Mateo, B. N. Mathur, J. Irving, H. L. Wang, M. Morales, D. M. Lovinger and J. F. Cheer (2012). "Selective activation of cholinergic interneurons enhances accumbal phasic dopamine release: setting the tone for reward processing." *Cell Rep* 2(1): 33-41.

Cagniard, B., T. D. Sotnikova, R. R. Gainetdinov and X. Zhuang (2014). "The dopamine transporter expression level differentially affects responses to cocaine and amphetamine." *J Neurogenet* 28(1-2): 112-121.

Calabresi, P., D. Centonze, P. Gubellini, A. Pisani and G. Bernardi (2000). "Acetylcholine-mediated modulation of striatal function." *Trends Neurosci* 23(3): 120-126.

Canales, J. J. and A. M. Graybiel (2000). "A measure of striatal function predicts motor stereotypy." *Nat Neurosci* 3(4): 377-383.

Carta, M., T. Carlsson, A. Munoz, D. Kirik and A. Bjorklund (2008). "Involvement of the serotonin system in L-dopa-induced dyskinesias." *Parkinsonism Relat Disord* 14 Suppl 2: S154-158.

Carta, M., T. Carlsson, A. Munoz, D. Kirik and A. Bjorklund (2008). "Serotonin-dopamine interaction in the induction and maintenance of L-DOPA-induced dyskinesias." *Prog Brain Res* 172: 465-478.

Case, D. T., J. Alamilla and D. C. Gillespie (2014). "VGLUT3 does not synergize GABA/glycine release during functional refinement of an inhibitory auditory circuit." *Front Neural Circuits* 8: 140.

Cazorla, M., U. J. Kang and C. Kellendonk (2015). "Balancing the basal ganglia circuitry: a possible new role for dopamine D2 receptors in health and disease." *Mov Disord* 30(7): 895-903.

Cenci, M. A., V. Francardo, S. S. O'Sullivan and H. S. Lindgren (2015). "Rodent models of impulsive-compulsive behaviors in Parkinson's disease: How far have we reached?" *Neurobiol Dis* 82: 561-573.

Centonze, D., P. Gubellini, G. Bernardi and P. Calabresi (1999). "Permissive role of interneurons in corticostriatal synaptic plasticity." *Brain Res Brain Res Rev* 31(1): 1-5.

Chaudhry, F. A., R. H. Edwards and F. Fonnum (2008). "Vesicular neurotransmitter transporters as targets for endogenous and exogenous toxic substances." *Annu Rev Pharmacol Toxicol* 48: 277-301.

Cherubini, E., P. L. Herrling, L. Lanfumey and P. Stanzione (1988). "Excitatory amino acids in synaptic excitation of rat striatal neurones in vitro." *J Physiol* 400: 677-690.

Chuhma, N., S. Mingote, A. Kalmbach, L. Yetnikoff and S. Rayport (2017). "Heterogeneity in Dopamine Neuron Synaptic Actions Across the Striatum and Its Relevance for Schizophrenia." *Biol Psychiatry* 81(1): 43-51.

- Chuhma, N., S. Mingote, H. Moore and S. Rayport (2014). "Dopamine neurons control striatal cholinergic neurons via regionally heterogeneous dopamine and glutamate signaling." *Neuron* 81(4): 901-912.
- Ciesielska, A., G. Mittermeyer, P. Hadaczek, A. P. Kells, J. Forsayeth and K. S. Bankiewicz (2011). "Anterograde axonal transport of AAV2-GDNF in rat basal ganglia." *Mol Ther* 19(5): 922-927.
- Citri, A. and R. C. Malenka (2008). "Synaptic plasticity: multiple forms, functions, and mechanisms." *Neuropsychopharmacology* 33(1): 18-41.
- Clark, B. A. and B. Barbour (1997). "Currents evoked in Bergmann glial cells by parallel fibre stimulation in rat cerebellar slices." *J Physiol* 502 ( Pt 2): 335-350.
- Cohen, J. Y., M. W. Amoroso and N. Uchida (2015). "Serotonergic neurons signal reward and punishment on multiple timescales." *Elife* 4.
- Cole, V. V. and A. H. Oikemus (1954). "Some stimulant effects of sodium glutamate, oxalo-acetate, pyruvate, and malate." *Curr Res Anesth Analg* 33(4): 282-284.
- Commons, K. G. and M. R. Serock (2009). "Coincidence of neurokinin 1 receptor with the vesicular glutamate transporter 3 (VGLUT3) in the rat forebrain." *Neurosci Lett* 464(3): 188-192.
- Cools, R., K. Nakamura and N. D. Daw (2011). "Serotonin and dopamine: unifying affective, activational, and decision functions." *Neuropsychopharmacology* 36(1): 98-113.
- Costall, B., R. J. Naylor and J. E. Olley (1972). "The substantia nigra and stereotyped behaviour." *Eur J Pharmacol* 18(1): 95-106.
- Cragg, S. J. (2006). "Meaningful silences: how dopamine listens to the ACh pause." *Trends Neurosci* 29(3): 125-131.
- Crawford, L. K., C. P. Craige and S. G. Beck (2011). "Glutamatergic input is selectively increased in dorsal raphe subfield 5-HT neurons: role of morphology, topography and selective innervation." *Eur J Neurosci* 34(11): 1794-1806.
- Creese, I. and S. D. Iversen (1973). "Blockage of amphetamine induced motor stimulation and stereotypy in the adult rat following neonatal treatment with 6-hydroxydopamine." *Brain Res* 55(2): 369-382.
- Creese, I. and S. D. Iversen (1975). "The pharmacological and anatomical substrates of the amphetamine response in the rat." *Brain Res* 83(3): 419-436.
- Crittenden, J. R., I. Cantuti-Castelvetri, E. Saka, C. E. Keller-McGandy, L. F. Hernandez, L. R. Kett, A. B. Young, D. G. Standaert and A. M. Graybiel (2009). "Dysregulation of CalDAG-GEFI and CalDAG-GEFII predicts the severity of motor side-effects induced by anti-parkinsonian therapy." *Proc Natl Acad Sci U S A* 106(8): 2892-2896.
- Crittenden, J. R. and A. M. Graybiel (2011). "Basal Ganglia disorders associated with imbalances in the striatal striosome and matrix compartments." *Front Neuroanat* 5: 59.
- Crittenden, J. R., C. J. Lacey, T. Lee, H. A. Bowden and A. M. Graybiel (2014). "Severe drug-induced repetitive behaviors and striatal overexpression of VAcHT in ChAT-ChR2-EYFP BAC transgenic mice." *Front Neural Circuits* 8: 57.
- Crittenden, J. R., C. J. Lacey, F. J. Weng, C. E. Garrison, D. J. Gibson, Y. Lin and A. M. Graybiel (2017). "Striatal Cholinergic Interneurons Modulate Spike-Timing in Striosomes and Matrix by an Amphetamine-Sensitive Mechanism." *Front Neuroanat* 11: 20.
- Crittenden, J. R., P. W. Tillberg, M. H. Riad, Y. Shima, C. R. Gerfen, J. Curry, D. E. Housman, S. B. Nelson, E. S. Boyden and A. M. Graybiel (2016). "Striosome-dendron bouquets highlight a unique striatonigral circuit targeting dopamine-containing neurons." *Proc Natl Acad Sci U S A* 113(40): 11318-11323.
- Curtis, D. R., J. W. Phillis and J. C. Watkins (1959). "Chemical excitation of spinal neurones." *Nature* 183(4661): 611-612.
- Curtis, D. R., J. W. Phillis and J. C. Watkins (1960). "The chemical excitation of spinal neurones by certain acidic amino acids." *J Physiol* 150: 656-682.
- Danbolt, N. C. (2001). "Glutamate uptake." *Prog Neurobiol* 65(1): 1-105.

- Daniels, R. W., C. A. Collins, K. Chen, M. V. Gelfand, D. E. Featherstone and A. DiAntonio (2006). "A single vesicular glutamate transporter is sufficient to fill a synaptic vesicle." *Neuron* 49(1): 11-16.
- Daniels, R. W., C. A. Collins, M. V. Gelfand, J. Dant, E. S. Brooks, D. E. Krantz and A. DiAntonio (2004). "Increased expression of the *Drosophila* vesicular glutamate transporter leads to excess glutamate release and a compensatory decrease in quantal content." *J Neurosci* 24(46): 10466-10474.
- Darmopil, S., A. B. Martin, I. R. De Diego, S. Ares and R. Moratalla (2009). "Genetic inactivation of dopamine D1 but not D2 receptors inhibits L-DOPA-induced dyskinesia and histone activation." *Biol Psychiatry* 66(6): 603-613.
- Darracq, L., G. Blanc, J. Glowinski and J. P. Tassin (1998). "Importance of the noradrenaline-dopamine coupling in the locomotor activating effects of D-amphetamine." *J Neurosci* 18(7): 2729-2739.
- Darracq, L., C. Drouin, G. Blanc, J. Glowinski and J. P. Tassin (2001). "Stimulation of metabotropic but not ionotropic glutamatergic receptors in the nucleus accumbens is required for the D-amphetamine-induced release of functional dopamine." *Neuroscience* 103(2): 395-403.
- Dautan, D., I. Huerta-Ocampo, I. B. Witten, K. Deisseroth, J. P. Bolam, T. Gerdjikov and J. Mena-Segovia (2014). "A major external source of cholinergic innervation of the striatum and nucleus accumbens originates in the brainstem." *J Neurosci* 34(13): 4509-4518.
- Daw, N. D., S. Kakade and P. Dayan (2002). "Opponent interactions between serotonin and dopamine." *Neural Netw* 15(4-6): 603-616.
- DeBoer, P., M. J. Heeringa and E. D. Abercrombie (1996). "Spontaneous release of acetylcholine in striatum is preferentially regulated by inhibitory dopamine D2 receptors." *Eur J Pharmacol* 317(2-3): 257-262.
- Deffains, M. and H. Bergman (2015). "Striatal cholinergic interneurons and cortico-striatal synaptic plasticity in health and disease." *Mov Disord* 30(8): 1014-1025.
- Denker, A. and S. O. Rizzoli (2010). "Synaptic vesicle pools: an update." *Front Synaptic Neurosci* 2: 135.
- Deroche-Gamonet, V., D. Belin and P. V. Piazza (2004). "Evidence for addiction-like behavior in the rat." *Science* 305(5686): 1014-1017.
- Di Chiara, G. (2002). "Nucleus accumbens shell and core dopamine: differential role in behavior and addiction." *Behav Brain Res* 137(1-2): 75-114.
- Di Chiara, G. and A. Imperato (1988). "Drugs abused by humans preferentially increase synaptic dopamine concentrations in the mesolimbic system of freely moving rats." *Proc Natl Acad Sci U S A* 85(14): 5274-5278.
- Di Chiara, G., G. Tanda, R. Frau and E. Carboni (1993). "On the preferential release of dopamine in the nucleus accumbens by amphetamine: further evidence obtained by vertically implanted concentric dialysis probes." *Psychopharmacology (Berl)* 112(2-3): 398-402.
- Dias, V., E. Junn and M. M. Mouradian (2013). "The role of oxidative stress in Parkinson's disease." *J Parkinsons Dis* 3(4): 461-491.
- Ding, J., J. N. Guzman, T. Tkatch, S. Chen, J. A. Goldberg, P. J. Ebert, P. Levitt, C. J. Wilson, H. E. Hamm and D. J. Surmeier (2006). "RGS4-dependent attenuation of M4 autoreceptor function in striatal cholinergic interneurons following dopamine depletion." *Nat Neurosci* 9(6): 832-842.
- Ding, Y., L. Won, J. P. Britt, S. A. Lim, D. S. McGehee and U. J. Kang (2011). "Enhanced striatal cholinergic neuronal activity mediates L-DOPA-induced dyskinesia in parkinsonian mice." *Proc Natl Acad Sci U S A* 108(2): 840-845.
- Disbrow, J. K., M. J. Gershten and J. A. Ruth (1982). "Uptake of L-[3H] glutamic acid by crude and purified synaptic vesicles from rat brain." *Biochem Biophys Res Commun* 108(3): 1221-1227.
- Divito, C. B., K. Steece-Collier, D. T. Case, S. P. Williams, J. A. Stancati, L. Zhi, M. E. Rubio, C. E. Sortwell, T. J. Collier, D. Sulzer, R. H. Edwards, H. Zhang and R. P. Seal (2015). "Loss of VGLUT3 Produces Circadian-Dependent Hyperdopaminergia and Ameliorates Motor Dysfunction and L-Dopa-Mediated Dyskinesias in a Model of Parkinson's Disease." *J Neurosci* 35(45): 14983-14999.

- Dong, Y., J. R. Taylor, M. E. Wolf and Y. Shaham (2017). "Circuit and Synaptic Plasticity Mechanisms of Drug Relapse." *J Neurosci* 37(45): 10867-10876.
- Dos Santos, M., M. Salery, B. Forget, M. A. Garcia Perez, S. Betuing, T. Boudier, P. Vanhoutte, J. Caboche and N. Heck (2017). "Rapid Synaptogenesis in the Nucleus Accumbens Is Induced by a Single Cocaine Administration and Stabilized by Mitogen-Activated Protein Kinase Interacting Kinase-1 Activity." *Biol Psychiatry*.
- Draxler, P., S. D. Honsek, L. Forsthuber, V. Hadschieff and J. Sandkuhler (2014). "VGLuT3(+) primary afferents play distinct roles in mechanical and cold hypersensitivity depending on pain etiology." *J Neurosci* 34(36): 12015-12028.
- Drevets, W. C., J. C. Price, D. J. Kupfer, P. E. Kinahan, B. Lopresti, D. Holt and C. Mathis (1999). "PET measures of amphetamine-induced dopamine release in ventral versus dorsal striatum." *Neuropsychopharmacology* 21(6): 694-709.
- Drew, L. J. and A. B. MacDermott (2009). "Neuroscience: Unbearable lightness of touch." *Nature* 462(7273): 580-581.
- Dumoulin, A., P. Rostaing, C. Bedet, S. Levi, M. F. Isambert, J. P. Henry, A. Triller and B. Gasnier (1999). "Presence of the vesicular inhibitory amino acid transporter in GABAergic and glycinergic synaptic terminal boutons." *J Cell Sci* 112 ( Pt 6): 811-823.
- Edwards, R. H. (2007). "The neurotransmitter cycle and quantal size." *Neuron* 55(6): 835-858.
- Eiden, L. E. (1998). "The cholinergic gene locus." *J Neurochem* 70(6): 2227-2240.
- El Mestikawy, S., A. Wallen-Mackenzie, G. M. Fortin, L. Descarries and L. E. Trudeau (2011). "From glutamate co-release to vesicular synergy: vesicular glutamate transporters." *Nat Rev Neurosci* 12(4): 204-216.
- Ena, S., A. de Kerchove d'Exaerde and S. N. Schiffmann (2011). "Unraveling the differential functions and regulation of striatal neuron sub-populations in motor control, reward, and motivational processes." *Front Behav Neurosci* 5: 47.
- Erecinska, M. and I. A. Silver (1990). "Metabolism and role of glutamate in mammalian brain." *Prog Neurobiol* 35(4): 245-296.
- Everitt, B. J. and T. W. Robbins (2013). "From the ventral to the dorsal striatum: devolving views of their roles in drug addiction." *Neurosci Biobehav Rev* 37(9 Pt A): 1946-1954.
- Fasano, C., J. Rocchetti, K. Pietrajtis, J. F. Zander, F. Manseau, D. Y. Sakae, M. Marcus-Sells, L. Ramet, L. J. Morel, D. Carrel, S. Dumas, S. Bolte, V. Bernard, E. Vigneault, R. Goutagny, G. Ahnert-Hilger, B. Giros, S. Daumas, S. Williams and S. El Mestikawy (2017). "Regulation of the Hippocampal Network by VGLUT3-Positive CCK- GABAergic Basket Cells." *Front Cell Neurosci* 11: 140.
- Favre-Besse, F. C., O. Poirel, T. Bersot, E. Kim-Grellier, S. Daumas, S. El Mestikawy, F. C. Acher and N. Pietrancosta (2014). "Design, synthesis and biological evaluation of small-azo-dyes as potent Vesicular Glutamate Transporters inhibitors." *Eur J Med Chem* 78: 236-247.
- Fischer-Smith, K. D., A. C. Houston and G. V. Rebec (2012). "Differential effects of cocaine access and withdrawal on glutamate type 1 transporter expression in rat nucleus accumbens core and shell." *Neuroscience* 210: 333-339.
- Fog, R. L., A. Randrup and H. Pakkenberg (1967). "Aminergic mechanisms in corpus striatum and amphetamine-induced stereotyped behaviour." *Psychopharmacologia* 11(2): 179-193.
- Fonnum, F. (1984). "Glutamate: a neurotransmitter in mammalian brain." *J Neurochem* 42(1): 1-11.
- Fowler, M. W. and K. Staras (2015). "Synaptic vesicle pools: Principles, properties and limitations." *Exp Cell Res* 335(2): 150-156.
- Franklin, K. M., L. Asatryan, M. W. Jakowec, J. R. Trudell, R. L. Bell and D. L. Davies (2014). "P2X4 receptors (P2X4Rs) represent a novel target for the development of drugs to prevent and/or treat alcohol use disorders." *Front Neurosci* 8: 176.
- Frederick, A. L., H. Yano, P. Trifilieff, H. D. Vishwasrao, D. Biezonski, J. Meszaros, E. Urizar, D. R. Sibley, C. Kellendonk, K. C. Sonntag, D. L. Graham, R. J. Colbran, G. D. Stanwood and J. A. Javitch (2015). "Evidence against dopamine D1/D2 receptor heteromers." *Mol Psychiatry* 20(11): 1373-1385.

Freneau, R. T., Jr., J. Burman, T. Qureshi, C. H. Tran, J. Proctor, J. Johnson, H. Zhang, D. Sulzer, D. R. Copenhagen, J. Storm-Mathisen, R. J. Reimer, F. A. Chaudhry and R. H. Edwards (2002). "The identification of vesicular glutamate transporter 3 suggests novel modes of signaling by glutamate." *Proc Natl Acad Sci U S A* 99(22): 14488-14493.

Freneau, R. T., Jr., M. D. Troyer, I. Pahner, G. O. Nygaard, C. H. Tran, R. J. Reimer, E. E. Bellocchio, D. Fortin, J. Storm-Mathisen and R. H. Edwards (2001). "The expression of vesicular glutamate transporters defines two classes of excitatory synapse." *Neuron* 31(2): 247-260.

Freneau, R. T., Jr., S. Voglmaier, R. P. Seal and R. H. Edwards (2004). "VGLUTs define subsets of excitatory neurons and suggest novel roles for glutamate." *Trends Neurosci* 27(2): 98-103.

Fujiyama, F., T. Furuta and T. Kaneko (2001). "Immunocytochemical localization of candidates for vesicular glutamate transporters in the rat cerebral cortex." *J Comp Neurol* 435(3): 379-387.

Gagnon, D. and M. Parent (2014). "Distribution of VGLUT3 in highly collateralized axons from the rat dorsal raphe nucleus as revealed by single-neuron reconstructions." *PLoS One* 9(2): e87709.

Gagnon, D., S. Petryszyn, M. G. Sanchez, C. Bories, J. M. Beaulieu, Y. De Koninck, A. Parent and M. Parent (2017). "Striatal Neurons Expressing D1 and D2 Receptors are Morphologically Distinct and Differently Affected by Dopamine Denervation in Mice." *Sci Rep* 7: 41432.

Gammelsaeter, R., T. Coppola, P. Marcaggi, J. Storm-Mathisen, F. A. Chaudhry, D. Attwell, R. Regazzi and V. Gundersen (2011). "A role for glutamate transporters in the regulation of insulin secretion." *PLoS One* 6(8): e22960.

Gan, Q., C. L. Salussolia and L. P. Wollmuth (2015). "Assembly of AMPA receptors: mechanisms and regulation." *J Physiol* 593(1): 39-48.

Gangarossa, G., M. Guzman, V. F. Prado, M. A. Prado, S. Dumas, S. El Mestikawy and E. Valjent (2016). "Role of the atypical vesicular glutamate transporter VGLUT3 in l-DOPA-induced dyskinesia." *Neurobiol Dis* 87: 69-79.

Gangarossa, G., J. Perroy and E. Valjent (2013). "Combinatorial topography and cell-type specific regulation of the ERK pathway by dopaminergic agonists in the mouse striatum." *Brain Struct Funct* 218(2): 405-419.

Gasnier, B. (2000). "The loading of neurotransmitters into synaptic vesicles." *Biochimie* 82(4): 327-337.

Gerfen, C. R. (1992). "The neostriatal mosaic: multiple levels of compartmental organization." *Trends Neurosci* 15(4): 133-139.

Gerfen, C. R. and D. J. Surmeier (2011). "Modulation of striatal projection systems by dopamine." *Annu Rev Neurosci* 34: 441-466.

Gertler, T. S., C. S. Chan and D. J. Surmeier (2008). "Dichotomous anatomical properties of adult striatal medium spiny neurons." *J Neurosci* 28(43): 10814-10824.

Geyer, M. A., A. Puerto, D. B. Menkes, D. S. Segal and A. J. Mandell (1976). "Behavioral studies following lesions of the mesolimbic and mesostriatal serotonergic pathways." *Brain Res* 106(2): 257-269.

Gillespie, D. C., G. Kim and K. Kandler (2005). "Inhibitory synapses in the developing auditory system are glutamatergic." *Nat Neurosci* 8(3): 332-338.

Goldman-Rakic, P. S. (1982). "Cytoarchitectonic heterogeneity of the primate neostriatum: subdivision into Island and Matrix cellular compartments." *J Comp Neurol* 205(4): 398-413.

Gonzales, K. K. and Y. Smith (2015). "Cholinergic interneurons in the dorsal and ventral striatum: anatomical and functional considerations in normal and diseased conditions." *Ann N Y Acad Sci* 1349: 1-45.

Goodman, L. S., E. A. Swinyard and J. E. Toman (1946). "Effects of I (+) glutamic acid and other agents on experimental seizures." *Archives of Neurology & Psychiatry* 56(1): 20-29.

Gras, C., B. Amilhon, E. M. Lepicard, O. Poirel, J. Vinatier, M. Herbin, S. Dumas, E. T. Tzavara, M. R. Wade, G. G. Nomikos, N. Hanoun, F. Saurini, M. L. Kemel, B. Gasnier, B. Giros and S. El Mestikawy (2008). "The vesicular glutamate transporter VGLUT3 synergizes striatal acetylcholine tone." *Nat Neurosci* 11(3): 292-300.

- Gras, C., E. Herzog, G. C. Bellenchi, V. Bernard, P. Ravassard, M. Pohl, B. Gasnier, B. Giros and S. El Mestikawy (2002). "A third vesicular glutamate transporter expressed by cholinergic and serotonergic neurons." *J Neurosci* 22(13): 5442-5451.
- Gras, C., J. Vinatier, B. Amilhon, A. Guerci, C. Christov, P. Ravassard, B. Giros and S. El Mestikawy (2005). "Developmentally regulated expression of VGLUT3 during early post-natal life." *Neuropharmacology* 49(6): 901-911.
- Graybiel, A. M., J. J. Canales and C. Capper-Loup (2000). "Levodopa-induced dyskinesias and dopamine-dependent stereotypies: a new hypothesis." *Trends Neurosci* 23(10 Suppl): S71-77.
- Graybiel, A. M., R. Moratalla and H. A. Robertson (1990). "Amphetamine and cocaine induce drug-specific activation of the c-fos gene in striosome-matrix compartments and limbic subdivisions of the striatum." *Proc Natl Acad Sci U S A* 87(17): 6912-6916.
- Graybiel, A. M. and C. W. Ragsdale, Jr. (1978). "Histochemically distinct compartments in the striatum of human, monkeys, and cat demonstrated by acetylthiocholinesterase staining." *Proc Natl Acad Sci U S A* 75(11): 5723-5726.
- Greengard, P. (2001). "The neurobiology of slow synaptic transmission." *Science* 294(5544): 1024-1030.
- Guzman, M. S., X. De Jaeger, S. Raulic, I. A. Souza, A. X. Li, S. Schmid, R. S. Menon, R. R. Gainetdinov, M. G. Caron, R. Bartha, V. F. Prado and M. A. Prado (2011). "Elimination of the vesicular acetylcholine transporter in the striatum reveals regulation of behaviour by cholinergic-glutamatergic co-transmission." *PLoS Biol* 9(11): e1001194.
- Hadamitzky, M., S. McCunney, A. Markou and R. Kuczenski (2012). "Development of stereotyped behaviors during prolonged escalation of methamphetamine self-administration in rats." *Psychopharmacology (Berl)* 223(3): 259-269.
- Hallett, P. J. and D. G. Standaert (2004). "Rationale for and use of NMDA receptor antagonists in Parkinson's disease." *Pharmacol Ther* 102(2): 155-174.
- Harkany, T., C. Holmgren, W. Hartig, T. Qureshi, F. A. Chaudhry, J. Storm-Mathisen, M. B. Dobszay, P. Berghuis, G. Schulte, K. M. Sousa, R. T. Fremeau, Jr., R. H. Edwards, K. Mackie, P. Ernfors and Y. Zilberter (2004). "Endocannabinoid-independent retrograde signaling at inhibitory synapses in layer 2/3 of neocortex: involvement of vesicular glutamate transporter 3." *J Neurosci* 24(21): 4978-4988.
- Hayashi, M., M. Otsuka, R. Morimoto, S. Hirota, S. Yatsushiro, J. Takeda, A. Yamamoto and Y. Moriyama (2001). "Differentiation-associated Na<sup>+</sup>-dependent inorganic phosphate cotransporter (DNPI) is a vesicular glutamate transporter in endocrine glutamatergic systems." *J Biol Chem* 276(46): 43400-43406.
- Hayashi, T. (1952). "A physiological study of epileptic seizures following cortical stimulation in animals and its application to human clinics." *The Japanese journal of physiology* 3: 46-64.
- Hayashi, T. (1954). "Effects of sodium glutamate on the nervous system." *The Keio Journal of Medicine* 3(4): 183-192.
- Hayashi, T. (1959). "The inhibitory action of beta-hydroxy-gamma-aminobutyric acid upon the seizure following stimulation of the motor cortex of the dog." *J Physiol* 145(3): 570-578.
- Heck, N., M. Dos Santos, B. Amairi, M. Sallery, A. Besnard, E. Herzog, T. Boudier, P. Vanhoutte and J. Caboche (2015). "A new automated 3D detection of synaptic contacts reveals the formation of cortico-striatal synapses upon cocaine treatment in vivo." *Brain Struct Funct* 220(5): 2953-2966.
- Heimer, L., D. S. Zahm, L. Churchill, P. W. Kalivas and C. Wohltmann (1991). "Specificity in the projection patterns of accumbal core and shell in the rat." *Neuroscience* 41(1): 89-125.
- Hepp, R., Y. A. Hay, C. Aguado, R. Lujan, L. Dauphinot, M. C. Potier, S. Nomura, O. Poirel, S. El Mestikawy, B. Lambollez and L. Tricoire (2015). "Glutamate receptors of the delta family are widely expressed in the adult brain." *Brain Struct Funct* 220(5): 2797-2815.
- Herculano-Houzel, S. (2009). "The human brain in numbers: a linearly scaled-up primate brain." *Front Hum Neurosci* 3: 31.
- Herzog, E., G. C. Bellenchi, C. Gras, V. Bernard, P. Ravassard, C. Bedet, B. Gasnier, B. Giros and S. El Mestikawy (2001). "The existence of a second vesicular glutamate transporter specifies subpopulations of glutamatergic neurons." *J Neurosci* 21(22): RC181.

Herzog, E., J. Gilchrist, C. Gras, A. Muzerelle, P. Ravassard, B. Giros, P. Gaspar and S. El Mestikawy (2004). "Localization of VGLUT3, the vesicular glutamate transporter type 3, in the rat brain." *Neuroscience* 123(4): 983-1002.

Herzog, E., F. Nadrigny, K. Silm, C. Biesemann, I. Helling, T. Bersot, H. Steffens, R. Schwartzmann, U. V. Nagerl, S. El Mestikawy, J. Rhee, F. Kirchhoff and N. Brose (2011). "In vivo imaging of intersynaptic vesicle exchange using VGLUT1 Venus knock-in mice." *J Neurosci* 31(43): 15544-15559.

Higley, M. J., A. H. Gittis, I. A. Oldenburg, N. Balthasar, R. P. Seal, R. H. Edwards, B. B. Lowell, A. C. Kreitzer and B. L. Sabatini (2011). "Cholinergic interneurons mediate fast VGLUT3-dependent glutamatergic transmission in the striatum." *PLoS One* 6(4): e19155.

Hikida, T., S. Kaneko, T. Isobe, Y. Kitabatake, D. Watanabe, I. Pastan and S. Nakanishi (2001). "Increased sensitivity to cocaine by cholinergic cell ablation in nucleus accumbens." *Proc Natl Acad Sci U S A* 98(23): 13351-13354.

Hikida, T., Y. Kitabatake, I. Pastan and S. Nakanishi (2003). "Acetylcholine enhancement in the nucleus accumbens prevents addictive behaviors of cocaine and morphine." *Proc Natl Acad Sci U S A* 100(10): 6169-6173.

Hintiryan, H., N. N. Foster, I. Bowman, M. Bay, M. Y. Song, L. Gou, S. Yamashita, M. S. Bienkowski, B. Zingg, M. Zhu, X. W. Yang, J. C. Shih, A. W. Toga and H. W. Dong (2016). "The mouse cortico-striatal projectome." *Nat Neurosci* 19(8): 1100-1114.

Hioki, H., F. Fujiyama, K. Nakamura, S. X. Wu, W. Matsuda and T. Kaneko (2004). "Chemically specific circuit composed of vesicular glutamate transporter 3- and preprotachykinin B-producing interneurons in the rat neocortex." *Cereb Cortex* 14(11): 1266-1275.

Hioki, H., H. Nakamura, Y. F. Ma, M. Konno, T. Hayakawa, K. C. Nakamura, F. Fujiyama and T. Kaneko (2010). "Vesicular glutamate transporter 3-expressing nonserotonergic projection neurons constitute a subregion in the rat midbrain raphe nuclei." *J Comp Neurol* 518(5): 668-686.

Hnasko, T. S. and R. H. Edwards (2012). "Neurotransmitter corelease: mechanism and physiological role." *Annu Rev Physiol* 74: 225-243.

Hokfelt, T., O. Johansson and M. Goldstein (1984). "Chemical anatomy of the brain." *Science* 225(4668): 1326-1334.

Hope, B. T., H. E. Nye, M. B. Kelz, D. W. Self, M. J. Iadarola, Y. Nakabeppu, R. S. Duman and E. J. Nestler (1994). "Induction of a long-lasting AP-1 complex composed of altered Fos-like proteins in brain by chronic cocaine and other chronic treatments." *Neuron* 13(5): 1235-1244.

Huh, C. Y., M. Danik, F. Manseau, L. E. Trudeau and S. Williams (2008). "Chronic exposure to nerve growth factor increases acetylcholine and glutamate release from cholinergic neurons of the rat medial septum and diagonal band of Broca via mechanisms mediated by p75NTR." *J Neurosci* 28(6): 1404-1409.

Hunnicut, B. J., B. C. Jongbloets, W. T. Birdsong, K. J. Gertz, H. Zhong and T. Mao (2016). "A comprehensive excitatory input map of the striatum reveals novel functional organization." *Elife* 5.

Ikemoto, A., D. G. Bole and T. Ueda (2003). "Glycolysis and glutamate accumulation into synaptic vesicles. Role of glyceraldehyde phosphate dehydrogenase and 3-phosphoglycerate kinase." *J Biol Chem* 278(8): 5929-5940.

Irving, A. J. and J. Harvey (2014). "Leptin regulation of hippocampal synaptic function in health and disease." *Philos Trans R Soc Lond B Biol Sci* 369(1633): 20130155.

Iversen, C. (1975). "The pharmacological and anatomical substrates of the amphetamine response in the rat brain."

Iversen, S. D., P. H. Kelly, R. J. Miller and P. Seviour (1975). "Proceedings: Amphetamine and apomorphine responses in the rat after lesion of mesolimbic or striatal dopamine neurones." *Br J Pharmacol* 54(2): 244P.

Jedynak, J. P., J. M. Uslaner, J. A. Esteban and T. E. Robinson (2007). "Methamphetamine-induced structural plasticity in the dorsal striatum." *Eur J Neurosci* 25(3): 847-853.

Jiang, Z. G. and R. A. North (1991). "Membrane properties and synaptic responses of rat striatal neurones in vitro." *J Physiol* 443: 533-553.

- Johnson, M. D. (1994). "Synaptic glutamate release by postnatal rat serotonergic neurons in microculture." *Neuron* 12(2): 433-442.
- Juge, N., Y. Yoshida, S. Yatsushiro, H. Omote and Y. Moriyama (2006). "Vesicular glutamate transporter contains two independent transport machineries." *J Biol Chem* 281(51): 39499-39506.
- Jung, H. J., C. H. Shin and S. B. Hong (2005). "Si distribution in silicoaluminophosphate molecular sieves with the LEV topology: a solid-state NMR study." *J Phys Chem B* 109(44): 20847-20853.
- Kaneko, S., T. Hikida, D. Watanabe, H. Ichinose, T. Nagatsu, R. J. Kreitman, I. Pastan and S. Nakanishi (2000). "Synaptic integration mediated by striatal cholinergic interneurons in basal ganglia function." *Science* 289(5479): 633-637.
- Kaneko, T. and F. Fujiyama (2002). "Complementary distribution of vesicular glutamate transporters in the central nervous system." *Neurosci Res* 42(4): 243-250.
- Karler, R., L. D. Calder, D. K. Thai and J. B. Bedingfield (1998). "The role of dopamine and GABA in the frontal cortex of mice in modulating a motor-stimulant effect of amphetamine and cocaine." *Pharmacol Biochem Behav* 60(1): 237-244.
- Karler, R., L. D. Calder, L. H. Thai and J. B. Bedingfield (1994). "A dopaminergic-glutamatergic basis for the action of amphetamine and cocaine." *Brain Res* 658(1-2): 8-14.
- Katz, B. (1979). "Elementary components of synaptic transmission." *Naturwissenschaften* 66(12): 606-610.
- Kawaguchi, Y., C. J. Wilson, S. J. Augood and P. C. Emson (1995). "Striatal interneurons: chemical, physiological and morphological characterization." *Trends Neurosci* 18(12): 527-535.
- Kehrl, J., J. C. Althaus, H. D. Showalter, D. M. Rudzinski, M. A. Sutton and T. Ueda (2017). "Vesicular Glutamate Transporter Inhibitors: Structurally Modified Brilliant Yellow Analogs." *Neurochem Res* 42(6): 1823-1832.
- Kelley, A. E. (2001). "Measurement of rodent stereotyped behavior." *Curr Protoc Neurosci Chapter 8: Unit 8 8*.
- Kelley, A. E. and J. M. Delfs (1994). "Excitatory amino acid receptors mediate the orofacial stereotypy elicited by dopaminergic stimulation of the ventrolateral striatum." *Neuroscience* 60(1): 85-95.
- Kelly, P. H., P. W. Seviour and S. D. Iversen (1975). "Amphetamine and apomorphine responses in the rat following 6-OHDA lesions of the nucleus accumbens septi and corpus striatum." *Brain Res* 94(3): 507-522.
- Kemel, M. L., M. Desban, J. Glowinski and C. Gauchy (1989). "Distinct presynaptic control of dopamine release in striosomal and matrix areas of the cat caudate nucleus." *Proc Natl Acad Sci U S A* 86(22): 9006-9010.
- Kim, S. J., M. Lewis and J. Veenstra-VanderWeele (2013). "The Developmental Neurobiology of Repetitive Behavior." 761-782.
- Kimura, M. (1986). "The role of primate putamen neurons in the association of sensory stimuli with movement." *Neurosci Res* 3(5): 436-443.
- Kimura, M., J. Rajkowski and E. Evarts (1984). "Tonically discharging putamen neurons exhibit set-dependent responses." *Proc Natl Acad Sci U S A* 81(15): 4998-5001.
- Kitabatake, Y., T. Hikida, D. Watanabe, I. Pastan and S. Nakanishi (2003). "Impairment of reward-related learning by cholinergic cell ablation in the striatum." *Proc Natl Acad Sci U S A* 100(13): 7965-7970.
- Kiyasova, V., S. P. Fernandez, J. Laine, L. Stankovski, A. Muzerelle, S. Doly and P. Gaspar (2011). "A genetically defined morphologically and functionally unique subset of 5-HT neurons in the mouse raphe nuclei." *J Neurosci* 31(8): 2756-2768.
- Kljakic, O., H. Janickova, V. F. Prado and M. A. M. Prado (2017). "Cholinergic/glutamatergic co-transmission in striatal cholinergic interneurons: new mechanisms regulating striatal computation." *J Neurochem* 142 Suppl 2: 90-102.
- Kochman, L. J., A. A. dos Santos, C. A. Fornal and B. L. Jacobs (2006). "Despite strong behavioral disruption, Delta9-tetrahydrocannabinol does not affect cell proliferation in the adult mouse dentate gyrus." *Brain Res* 1113(1): 86-93.

- Koizumi, H., R. Morigaki, S. Okita, S. Nagahiro, R. Kaji, M. Nakagawa and S. Goto (2013). "Response of striosomal opioid signaling to dopamine depletion in 6-hydroxydopamine-lesioned rat model of Parkinson's disease: a potential compensatory role." *Front Cell Neurosci* 7: 74.
- Kolb, B., G. Gorny, Y. Li, A. N. Samaha and T. E. Robinson (2003). "Amphetamine or cocaine limits the ability of later experience to promote structural plasticity in the neocortex and nucleus accumbens." *Proc Natl Acad Sci U S A* 100(18): 10523-10528.
- Koob, G. F. (2005). "The neurocircuitry of addiction: Implications for treatment." *Clinical Neuroscience Research* 5(2-4): 89-101.
- Koprach, J. B., S. H. Fox, T. H. Johnston, A. Goodman, B. Le Bourdonnec, R. E. Dolle, R. N. DeHaven, D. L. DeHaven-Hudkins, P. J. Little and J. M. Brotchie (2011). "The selective mu-opioid receptor antagonist ADL5510 reduces levodopa-induced dyskinesia without affecting antiparkinsonian action in MPTP-lesioned macaque model of Parkinson's disease." *Mov Disord* 26(7): 1225-1233.
- Kordower, J. H. and C. W. Olanow (2016). "Fetal grafts for Parkinson's disease: Decades in the making." *Proc Natl Acad Sci U S A* 113(23): 6332-6334.
- Korogod, N., C. C. Petersen and G. W. Knott (2015). "Ultrastructural analysis of adult mouse neocortex comparing aldehyde perfusion with cryo fixation." *Elife* 4.
- Koshimori, Y., J. H. Ko, R. Mizrahi, P. Rusjan, R. Mabrouk, M. F. Jacobs, L. Christopher, C. Hamani, A. E. Lang, A. A. Wilson, S. Houle and A. P. Strafella (2015). "Imaging Striatal Microglial Activation in Patients with Parkinson's Disease." *PLoS One* 10(9): e0138721.
- Krebs, H. A. (1935). "Metabolism of amino-acids: The synthesis of glutamine from glutamic acid and ammonia, and the enzymic hydrolysis of glutamine in animal tissues." *Biochem J* 29(8): 1951-1969.
- Krebs, H. A., L. V. Eggleston and R. Hems (1949). "Distribution of glutamine and glutamic acid in animal tissues." *Biochem J* 44(2): 159-163.
- Kreitzer, A. C. (2009). "Physiology and pharmacology of striatal neurons." *Annu Rev Neurosci* 32: 127-147.
- Kuczenski, R. and D. Segal (1989). "Concomitant characterization of behavioral and striatal neurotransmitter response to amphetamine using in vivo microdialysis." *J Neurosci* 9(6): 2051-2065.
- Kugler, S., E. Kilic and M. Bahr (2003). "Human synapsin 1 gene promoter confers highly neuron-specific long-term transgene expression from an adenoviral vector in the adult rat brain depending on the transduced area." *Gene Ther* 10(4): 337-347.
- Kuhar, M. J. and S. H. Snyder (1970). "The subcellular distribution of free H<sup>3</sup>-glutamic acid in rat cerebral cortical slices." *J Pharmacol Exp Ther* 171(1): 141-152.
- Kyte, J. and R. F. Doolittle (1982). "A simple method for displaying the hydropathic character of a protein." *J Mol Biol* 157(1): 105-132.
- Lamprecht, R. and J. LeDoux (2004). "Structural plasticity and memory." *Nat Rev Neurosci* 5(1): 45-54.
- Langen, M., M. J. Kas, W. G. Staal, H. van Engeland and S. Durston (2011). "The neurobiology of repetitive behavior: of mice." *Neurosci Biobehav Rev* 35(3): 345-355.
- Lei, W., Y. Jiao, N. Del Mar and A. Reiner (2004). "Evidence for differential cortical input to direct pathway versus indirect pathway striatal projection neurons in rats." *J Neurosci* 24(38): 8289-8299.
- Li, Y., B. Kolb and T. E. Robinson (2003). "The location of persistent amphetamine-induced changes in the density of dendritic spines on medium spiny neurons in the nucleus accumbens and caudate-putamen." *Neuropsychopharmacology* 28(6): 1082-1085.
- Lim, S. A., U. J. Kang and D. S. McGehee (2014). "Striatal cholinergic interneuron regulation and circuit effects." *Front Synaptic Neurosci* 6: 22.
- Liu, Z., J. Zhou, Y. Li, F. Hu, Y. Lu, M. Ma, Q. Feng, J. E. Zhang, D. Wang, J. Zeng, J. Bao, J. Y. Kim, Z. F. Chen, S. El Mestikawy and M. Luo (2014). "Dorsal raphe neurons signal reward through 5-HT and glutamate." *Neuron* 81(6): 1360-1374.

- Lobo, M. K. and E. J. Nestler (2011). "The striatal balancing act in drug addiction: distinct roles of direct and indirect pathway medium spiny neurons." *Front Neuroanat* 5: 41.
- Lobo, M. K., S. Zaman, D. M. Damez-Werno, J. W. Koo, R. C. Bagot, J. A. DiNieri, A. Nugent, E. Finkel, D. Chaudhury, R. Chandra, E. Riberio, J. Rabkin, E. Mouzon, R. Cachepe, J. F. Cheer, M. H. Han, D. M. Dietz, D. W. Self, Y. L. Hurd, V. Vialou and E. J. Nestler (2013). "DeltaFosB induction in striatal medium spiny neuron subtypes in response to chronic pharmacological, emotional, and optogenetic stimuli." *J Neurosci* 33(47): 18381-18395.
- Lodge, D. (2009). "The history of the pharmacology and cloning of ionotropic glutamate receptors and the development of idiosyncratic nomenclature." *Neuropharmacology* 56(1): 6-21.
- Luscher, C. (2016). "The Emergence of a Circuit Model for Addiction." *Annu Rev Neurosci* 39: 257-276.
- Luscher, C. and R. C. Malenka (2012). "NMDA receptor-dependent long-term potentiation and long-term depression (LTP/LTD)." *Cold Spring Harb Perspect Biol* 4(6).
- Luscher, C. and M. A. Ungless (2006). "The mechanistic classification of addictive drugs." *PLoS Med* 3(11): e437.
- Mandel, R. J., G. Leanza, O. G. Nilsson and E. Rosengren (1994). "Amphetamine induces excess release of striatal acetylcholine in vivo that is independent of nigrostriatal dopamine." *Brain Res* 653(1-2): 57-65.
- Marcus, E. M. and S. Jacobson (2003). *Physiology. Integrated Neuroscience*, Springer: 107-125.
- Marin, O., S. A. Anderson and J. L. Rubenstein (2000). "Origin and molecular specification of striatal interneurons." *J Neurosci* 20(16): 6063-6076.
- Matamales, M., J. Bertran-Gonzalez, L. Salomon, B. Degos, J. M. Deniau, E. Valjent, D. Herve and J. A. Girault (2009). "Striatal medium-sized spiny neurons: identification by nuclear staining and study of neuronal subpopulations in BAC transgenic mice." *PLoS One* 4(3): e4770.
- Matamales, M., J. Gotz and J. Bertran-Gonzalez (2016). "Quantitative Imaging of Cholinergic Interneurons Reveals a Distinctive Spatial Organization and a Functional Gradient across the Mouse Striatum." *PLoS One* 11(6): e0157682.
- Maycox, P. R., J. W. Hell and R. Jahn (1990). "Amino acid neurotransmission: spotlight on synaptic vesicles." *Trends Neurosci* 13(3): 83-87.
- McGeorge, A. J. and R. L. Faull (1989). "The organization of the projection from the cerebral cortex to the striatum in the rat." *Neuroscience* 29(3): 503-537.
- Meldrum, B. S. (2000). "Glutamate as a neurotransmitter in the brain: review of physiology and pathology." *J Nutr* 130(4S Suppl): 1007S-1015S.
- Meyerhoff, D. J. (2017). "Structural Neuroimaging in Polysubstance Users." *Curr Opin Behav Sci* 13: 13-18.
- Morin, N., V. A. Jourdain and T. Di Paolo (2014). "Modeling dyskinesia in animal models of Parkinson disease." *Exp Neurol* 256: 105-116.
- Morris, G., D. Arkadir, A. Nevet, E. Vaadia and H. Bergman (2004). "Coincident but distinct messages of midbrain dopamine and striatal tonically active neurons." *Neuron* 43(1): 133-143.
- Murer, M. G. and R. Moratalla (2011). "Striatal Signaling in L-DOPA-Induced Dyskinesia: Common Mechanisms with Drug Abuse and Long Term Memory Involving D1 Dopamine Receptor Stimulation." *Front Neuroanat* 5: 51.
- Mutch, S. A., P. Kensel-Hammes, J. C. Gadd, B. S. Fujimoto, R. W. Allen, P. G. Schiro, R. M. Lorenz, C. L. Kuyper, J. S. Kuo, S. M. Bajjalieh and D. T. Chiu (2011). "Protein quantification at the single vesicle level reveals that a subset of synaptic vesicle proteins are trafficked with high precision." *J Neurosci* 31(4): 1461-1470.
- Nagai, H., K. Kuwabara and G. Carta (2008). "Temperature Dependence of the Dissociation Constants of Several Amino Acids." *Journal of Chemical & Engineering Data* 53(3): 619-627.
- Nagy, A. (2000). "Cre recombinase: the universal reagent for genome tailoring." *Genesis* 26(2): 99-109.
- Nakamura, K., K. Matsumura, T. Hubschle, Y. Nakamura, H. Hioki, F. Fujiyama, Z. Boldogkoi, M. Konig, H. J. Thiel, R. Gerstberger, S. Kobayashi and T. Kaneko (2004). "Identification of

sympathetic premotor neurons in medullary raphe regions mediating fever and other thermoregulatory functions." *J Neurosci* 24(23): 5370-5380.

Nelson, A. B., T. G. Bussert, A. C. Kreitzer and R. P. Seal (2014). "Striatal cholinergic neurotransmission requires VGLUT3." *J Neurosci* 34(26): 8772-8777.

Nelson, N. (1987). "The vacuolar proton-ATPase of eukaryotic cells." *Bioessays* 7(6): 251-254.

Nestler, E. J. (2005). "Is there a common molecular pathway for addiction?" *Nat Neurosci* 8(11): 1445-1449.

Ni, B., P. R. Rosteck, Jr., N. S. Nadi and S. M. Paul (1994). "Cloning and expression of a cDNA encoding a brain-specific Na(+)-dependent inorganic phosphate cotransporter." *Proc Natl Acad Sci U S A* 91(12): 5607-5611.

Nicholls, D. and D. Attwell (1990). "The release and uptake of excitatory amino acids." *Trends Pharmacol Sci* 11(11): 462-468.

Niciu, M. J., B. Kelmendi and G. Sanacora (2012). "Overview of glutamatergic neurotransmission in the nervous system." *Pharmacol Biochem Behav* 100(4): 656-664.

Nickerson Poulin, A., A. Guerci, S. El Mestikawy and K. Semba (2006). "Vesicular glutamate transporter 3 immunoreactivity is present in cholinergic basal forebrain neurons projecting to the basolateral amygdala in rat." *J Comp Neurol* 498(5): 690-711.

Nistico, R., F. Mori, M. Feligioni, F. Nicoletti and D. Centonze (2014). "Synaptic plasticity in multiple sclerosis and in experimental autoimmune encephalomyelitis." *Philos Trans R Soc Lond B Biol Sci* 369(1633): 20130162.

Nowak, L., P. Bregestovski, P. Ascher, A. Herbet and A. Prochiantz (1984). "Magnesium gates glutamate-activated channels in mouse central neurones." *Nature* 307(5950): 462-465.

Oliveira, A. L., F. Hydling, E. Olsson, T. Shi, R. H. Edwards, F. Fujiyama, T. Kaneko, T. Hokfelt, S. Cullheim and B. Meister (2003). "Cellular localization of three vesicular glutamate transporter mRNAs and proteins in rat spinal cord and dorsal root ganglia." *Synapse* 50(2): 117-129.

Omote, H., T. Miyaji, N. Juge and Y. Moriyama (2011). "Vesicular neurotransmitter transporter: bioenergetics and regulation of glutamate transport." *Biochemistry* 50(25): 5558-5565.

Otis, T. S. (2001). "Vesicular glutamate transporters in cognition." *Neuron* 29(1): 11-14.

Ozkan, E. D. and T. Ueda (1998). "Glutamate transport and storage in synaptic vesicles." *Jpn J Pharmacol* 77(1): 1-10.

Paoletti, P., C. Bellone and Q. Zhou (2013). "NMDA receptor subunit diversity: impact on receptor properties, synaptic plasticity and disease." *Nat Rev Neurosci* 14(6): 383-400.

Park, M. R., J. A. Gonzales-Vegas and S. T. Kitai (1982). "Serotonergic excitation from dorsal raphe stimulation recorded intracellularly from rat caudate-putamen." *Brain Res* 243(1): 49-58.

Park, P., A. Volianskis, T. M. Sanderson, Z. A. Bortolotto, D. E. Jane, M. Zhuo, B. K. Kaang and G. L. Collingridge (2014). "NMDA receptor-dependent long-term potentiation comprises a family of temporally overlapping forms of synaptic plasticity that are induced by different patterns of stimulation." *Philos Trans R Soc Lond B Biol Sci* 369(1633): 20130131.

Pascoli, V., E. Valjent, A. G. Corbille, J. C. Corvol, J. P. Tassin, J. A. Girault and D. Herve (2005). "cAMP and extracellular signal-regulated kinase signaling in response to d-amphetamine and methylphenidate in the prefrontal cortex in vivo: role of beta 1-adrenoceptors." *Mol Pharmacol* 68(2): 421-429.

Perea, G., M. Navarrete and A. Araque (2009). "Tripartite synapses: astrocytes process and control synaptic information." *Trends Neurosci* 32(8): 421-431.

Perreault, M. L., A. Hasbi, M. Alijaniam, T. Fan, G. Varghese, P. J. Fletcher, P. Seeman, B. F. O'Dowd and S. R. George (2010). "The dopamine D1-D2 receptor heteromer localizes in dynorphin/enkephalin neurons: increased high affinity state following amphetamine and in schizophrenia." *J Biol Chem* 285(47): 36625-36634.

Perreault, M. L., A. Hasbi, B. F. O'Dowd and S. R. George (2011). "The dopamine d1-d2 receptor heteromer in striatal medium spiny neurons: evidence for a third distinct neuronal pathway in Basal Ganglia." *Front Neuroanat* 5: 31.

- Peter, Z., M. E. Oliphant and T. V. Fernandez (2017). "Motor Stereotypies: A Pathophysiological Review." *Front Neurosci* 11: 171.
- Pietrancosta, N., A. Kessler, F. C. Favre-Besse, N. Triballeau, T. Quentin, B. Giros, S. El Mestikawy and F. C. Acher (2010). "Rose Bengal analogs and vesicular glutamate transporters (VGLUTs)." *Bioorg Med Chem* 18(18): 6922-6933.
- Pinheiro, P. S. and C. Mulle (2008). "Presynaptic glutamate receptors: physiological functions and mechanisms of action." *Nat Rev Neurosci* 9(6): 423-436.
- Pond, D. and M. Pond (1951). "Glutamic acid and its salts in petit mal epilepsy." *The Journal of mental science* 97(409): 663.
- Prado, V. F., H. Janickova, M. A. Al-Onaizi and M. A. Prado (2017). "Cholinergic circuits in cognitive flexibility." *Neuroscience* 345: 130-141.
- Preobraschenski, J., J. F. Zander, T. Suzuki, G. Ahnert-Hilger and R. Jahn (2014). "Vesicular glutamate transporters use flexible anion and cation binding sites for efficient accumulation of neurotransmitter." *Neuron* 84(6): 1287-1301.
- Purves, D., G. J. Augustine, D. Fitzpatrick, W. C. Hall, A.-S. LaMantia and L. E. White (2012). *Neuroscience*, Sinauer.
- Pycock, C. J. (1980). "Turning behaviour in animals." *Neuroscience* 5(3): 461-514.
- Qi, J., S. Zhang, H. L. Wang, H. Wang, J. de Jesus Aceves Buendia, A. F. Hoffman, C. R. Lupica, R. P. Seal and M. Morales (2014). "A glutamatergic reward input from the dorsal raphe to ventral tegmental area dopamine neurons." *Nat Commun* 5: 5390.
- Quik, M., T. Bordia and K. O'Leary (2007). "Nicotinic receptors as CNS targets for Parkinson's disease." *Biochem Pharmacol* 74(8): 1224-1234.
- Ramet, L., J. Zimmermann, T. Bersot, O. Poirel, S. De Gois, K. Silm, D. Y. Sakae, N. Mansouri-Guilani, M. J. Bourque, L. E. Trudeau, N. Pietrancosta, S. Dumas, V. Bernard, C. Rosenmund and S. El Mestikawy (2017). "Characterization of a Human Point Mutation of VGLUT3 (p.A211V) in the Rodent Brain Suggests a Nonuniform Distribution of the Transporter in Synaptic Vesicles." *J Neurosci* 37(15): 4181-4199.
- Randrup, A. and I. Munkvad (1967). "Brain dopamine and amphetamine-induced stereotyped behaviour." *Acta Pharmacol Toxicol (Copenh)* 25: Suppl 4:62.
- Randrup, A. and I. Munkvad (1967). "Stereotyped activities produced by amphetamine in several animal species and man." *Psychopharmacologia* 11(4): 300-310.
- Randrup, A., I. Munkvad, R. Fog and I. Ayhan (1975). *Catecholamines in activation, stereotypy, and level of mood. Catecholamines and Behavior*. 1, Springer: 89-107.
- Rascol, O., S. Fox, F. Gasparini, C. Kenney, T. Di Paolo and B. Gomez-Mancilla (2014). "Use of metabotropic glutamate 5-receptor antagonists for treatment of levodopa-induced dyskinesias." *Parkinsonism Relat Disord* 20(9): 947-956.
- Ren, K., B. Guo, C. Dai, H. Yao, T. Sun, X. Liu, Z. Bai, W. Wang and S. Wu (2017). "Striatal Distribution and Cytoarchitecture of Dopamine Receptor Subtype 1 and 2: Evidence from Double-Labeling Transgenic Mice." *Front Neural Circuits* 11: 57.
- Renoir, T., T. Y. Pang and L. Lanfumey (2012). "Drug withdrawal-induced depression: serotonergic and plasticity changes in animal models." *Neurosci Biobehav Rev* 36(1): 696-726.
- Ritthausen, H. (1866). "Ueber die Glutaminsäure." *Journal für Praktische Chemie* 99(1): 454-462.
- Ritthausen, H. (1869). "Asparaginsäure und Glutaminsäure, Zersetzungsproducte des Legumins und Conglutins beim Kochen mit Schwefelsäure." *Journal für Praktische Chemie* 107(1): 218-240.
- Rizzoli, S. O. and W. J. Betz (2005). "Synaptic vesicle pools." *Nat Rev Neurosci* 6(1): 57-69.
- Roberts, E. and S. Frankel (1950). "gamma-Aminobutyric acid in brain: its formation from glutamic acid." *J Biol Chem* 187(1): 55-63.
- Robinson, T. E. and J. B. Becker (1986). "Enduring changes in brain and behavior produced by chronic amphetamine administration: a review and evaluation of animal models of amphetamine psychosis." *Brain Res* 396(2): 157-198.

- Robinson, T. E. and B. Kolb (2004). "Structural plasticity associated with exposure to drugs of abuse." *Neuropharmacology* 47 Suppl 1: 33-46.
- Robison, A. J. and E. J. Nestler (2011). "Transcriptional and epigenetic mechanisms of addiction." *Nat Rev Neurosci* 12(11): 623-637.
- Rondard, P., C. Goudet, J. Kniazeff, J. P. Pin and L. Prezeau (2011). "The complexity of their activation mechanism opens new possibilities for the modulation of mGlu and GABAB class C G protein-coupled receptors." *Neuropharmacology* 60(1): 82-92.
- Rossi, M. A. and H. H. Yin (2012). "Methods for studying habitual behavior in mice." *Curr Protoc Neurosci* Chapter 8: Unit 8 29.
- Ruel, J., S. Emery, R. Nouvian, T. Bersot, B. Amilhon, J. M. Van Rybroek, G. Rebillard, M. Lenoir, M. Eybalin, B. Delprat, T. A. Sivakumaran, B. Giros, S. El Mestikawy, T. Moser, R. J. Smith, M. M. Lesperance and J. L. Puel (2008). "Impairment of SLC17A8 encoding vesicular glutamate transporter-3, VGLUT3, underlies nonsyndromic deafness DFNA25 and inner hair cell dysfunction in null mice." *Am J Hum Genet* 83(2): 278-292.
- Russell, R. L. and R. O. Pihl (1978). "The effect of dose, novelty, and exploration on amphetamine-produced stereotyped behavior." *Psychopharmacology (Berl)* 60(1): 93-100.
- Russo, S. J., D. M. Dietz, D. Dumitriu, J. H. Morrison, R. C. Malenka and E. J. Nestler (2010). "The addicted synapse: mechanisms of synaptic and structural plasticity in nucleus accumbens." *Trends Neurosci* 33(6): 267-276.
- Russo, S. J. and E. J. Nestler (2013). "The brain reward circuitry in mood disorders." *Nat Rev Neurosci* 14(9): 609-625.
- Saka, E., M. Iadarola, D. J. Fitzgerald and A. M. Graybiel (2002). "Local circuit neurons in the striatum regulate neural and behavioral responses to dopaminergic stimulation." *Proc Natl Acad Sci U S A* 99(13): 9004-9009.
- Sakae, D. Y., F. Marti, S. Lecca, F. Vorspan, E. Martin-Garcia, L. J. Morel, A. Henrion, J. Gutierrez-Cuesta, A. Besnard, N. Heck, E. Herzog, S. Bolte, V. F. Prado, M. A. Prado, F. Bellivier, C. B. Eap, S. Crettol, P. Vanhoutte, J. Caboche, A. Gratton, L. Moquin, B. Giros, R. Maldonado, S. Daumas, M. Mameli, S. Jamain and S. El Mestikawy (2015). "The absence of VGLUT3 predisposes to cocaine abuse by increasing dopamine and glutamate signaling in the nucleus accumbens." *Mol Psychiatry* 20(11): 1448-1459.
- Salomon, L., C. Lanteri, J. Glowinski and J. P. Tassin (2006). "Behavioral sensitization to amphetamine results from an uncoupling between noradrenergic and serotonergic neurons." *Proc Natl Acad Sci U S A* 103(19): 7476-7481.
- Salomon, L., C. Lanteri, G. Godeheu, G. Blanc, J. Gingrich and J. P. Tassin (2007). "Paradoxical constitutive behavioral sensitization to amphetamine in mice lacking 5-HT2A receptors." *Psychopharmacology (Berl)* 194(1): 11-20.
- Sanders, A. C., A. J. Hussain, R. Hen and X. Zhuang (2007). "Chronic blockade or constitutive deletion of the serotonin transporter reduces operant responding for food reward." *Neuropsychopharmacology* 32(11): 2321-2329.
- Schafer, M. K., H. Varoqui, N. Defamie, E. Weihe and J. D. Erickson (2002). "Molecular cloning and functional identification of mouse vesicular glutamate transporter 3 and its expression in subsets of novel excitatory neurons." *J Biol Chem* 277(52): 50734-50748.
- Schenck, S., L. Kunz, D. Sahlender, E. Pardon, E. R. Geertsma, I. Savtchouk, T. Suzuki, Y. Neldner, S. Stefanic, J. Steyaert, A. Volterra and R. Dutzler (2017). "Generation and Characterization of Anti-VGLUT Nanobodies Acting as Inhibitors of Transport." *Biochemistry* 56(30): 3962-3971.
- Schiorring, E. (1979). "An open field study of stereotyped locomotor activity in amphetamine-treated rats." *Psychopharmacology (Berl)* 66(3): 281-287.
- Schultz, W., P. Dayan and P. R. Montague (1997). "A neural substrate of prediction and reward." *Science* 275(5306): 1593-1599.
- Schwartz, T. L., S. Sachdeva and S. M. Stahl (2012). "Glutamate neurocircuitry: theoretical underpinnings in schizophrenia." *Front Pharmacol* 3: 195.
- Schwerin, P., S. P. Bessman and H. Waelsch (1950). "The uptake of glutamic acid and glutamine by brain and other tissues of the rat and mouse." *J Biol Chem* 184(1): 37-44.

- Seal, R. P., O. Akil, E. Yi, C. M. Weber, L. Grant, J. Yoo, A. Clause, K. Kandler, J. L. Noebels, E. Glowatzki, L. R. Lustig and R. H. Edwards (2008). "Sensorineural deafness and seizures in mice lacking vesicular glutamate transporter 3." *Neuron* 57(2): 263-275.
- Seal, R. P., X. Wang, Y. Guan, S. N. Raja, C. J. Woodbury, A. I. Basbaum and R. H. Edwards (2009). "Injury-induced mechanical hypersensitivity requires C-low threshold mechanoreceptors." *Nature* 462(7273): 651-655.
- Shutoh, F., A. Ina, S. Yoshida, J. Konno and S. Hisano (2008). "Two distinct subtypes of serotonergic fibers classified by co-expression with vesicular glutamate transporter 3 in rat forebrain." *Neurosci Lett* 432(2): 132-136.
- Singh, R. A., T. A. Kosten, B. M. Kinsey, X. Shen, A. Y. Lopez, T. R. Kosten and F. M. Orson (2012). "Dose-dependent changes in the locomotor responses to methamphetamine in BALB/c mice: low doses induce hypolocomotion." *Pharmacol Biochem Behav* 103(2): 230-236.
- Slotboom, D. J., W. N. Konings and J. S. Lolkema (1999). "Structural features of the glutamate transporter family." *Microbiol Mol Biol Rev* 63(2): 293-307.
- Smith, A. D. and J. P. Bolam (1990). "The neural network of the basal ganglia as revealed by the study of synaptic connections of identified neurones." *Trends Neurosci* 13(7): 259-265.
- Smith, J. B., J. R. Klug, D. L. Ross, C. D. Howard, N. G. Hollon, V. I. Ko, H. Hoffman, E. M. Callaway, C. R. Gerfen and X. Jin (2016). "Genetic-Based Dissection Unveils the Inputs and Outputs of Striatal Patch and Matrix Compartments." *Neuron* 91(5): 1069-1084.
- Smith, Y., T. Wichmann, S. A. Factor and M. R. DeLong (2012). "Parkinson's disease therapeutics: new developments and challenges since the introduction of levodopa." *Neuropsychopharmacology* 37(1): 213-246.
- Somogyi, J., A. Baude, Y. Omori, H. Shimizu, S. El Mestikawy, M. Fukaya, R. Shigemoto, M. Watanabe and P. Somogyi (2004). "GABAergic basket cells expressing cholecystokinin contain vesicular glutamate transporter type 3 (VGLUT3) in their synaptic terminals in hippocampus and isocortex of the rat." *Eur J Neurosci* 19(3): 552-569.
- Sos, K. E., M. I. Mayer, C. Cserep, F. S. Takacs, A. Szonyi, T. F. Freund and G. Nyiri (2017). "Cellular architecture and transmitter phenotypes of neurons of the mouse median raphe region." *Brain Struct Funct* 222(1): 287-299.
- Spillantini, M. G., M. L. Schmidt, V. M. Lee, J. Q. Trojanowski, R. Jakes and M. Goedert (1997). "Alpha-synuclein in Lewy bodies." *Nature* 388(6645): 839-840.
- Staras, K. and T. Branco (2010). "Sharing vesicles between central presynaptic terminals: implications for synaptic function." *Front Synaptic Neurosci* 2: 20.
- Stensrud, M. J., F. A. Chaudhry, T. B. Leergaard, J. G. Bjaalie and V. Gundersen (2013). "Vesicular glutamate transporter-3 in the rodent brain: vesicular colocalization with vesicular gamma-aminobutyric acid transporter." *J Comp Neurol* 521(13): 3042-3056.
- Sudhof, T. C. (2004). "The synaptic vesicle cycle." *Annu Rev Neurosci* 27: 509-547.
- Sulzer, D. (2011). "How addictive drugs disrupt presynaptic dopamine neurotransmission." *Neuron* 69(4): 628-649.
- Swanson, C. J., M. Bures, M. P. Johnson, A. M. Linden, J. A. Monn and D. D. Schoepp (2005). "Metabotropic glutamate receptors as novel targets for anxiety and stress disorders." *Nat Rev Drug Discov* 4(2): 131-144.
- Tabb, J. S. and T. Ueda (1991). "Phylogenetic studies on the synaptic vesicle glutamate transport system." *J Neurosci* 11(6): 1822-1828.
- Takamori, S., M. Holt, K. Stenius, E. A. Lemke, M. Gronborg, D. Riedel, H. Urlaub, S. Schenck, B. Brugger, P. Ringler, S. A. Muller, B. Rammner, F. Gräter, J. S. Hub, B. L. De Groot, G. Mieskes, Y. Moriyama, J. Klingauf, H. Grubmuller, J. Heuser, F. Wieland and R. Jahn (2006). "Molecular anatomy of a trafficking organelle." *Cell* 127(4): 831-846.
- Takamori, S., P. Malherbe, C. Broger and R. Jahn (2002). "Molecular cloning and functional characterization of human vesicular glutamate transporter 3." *EMBO Rep* 3(8): 798-803.
- Takamori, S., J. S. Rhee, C. Rosenmund and R. Jahn (2000). "Identification of a vesicular glutamate transporter that defines a glutamatergic phenotype in neurons." *Nature* 407(6801): 189-194.

- Takamori, S., J. S. Rhee, C. Rosenmund and R. Jahn (2001). "Identification of differentiation-associated brain-specific phosphate transporter as a second vesicular glutamate transporter (VGLUT2)." *J Neurosci* 21(22): RC182.
- Takeuchi, T., A. J. Duzskiewicz and R. G. Morris (2014). "The synaptic plasticity and memory hypothesis: encoding, storage and persistence." *Philos Trans R Soc Lond B Biol Sci* 369(1633): 20130288.
- Tallman, J. F., S. M. Paul, P. Skolnick and D. W. Gallager (1980). "Receptors for the age of anxiety: pharmacology of the benzodiazepines." *Science* 207(4428): 274-281.
- Tamura, Y., K. Ogita and T. Ueda (2014). "A new VGLUT-specific potent inhibitor: pharmacophore of Brilliant Yellow." *Neurochem Res* 39(1): 117-128.
- Threlfell, S., T. Lalic, N. J. Platt, K. A. Jennings, K. Deisseroth and S. J. Cragg (2012). "Striatal dopamine release is triggered by synchronized activity in cholinergic interneurons." *Neuron* 75(1): 58-64.
- Tritsch, N. X., J. B. Ding and B. L. Sabatini (2012). "Dopaminergic neurons inhibit striatal output through non-canonical release of GABA." *Nature* 490(7419): 262-266.
- Trkanjec, Z. and V. Demarin (2001). "Presynaptic vesicles, exocytosis, membrane fusion and basic physical forces." *Med Hypotheses* 56(4): 540-546.
- Ueda, T. (2016). "Vesicular Glutamate Uptake." *Adv Neurobiol* 13: 173-221.
- Ungerstedt, U., L. L. Butcher, S. G. Butcher, N. E. Anden and K. Fuxe (1969). "Direct chemical stimulation of dopaminergic mechanisms in the neostriatum of the rat." *Brain Res* 14(2): 461-471.
- Vaaga, C. E., M. Borisovska and G. L. Westbrook (2014). "Dual-transmitter neurons: functional implications of co-release and co-transmission." *Curr Opin Neurobiol* 29: 25-32.
- Valjent, E., J. C. Corvol, J. M. Trzaskos, J. A. Girault and D. Herve (2006). "Role of the ERK pathway in psychostimulant-induced locomotor sensitization." *BMC Neurosci* 7: 20.
- Valjent, E., V. Pascoli, P. Svenningsson, S. Paul, H. Enslin, J. C. Corvol, A. Stipanovich, J. Caboche, P. J. Lombroso, A. C. Nairn, P. Greengard, D. Herve and J. A. Girault (2005). "Regulation of a protein phosphatase cascade allows convergent dopamine and glutamate signals to activate ERK in the striatum." *Proc Natl Acad Sci U S A* 102(2): 491-496.
- van Huijstee, A. N. and H. D. Mansvelder (2014). "Glutamatergic synaptic plasticity in the mesocorticolimbic system in addiction." *Front Cell Neurosci* 8: 466.
- Vandenberg, R. J. and R. M. Ryan (2013). "Mechanisms of glutamate transport." *Physiol Rev* 93(4): 1621-1657.
- Varga, V., A. Losonczy, B. V. Zemelman, Z. Borhegyi, G. Nyiri, A. Domonkos, B. Hangya, N. Holderith, J. C. Magee and T. F. Freund (2009). "Fast synaptic subcortical control of hippocampal circuits." *Science* 326(5951): 449-453.
- Varoqui, H., M. K. Schafer, H. Zhu, E. Weihe and J. D. Erickson (2002). "Identification of the differentiation-associated Na<sup>+</sup>/PI transporter as a novel vesicular glutamate transporter expressed in a distinct set of glutamatergic synapses." *J Neurosci* 22(1): 142-155.
- Vertes, R. P. (1991). "A PHA-L analysis of ascending projections of the dorsal raphe nucleus in the rat." *J Comp Neurol* 313(4): 643-668.
- Vigneault, E., O. Poirel, M. Riad, J. Prud'homme, S. Dumas, G. Turecki, C. Fasano, N. Mechawar and S. El Mestikawy (2015). "Distribution of vesicular glutamate transporters in the human brain." *Front Neuroanat* 9: 23.
- Virk, M. S., Y. Sagi, L. Medrihan, J. Leung, M. G. Kaplitt and P. Greengard (2016). "Opposing roles for serotonin in cholinergic neurons of the ventral and dorsal striatum." *Proc Natl Acad Sci U S A* 113(3): 734-739.
- Voisin, A. N., O. Mnie-Filali, N. Giguere, G. M. Fortin, E. Vigneault, S. El Mestikawy, L. Descarries and L. E. Trudeau (2016). "Axonal Segregation and Role of the Vesicular Glutamate Transporter VGLUT3 in Serotonin Neurons." *Front Neuroanat* 10: 39.
- Volpicelli-Daley, L. A., D. Kirik, L. E. Stoyka, D. G. Standaert and A. S. Harms (2016). "How can rAAV-alpha-synuclein and the fibril alpha-synuclein models advance our understanding of Parkinson's disease?" *J Neurochem* 139 Suppl 1: 131-155.

- Wallen-Mackenzie, A., H. Wootz and H. Englund (2010). "Genetic inactivation of the vesicular glutamate transporter 2 (VGLUT2) in the mouse: what have we learnt about functional glutamatergic neurotransmission?" *Ups J Med Sci* 115(1): 11-20.
- Watkins, J. C. (2000). "l-glutamate as a central neurotransmitter: looking back." *Biochem Soc Trans* 28(4): 297-309.
- Watt, A. J., M. C. van Rossum, K. M. MacLeod, S. B. Nelson and G. G. Turrigiano (2000). "Activity coregulates quantal AMPA and NMDA currents at neocortical synapses." *Neuron* 26(3): 659-670.
- Weihe, E., M. K. Schafer, B. Schutz, M. Anlauf, C. Depboylu, C. Brett, L. Chen and L. E. Eiden (1998). "From the cholinergic gene locus to the cholinergic neuron." *J Physiol Paris* 92(5-6): 385-388.
- Weston, M. C., R. B. Nehring, S. M. Wojcik and C. Rosenmund (2011). "Interplay between VGLUT isoforms and endophilin A1 regulates neurotransmitter release and short-term plasticity." *Neuron* 69(6): 1147-1159.
- White, F. J., A. Joshi, T. E. Koeltzow and X. T. Hu (1998). "Dopamine receptor antagonists fail to prevent induction of cocaine sensitization." *Neuropsychopharmacology* 18(1): 26-40.
- Wilson, C. J., H. T. Chang and S. T. Kitai (1990). "Firing patterns and synaptic potentials of identified giant aspiny interneurons in the rat neostriatum." *J Neurosci* 10(2): 508-519.
- Wilson, N. R., J. Kang, E. V. Hueske, T. Leung, H. Varoqui, J. G. Murnick, J. D. Erickson and G. Liu (2005). "Presynaptic regulation of quantal size by the vesicular glutamate transporter VGLUT1." *J Neurosci* 25(26): 6221-6234.
- Wojcik, S. M., J. S. Rhee, E. Herzog, A. Sigler, R. Jahn, S. Takamori, N. Brose and C. Rosenmund (2004). "An essential role for vesicular glutamate transporter 1 (VGLUT1) in postnatal development and control of quantal size." *Proc Natl Acad Sci U S A* 101(18): 7158-7163.
- Wolff, L. (1890). "Ueber Glyoxylpropionsäure und einige Abkömmlinge derselben." *Justus Liebigs Annalen der Chemie* 260(1): 79-136.
- Won, L., Y. Ding, P. Singh and U. J. Kang (2014). "Striatal cholinergic cell ablation attenuates L-DOPA induced dyskinesia in Parkinsonian mice." *J Neurosci* 34(8): 3090-3094.
- Woolf, N. J. and L. L. Butcher (1986). "Cholinergic systems in the rat brain: III. Projections from the pontomesencephalic tegmentum to the thalamus, tectum, basal ganglia, and basal forebrain." *Brain Res Bull* 16(5): 603-637.
- Wouterlood, F. G., W. Hartig, H. J. Groenewegen and P. Voorn (2012). "Density gradients of vesicular glutamate- and GABA transporter-immunoreactive boutons in calbindinand mu-opioid receptor-defined compartments in the rat striatum." *J Comp Neurol* 520(10): 2123-2142.
- Wu, X. S., L. Xue, R. Mohan, K. Paradiso, K. D. Gillis and L. G. Wu (2007). "The origin of quantal size variation: vesicular glutamate concentration plays a significant role." *J Neurosci* 27(11): 3046-3056.
- Yates, J. W., J. T. Meij, J. R. Sullivan, N. M. Richtand and L. Yu (2007). "Bimodal effect of amphetamine on motor behaviors in C57BL/6 mice." *Neurosci Lett* 427(1): 66-70.
- Zahm, D. S. and J. S. Brog (1992). "On the significance of subterritories in the "accumbens" part of the rat ventral striatum." *Neuroscience* 50(4): 751-767.
- Zander, J. F., A. Munster-Wandowski, I. Brunk, I. Pahner, G. Gomez-Lira, U. Heinemann, R. Gutierrez, G. Laube and G. Ahnert-Hilger (2010). "Synaptic and vesicular coexistence of VGLUT and VGAT in selected excitatory and inhibitory synapses." *J Neurosci* 30(22): 7634-7645.
- Zerari-Mailly, F., A. Braud, N. Davido, B. Toure, J. Azerad and Y. Boucher (2012). "Glutamate control of pulpal blood flow in the incisor dental pulp of the rat." *Eur J Oral Sci* 120(5): 402-407.
- Zhou, F. M., C. J. Wilson and J. A. Dani (2002). "Cholinergic interneuron characteristics and nicotinic properties in the striatum." *J Neurobiol* 53(4): 590-605.
- Zhou, Y. and N. C. Danbolt (2014). "Glutamate as a neurotransmitter in the healthy brain." *J Neural Transm (Vienna)* 121(8): 799-817.
- Zhu, S., D. Stroebel, C. A. Yao, A. Taly and P. Paoletti (2013). "Allosteric signaling and dynamics of the clamshell-like NMDA receptor GluN1 N-terminal domain." *Nat Struct Mol Biol* 20(4): 477-485.

Zhuang, X., J. Masson, J. A. Gingrich, S. Rayport and R. Hen (2005). "Targeted gene expression in dopamine and serotonin neurons of the mouse brain." *J Neurosci Methods* 143(1): 27-32.

Zhuo, M. (2014). "Long-term potentiation in the anterior cingulate cortex and chronic pain." *Philos Trans R Soc Lond B Biol Sci* 369(1633): 20130146.

Zimmermann, J., M. A. Herman and C. Rosenmund (2015). "Co-release of glutamate and GABA from single vesicles in GABAergic neurons exogenously expressing VGLUT3." *Front Synaptic Neurosci* 7: 16.

Ztaou, S., N. Maurice, J. Camon, G. Guiraudie-Capraz, L. Kerkerian-Le Goff, C. Beurrier, M. Liberge and M. Amalric (2016). "Involvement of Striatal Cholinergic Interneurons and M1 and M4 Muscarinic Receptors in Motor Symptoms of Parkinson's Disease." *J Neurosci* 36(35): 9161-9172.